Spring 2020

Using Human Granulosa Cells to Select the Most Competent Embryos for Uterine Transfer in in Vitro Fertilization Cycles

Richard John Kordus

USING HUMAN GRANULOSA CELLS TO SELECT THE MOST COMPETENT EMBRYOS FOR UTERINE TRANSFER IN IN VITRO FERTILIZATION CYCLES

by

Richard John Kordus

Bachelor of Science
Valparaiso University, 1997

Master of Science
University of South Carolina, 2010

Submitted in Partial Fulfillment of the Requirements

For the Degree of Doctor of Philosophy in

Biomedical Science

School of Medicine

University of South Carolina

2020

Accepted by:

Holly LaVoie, Major Professor

Wayne Carver, Committee Member

Carole Oskeritzian, Committee Member

Rekha Patel, Committee Member

Gail Whitman-Elia, Committee Member

Cheryl L. Addy, Vice Provost and Dean of the Graduate School

DEDICATION

I dedicate this work to my wife, Kelley Elizabeth Kordus, for your unending love and support. Thank you for the sacrifices you have made to make the completion of my doctorate possible. Not only have you given up your time, but you took on my responsibilities at home and made life as easy as possible for me. You accepted me having to travel the country as a consultant for us to stay in Columbia, SC and continue my degree. You agreed to move, in order for me to finish my degree. You took care of getting the house ready for sale and packing all on your own when we moved to Greenville, SC. You supported me in the times I wanted to give up, which were plenty. Most important you loved me through it all and were immensely patient.

I would also like to dedicate this work to all people who struggle with infertility. I have chosen to help those who cannot have children on their own to achieve their dreams of having a family. Kelley and I have struggled with infertility and we know the pain and heartache that comes along with that. It is my hope that someday my research may help those in need to achieve their goal of having a family. It is also my hope that this work may inspire other researchers to help those who struggle with infertility. Don’t give up, great things are coming in the future.

ACKNOWLEDGEMENTS

The completion of my degree would not have been possible without the help of so many people. First, I would like to thank my committee members, Dr. Wayne Carver, Dr Carole Oskerizitian, and Dr. Rekha Patel. Thank you for agreeing to be on my committee, thank you for asking thoughtful and probing questions, and thank you for your advice and guidance.

Second, I would like to thank my mentor, Dr. Holly LaVoie. I am more grateful than a few sentences can convey. I started my journey towards my PhD in 2006 and you have been guiding me the entire way. In 2010, you were understanding when I needed to step back and stop my studies and end with a MS instead. We collaborated while I continued to work at Advanced Fertility and Reproductive Endocrinology Institute, LLC. You encouraged me to come back and finish my PhD in 2015 which I really did not even think I wanted to do. You supported me when circumstances changed, and I had to start consulting for a and you helped me find my current position and Fertility Center of the Carolinas all the while continuing my research and mentoring. You pushed me when I needed it and were also compassionate when I needed it more. I could not have been more fortunate, and I am forever grateful that you accepted me as one of your students. The phrase, “When the student is ready, the Master will appear.” Truly applies to my journey.

Third, I would like to thank Dr. Gail Whitman-Elia. I would not be where I am today without you. Perhaps fate brought us together in 2003 when I first consulted for you. You offered me a position and the flexibility to continue my education which was a wonderful gift. You also introduced me to my wife, Kelley, and that has changed my life for the better even more than my degree.

I also need to thank all my colleagues who were my support, encouragement, and people who worked a little bit harder when they did not have to so I could finish my dissertation. Mandy Schultz, you were my right hand, friend, and I still miss you dearly. Charlotte Taunton, you were a joy to work with and a blessing when I needed help with statistics. Henry Malter, thank you for hiring me and supporting me while I finished my research. Heather Stowe, thank you for your strength, sacrifices, and editing skills. Thank you to all the Doctors at Fertility Center of the Carolinas, David Forstein, Lisa Green, Bruce Lessey, Creighton Likes, Paul Miller, and Johanna Von Hofe for the opportunity to work with you and the support I received from all of you through this journey. I would also like to thank the rest of the staff at both clinics although I do not have the space to mention everyone individually, each of you in some way have impacted my journey.

Finally, I need to thank Dr Michael Corso. We started as coworkers and end as life-long friends. We journeyed together to get where we are, but I couldn't have done it without your help in both labs. Now we are both graduating together and that is bittersweet. You are like a brother to me. Thank you always.

ABSTRACT

Infertility is a worldwide epidemic often treated with in vitro fertilization. The success of in vitro fertilization is directly dependent upon the quality of oocytes produced during the controlled stimulation of the patient's ovaries. There is a need for improved methods to allow embryologists to select the most viable embryos with the highest probability of leading to live births since in vitro fertilization success is far from optimal.

Oocyte and subsequent embryo quality are intimately influenced by the granulosa cells which surround the oocyte during follicular maturation. The oocytes require proper signaling and energy production form the surrounding granulosa cells for ideal maturation which will allow the oocyte to fertilize and produce a viable embryo. We hypothesize that mRNA levels of certain genes in granulosa cells will allow for the identification oocytes that will produce euploid embryos and the most viable embryos within a cohort. Secondly, we hypothesize that the rate by which mitochondria from granulosa cells are able to utilize certain metabolic substrates will be able to identify patients that have increased probability of producing high quality embryos leading to live births.

This dissertation attempts to identify a group of genes within individual cumulus cells that show differential mRNA gene expression between oocytes of euploid embryos and oocytes leading to live birth compared to oocytes that do not. From these genes we further attempt to create a model using multiple genes to

identify the most viable oocytes within a cohort. This dissertation also attempts to identify metabolic substrates differentially utilized by granulosa cell mitochondria based on patient demographics or embryo development and determine if individual substrates can be used as mitochondrial biomarkers for assisted reproduction. As a whole, the work in this dissertation seeks to provide a panel of biomarkers that can be used by clinicians to better identify embryos that will help improve overall assisted reproductive success.

TABLE OF CONTENTS

LIST OF TABLES

LIST OF FIGURES

LIST OF SYMBOLS

α	Alpha
β	Beta
°C	Degrees Celsius
CO_2	Carbon Dioxide
Ct	Threshold Cycle
g	Gravity
>	Greater than
≥	Greater than or equal to
H_2O	Water
hrs	Hours
IUs	International Units
IU/mL	International Unit per Milliliter
kb	Kilobase
kg/m^2	Body mass index (kilogram per meter squared)
<	Less than
≤	Less than or equal to
LN_2	Liquid Nitrogen
mg/mL	Milligram per Milliliter
µL	Microliter

mm	Millimeter
mM	Millimolar
min	Minute(s)
x	Multiplied by
N_2	Nitrogen
ng	Nanogram
ng/mL	Nanograms per Milliter
nM	Nanomolar
nm	Wavelength
O_2	Oxygen
%	Percent
pg/mL	Picogram per Milliliter
pH	Potential Hydrogen
®	Registered trademark symbol
sd	Standard deviation
U/mL	Units per Milliliter

LIST OF ABBREVIATIONS

ACE2 ..... Angiotensin 1 Converting Enzyme 2

aCGH ..... Array Comparative Genomic Hybridization

ACTB ..... Actin Beta

ACVR1 ..... Activin A Receptor Type 1

ACVR1B ..... Activin A Receptor Type 1B

ADP ..... Adenosine Diphosphate

AKAP11 ..... A Kinase Anchoring Protein 11

Akt1 ..... AKT Serine/Theronine Kinase 1

AHR ..... Aryl Hydrocarbon Receptor

ALCAM ..... Activated Leukocyte Cell Adhesion Molecule

ALDOA ..... Aldolase, Fructose-Bisphosphate A

AMA ..... Advanced Maternal Age

AMH ..... Anti-Müllerian Hormone

AMP ..... Adenosine 5'-Monophosphate

ANG ..... Angiogenin

ANOVA ..... Analysis of Variance

AQP1 ..... Aquaporin 1 (Colton blood group)

AQP2 ..... Aquaporin 2

AQP3 ..... Aquaporin 3 (Gill blood group)

AQP4 ..... Aquaporin 4

AQP5 ..... Aquaporin 5

AQP6 .....Aquaporin 6

AQP7 .....Aquaporin 7

AQP9 .....Aquaporin 9

AQP11 .....Aquaporin 11

AQP12A ..... Aquaporin 12A

AR .....Androgen Receptor

AREG ..... Amphiregulin

ARID1B .....AT-Rich Interaction Domain 1B

ART ..... Assisted Reproductive Technologies

ASRM .....American Society for Reproductive Medicine

ATP ..... Adenosine Triphosphate

AUC ..... Area Under the Curve

BACH2 .....BTB Domain and CNC Homolog 2

Bcl2l1 ..... BCL2 Like 1

BCL2L11 ..... BCL2 Like 11

BDNF .....Brain Derived Neurotrophic Factor

BIRC5 ..... Baculoviral Inhibitor of Apoptosis Repeat Containing 5

BMI ..... Body Mass Index

BMP6 .....Bone Morphogenetic Protein 6

BMP15 .....Bone Morphogenetic Protein 15

BMPR2 ..... Bone Morphogenetic Protein Receptor Type 2

BSG ..... Basigin

CA.....Corpus Albicans

CACNA1C..... Calcium Channel, Voltage-Dependent, L Type, Alpha-1C Subunit

CALM1 .....Calmodulin 1

CALM2 ..... Calmodulin 2

CALU ..... Calumenin

CAMK1D ..... Calcium/Calmodulin Dependent Protein Kinase 1D

cAMP ..... Adenosine 3',5'-Cyclic Monophosphate

CC..... Cumulus Granulosa Cell

CD117..... c-KIT receptor

cDNA .....Complementary Deoxyribonucleic Acid

CDC42 ..... Cell Division Cycle 42

CG ..... Chorionic Gonadotropin

cGMP..... Cyclic Guanosine Monophosphate

CH..... Corpus Hemorrhagicum

CHD9 ..... Chromodomain Helicase DNA Binding Protein 9

CHGB ..... Chromogranin B

CL ..... Corpus Luteum

COC..... Cumulus Oocyte Complex

COX20 ..... COX20, Cytochrome C Oxidase Assembly Factor

CSCC..... Cholesterol Side-Chain Cleavage Complex

Cx43 ..... Connexin 43

CXCL2 ..... C-X-C Motif Chemokine Ligand 2

CXCL8 ..... C-X-C Motif Chemokine Ligand 2

CYP11A1 .....Cytochrome P450 Family 11 Subfamily A Member 1

CYP17A1 .....Cytochrome P450 Family 17 Subfamily A Member 1

CYP19A1/Cyp19a1.....Aromatase

DHEA.....Dehydroepiandrosterone

DNA .....Deoxyribonucleic Acid

DNAJC15 ..... DnaJ Heat Shock Protein Family (Hsp40) Member C15

DOK5 ..... Docking Protein 5

DOR ..... Diminished Ovarian Reserve

DPC ..... Days Post Coitum

DPP8 ..... Dipeptidyl Peptidase 8

DPYSL3 ..... Dihydropyrimidinase Like 3

DRGE ..... Differential mRNA Gene Expression

DUSP6 ..... Dual Specificity Phosphatase 6

E2 ..... Estrogen

EDIL3 ..... Epidermal Growth Factor Like Repeats and Discoidin Domains 3

EFNB2 ..... Ephrin B2

EGF ..... Epidermal Growth Factor

EGR1 ..... Early Growth Response 1

EREG ..... Epiregulin

ESR1 ..... Estrogen Receptor 1

ET ..... Embryo Transfer

ETC ..... Electron Transport Chain

$FADH_2$ ..... Flavin Adenine Dinucleotide Hydride

FDX1 ..... Ferredoxin 1

FDXR ..... Ferredoxin Reductase

FET ..... Frozen Embryo Transfer

FGF ..... Fibroblast Growth Factor

FGF12 ..... Fibroblast Growth Factor 12

FGG ..... Fibrinogen Gamma Chain

FOSB ..... FosB Proto-Oncogene, AP-1 Transcription Factor Subunit

FOXO1 ..... Forkhead Box O1

FOXO3 ..... Forkhead Box O3

FOXO4 ..... Forkhead Box O4

FSH ..... Follicle Stimulating Hormone

FSHβ ..... Follicle Stimulating Hormone Beta Subunit

FSHR ..... Follicle Stimulating Hormone Receptor

GABPB1 ..... GA Binding Protein Transcription Factor Beta Subunit 1

GAP43 ..... Growth Associated Protein 43

GC ..... Granulosa Cell

GDF9 ..... Growth-Differentiation Factor 9

GHR ..... Growth Hormone Receptor

GJA1/Gja1 ..... Gap Junction Alpha-1

GJA4 ..... Gap Junction Alpha-4

GLMM ..... Generalized Linear Mixed Model

GnRH ..... Gonadotropin Releasing Hormone

GPR137B ..... G Protein-Coupled Receptor 137B

GPX3 ..... Glutathione Peroxidase 3

GREM1 ..... Gremlin 1, DAN family BMP antagonist

GSR ..... Glutathione-Disulfide Reductase

GSTA3 ..... Glutathione S-Transferase Alpha 3

GSTA4 ..... Glutathione S-Transferase Alpha 4

GV ..... Germinal Vesical

GVBD ..... Germinal Vesical Break Down

HAS2 ..... Hyaluronan Synthase 2

hCG ..... Human Chorionic Gonadotropin

HEPES.....N-2-Hydroxyethylpiperazine-N'-2- Ethanesulfonic Acid

HIF1A..... Hypoxia Inducible Factor 1 Alpha Subunit

HIPK1 .....Homeodomain Interacting Protein Kinase 1

H4C3.....H4 Clustered Histone 3

hMG ..... Human Menopausal Gonadotropin

HOMER1 ..... Homer Scaffolding Protein 1

HPG .....Hypothalamic/Pituitary/Gonadal

HP-hMG .....High-Purity Human Menopausal Gonadotropin

HSD3B1..... ...Hydroxy-Delta-5-Steroid Dehydrogenase, 3 Beta and Steroid Delta-Isomerase 1

HSD3B2..... ...Hydroxy-Delta-5-Steroid Dehydrogenase, 3 Beta and Steroid Delta-Isomerase 2

HSD17B..... 17-Beta Hydroxysteroid Dehydrogenase

HTF.....Human Tubal Fluid

HTRA1 .....HtrA Serine Peptidase 1

ICM ..... Inner Cell Mass

ICSI..... Intracytoplasmic Sperm Injection

IGF..... Insulin Like Growth Factor

IGF1..... Insulin Like Growth Factor

IGF2..... Insulin Like Growth Factor 2

IGFBP4 ..... Insulin Like Growth Factor Binding Protein 4

IGFBP5 ..... Insulin Like Growth Factor Binding Protein 5

IL7R .....Interleukin 7 Receptor

IL8..... C-X-C Motif Chemokine Ligand 8

IL1B ..... Interleukin 1 Beta

IL6ST ..... Interleukin 6 Signal Transducer

ING1 ..... Inhibitor of Growth Protein 1

INHBA .....Inhibin Subunit Beta A

INHBB .....Inhibin Subunit Beta B

INHBC ..... Inhibin Subunit Beta C

IRB .....Institutional Review Board

ITM2A .....Integral Membrane Protein 2

ITPKA ..... Inositol-Trisphosphate 3-Kinase A

ITPR1 ..... Inositol 1,4,5-Trisphosphate Receptor Type 1

IVF ..... In Vitro Fertilization

KDM4A ..... Lysine Demethylase 4A

KDM4B ..... Lysine Demethylase 4A

KHDRBS3 ..... KH RNA Binding Domain Containing, Signal Transduction Associated 3

KRT6A ..... Keratin 6A

LDHA .....Lactate Dehydrogenase A

LH ..... Luteinizing Hormone

LHCGR ..... Luteinizing Hormone/Choriogonadotropin Receptor

LHR .....Luteinizing Hormone Receptor

LHRH .....Luteinizing Hormone Releasing Hormone

LRP8 ..... LDL Receptor Related Protein 8

MII .....Metaphase 2 Oocyte

MAPK..... Mitogen-Activated Protein Kinase

MARCKS .....Myristoylated Alanine Rich Protein Kinase C Substrate

MAS ..... Mitochondrial Assay Solution

MFI .....Male Factor Infertility

MGC ..... Mural Granulosa Cell

MPF .....Maturation [M-phase] Promoting Factor

MPI ..... Meiotic Prophase 1

mRNA .....Messenger Ribonucleic Acid

MT-ATP8 ..... Mitochondrially Encoded ATP Synthase 8

mtDNA .....Mitochondrial Deoxyribonucleic Acid

MTUS1..... Microtubule Associated Tumor Suppressor 1

NAD^+..... Nicotinamide Adenine Dinucleotide

NADH..... Nicotinamide Adenine Dinucleotide Hydride

NADPH ..... Nicotinamide Adenine Dinucleotide Phosphate Hydride

NCBI .....National Center for Biotechnology Information

nDNA ..... Nuclear Deoxyribonucleic Acid

NFIB..... Nuclear Factor I B

NGS .....Next-Generation Sequencing

NOR.....Normal Ovarian Reserve

NR2F6 ..... Nuclear Receptor Subfamily 2 Group F Member 6

NRP1 ..... Neuropilin 1 Receptor

NTS.....Neurotensin

NUP133 .....Nucleoporin 133

NUDT10.....Nudix Hydrolase 10

OXPHOS ..... Oxidative Phosphorylation

P4 ..... Progesterone

PAPPA..... Pappalysin-1

PBS..... Phosphate Buffered Saline

PC1.....First Principal Component

PC2 ..... Second Principal Component

PCA ..... Principle Component Analysis

PCK1 ..... Phosphoenolpyruvate Carboxykinase 1

PCOS ..... Polycystic Ovarian Syndrome

PCR ..... Polymerase Chain Reaction

PDGF ..... Platelet Derived Growth Factor

PEDF ..... Pigment Epithelium-Derived Factor

PFKP ..... Phosphofructokinase, Platelet

PGA3 ..... Pepsinogen 3, Group 1 (Pepsinogen A)

PGA4 ..... Pepsinogen 4, Group 1 (Pepsinogen A)

PGA5 ..... Pepsinogen 5, Group 1 (Pepsinogen A)

PGC ..... Primordial Germ Cell

PGK1 ..... Phosphoglycerate Kinase 1

PGR ..... Progesterone Receptor

PGRMC1 ..... Progesterone Receptor Membrane Component 1

PGT-A ..... Preimplantation Genetic Testing For Aneuploidy

PHLDA1 ..... Pleckstrin Homology Like Domain Family A Member 1

PIK3CA ..... Phosphatidylinositol-4,5-Bisphosphate 3-Kinase Catalytic Subunit Type 2 Alpha

PI3K/AKT ..... Phosphoinositol 1,3-Kinase/ Serine/Threonine Kinase 1

PIR ..... Pirin

PKA ..... Adenylyl Cyclase/cAMP/Protein Kinase A

PKM ..... Pyruvate Kinase, Muscle

PKN2 ..... Protein Kinase N2

PLIN2 ..... Perilipin 2

PNCK ..... Pregnancy Upregulated Nonubiquitous CaM Kinase

PROK2 ..... Prokineticin 2

PSMD6 ..... Proteasome 26S Subunit, Non-ATPase 6

Pt ..... Patient

PTGS2 ..... Prostaglandin-Endoperoxide Synthase 2

PTHLH ..... Parathyroid Hormone Like Hormone

PTMA ..... Prothymosin Alpha

PTX3 ..... Pentraxin 3

qRT-PCR ..... Quantitative Real-Time Polymerase Chain Reaction

rFSH ..... Recombinant Follicle Stimulating Hormone

rLH ..... Recombinant Luteinizing Hormone

RGS2 ..... Regulator of G Protein Signaling 2

RGS3 ..... Regulator of G Protein Signaling 3

RHBDL2 ..... Rhomboid Like 2

RNA ..... Ribonucleic Acid

ROC ..... Receiver Operating Characteristic

ROS ..... Reactive Oxygen Species

RPL9 ..... Ribosomal Protein L9

RPS6KA2 ..... Ribosomal Protein S6 Kinase A2

RT ..... Room Temperature

RT-PCR ..... Real-Time Polymerase Chain Reaction

RUNX2 ..... RUNX Family Transcription Factor 2

RYR2 ..... Ryanodine Receptor 2

SART ..... Society for Assisted Reproductive Technology

SASH1 ..... SAM and SH3 Domain Containing 1

SCARB1 ..... Scavenger Receptor Class B Member 1

SCF ..... Stem Cell Factor

SDC4 ..... Syndecan 4

SEMA3A ..... Semaphorin 3A Membrane Protein

SERPINA3 ..... Serpin Family A Member 3

SERPINE2 ..... Serpin Family E Member 2

SERPINF1 ..... Serpin Family F Member 1

SFRP1 ..... Secreted Frizzled Related Protein 1

SFRP2 ..... Secreted Frizzled Related Protein 2

Shc1 ..... SHC Adaptor Protein 1

SIRT3 ..... Sirtuin 3

SLC2A1 ..... Solute Carrier Family 2 Member 1

SLC2A4 ..... Solute Carrier Family 2 Member 4

SLC2A9 ..... Solute Carrier Family 2 Member 9

SPHKAP ..... SPHK1 Interactor, AKAP Domain Containing

SPRY2 ..... Sprouty RTK Signaling Antagonist 2

SPRY4 ..... Sprouty RTK Signaling Antagonist 4

SPSB2 ..... SplA/Ryanodine Receptor Domain and SOCS Box Containing 2

StAR ..... Steroidogenic Acute Regulatory Protein

STARD1 ..... Steroidogenic Acute Regulatory Protein

STC1 ..... Stanniocalcin 1

STC2 ..... Stanniocalcin 2

STS ..... Steroid Sulfatase (Microsomal), Isozyme S

SYT11 ..... Synaptotagmin 11

TBP ..... TATA-Box Binding Protein

TBX6 ..... T-Box 6

TC ..... Theca Cell

TGFB1 ..... Transforming Growth Factor Beta 1

TGF-β ..... Transforming Growth Factor Beta

THBS1 ..... Thrombospondin 1

THOC2 ..... THO Complex 2

TLDA ..... TaqMan Low-Density Array

TMEM64 ..... Transmembrane Protein 64

TNC ..... Tenascin C

TNFAIP6 ..... TNF Alpha Induced Protein 6

TOM1 ..... Target of myb1 Membrane Trafficking Protein

TP5313 ..... Tumor Protein p53 Inducible Protein 3

TRPM7 ..... Transient Receptor Potential Cation Channel Subfamily M Member 7

TUG1 ..... Taurine Upregulated 1 (Non-Protein Coding)

UBQLN1 ..... Ubiquilin 1

UGP2 ..... UDP-Glucose Pyrophosphorylase 2

ULBP1 ..... UL16 Binding Protein 1

VCAN ..... Versican

WRB ..... Tryptophan Rich Basic Protein

YWHAZ ..... Tyrosine 3-Monooxygenase/Tryptophan 5-Monooxygenase Activation Protein Zeta

ZNF93 ..... Zinc Finger Protein 93

ZNF132 ..... Zinc Finger Protein 132

Chapter 1

Introduction[1,2]

---

[1]Portions adapted from Kordus, R.J. 2010, Expression of DIO2 in the porcine ovary and the granulosa cells of humans (Master's thesis). Retrieved from https://scholarcommons.sc.edu/etd/202

[2]Portions adapted from R.J. Kordus and H.A. LaVoie. Granulosa cell biomarkers to predict pregnancy in ART: pieces to solve the puzzle. 2017. Reproduction. 153(2):R69-R83. Epub 2016 Nov 4. Review. Reprinted here with permission of publisher

1.1 Significance of Study

In vitro fertilization (IVF) is a common intervention for treating women struggling with infertility. IVF involves hormonally priming a woman's ovaries to mature multiple follicles, retrieving oocytes from the follicles, inseminating the mature oocytes with the partner's or donor sperm, and after several days selecting cultured embryos for transfer to the patient's uterus. Most IVF cycles fail to lead to a live birth. Each round of IVF has a tremendous cost to the patient ranging from $10,000 to $20,000 per fresh oocyte retrieval and around $4,000 for subsequent frozen embryo transfers (FETs). The low take-home baby rate means that many patients will incur each of these costs multiple times.

To improve live birth outcomes, the use of preimplantation genetic testing for aneuploidy (PGT-A) has been employed to identify genetically euploid embryos before uterine transfer. In some cases, PGT-A has been shown to increase implantation, ongoing pregnancy, and delivery rates (Chen et al., 2015a, Schoolcraft et al., 2010, Scott et al., 2013, Yang et al., 2012). However, PGT-A is also an invasive method that requires the removal of several cells from the embryo's trophectoderm layer of the blastocyst. Using euploid embryos for uterine transfer does not guarantee implantation, however, and some studies have indicated there is a decreased pregnancy rate following PGT-A (Kushnir et al., 2016, Chang et al., 2016). One study has shown that only certain age groups benefit from PGT-A testing (Kang et al., 2016). Additionally, implantation failure has been positively correlated with the number of cells removed during the biopsy procedure (Zhang et al., 2016). There is also concern that mosaicism (two distinct

cells lines within the same embryo) will give rise to erroneous PGT-A results and that some embryos which would lead to genetically normal live births will not be transferred because of these misleading results (Kushnir et al., 2018, Gleicher et al., 2016, Taylor et al., 2014). Therefore, finding a non-invasive and reliable method to select the most viable oocytes and subsequent embryos for uterine transfer would be highly desirable in the field of IVF.

The ultimate success of an IVF cycle is determined by ovarian stimulation protocols and patient characteristics that control the quality of the oocytes retrieved (Adriaenssens et al., 2010a). These various factors will influence the development of the somatic cells of the ovarian follicle, specifically, the granulosa cell (GC) population. In turn, the GCs will impact the developing oocytes they enclose (Eppig et al., 1996, Gilchrist et al., 2008, Matzuk et al., 2002). In an ideal IVF stimulation, the interactions of the GCs and oocytes will result in optimal conditions for oocyte maturation (Tanghe et al., 2002, Uyar et al., 2013). Since the GCs are readily obtained as a by-product of the IVF process, they are an ideal source of materials for non-invasive analysis of oocyte potential. Techniques which assess mRNA biomarker levels and mitochondrial substrate utilization in GCs allow rapid profiling that could potentially identify the most viable oocytes and subsequent embryos and still be incorporated into the standard workflow of an IVF laboratory without much difficulty. mRNA expression analysis and mitochondrial metabolic assessment of GCs can be performed before embryo transfer (ET) allowing for the selection of the embryo with the highest implantation potential. Several recent studies suggest that GC mRNA biomarkers can be used to generate models that

can identify oocytes/embryos with the highest probabilities of leading to pregnancies and live births (Borup et al., 2016, Ekart et al., 2013, Iager et al., 2013, Wathlet et al., 2011, Wathlet et al., 2012, Wathlet et al., 2013). Mitochondrial function and mitochondria content have also been shown to be related to oocyte maturation and IVF pregnancies as well (Dalton et al., 2014, Huang and Wells, 2010, Tsai et al., 2010).

The developing ovarian follicle is comprised of an oocyte, follicular fluid, and distinct somatic cell populations. The preovulatory follicle, whose cells are harvested during the IVF procedure, contains two distinct GC types: the cumulus granulosa cell (CC) and the mural granulosa cell (MGC). The CCs surround and share gap junctions with their individual oocytes. Cumulus cells remain attached to their oocytes following oocyte retrieval and must be mechanically and enzymatically removed before intracytoplasmic sperm injection (ICSI) of spermatozoa for insemination in male factor and PGT-A cases. Cumulus cells will remain attached to the oocyte during conventional insemination procedures. Cumulus cells have bi-directional communication with the oocytes and tend to reflect the oocyte's overall health (Huang and Wells, 2010). Biomarkers of GCs associated with individual oocytes could potentially be used in assisted reproduction procedures to indicate which embryos have the best chance of implanting in the uterus and completing gestation.

Successful embryo development relies upon sufficient energy metabolism generated by adenosine triphosphate (ATP) processed through the mitochondria. Cumulus cells produce ATP and augment oocyte ATP supply during follicular

growth. The CCs also provide pyruvate for the oocyte, generated from glycolysis, via gap junctions. Pyruvate is converted by pyruvate dehydrogenase to acetyl-CoA which enters the tricarboxylic acid cycle where it is metabolized and ultimately produces ATP through the process of oxidative phosphorylation (OXPHOS) within the mitochondria of the oocyte (Su et al., 2009, Sutton-McDowall et al., 2010). Several studies have evaluated CCs, MGCs, and trophectoderm cells from blastocysts, and it appears there is a high correlation between the mitochondrial DNA (mtDNA) content found in oocytes and CCs indicating that CC mtDNA levels might serve as a biomarker for oocyte competence (Boucret et al., 2015, Desquiret-Dumas et al., 2017, Diez-Juan et al., 2015, Fragouli and Wells, 2015, Ogino et al., 2016, Taugourdeau et al., 2019).

We hypothesize that specific biomarkers in GCs can be used to select individual oocytes and their subsequent embryos that have the best chances of leading to viable pregnancies and resulting in live births. We propose a series of studies to determine if (1) a set of CC mRNA biomarkers and (2) GC mitochondrial metabolic substrate utilization can be used to improve IVF outcomes. Successful completion of the first study will result in a mRNA biomarker model that can be used to select the embryos for uterine transfer that have the best chance of resulting in a live birth. Accomplishment of our second goal will result in determination if mitochondrial metabolic substrate utilization in pooled MGCs and CCs can be used as biomarkers relating to patient demographics and embryo development. A future goal would be to utilize a small subset of mitochondrial

substrates as biomarkers to analyze individual CC masses to choose individual embryos for uterine transfer.

1.2 Ovarian Structure

The female gonad is called the ovary, and it is analogous to the testis in the male. The ovary's primary function is oocyte production or oogenesis. It will store oocytes arrested at the primordial stage of development until they are recruited to initiate maturation. After puberty and through menopause, the ovary will mature a cohort of oocytes each reproductive cycle and ovulate one or more oocytes each cycle. The ovary also acts as an endocrine gland producing hormonal secretions such as steroids prior to ovulation and from the luteinized cells of the follicle which remain in the ovary and form the corpus luteum (CL) following ovulation.

A single ovary is located on each side of the uterus and attached with an ovarian ligament (Figure 1.1). Each ovary lies near the fimbriae of each oviduct or Fallopian tube. The Fallopian tube acts as a conduit to transport spermatozoa from the male, oocytes from the female, and the resulting embryo following fertilization. The Fallopian tubes will also provide a nutrient-rich environment for the gametes and embryos. A spermatozoon will fertilize the oocyte in the ampulla of the Fallopian tube and the resulting fertilized oocyte, also known as the zygote, will be transported to the uterus for implantation. The uterus has an external wall called the perimetrium, a muscular middle layer called the myometrium, and an inner layer called the endometrium. Both the myometrium and endometrium are responsive to hormones of the reproductive cycle. The endometrium has two layers the stratum functionalis and the stratum basalis. The stratum functionalis

lines the inside of the uterus and is where the embryo will attach and grow into a fetus or it will be shed during menstruation if the embryo does not implant.

The ovary (Figure 1.2) is a complex structure containing multiple cell types with diverse and dynamic functions. The innermost layer is the ovarian medulla and the outermost layer is the ovarian cortex. The outer cortex, known as the tunica albuginea, is composed of only dense connective tissues which protect the ovary. The ovary contains female gametes, termed oogonia or oocytes, and somatic cells within the ovarian follicles and specialized dense connective tissue, termed stroma, and blood vessels. Ovarian nerves, as well as blood and lymphatic vessels, reside within the medulla. The main difference between the medulla and cortex is that ovarian follicles are only present in the cortex.

The main functional components of the ovary are the ovarian follicles. The follicles consist of oocytes, GCs, and theca cells (TCs). The GCs and TCs provide the oocyte they surround with a protected environment in which they grow and mature, allowing for fertilization by a spermatozoon following ovulation (Buccione et al., 1990). There is bi-directional communication between the GCs and oocytes, which promotes oocyte maturation (Tanghe et al., 2002, Uyar et al., 2013). This close association between the oocytes and their GCs make the GCs good candidates for research related to oocyte developmental competence.

1.3 Oogenesis

Oogonia are derived from primordial germ cells (PGCs). In humans, PGCs appear early during the second week of embryonic development from the primary ectoderm (Larsen, 2001, Wylie, 1999). PGCs can travel to various locations

throughout the embryo and yolk sac but will finally colonize the gonadal ridges (Richardson and Lehmann, 2010). Human PGCs migrate from the primary ectoderm to the extra-embryonic yolk sac after their formation. Around week 5 of embryonic development, human PGCs travel back to the embryo where they colonize the epithelial-derived sex cords within the gonadal ridges, which ultimately form the primordial gonads. Concomitant with cortical sex cords proliferation, the epithelial cells which surround the PGCs will eventually transform into somatic GCs within the ovarian follicles and ovarian TCs will derive from the mesenchyme of the genital ridge.

In humans, PGCs will undergo mitosis until around the seventh month of fetal development. At that point, they will begin meiosis and give rise to the oogonia within the ovary. PGCs are unique as they are the only cells that can initiate and undergo meiosis. The oogonia experience incomplete cytokinesis and remain linked through cellular bridges and will cluster together into nests surrounded by a single layer of pre-granulosa cells (Pepling and Spradling, 1998). It has been suggested that most of the oocytes within an individual nest will not ultimately undergo folliculogenesis but undergo atresia, so only the most competent oocytes from each nest will survive (Hernandez-Ochoa et al., 2009).

At birth, female humans will have approximately 1 million oogonia. All the oogonia will undergo arrest at the diplotene stage of meiotic prophase I (MPI), as primary oocytes, where they will persist until the onset of sexual maturity (Whitaker, 1996). The primary oocytes will remain in a quiescent state until a small cohort of primary oocytes is recruited with each reproductive cycle, due to

hormonal signals from the pituitary gland, and transform into secondary oocytes (McGee and Hsueh, 2000). Secondary oocytes will mature and gain meiotic competence to form a viable metaphase II (MII) oocyte throughout the follicular stage of the reproductive cycle. In response to the luteinizing hormone (LH) surge, the oocyte will be expelled from the follicle and ovulated into the oviduct in preparation for fertilization by a spermatozoon. The ovary will reabsorb the remaining oocytes of the cohort that do not gain competence and complete ovulation. Follicular oocyte quantity dwindles with increasing age and it is widely accepted that the supply is finite and females will stop ovulating when the stock of oocytes is depleted (Gosden et al., 1983, te Velde et al., 1998). However, there is growing evidence that germline stem cells could potentially replenish part of the ovarian oocyte pool and form new primordial follicles; this is still a topic of debate. Surface epithelial cells from tunica albuginea in human ovaries have been shown to differentiate into GCs and oocytes, which combine form new follicles (Bukovsky et al., 2004, Bukovsky, 2005).

During oogenesis mitochondria, other organelles, RNA, proteins, and energetic repositories will accumulate in the oocytes in preparation for the early stages of pre-embryonic development. Mitochondria will proliferate within the oocyte and a bottleneck appears to exist where the healthiest mitochondria with minimal mutations are preferentially selected to be passed to the next generation (Figure 1.3) (May-Panloup et al., 2016, Marlow, 2017). Estimates suggest pre-migratory PGCs have 10 mitochondria, increasing to 100 when the PGCs migrate to the gonadal ridges, and nearly 10,000 in the primordial follicle in the human

(Jansen and de Boer, 1998) with other estimates suggesting up to 250,000 mitochondria or more in the oocyte (Barritt et al., 2002, May-Panloup et al., 2005b, Reynier et al., 2001, Santos et al., 2006). It has been proposed that the bottleneck serves to maintain a uniform genome of mtDNA, termed homoplasmy, and reduce multiple mtDNA genomes, termed heteroplasmy (Cummins, 2001). Mitochondria are also found within the early flattened GCs which surround the oocyte at this early stage of development. Regions of concentrated mitochondria and other organelles, termed Balbiani bodies, are found in the cytoplasm near the nuclei of primary oocytes humans (Motta et al., 2000). Multiple metabolic pathways are present during oocyte maturation. Primordial follicles utilize both glucose and pyruvate as substrates meaning they use both glycolysis and OXPHOS to generate ATP (Shoubridge and Wai, 2007). Additionally, pyruvate is supplied to the oocyte from the breakdown of glucose by the CCs through gap junctions (Jansen and Burton, 2004).

Following a period of dormancy, which can last for several years in humans, the primary oocyte begins to grow and prepare for fertilization. The nucleus of the oocyte is termed the germinal vesicle (GV). The GCs and TCs surrounding the oocyte will transform through varying stages, beginning with a single layer of flattened squamous pre-GCs into a multilaminar antral follicle containing both GCs and TCs (Lintern-Moore and Moore, 1979). Germinal vesicle breakdown (GVBD) is a necessary first step in the resumption of meiosis by the oocytes and the process is initiated in several animal species by maturation [M-phase] promoting factor (MPF) following the LH surge (Eppig et al., 1983, Jones, 2004). It has been

postulated that within the antral follicle that the CCs, MGCs, and TCs all generate adenosine 3',5'-cyclic monophosphate (cAMP) which is shuttled into the oocyte. It has been shown that gap junctions are the gateways by which cAMP is transferred from the somatic cells to the oocyte leading to the redeployment of the catalytic subunit of adenylyl cyclase/cAMP/protein kinase A (PKA) (Webb et al., 2002). The cAMP keeps MPF in its inactive form, maintaining the oocyte in the diplotene phase of meiosis I (Dekel et al., 1981).

The causal mechanism behind the resumption of meiosis is a marked decrease of cyclic guanosine monophosphate (cGMP) in GCs following the LH surge. There is also a concomitant decrease of cGMP levels in the oocyte increasing phosphodiesterase 3A enzyme activity which promotes conversion of cAMP to adenosine 5'-monophosphate (AMP) resulting in lower cAMP levels and triggers MPF to resume meiotic development (Celik et al., 2015, Jaffe and Egbert, 2017, Mehlmann, 2005). It has been demonstrated that when oocytes from vertebrates and mammals are removed from antral follicles and cultured in control media and somatic cell conditioned media, the oocytes in the somatic cell media exhibit reduced GVBD which suggest CCs and MGCs play a role in maintaining oocytes in the arrested meiotic state (Liang et al., 2007). When an oocyte is removed from the follicle, spontaneous maturation will occur because the communication between the somatic cells and the oocyte ceases (Conti et al., 2012, Zhang et al., 2010).

1.4 Folliculogenesis

The pre-antral phase of folliculogenesis is gonadotropin independent, while the antral phased is governed by the gonadotropins of the reproductive cycle (Figure 1.4). At any point in time, the ovary contains follicles at many stages of development. The reproductive cycle begins with the follicular phase when a small cohort of primary oocytes within small (~2 mm) antral follicles resume growing in response to follicle stimulating hormone (FSH), the critical regulator of folliculogenesis, from the anterior pituitary. Follicles will grow for several months in the primordial, pre-antral, and early antral stages of folliculogenesis prior reaching the small antral stage. In addition to the oocytes, the somatic cells surrounding each primary oocyte also grow and transform in response to the hormones of the reproductive cycle. Throughout the follicular phase, the somatic cells differentiate into distinct cell types. The cells near the oocyte will become the GCs (CCs and MGCs) while those most distal from the oocytes will become internal and external TCs. Both sets of cells will support the oocyte as it matures and provide nourishment for the oocyte (McGee and Hsueh, 2000, Suh et al., 2002). The oogonia impact the development of both the GCs and the TCs. The somatic cells, in turn, also influence the nuclear and cytoplasmic maturation of oogonia (Eppig, 2001). This interaction implies that the developmental competence of the oocyte relies on the complete ultrastructure of the follicle, indicating that CCs and MGCs are ideal for assessing oocyte and embryo quality.

The various types of follicles exhibited throughout the reproductive cycle include oocyte nests, primordial follicles, primary unilaminar pre-antral follicles,

primary multi-laminar pre-antral follicles, antral follicles, and pre-ovulatory or Graafian follicles (Figure 1.4). The distinguishing property of primordial follicles is a solitary layer of flattened pre-GCs that surround dormant primary oocytes (Fortune, 2003). When primary oocytes enter the growth phase, the follicles become primary unilaminar pre-antral follicles as a single layer of pre-granulosa cells transforms into cuboidal granulosa cells (Hirshfield, 1989). Granulosa cells are unlike other somatic cell types, both phenotypically and transcriptionally.

As the follicle continues to develop, cuboidal granulosa cells proliferate into a primary multi-laminar pre-antral follicle and give rise to primary and secondary follicles. During this time, each follicle will continue to add GC layers. The somatic cells at the developing follicle's periphery, originating from mesodermal embryonic tissue and exterior to the basement membrane termed the basal lamina, will transform into TCs (Fortune, 2003). Theca cells produce androgens that diffuse across the basement membrane to GCs where they are converted into estrogen (E2).

The pre-antral follicle will contain the oocyte surrounded by multiple distinct somatic cells layers. The TCs differentiate into both internal and external stratums at the periphery of the follicle. Within the basement membrane, there are also two strata of GCs surrounding the oocytes, the MGCs and CCs. The CCs reside closest to their individual oocyte and they share gap junctions. When the oocyte is ovulated in a natural reproductive cycle or aspirated during assisted reproductive technologies (ART) the CC layer, also termed the corona radiata, will remain

associated with the oocyte. Collectively, the oocyte and the CCs that surround it are referred to as the cumulus-oocyte complex (COC).

As the follicle continues to increase in size, fluid will collect in the space between the GCs creating a fluid-filled cavity, or antrum. Oocytes isolated from smaller antral follicles have been shown to have decreased meiotic competence and are less likely to undergo final maturation (Hunter et al., 2000). The capacity for an oocyte to recommence meiosis I is referred to as meiotic competence and will occur following the LH surge. The antrum will increase in size until it becomes a pre-ovulatory or Graafian follicle, just before ovulation. The size of Graafian follicles in human ovaries between 22 to 25 mm. The LH surge will cause the follicle to rupture releasing the COC and triggering the final maturation of the oocyte from the GV stage to the MII stage in preparation for fertilization (Stocco et al., 2007). The MGCs and TCs remaining in the post-ovulatory follicle will become the CL due to luteinization. In most higher mammals, the TCs transform into small luteal cells and the GCs will become large luteal cells (Murphy, 2000). The follicular blood supply of the pre-antral follicles originates from the ovarian stromal cells. During the antral stage of development, the TCs also develop their own separate blood supply (Stouffer et al., 2001). When the oocyte ruptures from the follicle, the blood vessels that surround the follicle will bleed forming a post-ovulatory structure known as the corpus hemorrhagicum (CH). The CH will quickly transform into the CL (Niswender et al., 2000). The CL is a temporary endocrine gland that, in humans, produces both progesterone (P4) and E2. The hormones are produced for the first few months of the pregnancy, if established, and are needed until the

placenta takes over production of the hormones. If pregnancy fails to transpire, the CL will degenerate into a corpus albicans (CA) which over time will be reabsorbed into the stroma of the ovary.

Two distinct granulosa cell populations exist in the mature follicle, the MGCs and the CCs. Cumulus cells surround the oocyte during follicular maturation and ovulation and remain attached to the oocyte following oocyte retrieval during ART. Mural granulosa cells and CCs share many similarities but also have individual transcriptional patterns consistent with their specialized relationship with the oocyte (Huang and Wells, 2010) and differential responsiveness to pituitary gonadotropins (Khamsi and Roberge, 2001). Both MGCs and CCs are under the influence of oocyte secreted factors, most notably growth-differentiation factor 9 (GDF9), bone morphogenetic protein 15 (BMP15) and possibly bone morphogenetic protein 6 (BMP6*)*. These factors influence CCs and MGCs by controlling apoptotic activities as well as metabolism and steroidogenesis (Su et al., 2008). These factors regulate MGC and CC functions by activating the SMAD and/or mitogen-activated protein kinases (MAPK) intracellular cascade pathways through Transforming Growth Factor beta (TGF-β) superfamily receptors (Gilchrist et al., 2008, Liang et al., 2007). Oocyte-secreted factors influence the stem cell factor (SCF), which binds to the c-KIT receptor (CD117), causing GC proliferation, inhibiting CC apoptosis and luteinization, and modulating CC metabolism. Pyruvate metabolism doubles along with a rise in oxygen (O2) utilization in mouse pre-ovulatory oocytes compared to primary oocytes (Harris et al., 2009). Anti-Müllerian hormone (AMH), another member of the TGF-β superfamily, is produced

by growing follicles and may inhibit primordial follicle activation but the mechanism by which it acts has not been elucidated.

Three studies utilizing microarray have demonstrated that MGCs and CCs isolated from the follicles of women undergoing ART exhibit vastly diverse RNA expression patterns with thousands of genes being differentially expressed. Many of these differences were confirmed by quantitative real-time polymerase chain reaction (qRT-PCR). Koks and coworkers (Koks et al., 2010) found that the mRNAs for fibrinogen gamma chain (*FGG),* neurotensin (*NTS),* FosB proto-oncogene, AP-1 transcription factor subunit *(FOSB),* and dual specificity phosphatase 6 (*DUSP6)* showed a greater than 2-fold decrease in pooled CCs compared to pooled MGCs, while tenascin C (*TNC),* epidermal growth factor like repeats and discoidin domains 3 (EDIL3), UL16 binding protein 1 *(ULBP1),* and ryanodine receptor 2 *(RYR2)* transcripts showed more than a 2-fold increase in CCs compared to MGCs. This study did not consider differences in oocyte maturational status when pooling cells and may have confounded the data as an oocyte's maturity does affect gene expression. A study by Grondahl and colleages (Grondahl et al., 2012) analyzed paired CCs and MGCs taken from a single large pre-ovulatory follicle containing a mature oocyte from each patient thereby controlling for oocyte maturational differences and oocyte yield. When comparing CCs to MGCs, the mRNAs for growth hormone receptor (*GHR), NTS,* pepsinogen 3, group I (pepsinogen A) (*PGA3),* pepsinogen 4, group I (pepsinogen A*) (PGA4),* pepsinogen 5, group I (pepsinogen A*) (PGA5),* progesterone receptor membrane component 1*(PGRMC1),* and cytochrome P450 family 11 subfamily A member 1

(CYP11A1) were significantly increased, while mRNAs for calcium channel, voltage-dependent, L type, alpha-1C subunit *(CACNA1C),* interleukin 7 receptor (*IL7R*), growth-associated protein 43 (*GAP43*), *AMH, TNC,* and *RYR2* were significantly decreased. A third study examined MGCs and CCs samples from mature oocytes (Burnik et al., 2015b). These authors also conducted a meta-analysis with the data generated from the previous two studies (Burnik et al., 2015a, Grondahl et al., 2012) and collectively found 3156 genes differentially expressed. The later study identified two unique genes that were not previously reported in human follicular cells: prokineticin 2 (*PROK2*) and pregnancy upregulated nonubiquitous CaM kinase (*PNCK*). Further, validation of microarray results by qRT-PCR showed mRNA levels increased for angiotensin I converting enzyme 2 (*ACE2),* HtrA serine peptidase 1 *(HTRA1), PNCK,* and *RYR2,* while they decreased for *DUSP6, FGG,* interleukin 1 beta (*IL1B*), and *PROK2* when comparing CCs to MGCs. These three studies showed clear differences between the two distinct granulosa cell types however, the differential mRNA gene expression (DRGE) among the studies could be due to pooling or not pooling cells of different oocyte maturational status, different samples sizes in the number of oocytes per patient used and number of individual patients, stimulation types between studies, freezing and handling of cells, and varying infertility diagnoses. Regardless, these studies demonstrate that the different expression profiles of the MGC and CC populations should be taken into consideration when examining possible pregnancy and live birth biomarkers.

1.5 The Menstrual Cycle

The reproductive cycle is a repetitive cyclical process. During the cycle, several events will occur, including follicular growth, oocyte development, ovulation, alterations of the endometrial lining of the uterus, and maintenance of pregnancy or menstruation. This process is governed by modulations of the hormones of hypothalamic/pituitary/gonadal (HPG) axis (Figure 1.5) which include pituitary gonadotropins, follicle stimulating hormone and luteinizing hormone, and ovarian steroids, estradiol and progesterone. The hormones of the HPG axis act upon a variety of tissues in a concerted manner through an elaborate feedback system. The actions of FSH are initiated by binding to specific membrane receptors which cause the GC population to proliferate, E2 production to increase, and also promote LH/chorionic gonadotropin receptor (LHR or LHCGR) expression. The actions of LH on the TCs serve to stimulate steroidogenesis by increasing the production of androgens which are used by GCs to produce E2. LH is also responsible for ovulation of the mature oocyte and after the CL forms, LH stimulates luteal P4 production.

Both FSH and LH are heterodimeric glycoproteins. They both, along with chorionic gonadotropin (CG) and thyroid stimulating hormone share a common α-subunit while retaining their own unique β-subunits (Richards et al., 2002). Each receptor is a G-protein-coupled transmembrane receptor. When the ligands bind to their respective receptors, they generate a second messenger in the form of cAMP via the PKA pathway. The levels of cAMP are vital during folliculogenesis and oocyte maturation. FSH sustains higher cAMP levels and modulates gap

junctions by enhancing permeability and altering the gap-junction alpha-1 gene (*GJA1*) within the oocyte (Burghardt et al., 1995). It has also been demonstrated that GC signaling also involves other signaling pathways, including RAS and MAPKs (Fan et al., 2012).

In primates, the reproductive cycle is termed the menstrual cycle (Figure 1.6). The HPG axis is a finely tuned feedback loop. The menstrual cycle begins with menstruation when the levels of E2 and P4 are low. Lack of circulating E2 prompts the hypothalamus to commence pulsatile secretion of gonadotropin releasing hormone (GnRH). Gonadotropin releasing hormone acts upon the anterior pituitary to release the pituitary hormones, FSH and LH. Follicle stimulating hormone and LH are the principal drivers of female follicular and oocyte development (Richards, 1994). Follicle stimulating hormone and LH, in turn, stimulate the ovaries. As E2 increases, a negative feedback signal is received by the hypothalamus which will pause GnRH secretion until the E2 levels drop so the cycle can start again (Emanuele et al., 2002). Additionally, GCs and TCs produce inhibins, which have also been shown to inhibit FSH secretion by the pituitary (Knight and Glister, 2006).

The menstrual cycle consists of a follicular phase and a luteal phase. The number of primary follicles that mature each cycle is related to a female's age and to the number of oocytes within the ovary. Cohort growth is initiated by stimulation from the hormones produced by the pituitary gland and paracrine factors generated by the ovary (Hsueh et al., 2000). During the follicular phase, secondary follicles grow and differentiate while the oocyte matures. FSH levels are highest

on days 2-5 during the middle of the cycle. During the follicular phase, GCs have FSH receptors (FSHRs) and the TCs have LHCGRs and produce androstenedione (Hillier, 2001). *FSHR* mRNA levels are most abundant in human GCs in small antral (~6 mm) follicles in the early follicular phase and then decrease, whereas, *LHCGR* mRNA levels in human GCs increase starting during the mid-follicular phase and peak in preovulatory follicles (~15 mm) (Richards, 1994, Jeppesen et al., 2012). Granulosa cell E2 expression increases in response to androstenedione produced by the TCs, which is generated from cholesterol through the steroidogenic pathway as described below. Androstenedione disseminates from the TCs via the basal lamina to the GCs. Follicle stimulating hormone then acts, by way of a cAMP signaling pathway, to induce aromatase (CYP19A1) to convert androstenedione to E2 augmenting overall E2 production (Magoffin, 2005).

As the follicular phase progresses and GC FSHRs decrease and LHCGRs increase, GCs are now able to respond to LH. The LH surge causes the follicle to rupture, the oocyte to resume meiosis, and the CCs to radiate outward from the oocyte. It also causes luteinization of GCs and TCs which form the CL. The follicular phase culminates, and the luteal phase commences with the ovulation of the oocyte from the pre-ovulatory, or Graafian follicle, in response to the LH surge (Jeppesen et al., 2012). Near mid-cycle, the negative feedback generated by E2 switches to positive feedback causing the LH surge with E2 levels exceeded 150-200 pg/mL for 36 hrs in humans. Increased E2 levels suppress pituitary FSH secretion but promote LH secretion. However, there is also a small surge of FSH at this time, which may signal a new set of follicles to begin recruitment for the next

cycle. Luteinizing hormone is also necessary for completion of steroidogenesis as the surge stimulates the formation of the cells of the CL. Amphiregulin (*AREG*), an epidermal growth factor-like growth factor found in CCs and MGCs, is induced by the LH surge and causes expansion of the CCs and mediates oocyte maturation. Reduced *AREG* mRNA levels in CCs of oocytes have been shown to be associated with high-quality blastocysts derived from IVF (Feuerstein et al., 2007). Additionally, higher *AREG* mRNA levels in pooled human IVF derived CCs and MGCs have been shown to be associated with pregnancy (Huang and Wells, 2010).

The luteal phase is notable due to heightened P4 produced from the CL and modest E2 levels that prepare the uterine environment to be highly receptive to embryo implantation and the continuation of an ongoing pregnancy. The LH surge causes TCs to proliferate, luteinize, and secrete increased amounts of androstenedione and promotes P4 secretion from the CL. GCs transform into large luteal cells and TCs transform into small luteal cells of the CL (Devoto et al., 2009, Niswender et al., 1994). The gonadotropin surge has been shown to alter the gene expression in the CCs and MGCs in humans (Borgbo et al., 2013).

When an embryo implants initiating a pregnancy, the menstrual cycle temporarily pauses until the pregnancy is complete. In response to an embryo failing to implant, or when the pregnancy is concluding, GnRH secretion will increase as P4 levels decline. In either case, the luteal cells of the CL will regress and develop into scar tissue known as the corpus albicans.

1.6 Steroidogenesis

Granulosa cells and TCs produce androgens, estrogens, and/or progestins for use during the reproductive cycle. The collaborative relationship exhibited by the GCs and TCs is termed the two-cell, two-gonadotropin theory (Figure 1.7). The reproductive steroids are all derived from their common precursor, cholesterol. Cholesterol in the body originates from low- or high-density lipoproteins or hydrolysis of cholesterol esters. Free cholesterol arrives at the mitochondria with the aid of the cytoskeletal system within the cell (Niswender et al., 2000). Steroidogenic acute regulatory protein (StAR) shuttles cholesterol into the mitochondria (Manna et al., 2001). Cholesterol will be modified to pregnenolone by cytochrome P450 family 11 subfamily A member 1 (CYP11A1), also known as the cholesterol side-chain cleavage enzyme, irrespective of the final steroid generated. CYP11A1, ferredoxin 1 (FDX1), and ferrodoxin reductase (FDXR) are all members of the cholesterol side-chain cleavage complex (CSCC) located on matrix portion of the inner mitochondrial membrane (Hanukoglu et al., 1990, Miller, 2005). The components of the CSCC serve as an oxidation/reduction system as part of the process of steroidogenesis. FDX1 and FDXR act as acceptors for electrons from nicotinamide adenine dinucleotide phosphate hydride (NADPH) (Hanukoglu and Jefcoate, 1980). They hydrolyze the cholesterol side-chain two times cleaving the bonds of carbons 20 and 22 forming pregnenolone and isocaproic acid. Next, cytochrome P450 family 17 subfamily A member 1 (CYP17A1) transforms pregnenolone to dehydroepiandrosterone (DHEA) (Edson et al., 2009). The final step before leaving the TCs, is the conversion of DHEA to

androstenedione by hydroxy-delta-5-steroid dehydrogenase, 3 beta- and steroid delta-isomerase 1 (HSD3B1). Androstenedione passes across the basement membrane to GCs. Follicle stimulating hormone stimulates GC expression of CYP19A1 and 17-beta hydroxysteroid dehydrogenase (HSD17B) to convert androstenedione into E2. Aromatase mRNA levels in human GCs increase starting during the mid-follicular phase and peak in preovulatory follicles (~15 mm) (Jeppesen et al., 2012). DNA microarray studies in human CCs and GCs have shown that *HSD3B1*, *CYP11A1*, and *StAR* mRNA are upregulated in response to human chorionic gonadotropin (hCG) (Assou et al., 2006).

In addition to the TCs and the MGCs, the COCs coordinate metabolic processes necessary for the energy requirements of the oocyte needed for fertilization and early development (Figure 1.8). This means that mitochondrial functions within the CCs are intimately related to the overall developmental competence of the oocyte (Dumesic et al., 2016). Therefore, mitochondria within the CCs and or MGCs may be a viable indirect biomarker to assess oocyte developmental competence.

Mitochondria are abundant in the oocyte and GCs, with each mature human oocyte containing approximately 100,000-250,000 mtDNA copies. Mitochondria are small double-membrane organelles transmitted to offspring through maternal inheritance, with infrequent rare exceptions (Cummins, 2000, Song et al., 2014). While spermatozoa do possess mitochondria, once an oocyte has been fertilized and the subsequent embryo progresses through development, animal and human

studies have shown that the paternal mitochondria are not present when the embryo surpasses the 4-cell stage (Cummins, 2000, Sutovsky et al., 2000).

Mitochondria are unique because they contain their own genome. mtDNA contains 16.6 kb of circular double-stranded DNA with 37 genes encoding for 13 proteins, two ribosomal RNAs, and 22 transfer RNAs (Benkhalifa et al., 2014). The proteins and RNAs are necessary for OXPHOS and constituents of the electron transport chain (ETC) with nuclear DNA (nDNA) providing the other components needed for proper mitochondrial function.

Oxidative phosphorylation accounts for about 88% percent of a cell's ATP production with the remainder of the ATP is produced via glycolysis and the tricarboxylic acid cycle (Seyfried and Shelton, 2010). OXPHOS takes place across the inner membrane of the mitochondria and is the result of the transfer of electrons through the linked protein complexes of the ETC (Figure 1.9) which generate mitochondrial membrane potential by transporting protons across the membrane (Veatch et al., 2009). Electrons are transferred from electron donors, nicotinamide adenine dinucleotide hydride (NADH), NADPH, and flavin adenine dinucleotide hydride ($FADH_2$) to electron acceptors (i.e. O_2) during redox reactions. The flow of electrons in turn transports protons across the inner mitochondrial membrane. Both the pH gradient and the electrical potential generated through this process generate potential energy, which converts adenosine diphosphate (ADP) to ATP, as protons flow through the ATP synthase enzyme.

Cumulus cells have high glycolytic activity and provide oocytes with pyruvate via gap junctions (Collado-Fernandez et al., 2012). Oocytes exhibit

minimal glycolytic capacity due to low phosphofructokinase activity and rely upon pyruvate utilization for proper maturation (Barbehenn et al., 1974, Biggers et al., 1967). Oocytes overcome this energy deficiency due to low glycolytic activity by receiving ATP and other energy precursors including amino acids, pyruvate, nucleotides, and cholesterol from the highly glycolytic CCs through shared gap junctions (Figure 1.8) (Anderson and Albertini, 1976, Downs, 1995, Downs and Utecht, 1999, Johnson et al., 2007, Su et al., 2009). The association of the oocyte and the CCs may be beneficial for better embryo development. Human oocytes maintained within CCs in culture exhibit higher levels of ATP and improved embryo development (Van Blerkom et al., 1995).

1.7 In Vitro Fertilization

In vitro fertilization is a type of ART for humans where both the oocytes from the female and spermatozoa from the male are collected and combined in the laboratory as opposed to within the female's body. Once inseminated, the oocyte will fertilize and develop into a pre-embryo. Fertilization is confirmed with the presence of both the male and female pronuclei and two polar bodies. This first stage of development before syngamy, or fusion of the two pronuclei, is termed a pre-zygote (Braude and Rowell, 2003). The fused pronuclei will undergo pronuclear breakdown before the first cleavage division. The fertilized oocyte is called a zygote from the time immediately after syngamy until the first cell division. From that point forward through day 14, the conceptus is referred to as a pre-embryo, although many use embryo and pre-embryo interchangeably. Somewhere between 72 to 96 hrs post insemination, the pre-embryo will undergo

compaction and progress from 16 cells to the blastocyst stage. The cells of the blastocyst will differentiate into an inner cell mass (ICM), which ultimately forms the fetus and the trophectoderm, which gives rise to the placenta. When the primitive streak develops on day 14, the conceptus will be considered an embryo. From the end of the 8th-week post-ovulation until birth, the human conceptus is considered a fetus. In the context of IVF, pre-embryos will be transferred to the uterus on day 3 (at the cleavage stage) or more commonly on day 5 or day 6 (at the blastocyst stage). Untransferred supernumerary pre-embryos will be frozen for use in subsequent FET cycles. Women undergo IVF for many different types of female infertility including but not limited to age, ovulation disorders, tubal disease, uterine factors, polycystic ovarian syndrome (PCOS), endometriosis, diminished ovarian reserve (DOR), and idiopathic or unexplained infertility.

1.8 Patient Characteristics Influencing In Vitro Fertilization Biomarkers

One of the main difficulties when evaluating microarray and qRT-PCR data in CCs and MGCs for biomarkers that relate to embryo quality and other reproductive endpoints used with IVF is the heterogeneous population of patients. Among the potentially complicating factors are the large variability in patient characteristics and the multiple stimulation types used during IVF procedures. Patient characteristics influencing IVF outcome and gene expression include age, body mass index (BMI), diagnosis, stimulation type, hormonal levels during stimulation, and oocyte yield (Adriaenssens et al., 2010a). To further complicate matters, uterine receptivity also influences the interpretation of transcriptomic data such that a non-receptive uterus will cause implantation failure regardless of the

quality of the transferred embryo. This will affect the statistical sensitivity (# of true positives)/ (# of true positives + # of false negatives)) of studies. In light of this fact, for a small number of cases, ETs resulting in “not pregnant” or “no implantation” results will actually be false negatives due to poor uterine receptivity rather than embryo characteristics. This section will review studies that demonstrate how these variables can impact the transcriptional profile of granulosa cells.

In terms of heterogeneous patient populations, the mixture of multiple diagnoses and stimulation types will skew many analyses. Andrianenssens and coworkers (Adriaenssens et al., 2010a) showed that mRNA gene expression profiles are influenced by a patient’s biological characteristics, type of stimulation used for the patient’s IVF cycle, and oocyte developmental features. In this study, CCs of 63 patients were evaluated by qRT-PCR for expression of 10 genes; gene expression was then related to 13 different IVF cycle characteristics. Thirty-five patients were stimulated with gonadotropin releasing hormone agonist with high-purity-human menopausal gonadotropin (HP-hMG) and 28 patients were stimulated with GnRH-agonist with recombinant follicle stimulating hormone (rFSH). Patient characteristics, biological variables and embryo development were similar between the two treatment groups. Most of the patients had male factor infertility (MFI) with subsets having female subfertility (<10%), idiopathic subfertility (<10%), and a combination of male and female subfertility combined (<15%). These subgroupings may have influenced the outcome of the statistical analysis of the gene expression. The analyses may have been stronger if only MFI patients were used, but on the other hand statistical power would be lost by

reducing sample size. Using a linear regression model, 5 of the 10 genes examined syndecan 4 (*SDC4*), versican (*VCAN*), gremlin 1, DAN family BMP antagonist (*GREM1)*, sprouty RTK signaling antagonist 4 (*SPRY4*) and ribosomal protein S6 kinase A2 (*RPS6KA2*) showed differential expression based on the type of stimulation. Patients stimulated with rFSH showed higher *SPRY4* and lower *SDC4* mRNA levels when compared with HP-hMG stimulated patients. *VCAN* was negatively correlated with oocyte maturity in the rFSH group and *RPS6KA2* was positively correlated with increasing age in the rFSH stimulated group. *GREM1* showed a positive correlation with age and embryos having greater than seven cells and a negative correlation with serum progesterone on day of hCG administration in rFSH stimulated patients. Interestingly, *SDC4*, *GREM1*, *SPRY4*, and *RPS6KA2* are all involved in signaling TGF-β or epidermal growth factor (EGF) signaling pathways. The above study provides evidence that the type of gonadotropin treatment can affect certain signaling pathways thereby altering gene expression.

An individual patient's diagnosis may also influence differential mRNA gene DRGE in CCs and MGCs. PCOS compared to non-PCOS (Catteau-Jonard et al., 2008, Wei et al., 2012, Schmidt et al., 2014, Chen et al., 2015b) endometriosis compared to non-endometriosis (Yanaihara et al., 2005, Allegra et al., 2014, Barcelos et al., 2015), and DOR compared to normal ovarian reserve (NOR) (Greenseid et al., 2011, Jindal et al., 2012, May-Panloup et al., 2012, Meng et al., 2013) have all been shown to alter gene expression. In fact, PCOS patients with or without insulin resistance were shown to have DRGE compared to non-PCOS

normal control patients (Kaur et al., 2012). Other pathologies may also alter gene expression but have not been examined. Including any of these diagnoses in studies may also alter the actual transcriptional profiles and should be avoided if possible or analyzed separately.

The major contributing factor to reduced fecundity is advanced maternal age (AMA), even among females who do not have other infertility problems. Advanced maternal age is becoming an increasing concern as more and more women are choosing to delay starting families past the ideal reproductive age. Reproduction in human females peaks around 25 years old, exhibits a moderate decline after the age of 30 and drops steeply following 37 years of age (O'Connor et al., 1998). This decrease in reproductive potential is due to reduced oocyte quality and production of more aneuploid embryos associated with aging (Hassold and Hunt, 2001, Hassold et al., 2007, Heffner, 2004). Comprehensive chromosomal screenings from trophectoderm biopsies of 15,169 human blastocysts showed the lowest aneuploidy rates of <30% occurred between the ages of 26 and 30 years of age, rates increased above 40% for patients younger than 26 and older than 36 years old, and peaked above 80% for patients over 42 years old (Figure 1.10) (Franasiak et al., 2014). Between 70-90% of aneuploidies occur within the oocytes due to chromosomal nondisjunction at meiosis I during oogenesis (Capalbo et al., 2017, Nagaoka et al., 2012). This increase in aneuploidy is partially due to the years human oocytes spend in a prolonged arrested state in meiosis I when they may incur physiological alterations.

It has been postulated that developmental abnormalities seen in oocytes with AMA are directly related the mitochondrial dysfunction owing to increased point mutations in mtDNA (Barritt et al., 2000, Bentov and Casper, 2013) and decreased mtDNA content (Chan et al., 2005, Duran et al., 2011, Murakoshi et al., 2013). mtDNA mutations are about 25-times higher than mutations in (nDNA) because mtDNA does not have associated histones or effective DNA repair processes to repair mutations caused from reactive oxygen species (ROS) and free radicals within the mitochondrial matrix (Lynch et al., 2006). Since accumulation of abnormal mitochondria affects overall mitochondrial function, the investigation of mitochondrial metabolism may provide some insight into oocyte developmental competence and help to select the best oocyte and embryos for uterine transfer.

The overall appearance of mitochondria is altered with increased age in humans as exhibited by cristae malformation, swelling, and vacuolization (Muller-Hocker et al., 1996, Van Blerkom, 2011). In addition to altered appearance, there are functional changes in the mitochondria of aging oocytes as well. Mitochondrial membrane potential, which correlates to mitochondrial activity, is inversely related to age and reduced embryo development, which may be responsible for declining fertility with AMA (Wilding et al., 2001). This decrease in mitochondrial membrane potential corresponds to other studies where ATP production and metabolic activity decreased with advancing age (Eichenlaub-Ritter et al., 2011, Van Blerkom, 2011). Oxidative damage due to ROS accumulation has also been implicated in reducing oocyte competence (Tatone et al., 2008). It has been suggested that impaired

mitochondria, which typically begin resumption of biogenesis at the blastocyst stage (Figure 1.3), may begin replicating early to compensate for impaired function (May-Panloup et al., 2016). This premature replication may account for increased mtDNA copy numbers seen by Fragouli and colleagues in trophectoderm biopsies from blastocysts from older patients (Fragouli et al., 2015). These observations, taken together, may indicate a disruption of the follicular environment compromising oocyte and GC communication, disruption of the cell cycle, and altered meiotic spindle assembly and chromosomal segregation (Eichenlaub-Ritter et al., 2004, Schon et al., 2000). All these perturbations may contribute to decreased oocyte competence and result in reduced embryo development and account for the decline in fertility with AMA.

Patient age has been shown to be associated with DRGE in CCs and MGCs (Al-Edani et al., 2014, Kedem et al., 2014, Hurwitz et al., 2010, Liu et al., 2010, McReynolds et al., 2012) as well as oocytes (Grondahl et al., 2010). Patient BMI alters CC gene expression in both PCOS (Kenigsberg et al., 2009) and non-PCOS women (Robker et al., 2009). Therefore, studies with a large range of ages or BMIs may show DRGE profiles that would not exist if the age ranges or BMI were controlled for in the studies.

Lower mtDNA mRNA transcripts of genes associated with defending against ROS have been demonstrated to be associated with AMA in human MCGs (Tatone et al., 2006). Another group demonstrated that mRNA of sirtuin 3 (*SIRT3*), which is a mitochondrial protein associated with metabolism and which alters mitochondrial function, was lower in MGCs from women with AMA and young

women with DOR compared to younger women with NOR and lower in CCs from women with AMA compared to younger women (Pacella-Ince 2014). Additionally, a common mtDNA 4977 base pair deletion was observed at increased levels in GCs from women with AMA compared to younger women (Seifer et al., 2002). Furthermore, the 4977 base pair deletion in mtDNA was found to be higher in the CCs of non-pregnant women than pregnant women, with a higher incidence in women more than 34 years old (Tsai et al., 2010). These studies suggest that women with AMA and DOR have altered mtDNA within their follicular cells, and this may affect oocyte developmental competence and ability to establish a pregnancy.

1.9 Stimulation Protocols Influencing In Vitro Fertilization Biomarkers

The goal of IVF is to harvest as many good quality oocytes as possible from the pool of oocytes ready to begin maturation at the start of the patient's cycle in anticipation that one or more will lead to live birth. This process is accomplished using controlled ovarian stimulation protocols. The patient's HPG axis is stimulated with medications in order to produce many oocytes from multiple follicles within a single reproductive cycle, as opposed to a single dominant follicle with a single oocyte typical of unstimulated cycles. The injectable medications used are called GnRH agonists or GnRH antagonists and are used in combination with gonadotropins to stimulate follicular growth. The exact protocols used will vary between IVF clinics. These protocols suppress the endogenous LH production from the pituitary and therefore a "trigger" medication, usually hCG or recombinant luteinizing hormone (rLH), is necessary to induce ovulation.

The impact of different gonadotropin treatments on gene expression profiles of GCs has been corroborated by other groups. Grondahl and coworkers (Grondahl et al., 2009) published the first study to report DRGE profiles by microarray in MGCs with GnRH agonist protocols with either rFSH or HP-hMG. In their study, 85 genes showed DRGE of which *LHCGR* and genes involved in cholesterol and steroid synthesis had lower expression in the HP-hMG group compared to the rFSH group. This DRGE seen between the agonist HP-hMG and rFSH treatments in MGC was also demonstrated in a subsequent study (Brannian et al., 2010). Of the 1736 genes exhibiting a ≥ 2-fold expression difference 400 were related to signal transduction. This data was validated by qRT-PCR and insulin like growth factor binding protein 4 (*IGFBP4*), insulin like growth factor binding protein 5 (*IGFBP5*), and basigin (*BSG*) mRNA showed at least a 3-fold increase in mRNA levels when comparing the HP-hMG to rFSH group, whereas AKAP11: A-kinase anchoring protein 11 (*AKAP11*), hypoxia inducible factor 1 alpha subunit (*HIF1A*), and bone morphogenetic protein receptor type 2 (*BMPR2*) were decreased.

Gatta and coworkers (Gatta et al., 2013) evaluated different stimulation protocols comparing rFSH plus rLH or HP-hMG and found DRGE in CCs by stimulus type. Two main clusters of genes varied with stimulation type with 61 genes being upregulated with HP-hMG and downregulated with rFSH plus rLH, and 84 genes being upregulated with rFSH plus rLH and downregulated with HP-hMG, compared to rFSH alone. The genes identified mediated functions related to retinoic acid transport, phosphatase enzymes, DNA methylation and

transcription, and oocyte/follicle development. An additional 53 genes were upregulated in both groups compared to rFSH alone. Assou and coworkers (Assou et al., 2013) retrospectively examined individual cumulus mass transcripts by microchip and embryo development using GnRH antagonist protocols with either HP-hMG or rFSH. In the HP-hMG group 45 genes were significantly upregulated including those related to cell-cell interaction and lipid metabolism whereas 49 genes were significantly upregulated in the rFSH group including extracellular matrix assembly and tumor necrosis factor family members. No differences were observed between HP-hMG and rFSH treatments in CC mRNA levels of *LHCGR*, *BMPR2*, cytochrome P450 family 19 subfamily A member 1 (*CYP19A1*), *CYP11A1*, steroidogenic acute regulatory protein (*STARD1*), hydroxy-delta-5-steroid dehydrogenase, 3 beta- and steroid delta-isomerase 2 (*HSD3B2*), activin A receptor type 1 (*ACVR1*), activin A receptor type 1B (*ACVR1B*), inhibin beta C subunit (*INHBC*), and inhibin beta B subunit (*INHBB*) or in fibroblast growth factor (*FGF*), insulin like growth factor (*IGF*), *EGF,* and platelet derived growth factor (*PDGF*) pathways. Not only does the type of GnRH-mediated stimulation alter the gene expression of CCs and MGCs but the “trigger” medication that induces the final maturation prior to oocyte retrieval modifies gene expression as well. After GnRH-antagonist priming, hCG and GnRH agonist “triggers” exhibit differing expression patterns related to steroidogenic pathways in CCs and angiogenic pathways in the MGCs (Borgbo et al., 2013). The GnRH agonist “trigger” also showed higher *LHCGR* mRNA in CCs than the hGC “trigger”. In another study, patient groups were given 0, 5,000 or 10,000 IUs of hCG (Coskun

et al., 2013). The gene expression profiles differed between the hCG groups and the non-hCG group with approximately 2000 genes up or downregulated in each hCG group, yet only 15 genes differed significantly between the two hGC doses. The GnRH “trigger” leads to an endogenous increase in LH, whereas hCG serves to mimic the LH surge. hCG has a longer half-life and higher affinity than LH for the LHCGR (Choi and Smitz, 2014), yet LH is more potent at activating downstream signals such as cAMP accumulation, extracellular signal–regulated kinases and protein kinase B activation. Another group examined the effects of a double “trigger” to produce final oocyte maturation using a GnRH agonist at 40 hrs before oocyte retrieval and hCG 34 hrs before oocyte retrieval. They found that *AREG*, epiregulin (*EREG*), and serpin family f member (*SERPINF1*), also called pigment epithelium-derived factor (*PEDF*), mRNA levels were significantly higher while *GJA1* mRNA levels were significantly lower in MGCs in the double trigger group (Haas et al., 2019). Finally, a recent study small study examined the effects for hCG, GnRH agonist, or a double “trigger” using both medications on the CC transcriptome in a total of 30 poor, normal and high responder patients by next-generation sequencing (NGS) (Fuchs Weizman et al., 2019). The CC samples from patients with higher than average ovarian reserve tended to cluster together more closely than CC samples from the other groups. mRNA levels differed between the 3 treatment groups and the 3 trigger types, including genes related to apoptosis, cell-cycle regulation, oocyte maturation, immune response, and inflammation. These findings suggest that possible differences in activation of the LH receptor may account for trigger differences in CC gene profiles. Moreover,

these studies indicate the type of gonadotropin stimulus should be considered when interpreting biomarker data, as different stimuli yield different gene expression profiles.

1.10 Improving IVF Outcomes with Non-Invasive Biomarkers

Even with improvements in ART over the past couple of decades, the success rates for procedures treating infertility and leading to live births is still less than optimal. European data from 2011, as reported by the European IVF-Monitoring Consortium and the European Society of Human Reproduction and Embryology showed the non-donor ET rate was 33% with the pregnancy rate per embryo thaw cycle being 21% (Kupka et al., 2016). Recent national summary data from 2017, as reported by the Society for Assisted Reproductive Technology (SART) website (SART, 2019), indicate the cumulative live birth rate per oocyte retrieval including fresh and subsequent frozen transfers in the United States from IVF in patients less than 35 years old was approximately 54% and decreased with increasing maternal age. There is a need to improve outcomes of IVF, which may require improved stimulation protocols to yield better oocytes/embryos or identifying new methods for assessing the most viable oocytes/embryos. Several approaches are being investigated to find reliable and reproducible surrogate biomarkers for oocyte competence and selection of the embryos with the best probability of producing live births.

This suboptimal success rate of IVF may be due to the fact that most embryos selected for uterine transfer are chosen based on the morphological appearance of the embryos and their cleavage rates. In fact, Munne and

coworkers (Munne et al., 2007b) reported that most morphologically normal appearing embryos (based on shape, size, blastomere number, and fragmentation) may be aneuploid. In an analysis of 6000 embryos produced from oocytes of women less than 35 years of age, approximately 56% of embryos with the best morphology and development rate were actually aneuploid (Munne et al., 2007a). Furthermore, morphologically good, aneuploid embryos increased to nearly 80% for the women age 41 and older. These data indicate the need for better methodologies to reduce selection of aneuploid embryos.

In a later study, Munne and coworkers (Munne et al., 2009) suggested that the best way to select euploid embryos for uterine transfer was to use a combination of both morphological appearance and PGT-A. For PGT-A, 3-10 cells are biopsied from the trophectoderm of a day 5 or day 6 blastocyst for chromosome analysis. This approach has been validated by several groups that have demonstrated increased ongoing pregnancy, implantation, and delivery rates of nearly 20% with PGT-A screened versus non-PGT-A screened embryos (Schoolcraft et al., 2010, Yang et al., 2012, Scott et al., 2013, Forman et al., 2013).

While PGT-A has been shown to increase positive IVF outcomes in several studies, it requires invasive manipulation which might harm the embryo potentially decreasing successful outcomes. This idea is supported by a recent report which reviewed PGT-A embryo data in the United States for 2011 and 2012 and showed that utilizing PGT-A-screened embryos did not increase IVF success rates. In actuality, the success rate per uterine transfer was reduced from 46.2% to 39.3% when PGT-A was utilized (Kushnir et al., 2016). The authors of this study

concluded that PGT-A decreases the chance of live birth, and that improvements previously reported with PGT-A in women over 37 years-old are due to selection bias.

There are several non-invasive methods for embryo selection that have been used in conjunction with embryonic morphological appearance and development rate. Numerous studies have evaluated the characteristics of GCs which surround the oocyte, follicular fluid contents or the secretions of the embryos while in culture. Several non-invasive methods for embryo assessment have been reviewed elsewhere and include the study of epigenomics which consists of bisulfite sequencing to analyze DNA methylation of the GCs (Egea et al., 2014); proteomics, including electrophoresis, chromatography, and mass spectrometry of follicular fluid or oocyte culture media (Nel-Themaat and Nagy, 2011); metabolomics of spent human embryo culture media by gas chromatography, high pressure liquid chromatography, or nuclear magnetic resonance (Uyar and Seli, 2014); and time-lapse imaging of embryos (Kirkegaard et al., 2015). A recent meta-analysis examining studies using time-lapse to select embryos for uterine transfers has shown improved pregnancy and live birth rates compared to embryo scoring methods alone (Pribenszky et al., 2017).

The basis for using CCs and MGCs as biomarkers for oocyte health is the evidence that there is bi-directional signaling shared between the oocytes the somatic cells of the follicles providing the optimal environment for oocyte maturation, fertilization, and embryo development (Assou et al., 2008, Dumesic et al., 2015, Tsai et al., 2010). These somatic cells are a great source of materials

for the studies of epigenomics (Egea et al., 2014), mitochondrial function and mtDNA content (Cecchino et al., 2018), and transcriptomics (Kordus and LaVoie, 2017). Epigenomics uses bisulfite sequencing to examine DNA methylation patterns. Mitochondrial function examines both ATP production and OXPHOS. Transcriptomics uses RT-PCR or microarrays to observe differences in gene expressions patterns.

1.11 mRNA in Cumulus Cells and Mural Granulosa Cells as Non-Invasive Biomarkers in IVF

The ability of an embryo to develop appropriately and ultimately implant, grow, and result in a live birth is dependent upon the original oocyte's developmental competence. Therefore, any of the methods mentioned above that can reliably determine which oocytes are the most developmentally competent will be invaluable to help improve embryo selection before uterine transfer and increase IVF success. One of the best sources for biomarkers for non-invasive study for oocyte development competence is the GCs for the reasons described above (Feuerstein et al., 2012).

Early assessment of RNA transcripts in GCs addressed small numbers of genes and techniques utilized were less quantifiable. Such reports included semi-quantitative analyses of RT-PCR and northern blotting of a single or handful of expressed genes. The ability to analyze thousands of transcripts simultaneously was made possible with the availability gene microarrays. Furthermore, the application of qRT-PCR allowed more accurate quantification and validation of transcript changes. A single microarray can exhibit hundreds, if not thousands, of DRGE patterns. It is important to validate mRNA level changes by qRT-PCR as

microarray can produce false positive signals (Provenzano and Mocellin, 2007). Groundbreaking early microarray work, which evaluated the transcriptomes of human luteinized granulosa cells from IVF patients, showed differences in thousands of mRNA transcripts between women with NOR and DOR, however changes were not validated through qRT-PCR thereby limiting the data interpretation (Chin et al., 2002). RNA-seq is a more recent method that can replace microarrays; in this technique, RNA is converted to cDNA then undergoes deep-sequencing to identify transcripts.

An important factor to consider when evaluating DRGE in transcriptomic studies in whether or not mature and immature oocyte granulosa cells have been mixed together. Mature and immature oocyte CCs have differing mRNA expression patterns (Assou et al., 2006, Gasca et al., 2007, Kwon et al., 2010, Ouandaogo et al., 2011, Ouandaogo et al., 2012, Devjak et al., 2012, Huang et al., 2013, Grondahl et al., 2013). A more recent study using ovarian cortical tissue from patients undergoing oophorectomy before treatment for cancer showed DRGE between GCs from primordial follicles and primary follicles (Ernst et al., 2018). This knowledge may help in finding appropriate biomarkers to determine pregnancy potential as there may be visually mature oocytes that exhibit immature gene expression profiles. If the mature oocyte expression pattern can be linked to live birth, the embryos resulting from those oocytes can be preferentially selected for uterine transfer.

At this time there is no one single gene transcript that appears to be capable of predicting which embryos produced by IVF will implant and lead to a live birth.

The gene biomarker studies undertaken have varied among the chosen endpoints which include oocyte nuclear maturation, fertilization, day 2 and day 3 embryo morphologies, day 5 and day 6 blastocyst morphologies, implantation, ongoing pregnancy, and live birth. Appendices A-C summarize the findings of studies that show genes positively associated with pregnancy or live birth (Appendix A), genes that have conflicting findings between different studies (Appendix B), and genes whose data do not support an association with pregnancy or live birth (Appendix C). While the most desirable endpoint for transcriptomics studies is live birth, several studies examined the gene expression of CCs in relation to embryo development (Anderson et al., 2009, Assou et al., 2013, Cillo et al., 2007, Dhali et al., 2017, Feuerstein et al., 2007, Hammond et al., 2015, Liu et al., 2018, Hasegawa et al., 2005, McKenzie et al., 2004, Nivet et al., 2016, Scarica et al., 2019, Zhang et al., 2005). Since embryos with the best morphological appearance are usually selected for uterine transfer and have been shown to implant at a higher rate than morphologically low quality embryos (van Loendersloot et al., 2010), the gene expression profiles of these studies may serve as an indirect marker of embryo viability and be at least loosely related to live birth rates.

The first retrospective study to look at CC transcripts and pregnancy as the end point was conducted by Assou and coworkers (Assou et al., 2008). Thirty patients less than 35 years old with MFI were included in the study. The stimulation protocols were varied and included GnRH agonist or antagonist with rFSH or hMG. The data showed that there was DRGE between the pregnant and not pregnant groups. Out of the 569 upregulated genes in the pregnant group, pathway analysis

showed enrichment in genes associated with oxidative stress and nuclear factor kappa-light-chain-enhancer of activated B cells signaling. Of the 61 downregulated genes associated with pregnancy, pathways included insulin-like growth factor 1 (*IGF1*) and Sonic hedgehog signaling. Five CC masses each from pregnant patients and non-pregnant patients were used to further validate the microarray data. BCL2 like 11 (*BCL2L11*) and phosphoenolpyruvate carboxykinase 1 (*PCK1*) were downregulated while nuclear factor I B (*NFIB*) was upregulated in pregnant versus non-pregnant samples. There was no analysis performed for the mixed stimulation protocols, and thus it is difficult to determine the impact of stimulation type. The qRT-PCR analyses were only performed on 5 samples each, which does not provide much statistical power. The upregulation of nearly 600 genes in the pregnant group may indicate that the genome of CC may need to become transcriptionally activated to achieve pregnancy.

As a follow-up to their 2008 study, Assou and coworkers (Assou et al., 2010) identified 45 genes as CC biomarkers associated with pregnancy. They conducted a prospective study with patients < 36 years old undergoing IVF with ICSI. The study was split into two groups where the two day 3 embryos selected for transfer were chosen either based on the CC mRNA expression profile or embryo morphology. In the first group, 267 individual CC from 30 patients were analyzed by qRT-PCR. Ongoing pregnancy rates per retrieval were 70% in the group which used qRT-PCR versus 47% for the morphology group alone demonstrating the use of CC mRNA expression as a useful prognostic tool. The authors note a large

cohort study would be the best way to confirm this data. Unfortunately, the genes examined in this study were not specified.

A similar study was the first to look at the CC gene expression transcriptome based on single ET (Hamel et al., 2008). Forty women undergoing IVF with tubal factor, endometriosis, or idiopathic infertility were part of the study. MGCs and CCs were pooled into 2 groups for those that formed a positive pregnancy and embryos that arrested. From the hybridizations of the positive pregnancy and negative pregnancy MGC forward-subtracted PCR products were used as probes to hybridize a custom-made microarray. Following microarray analyses 18 candidate genes were validated by qRT-PCR with the pooled MGC samples. Five genes showed DRGE in the positive versus negative pregnancy groups with *CYP19A1*, cell division cycle 42 (*CDC42*), serpin family E member 2 *(SERPINE2)*, *HSD3B1* and *FDX1* showing a statistically significant increase in the positive pregnancy groups. Drawbacks of the study are that the methods did not mention what type of stimulation protocols were used, and the study included endometriosis and idiopathic infertility patients and did not take these diagnoses into account or specify the number of each patient with each diagnosis.

In a follow-up study, the MGCs of transferred embryos from 18 patients were pooled from embryos that formed an ongoing pregnancy at 6-8 weeks or embryos that failed to implant (Hamel et al., 2010b). The patient population was mixed with tubal factor, idiopathic infertility, and endometriosis and the stimulation was unspecified. Microarray analysis showed DRGE preferentially expressed for 25 genes in the pregnancy group and 19 genes in the non-pregnant group.

Validation of 10 genes was performed using qRT-PCR and showed UDP-glucose pyrophosphorylase 2 (*UGP2*) and pleckstrin homology like domain family A member 1 (*PHLDA1*) gene expression was significantly higher in the pregnant group. In addition, the same lab performed a slightly different study and performed logistical regression analysis to determine which genes would best predict pregnancy (Hamel et al., 2010a). Included in these analyses were 9 patients for intra-patient analysis with successful pregnancies versus arrested embryos, and 38 patients for interpatient analysis which included a third group with unsuccessful pregnancies. Successful pregnancies were those in which either the single transfer or one or both of two transferred embryos implanted. With two transferred embryos resulting in a singleton pregnancy, determining which embryo implanted is difficult, so the study employed principal component analysis (PCA) to predict which embryo most likely implanted. PCA is a statistical method whereby the correlated variables from the embryos known to implant were used to estimate which one of a pair of embryos implanted when two were transferred but only one implanted. Phosphoglycerate kinase 1 (*PGK1*) and regulator of G-protein signaling 2 (*RGS2*) were determined to be the best predictors of pregnancy from the intrapatient analysis and *PGK1* and *CDC42* were the best predictors of pregnancy from the interpatient analysis.

Two separate studies combined traditional embryo morphology and zona pellucida birefringence (refractive index) to examine gene expression (Assidi et al., 2011, Assidi et al., 2015). In the first study, CCs from 8 patients having the same stimulation protocol were divided into two groups base on positive or negative

pregnancy results. Day 3 post-insemination embryos for transfer were selected based on good embryo morphology and high zona pellucida birefringence. Dipeptidyl peptidase 8 (*DPP8*), H4 clustered histone 3 (*H4C3*), ubiquilin 1 (*UBQLN1*), calmodulin 1 (*CALM1*), neuropilin 1 (*NRP1*), and proteasome 26S subunit, non-ATPase 6 (*PSMD6*) mRNA levels were all shown to be related to a positive pregnancy while target of myb1 membrane trafficking protein (*TOM1*) was related to a negative pregnancy following ET. In the second study, seven patients with MFI were stimulated with GnRH agonist with hMG/FSH. The embryos were divided into CCs with high zona pellucida birefringence and positive pregnancy and CCs with low zona pellucida birefringence and negative pregnancy and compared. By microarray analysis, 48 genes were overexpressed and 27 genes were under expressed. These genes included *CALM1, NRP1, and PSMD6* as seen in the previous study. *DPP8* and *UBQLN1,* as well as the 3 genes listed previously showed DRGE by qRT-PCR between the two groups, however, no correlation was seen between oocyte competence and zona pellucida birefringence, thereby indicating DRGE is a viable option for embryo selection while refractive index may not be.

Prostaglandin-endoperoxide synthase 2 (*PTGS2*) and *VCAN* mRNA expression were shown to be significantly higher in CCs from oocytes that led to a live birth, and *GREM1* and phosphofructokinase, platelet (*PFKP*) mRNA expression was correlated with the baby's birth weight (Gebhardt et al., 2011). These results came from a retrospective study evaluating pregnancy resulting from 38 single ETs. All patients had long down-regulation protocols with rFSH.

Feuerstein et al. (Feuerstein et al., 2012) performed 96 microarray hybridizations and qRT-PCR with 197 individual CC masses from oocytes of 106 IVF patients and compared the results with embryo development and pregnancy. The samples were separated by oocyte nuclear maturation. *RGS2* was shown to be linked to pregnancy potential while pentraxin 3 (*PTX3*) showed a significant correlation with blastocyst development but only showed a positive correlation with pregnancy. Perilipin 2 (*PLIN2*) and angiogenin (*ANG*) were also associated with developmental competence. Biomarkers related to LH signaling have also been examined in relation to IVF success. Papamentzelopoulou and coworkers (Papamentzelopoulou et al., 2012b) showed that a more robust CC *LHCGR* mRNA expression was positively associated with pregnancy. Forty patients with GnRH-agonist protocols with rFSH treatment were examined. Medium to high *LHCGR* expression was exhibited in 6 out of 7 patients who became pregnant. RUNX family3K transcription factor 2 (*RUNX2*) gene expression, which is induced by the preovulatory LH surge, was examined in CCs (Papamentzelopoulou et al., 2012a). This study examined 41 ICSI patients between 24 and 45 years old being treated for MFI and each had at least one prior unsuccessful IVF cycle. All the patients were treated with a GnRH-agonist protocol. The *RUNX2* gene was detected in 12 out of 41 women. Of the 12 expressing *RUNX2* in the cumulus mass only 1 became pregnant, while 7 of the remaining 28 patients who did not express the gene did become pregnant. The presence of *RUNX2* in CCs may signify an oocyte that will likely not yield a pregnancy while the presence of *LHCGR* mRNA could

indicate embryos capable of forming a pregnancy and both could be potentially useful biomarkers for embryo selection.

Increased levels of *GDF9* and *BMP15* expression have both been associated with positive pregnancy as well as mature oocytes, fertilization rate, and embryo quality (Li et al., 2014). This study utilized one of the largest sample sizes to date, using 2426 CC masses from 196 patients with MFI, normal BMI, age 27 to 37 years old, and stimulated with a GnRH protocols. *GDF9* and *BMP15* expression was analyzed by qRT-PCR. Considering that downstream genes affected by GDF9 and BMP15 such as *PTGS2* and *GREM1* have been shown to be related to pregnancy it is not surprising that their own gene expression would serve as potential biomarkers for IVF success.

In a small retrospective study assessing the CCs from 16 individual embryos transferred in 16 IVF patients, mRNA levels of 11 out of 92 mRNA transcripts associated with the phosphoinositol 1,3-kinase/serine/threonine kinase 1 (PI3K/AKT) pathway were lower in CCs from oocytes resulting in implanted embryos (Artini et al., 2017). The researchers also looked at 4 transcripts from 4 pregnant patients and 4 non-pregnant patients by RT-PCR. Estrogen repector 1 (*ESR1*) showed lowered mRNA levels in the pregnant group while forkhead box O4 (*FOXO4*) showed higher mRNA levels. Forkhead box O1 (*FOXO1*) and forkhead box O3 (*FOXO3*) did not show a difference. Since this data only used eight patients total it is difficult to discern the accuracy of this data. To validate their array results, the investigators selected three genes out of the 11 showing DRGE and collected CCs from CD-1 mice at various time points following hCG

injection. Lower levels of AKT serine/threonine kinase 1 (*Akt1*), BCL2-like 2 (*Bcl2l2*) and SHC adaptor protein 1 (*Shc1*) mRNAs were noted from oocytes that fell within the optimal maturation window of 12-15 hrs post-hCG whereas higher levels were seen in CCs immature and post-mature oocytes. These results indicate there may be an optimal maturation window which will have a distinct expression profile that may be able to identify the most competent embryos and the genes of the PI3K/AKT pathway may play an essential role in that determination.

Another interesting study examined the role genes related to histone demethylation may have in contributing to oocytes competence. It was noted that by immunohistochemical staining that lysine demethylase 4A (*KDM4A*) was present in oocytes, GCs, and CLs and that lysine demethylase 4B (*KDM4B*) was present in oocytes, GCs, TCs, and CLs (Krieg et al., 2018). This observation prompted the investigators to determine the mRNA expression of the two genes in the GCs of IVF patients. Examining both CCs and MGCs of 84 women, it was demonstrated that *KDM4A* and *KDM4B* mRNA levels were lower in the CCs and MGCs from oocytes resulting in embryos that resulted in pregnancies. This data should be interpreted with caution as there were significant differences in age, AMH levels, E2 levels, FSH levels, numbers of oocytes retrieved, number of fertilized oocytes, and there were very diverse reasons for infertility which may confound the data. However, this study may provide early evidence that epigenetics plays a role in modifying GC gene expression in relation to oocyte developmental competence.

Another group examined 10 individual CC samples from 10 idiopathic patients and looked at the differences in 10 microarray expression profiles between oocytes that resulted in pregnancies versus no-pregnancies and live births versus no-pregnancies (Demiray et al., 2019). The authors found that in the pregnancy assessment group that the genes related to circadian entrainment exhibited the most DRGE while the genes of the apoptosis and the neurotrophin signaling showed the highest DRGE in the live birth assessment group. They also identified 20 genes presenting the highest DRGE in the two groups; however, they did not confirm any of the results by RT-PCR. Also, this data should be viewed with caution as only three patients out of ten became pregnant, and only two patients gave birth, indicating the power of this study was low.

In the most recent study to date, microarray analysis indicated that DRGE was present in 165 genes when comparing oocytes resulting in pregnancy and oocytes that did not implant (Fortin et al., 2019). The study compared gene expression of MGCs from 16 patients with each group consisting of 4 pools of 4 patients each. The microarray analyses indicated higher levels of pro-inflammatory cytokines and other inflammatory genes. They validated their microarray data with six genes by RT-PCR using material from the 32 patients used in the microarray study, and they also performed a second validation adding 12 more patient samples that were not pregnant and 53 patient samples from patients who became pregnant. In the first analysis, C-X-C motif chemokine ligand 2 (*CXCL2*) and docking protein 5 (*DOK5*) mRNA levels significantly decreased in the pregnant group. In the second analysis, *DOK5* and *NTS* mRNA levels

significantly decreased in the pregnant group. The study may indicate that overexpression of genes related to inflammation may play a role in interfering with the ability of an oocyte to lead to a viable pregnancy.

While several studies have shown DRGE between the CCs of embryos which form viable pregnancy and those that do not, several studies have also shown no significant DRGE between the groups. For example, Anderson and coworkers (Anderson et al., 2009) examined the genes hyaluronan synthase 2 (*HAS2*), brain derived neurotrophic factor (*BDNF*), *GREM1*, *PTGS2*, tumor necrosis factor alpha induced protein 6 (*TNFAIP6*) and *PTX3* and showed no correlation between the gene expression and pregnancy. Only *GREM1* showed a higher gene expression trend with pregnancy but it was not statistically significant. In two recent studies, evaluating CC and MGC gene profiles and implantation potential or fertilization, no gene differences were found to be significantly associated with these endpoints (Burnik et al., 2015a, Burnik et al., 2015c). The authors selected 3 genes from the published literature that were proposed biomarkers in CCs for pregnancy in at least 2 studies and were validated with qRT-PCR. *RGS2* and *VCAN* showed no DRGE between CCs of embryos that formed a pregnancy or did not, whereas ephrin B2 (*EFNB2*) showed a trend toward higher expression in the embryos that failed to form a pregnancy. In contrast to a previous GC study (Fujino et al., 2008), CC expression of survival factor gene baculoviral inhibitor of apoptosis repeat containing 5 (*BIRC5*) showed no correlation with pregnancy when examined in Greek women (Varras et al., 2012).

In a study examining ten aquaporin (AQP) subtypes, *LHCGR*, and *STARD1* from GCs of 111 women, no statistical differences were noted between women who were pregnant and those that were not pregnant (Lee et al., 2016). More recently a group engaged in a paired prospective study of 34 CCs from euploid sibling embryos using RNAseq and found no differences in the transcriptome of those oocytes resulting in embryos that resulted in a live birth and those that did not (Green et al., 2018). This study differed from all the other studies reviewed so far because it controlled for the uterine environment. By transferring two embryos into each patient, the CC transcripts between the two embryos could be assessed without the false-negative results due to uterine environments in other studies. Although there were no differences seen, it is important to note that the embryos transferred were most likely very similar as they had already been tested by PGT-A meaning these were blastocysts of high enough quality to undergo biopsy and were genetically normal. If the entire cohort of embryos was transferred back into a single patient over time, and many more patients were analyzed, DRGE may become apparent. Variations in those studies showing DRGE differences and those with no differences may be due to the more restrictive inclusion criteria in studies with negative findings such as exclusion of patients with particular diagnoses such as endometriosis or sample size differences.

To better identify abnormal embryos, Fragouli and coworkers (Fragouli et al., 2012) used first polar bodies to access oocyte ploidy. Differential mRNA gene expression between euploid and aneuploid oocytes was evaluated in CCs. Women (n=28) ranging in age from 23 to 46 with varied ovarian stimulation

protocols which included GnRH agonist started in the mid-luteal phase of the previous cycle with rFSH, a combination of either GnRH agonist or an antagonist with rFSH, with or without hMG participated in the study. Customized TaqMan low-density arrays (TLDAs) were utilized to evaluate CC transcriptomes and initially showed 729 potentially altered genes in CCs associated with aneuploid oocytes. SplA/ryanodine receptor domain and SOCS box containing 2 (*SPSB2*) and putative quinone oxidoreductase (*TP5313*) were significantly downregulated in CCs of aneuploid oocytes. *SPSB2* showed a positive but non-significant correlation with live birth. If oocytes that lead to aneuploid embryos could be identified using CC gene profiles it would be an asset to the embryologist. The combined use of morphological endpoints with gene expression profiles may lead to more precise prediction models.

All the previously discussed studies have examined the transcriptomes of CCs or MGCs based on the various endpoints of interest. However, none of the studies attempted to generate a predictive model for prospective embryo selection based upon the gene expression profiles until Wathlet and coworkers (Wathlet et al., 2011). This study examined 25 patients stimulated with GnRH antagonist with rFSH and compared them to 20 patients stimulated with GnRH agonist with HP-hMG. The causes of infertility were mixed with 10% idiopathic, 55% male factor only, 19% combined male and female (3% PCOS, tubal 6%, endometriosis 10%), and 16% endometriosis. Multivariable stepwise regression analysis was performed to develop several predictive models of embryo competence and pregnancy. Better day 3 embryo quality prediction models included transient

receptor potential cation channel subfamily M member 7 (*TRPM7*) and inositol-trisphosphate 3-kinase A (*ITPKA*), while pregnancy prediction models included *VCAN* and *SDC4*. The best pregnancy prediction model had a sensitivity of 74% and a specificity of 91%. It is worth noting that the strongest prediction models not only included the CC gene transcription profiles, but also included other parameters such as the number of COCs retrieved/gonadotropin dose and the number of cells in day 3 embryos.

Wathlet and coworkers (Wathlet et al., 2012) performed a follow-up study using a different set of genes. In this study, 11 genes in 99 CC masses from 33 patients were examined. The patient population was again mixed with 55% male factor only, 9% female factor (endometriosis, ovulation disorder, and myomatosis), male and female factor 12% (tubal and PCOS), and 24% idiopathic infertility. All patients were stimulated with GnRH antagonist protocols with rFSH (Gonal-f or Puregon). For all pregnancy and live birth analyzes only the transferred oocytes were considered. The best live birth prediction model with gene expression utilized calcium/calmodulin dependent protein kinase ID (*CAMK1D*), *EFNB2,* and stanniocalcin 2(*STC2*). The full predictive model for live birth contained the same genes as well as the days of stimulation. While *VCAN* was again assessed in this study its gene expression did not differ between the pregnant and non-pregnant patients. This may be due to the fact that the patient infertility diagnoses differed between the two studies with respect to the proportion of each type of infertility as PCOS and endometriosis have both been shown to alter the transcriptome as mentioned previously.

Building upon the two previous studies, a third study was conducted validating the *CAMK1D, EFNB2,* and *STC2* model and evaluating 9 additional candidate genes (Wathlet et al., 2013). Also, for the first time, an intra-patient model in relation to frozen/thawed embryos from the same patient was examined. CC from 47 patients undergoing single ET and stimulated with GnRH antagonist protocols were analyzed. Using just *CAMK1D, EFNB2,* and *STC2* in the model, an accuracy of 72% was obtained. Five of the 12 genes gave the best predictive model and included *EFNB2,* glutathione peroxidase 3 (*GPX3*), glutathione S-transferase alpha 3 (*GSTA3*), glutathione S-transferase alpha 4 (*GSTA4*), and progesterone receptor (*PGR*). The model gave a positive predictive value of 78%, a negative predictive value of 83%, and an accuracy of 81%. Adding the days of stimulation, relative serum estradiol, and age to the model increased all three model endpoints to 93%. The receiver operating characteristic (ROC) curves for the two models were 0.93 and 0.95. For intra-patient pregnancy prediction, the 5 gene predictive model was used since the patient characteristics were the same in each patient. The model was able to correctly rank the embryos in 6 of 7 patients. These three studies taken together represent, as the authors state, a "cascade" strategy for selecting candidate genes. The genes yielding the best predictive model from one set of candidate genes are kept and the ones that do not show any predictive value are discarded, then a new set of genes are tested along with the predictive set and kept or discarded in the same way in order to yield the best model.

Iager and coworkers (Iager et al., 2013) conducted a retrospective study between 3 different clinical sites to compare a pregnancy prediction model accounting for patient and clinic variation. The endpoints for this study were pregnancy and live birth. The training set revealed 1,180 differentially expressed genes which were narrowed down to 227 genes in the validation set using weighted voting analysis with a 97% prediction accuracy on the training set and 87% on the validation set. From the 227 predictive genes a custom TLDA with 196 genes was made. This array was used to further narrow the predictive gene set down to 12 genes fibroblast growth factor 12 (*FGF12*), G protein-coupled receptor 137B (*GPR137B)*, solute carrier family 2 member 9 (*SLC2A9*), AT-rich interaction domain 1B (*ARID1B*), nuclear receptor subfamily 2 group F member 6 (*NR2F6*), zinc finger protein 132 (*ZNF132*), COX20, cytochrome c oxidase assembly factor (COX20), zinc finger protein 93 (*ZNF93*), rhomboid like 2 (*RHBDL2*), DnaJ heat shock protein family (Hsp40) member C15 (*DNAJC15*), microtubule associated tumor suppressor 1 (*MTUS1*), and nucleoporin 133 (*NUP133*). This pregnancy prediction model resulted in an accuracy of 78% and a ROC curve of 0.76.

By examining the previous published literature Ekart and coworkers (Ekart et al., 2013) developed a ranking system for selection of mature oocytes that would theoretically lead to pregnancy based on CC gene transcription. In this retrospective study, they selected an 8 gene panel, *HAS2*, follicle stimulating hormone receptor (*FSHR*), solute carrier family 2 member 4 (*SLC2A4*), activated leukocyte cell adhesion molecule (*ALCAM*), secreted frizzled related protein 2

(*SFRP2*), *VCAN*, *NRP1* and *PGR* based on prior published studies (McKenzie et al., 2004, Gebhardt et al., 2011, Wathlet et al., 2011, Fragouli et al., 2012, Iager et al., 2013) to predict the mature oocytes that would lead to live birth. Based on their qRT-PCR results, it was determined that *HAS2, FSHR, VCAN,* and *PGR* would be the best genes to rank the oocytes. If embryos had been chosen based on the model from the four gene transcript levels, a single good blastocyst capable of implantation for transfer would have been selected 76% of the time. As the authors acknowledge, the method needs to be validated in a large unselected population to assess its validity on a larger scale. This implies that an embryologist could choose which oocytes to inseminate based on the gene expression of the CCs.

The difference in MGC and CC transcriptomes were analyzed to develop a statistical classification system using a support vector machine algorithm to predict live birth (Borup et al., 2016). Samples were collected from 60 women stimulated with long GnRH agonist protocols. Sixteen individual CCs and their paired MGCs which were associated with a live birth and embryo morphology-matched CCs and their paired MGCs which failed to form a pregnancy were analyzed. In total 30 genes found in CCs were predictive of live birth with an accuracy of 81%, a positive predictive value of 77%, a negative predictive value of 86%, and a ROC curve of 0.86. This model was further applied to three other data sets using blastocyst formation as the endpoint and had a prediction accuracy of 62%, 75%, and 88%, respectively. The genes included in the model were related to apoptosis and extracellular matrix formation.

In a recent study, the creation of a newer model of CC predictive genes was prospectively analyzed in IVF patients (Adriaenssens et al., 2019). Further refining the previous works of Wathlet and colleagues, the researchers used three genes in their model, *EFNB2*, *CAMK1D*, and SAM and SH3 domain containing 1 (*SASH1*). The researchers termed their model the "Corona Test". The results of the Corona Test were given to the embryologists 2 days following oocyte retrieval and before ET on day 3. Patients with 2 or more high-quality embryos on day 3 had the embryo with the highest Corona Test rank transferred. This group (n=62) was compared to 2 control groups with a matched single embryo transferred on day 3 (n=62) and day 5 (n=44) without Corona Test results. The Corona Test group had a clinical pregnancy rate of 63%, followed by day 5 at 43% and day 3 at 27%. Live birth rates were 55%, 39%, and 23% in each group, respectively. The ROC analysis had an area under the curve (AUC) of 0.8081, implying it had very good predictive accuracy. Subsequently, 26 frozen ETs were also analyzed for those patients who did not get pregnant in the fresh Corona Test group. In that analysis, the experimental group had a cumulative pregnancy rate (those who were pregnant following the fresh or subsequent frozen ETs) of 78% in the Corona Test group compared to 65% and 56% in the day 5 and day 3 controls, respectively. The time to pregnancy from the first transfer until a successful pregnancy was established was significantly reduced in the Corona Test group. Corona Test scores were discordant compared to embryo morphology in 73% of all embryos, which means that either that best-looking embryo was not the one with the highest Corona Test score or that the Corona Test score differed between

at least 2 embryos that were morphologically the same. This study demonstrates the proposed utility of using CCs as putative biomarkers to select the best embryos for transfer using non-invasive methods.

These above studies show that the use of several genes can generate predictive models with good accuracy and ROC curves. It is also apparent that the models are incomplete and need further testing. The addition of patient characteristics to the models seems to improve the specificity as well. None of these models, with the exception of the (Iager et al., 2013) study, have been validated by an outside group to confirm the accuracy of the models across different labs.

1.12 Mitochondria as Non-Invasive Biomarkers for IVF

Mitochondrial function and its relationship to human reproductive potential is poorly understood, and further research needs to be conducted regarding oocyte developmental competence and embryonic development. Studies have shown that mature human oocytes contain more mtDNA than immature oocytes and more mitochondria than other cells types in general. Mitochondria are abundant in GCs as well (Ramalho-Santos et al., 2009). What differentiates high-quality oocytes which will form high-quality embryos and lead to a live birth is not well understood, and the molecular mechanisms remain to be elucidated. One potential explanation includes deficient mitochondrial function (Bentov et al., 2011).

Embryos require large amounts of energy throughout the cleavage divisions that occur during early embryogenesis; therefore, embryo viability may be related to energy production via the mitochondria (May-Panloup et al., 2005a, Reynier et

al., 2001, Zhao et al., 2010). Van Blerkom and associates demonstrated increased ATP content in unfertilized oocytes was more likely to be associated with embryos that displayed good development in the same cohort (Van Blerkom et al., 1995). Mitochondrial content amplifies significantly within the oocyte during oogenesis until ovulation (Figure 1.3). As the embryo undergoes cell division, each cell, also called blastomere, should receive half of the amount of the mitochondria from that starting pool. This means the number of mitochondria per blastomere decreases as the amount of energy required by the embryo increases. This inverse relationship indicates oocytes with higher ATP production, and by association higher mitochondrial content or better metabolism, will be more likely to develop appropriately to the blastocyst stage when the mtDNA starts to replicate again (May-Panloup et al., 2016, Chappel, 2013). This observation shows that mtDNA copy number may be a good surrogate biomarker for embryo development (de Los Santos et al., 2018, Diez-Juan et al., 2015, Fragouli et al., 2017, Fragouli et al., 2015, Ravichandran et al., 2017). However, mtDNA copy number alone does not account for how efficiently the mitochondria function.

Early mitochondrial studies in IVF examined mtDNA content in oocytes. The average mtDNA content between individual oocytes varies in humans even within the same patient (Reynier et al., 2001). However, it appears there are some consistent observations, including lower mtDNA levels associated with oocytes that fail to fertilize, AMA, and aneuploidy. Studies have demonstrated higher mean mtDNA levels in fertilized human oocytes compared to both unfertilized oocytes and degenerated oocytes (Reynier et al., 2001, Santos et al., 2006), although large

variations were seen between individual oocytes and no threshold had been established. Higher mtDNA levels were again seen in unfertilized oocytes and embryos that failed to cleave in patients older than 40 years old (Murakoshi et al., 2013).

Recent mitochondrial research in IVF has focused mtDNA content in trophectoderm cells related to blastocyst development. In an elegant study by Fragouli and colleagues, 379 trophectoderm biopsies from blastocysts were examined by array comparative genomic hybridization (aCGH), RT-PCR, and NGS (Fragouli et al., 2015). Euploid blastocysts compared to aneuploid blastocysts, embryos from younger women compared to older women, and blastocysts that implanted compared to blastocysts that did not implant all exhibited lower mtDNA levels in trophectoderm cells. Additionally, the researchers established a predictive threshold value and found that 30% of the euploid embryos that did not implant were above the threshold value. Blastocysts which failed to implant, having higher mtDNA levels in trophectoderm cells, were corroborated in a separate study (Diez-Juan et al., 2015). In another retrospective study examining 1641 trophectoderm biopsies from 402 patients, mtDNA levels in the trophectoderm biopsies were higher in aneuploid embryos, embryos from patients with higher BMIs, lower P4 levels, and poor grade trophectoderm (de Los Santos et al., 2018). In another blinded retrospective study 282 euploid blastocysts were transferred (Ravichandran et al., 2017). A total of 185 embryos with lower relative mtDNA levels in trophectoderm cells resulted in pregnancies while 0 out of 33 embryos with elevated mtDNA above the predicted threshold value failed to implant. This

100% negative predictive value may indicate that mtDNA copy number in trophectoderm cells may be a possible method to improve the odds of selecting the most viable embryos. Finally, in a prospective blinded non-selection study, 199 euploid blastocysts were transferred, and mtDNA levels in trophectoderm cells were analyzed. This study also showed a 100% negative predictive value with the nine embryos with mtDNA content above the threshold level failing to produce a pregnancy (Fragouli et al., 2017).

Other groups have refuted these observations. Victor and associates postulate the data of the above studies may be biased due to a lack of mathematical corrections necessary to appropriately determine mtDNA copy number in trophectoderm cells (Victor et al., 2017). When they retrospectively analyzed 1396 trophectoderm biopsies, they found no difference in mtDNA trophectoderm copy numbers based on age, ploidy status, or implantation. Another retrospective study where PGT-A tested blastocysts were transferred in pairs, showed no predictive value of mtDNA trophectoderm copy number indicating the need for further analysis before being applied to make clinical decisions about which embryos to transfer (Treff et al., 2017). In a retrospective study of 1510 trophectoderm biopsies from patients between 31 and 38 years old, poor quality embryos exhibited higher mtDNA trophectoderm content overall, but when reanalyzed only assessing euploid embryos, this predictive trend was abolished. Additionally, mtDNA trophectoderm levels did not show differences in terms of pregnancy or implantation (Klimczak et al., 2018). Most recently, a prospective study of 109 trophectoderm biopsies from 100 IVF patients showed no differences

in mtDNA levels between embryos that implanted and those that did not (Victor et al., 2019).

It has been hypothesized that the mtDNA pool in CCs and MGCs are responsible for proper oocyte maturation and that the mtDNA originating in oocytes supports the early embryonic cleavage divisions making both key players in ultimate embryo viability. Evidence for this hypothesis has been shown with correlations between oocyte and CC mtDNA content in IVF patients (Boucret et al., 2015). Additionally, the presence of the mtDNA 4977 base pair deletion in human CCs is associated with lower pregnancy rate (Tsai et al., 2010).

While lower mtDNA copy numbers were associated with better blastocyst development and implantation as described above, in three separate studies, increased mtDNA copy numbers in CCs have been shown to be associated with embryos that developed into high- versus low-quality embryos and embryos more likely to implant than those that did not implant. Ogino and colleagues first proposed using mtDNA in CCs as a biomarker and were also the first to demonstrate increased mtDNA copy number in CCs using RT-PCR to determine copy number in humans. In this prospective study, 60 individual COCs were collected from women undergoing IVF. They used a mtDNA copy number threshold value of 86 to distinguish between good- and poor-quality embryos with a positive predictive value of 84.4 and a negative predictive value of 82.1. The mean values of good- and poor-quality embryos were 140 (25–75% quartile, 97–264) and 57 (25–75% quartile, 34–74), respectively. In this study, there was no difference in good and poor embryo development based on maternal age (Ogino

et al., 2016). A larger study examined the mtDNA content in CCs by RT-PCR from 452 COCs from 62 patients undergoing IVF (Desquiret-Dumas et al., 2017). Increased mtDNA copy number in CCs was associated with good- and poor-quality embryos although there was a much larger interquartile range 738 (25-75% quartile, 250–1228) and 342 (25-75%, quartile, 159–818) between this study and the first study. Additionally, the patient's with lower BMIs and those that were smokers had higher CC mtDNA copy numbers. The third study from the same group as the previous study, focused on mtDNA copy number in CCs relating to implantation and ongoing pregnancy. 84 COCs were analyzed with RT-PCR from 71 patients undergoing IVF. Those embryos that implanted showed a significantly higher mtDNA copy number in CCs than those that did not implant, independently of other patient variables with means of 215 [sd 375] and 59 [sd 72], respectively (Taugourdeau et al., 2019). Interestingly, while increased mtDNA copy numbers in CCs have been associated with better embryo development and implantation the inverse was seen in trophectoderm cells. It has been postulated that increased mitochondria within a blastocyst may serve to compensate for reduced mitochondrial energy dysfunction due to metabolic stress from ROS and free radicals (Diez-Juan et al., 2015, Fragouli et al., 2015, Grindler and Moley, 2013, May-Panloup et al., 2016).

1.13 Specific Aims

Infertility affected approximately 1 in 7 couples from 2015-2017 in the United States, according to the Centers for Disease Control National Survey of Family Growth (CDC, 2019). Many of these couples turn to IVF to treat this disease. It

has been estimated that less than 10% of all oocytes harvested during an IVF cycle will produce a live a birth (Lemmen et al., 2016) and the odds of taking home a child in the United States following IVF is only 30% per oocyte retrieval based on data tracked by the SART (SART, 2019). Additionally, as a woman ages the probability of taking home a baby from IVF drastically decreases. These statistics indicate that current approaches of selecting embryos for uterine transfer are insufficient, and newer methods for embryo selection are required. Since IVF procedures have high costs, there is a critical need to identify the embryos with the highest potential of leading to implantation and live birth as quickly as possible to reduce IVF costs and offset the effects of advancing age with subsequent procedures.

Our long-term goal is to create a panel of biomarkers that can help embryologists quickly and easily select an embryo from a patient's cohort of embryos that has the best chance of implanting, leading to live birth, and improving patients' odds of success using IVF the first time. We hypothesize that this can be accomplished using the cells which surround the oocytes during follicular maturation. Cumulus cells and mural granulosa cells collectively comprise the granulosa cell pool. Granulosa cells are by-products harvested during the oocyte retrieval in assisted reproduction procedures, and they closely reflect the oocyte's maturational status and developmental potential (Dumesic et al., 2015).

Our objectives are to determine a set of non-invasive biomarkers in GCs which identify the oocytes that will result in a live birth within a patient's cohort of

oocytes. In Aim 1, we will analyze several carefully selected mRNA biomarkers in individual CC masses to determine if a single or panel of biomarkers can be used to predict euploid embryos that will have the best odds of resulting in a live birth. In Aim 2, we will examine the mitochondrial metabolic substrate utilization in pooled granulosa cells and compare between patients based on age, serum AMH levels, BMI, and number of mature oocytes retrieved per cohort, and embryo cohort development. We will also examine selected mRNA biomarkers of interest from Aim 1 and compare them within the same Aim 2 groups.

AIM1: To test the hypothesis that out of the group of selected cumulus cell mRNA biomarkers there will be one or a panel that will allow selection of the embryo with the highest odds of implanting and leading to live birth. Levels of 19 mRNA biomarkers will be assessed via qRT-PCR and related to the development of their corresponding individually cultured oocytes and subsequent embryos, embryo ploidy status, and live birth outcomes.

AIM2: (A) To determine if mitochondrial function differs between patients based on age, serum AMH levels, BMI, number of mature oocytes, and embryo cohort development and (B) to determine of individual substrates can be used as mitochondrial biomarkers for IVF. The rates of mitochondrial metabolic substrate utilization by mitochondria in pooled CCs and MGCs will be assessed and related to patient demographics including age, serum AMH level, BMI, percent of mature oocytes, fertilization rate, day 3 embryo development, blastocyst development, mitochondrial content, and mRNA levels of selected genes.

Successful identification of non-invasive biomarkers to select the most competent oocytes will revolutionize the field of IVF. Once a panel is created that faithfully identifies the oocytes with the best chance of success, an embryologist would select the embryos with the best probability of resulting in live birth from the cohort of embryos created. This procedure would reduce the number of procedures needed to have a viable pregnancy resulting in a live birth, increasing the overall success IVF and reduce cost to the patient. In theory, an embryologist may only need to inseminate a small number of oocytes from the cohort rather than all of them. This change in procedure would prevent creation of excess embryos and the moral dilemma of what to do with any extra unused embryos.

1.14 Innovation

Few studies have examined the link between CC mRNA levels and oocyte/embryo ploidy status (Fragouli et al., 2010, Fragouli et al., 2012, Parks et al., 2016, Green et al., 2018). Our study will employ a focused set of CC mRNA biomarkers related to CC expansion and oocyte maturation, steroidogenesis, and hormone modulation and signaling to determine if specific mRNA levels correlate with oocyte maturity, abnormal embryo development, embryo ploidy status, and live birth outcomes. Using data collected, we will create a model of specific CC mRNA biomarker levels to identify a mature oocyte's ability to produce euploid embryos with best live birth potential.

Most studies of GC, oocyte, and embryo mitochondria have exclusively evaluated mitochondrial copy numbers. These proposed studies will evaluate GC mitochondrial activity in a novel way. This will be the first examination of a

new mitochondrial function assay that has not previously been used to assess mitochondrial substrates in GCs. It measures the rate of electron flow through the electron transport chain from varying metabolic substrates that produce NADH or $FADH_2$. The goal will be to see how substrate utilization differs between various patient groups. Additionally, we will examine fertilization rates, day three embryo development, blastocyst development, and mRNA levels of selected genes between the groups to see if one or more substrates can be used for future individual CC biomarker screening purposes and improve IVF outcomes.

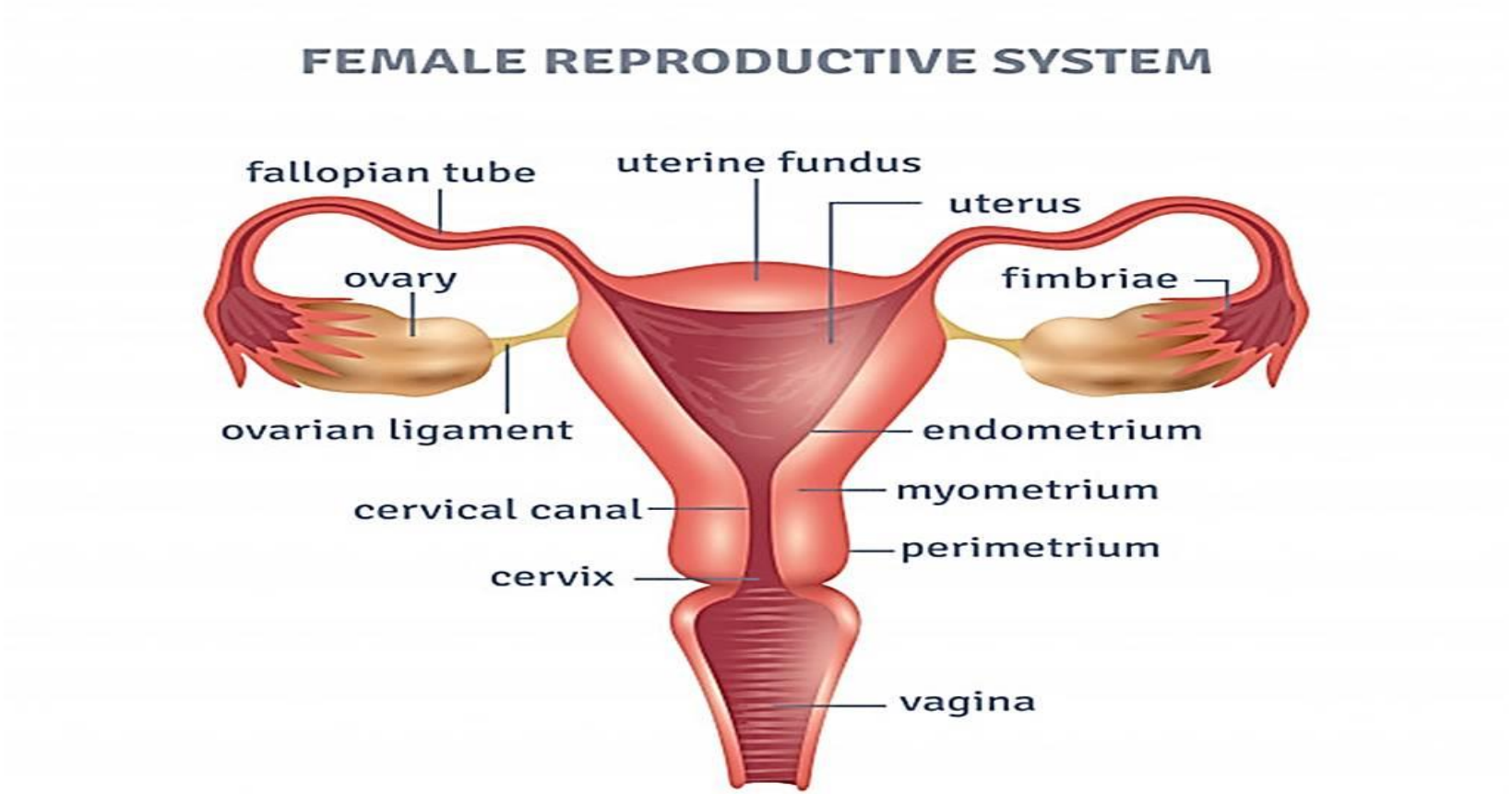

Figure 1.1. Midsagittal section of the female reproductive tract. Uterus-poster 3791876: freepik.com. This cover has been designed using resources form Freepik.com.

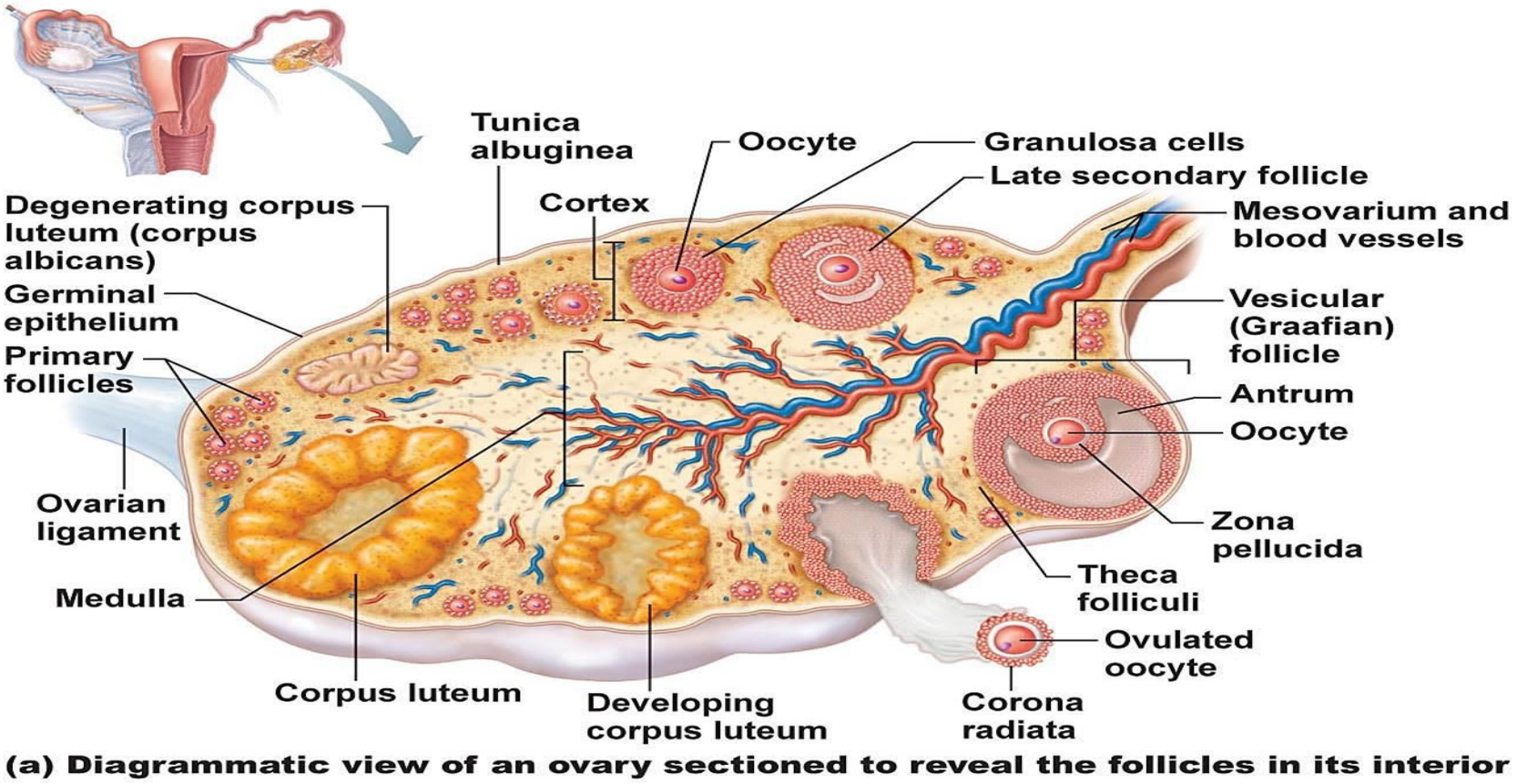

Figure 1.2. The ovary exhibiting different stages of follicular development. A random cross-sectional view as seen here would exhibit follicles and corpora lutea at various stages from development from primordial follicles through corpus albicans. Typically Graafian follicles, developing corpus luteum, and corpus luteym are not present in the ovary concurrently but rather in succession (Marieb, 2016). Reprinted by permission of Pearson Education, Inc., New York, New York.

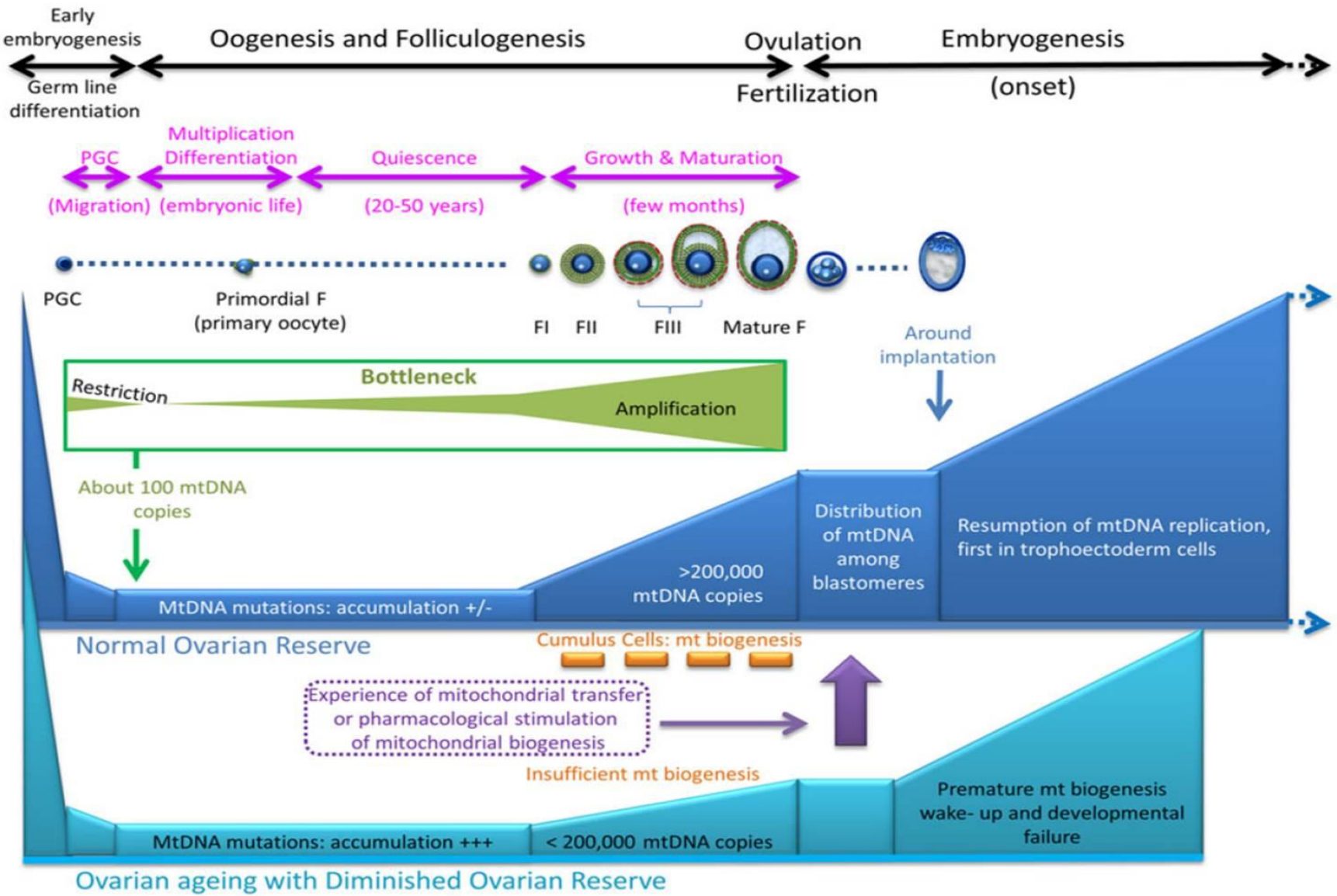
Early embryogenesis
Germ line differentiation
Oogenesis and Folliculogenesis
Ovulation
Fertilization
Embryogenesis
(onset)
PGC
(Migration)
Multiplication Differentiation
(embryonic life)
Quiescence
(20-50 years)
Growth & Maturation
(few months)
PGC
Primordial F
(primary oocyte)
FI
FII
FIII
Mature F
Around implantation
Bottleneck
Restriction
Amplification
About 100 mtDNA copies
MtDNA mutations: accumulation +/-
>200,000 mtDNA copies
Distribution of mtDNA among blastomeres
Resumption of mtDNA replication, first in trophoectoderm cells
Normal Ovarian Reserve
Cumulus Cells: mt biogenesis
Experience of mitochondrial transfer or pharmacological stimulation of mitochondrial biogenesis
Insufficient mt biogenesis
MtDNA mutations: accumulation +++
< 200,000 mtDNA copies
Premature mt biogenesis wake- up and developmental failure
Ovarian ageing with Diminished Ovarian Reserve

Figure 1.3. Mitochondrial biogenesis during oogenesis, folliculogenesis (F = Follicle, I primary, II pre-antral, III antral) and early embryonic development in humans. During early maternal embryogenesis, the mtDNA content of each embryonic cell undergoes a drastic reduction. This is followed, during oogenesis, by a restriction and amplification of mtDNA content leading to a refreshed and purified mtDNA pool as illustrated in the bottleneck (green), quantitatively sufficient for allocation among the embryonic blastomeres. The close relationship between the oocyte and the surrounding cumulus cells appears to be important for the constitution of the oocyte mitochondrial pool (orange). Modified from (May-Panloup et al., 2016). Reprinted with permission.

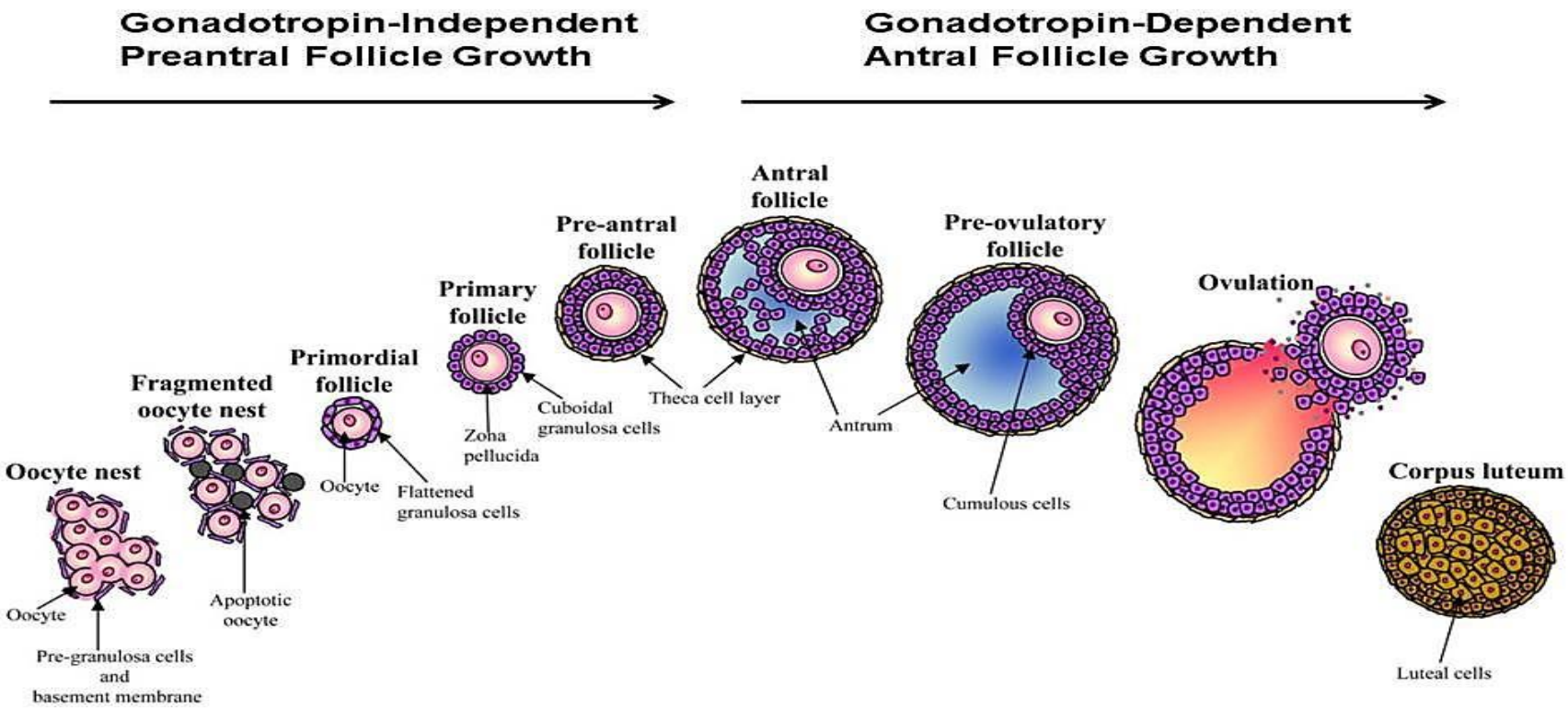

Figure 1.4. Follicular development. The diagram summarizes the process of ovarian follicle development and growth, from oocyte nests present in the fetal ovary through follicle growth, ovulation and corpus luteum formation during adulthood. Modified from (Hernandez-Ochoa et al., 2009). Reprinted with permission.

Hypothalamus
GnRH
Pituitary
LH
FSH
Ovaries
Progesterone
Estrogen

Figure 1.5. The female hypothalamic–pituitary–gonadal axis. The hypothalamus produces and secretes gonadotropin releasing hormone (GnRH) into a system of blood vessels that link the hypothalamus and the pituitary gland. GnRH stimulates the pituitary gland by attaching to specific molecules (i.e., receptors). After the coupling of GnRH with these receptors, a cascade of biochemical events causes the pituitary gland to produce and secrete two hormones, luteinizing hormone (LH) and follicle–stimulating hormone (FSH). LH and FSH are two of a class of hormones commonly known as gonadotropins. They are secreted into the general circulation and attach to receptors on the ovary, where they trigger ovulation and stimulate ovarian production of the hormones estrogen and progesterone. These female hormones cause monthly menstrual cycling and have multiple effects throughout the body. In particular, estrogen has profound effects on the skeletal system and is crucial to maintaining normal bone health. Modified from (Emanuele et al., 2002).

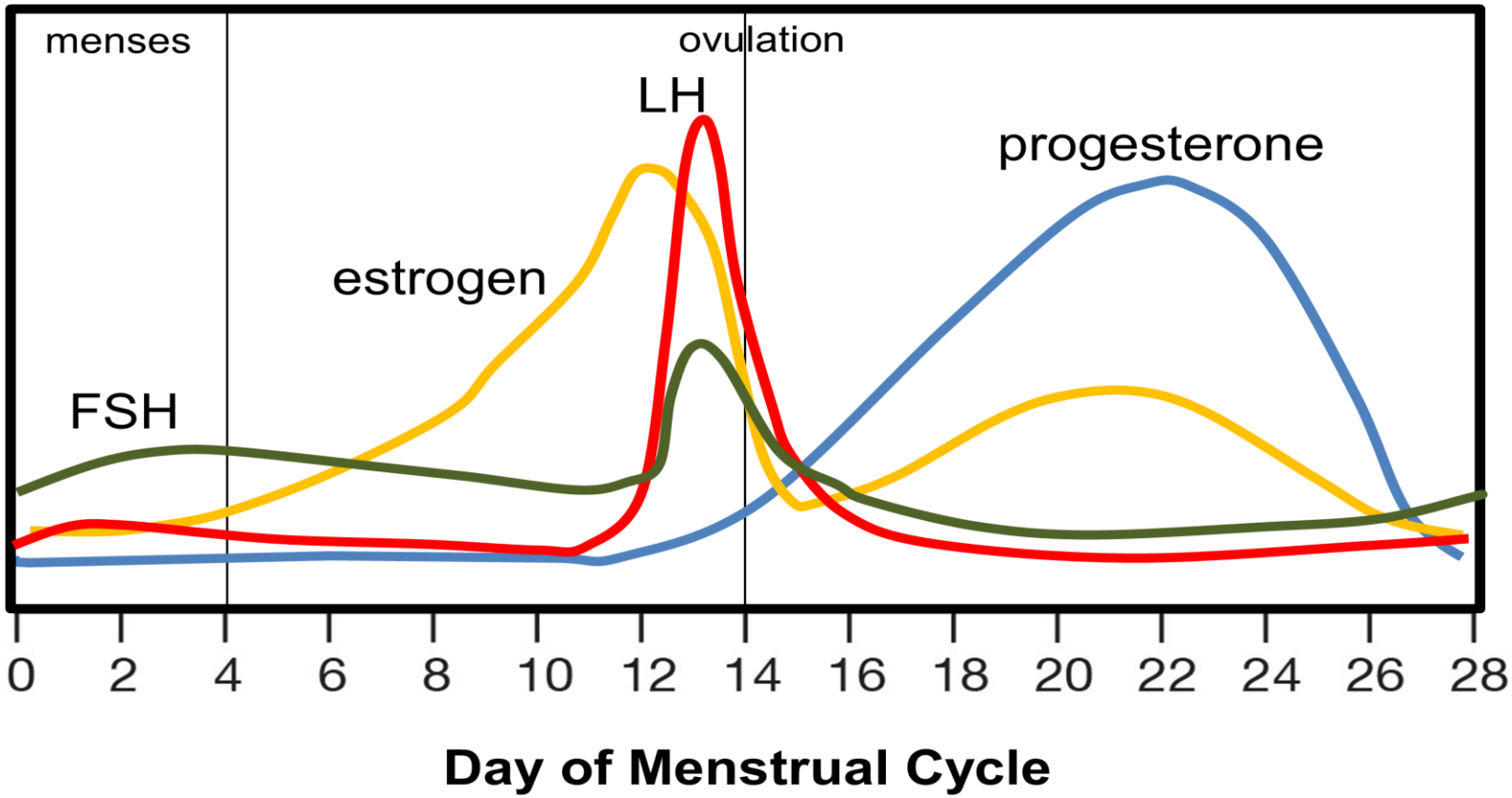
menses
ovulation
LH
progesterone
estrogen
FSH
0
2
4
6
8
10
12
14
16
18
20
22
24
26
28
Day of Menstrual Cycle

Figure 1.6. The human menstrual cycle. A typical human menstrual cycle lasts 28 days, with ovulation occurring at midpoint, at day 14. The first day of vaginal bleeding is day 1. The first phase of the cycle is the follicular phase, during which progesterone levels are very low, and estrogen levels start low and slowly increase. At approximately day 12, estrogen levels peak, causing increased secretion of pituitary LH and FSH, with levels peaking on day 13-14. The LH surge results in ovulation, and a transient drop in estrogen, and a new increase in progesterone levels. During the post-ovulation period, called the luteal phase, estrogen and progesterone levels first rise, then fall back to very low levels, at which point the next menses starts. The progesterone scale is 1000-fold higher than the estrogen scale. Modified from (Emanuele et al., 2002).

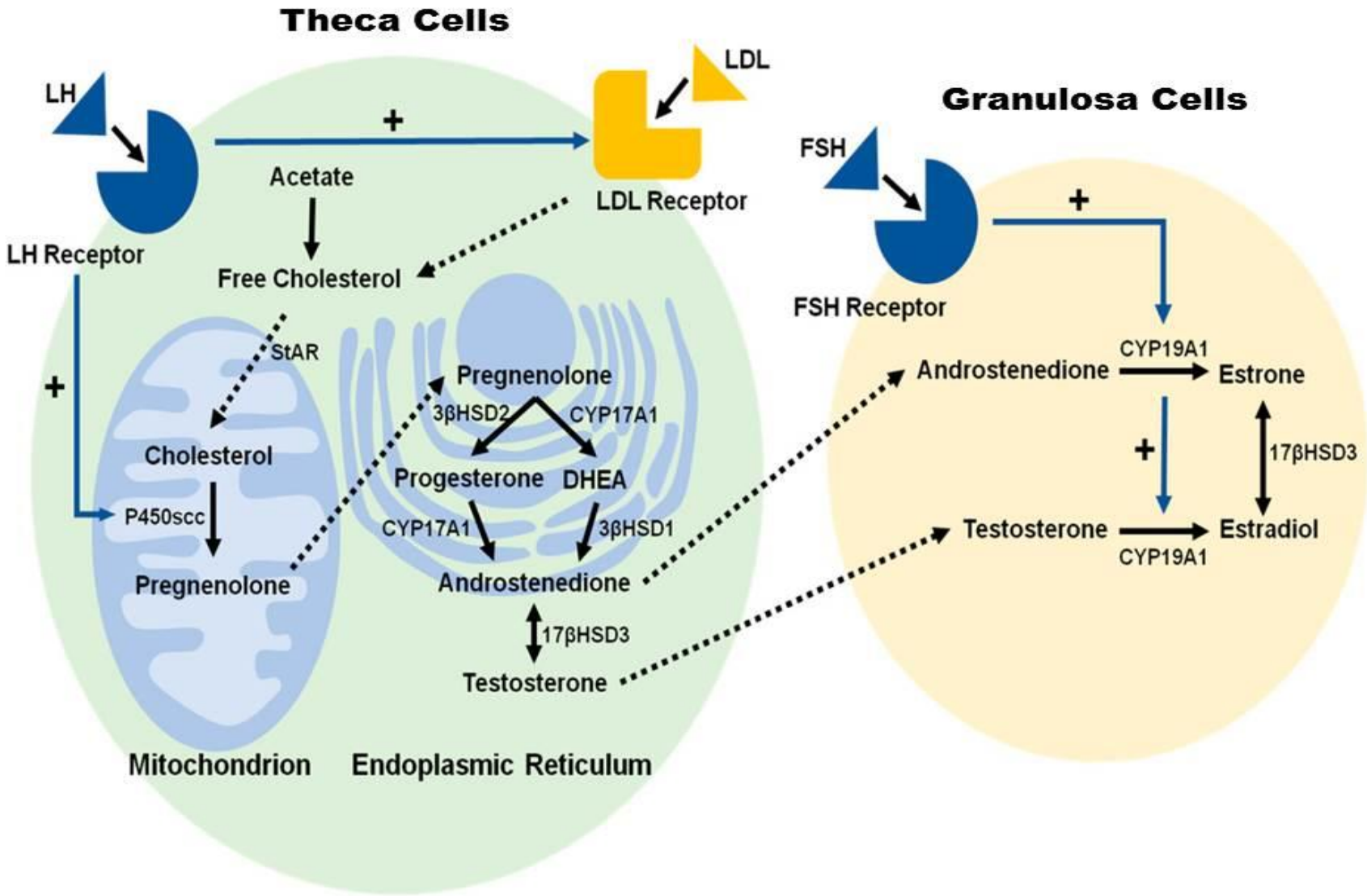
Theca Cells
LH
LDL
+
Acetate
LDL Receptor
LH Receptor
Free Cholesterol
StAR
+
Pregnenolone
3βHSD2
CYP17A1
Cholesterol
Progesterone
DHEA
P450scc
CYP17A1
3βHSD1
Pregnenolone
Androstenedione
17βHSD3
Testosterone
Mitochondrion
Endoplasmic Reticulum
Granulosa Cells
FSH
+
FSH Receptor
CYP19A1
Androstenedione
Estrone
+
17βHSD3
Testosterone
Estradiol
CYP19A1

Figure 1.7. The two-cell, two-gonadotropin theory of follicular conversion of cholesterol to steroid hormones. Free cholesterol is deposited into theca cells by low-density lipoprotein (LDL) receptor-mediated LDL endocytosis. The conversion of cholesterol to pregnenolone by CYP11A1 in the inner membrane of the mitochondria is initiated by the binding of luteinizing hormone (LH) to the luteinizing hormone receptor (LHR). Pregnenolone is converted to dehydroepiandrosterone (DHEA) by CYP17A1 in the endoplasmic reticulum (ER). DHEA is converted to androstenedione by HSD3B1. Androstenedione diffuses across the basement membrane to the granulosa cells (GCs). Finally, androstenedione is converted to estradiol (E_2) by aromatase (CYP19A1) which is initiated by the binding of follicle-stimulating hormone (FSH) to the follicle-stimulating hormone receptor (FSHR). (Black solid line arrows: synthesis step; blue solid line arrow with + symbol: activation; dotted line arrows: transfer step). Modified from (Hebert-Schuster et al., 2018). Reprinted with permission.

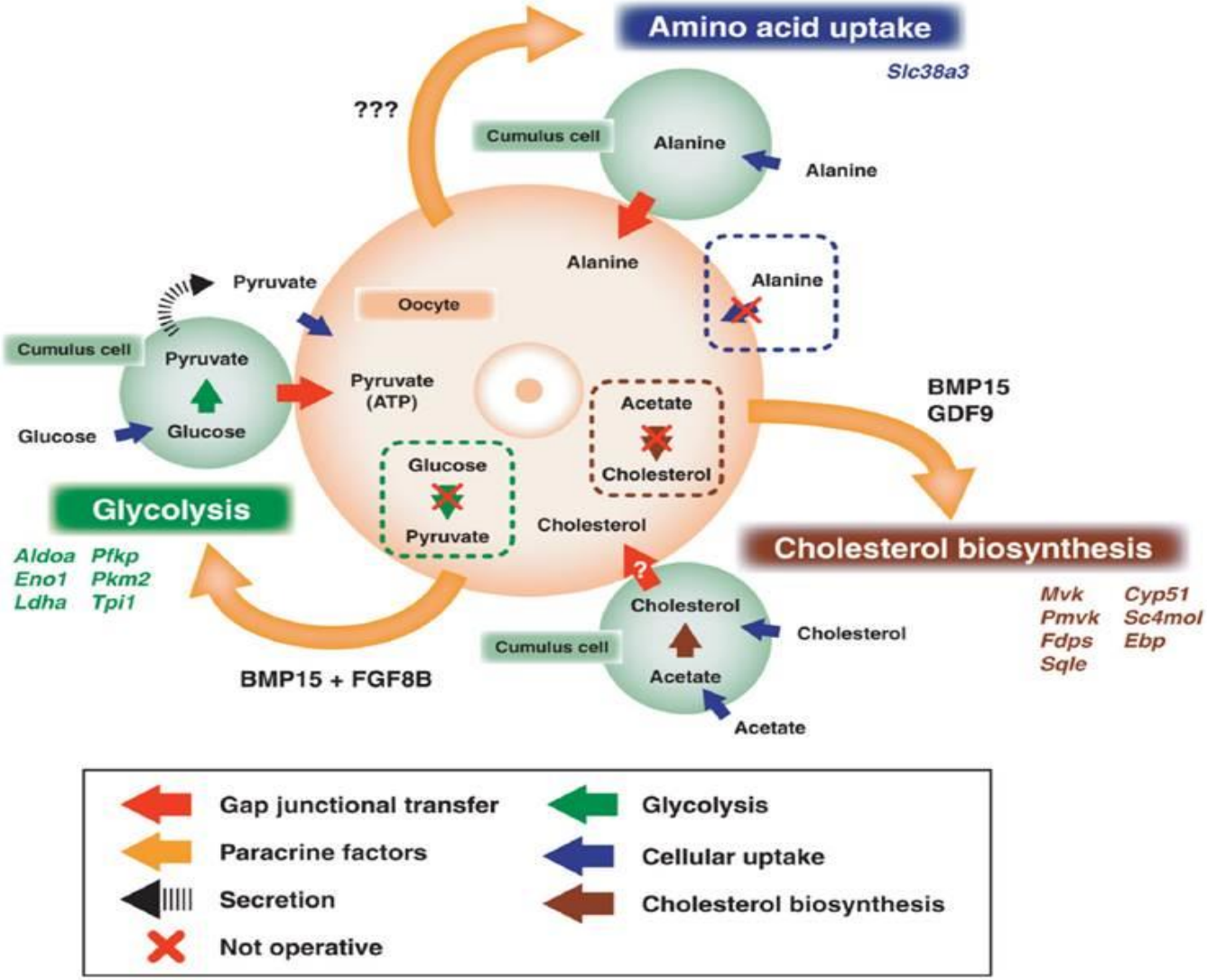
Amino acid uptake
Slc38a3
???
Cumulus cell
Alanine
Alanine
Alanine
Alanine
Oocyte
Pyruvate
Cumulus cell
Pyruvate
Glucose
Glucose
Pyruvate
(ATP)
Acetate
Cholesterol
BMP15
GDF9
Glucose
Pyruvate
Cholesterol
Glycolysis
Aldoa Pfkp
Eno1 Pkm2
Ldha Tpi1
Cholesterol biosynthesis
Mvk Cyp51
Pmvk Sc4mol
Fdps Ebp
Sqle
?
Cholesterol
Cholesterol
Cumulus cell
Acetate
Acetate
BMP15 + FGF8B
Gap junctional transfer
Paracrine factors
Secretion
Not operative
Glycolysis
Cellular uptake
Cholesterol biosynthesis

Figure 1.8. Metabolic cooperativity between oocytes and cumulus cells, and the role of oocyte-derived paracrine factors in promoting metabolism in cumulus cells. Oocytes are deficient in metabolizing glucose by glycolysis, synthesizing cholesterol from acetate and taking up alanine directly, as compared with cumulus cells. Oocytes obtain products of the glycolysis (e.g., pyruvate) and cholesterol biosynthesis (e.g., cholesterol) pathway, as well as alanine from cumulus cells. Oocytes, via secreting paracrine factors, promote these metabolic processes in cumulus cells by promoting the expression of transcripts encoding key enzymes in the corresponding pathways, as well as the expression Slc38a3 encoding an amino acid transporter for L-alanine. GDF9 and BMP15 are involved in promoting cholesterol biosynthesis in cumulus cells, while cooperation between BMP15 and FGFs are required for promoting glycolysis. Which oocyte-derived paracrine factor(s) participate in the induction of Slc38a3 expression, as well as L-alanine uptake by cumulus cells are unknown. (Su et al., 2009). Reprinted with permission.

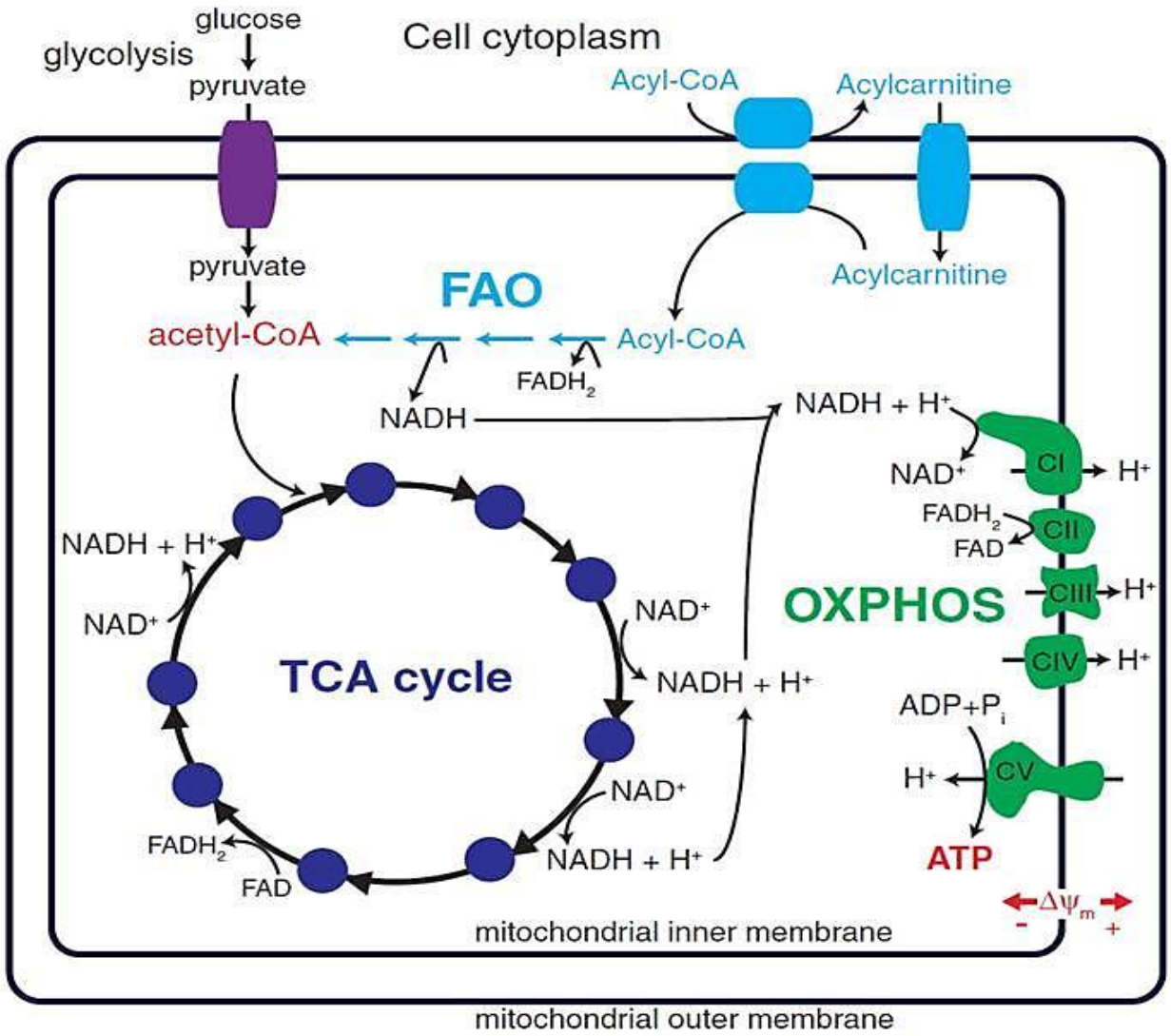
glucose
glycolysis
pyruvate
Cell cytoplasm
Acyl-CoA
Acylcarnitine
pyruvate
FAO
acetyl-CoA
Acyl-CoA
FADH2
NADH
NADH + H+
NAD+
CI
H+
FADH2
FAD
CII
CIII
H+
OXPHOS
CIV
H+
NADH + H+
NAD+
TCA cycle
NAD+
NADH + H+
ADP+Pi
H+
CV
NAD+
NADH + H+
FADH2
FAD
ATP
ΔΨm
-
+
mitochondrial inner membrane
mitochondrial outer membrane

Figure 1.9. Mitochondrial metabolism. Glucose breakdown through glycolysis and the tricarboxylic acid cycle (dark blue) generates reduced NADH and $FADH_2$. Fatty acid β-oxidation (FAO, light blue) of fatty acyl-CoA esters is performed in four enzymatic reactions that also generate NADH and $FADH_2$, as well as acetyl-CoA. Electrons derived from NADH and $FADH_2$ are utilized by the five OXPHOS complexes (green) to generate ATP. Complex I (CI, NADH: ubiquinone oxidoreductase), complex III (CIII, ubiquinol: ferricytochrome *c* oxidoreductase) and complex IV (CIV, cytochrome *c* oxidase) pump electrons out of the mitochondrial matrix to generate a membrane potential ($\Delta\psi_m$) that drives the synthesis of ATP by complex V (CV, F_oF_1-ATP synthetase). CII, complex II (succinate: ubiquinone oxidoreductase). (Nsiah-Sefaa and McKenzie, 2016). Reprinted with permission.

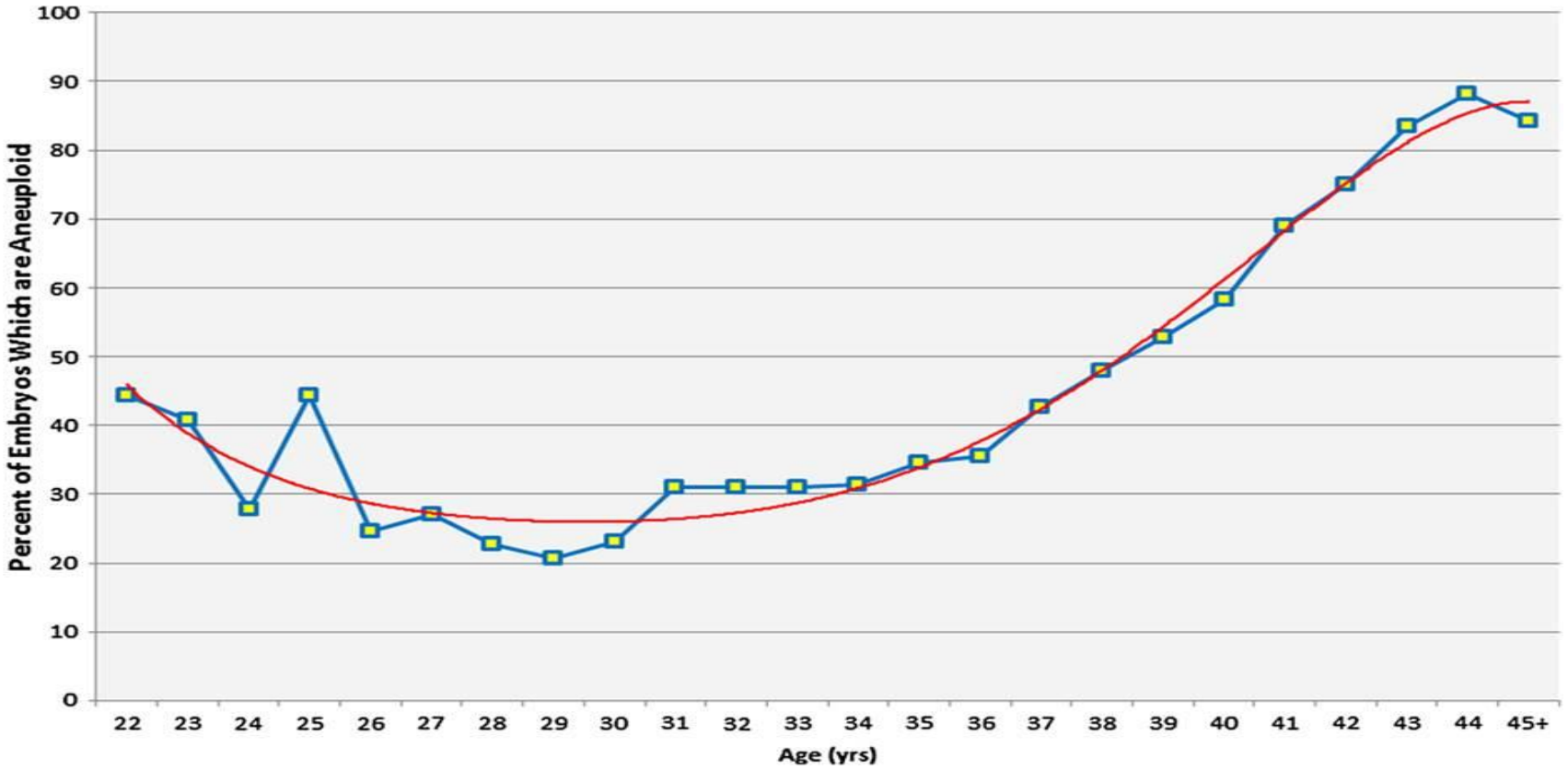

Figure 1.10. Prevalence of aneuploidy in human women. The prevalence of aneuploidy relative to the age of the female partner demonstrates the lowest risk in women from their middle to late twenties, with significantly higher rates in embryos obtained from both younger and older women ($P<1*10^{-6}$). The relationship between age and the rate of aneuploidy is a best fit at the 5th degree polynomial (regression line shown). Modified from (Franasiak et al., 2014). Reprinted with permission.

CHAPTER 2

Materials and Methods

2.1 Ethical Approval

These studies were approved by the University of South Carolina Institutional Review Board (IRB registration number: 00000240) and Greenville Health System Institutional Review Board (IRB number: Pro00072006).

2.2 Patient Controlled Ovarian Stimulation and Granulosa Cell Harvest

Granulosa cells were harvested from patients undergoing infertility treatment at Advanced Fertility and Reproductive Endocrinology Institute (Columbia, SC, USA) and Fertility Center of the Carolinas (Greenville, SC, USA). Patient demographics, cycle information, pregnancy, and live birth data were collected. Each patient's ovaries were stimulated using either a long luteal protocol or an antagonist controlled ovarian stimulation protocol. In the antagonist cycles, when one follicle reached at least 13 mm or the patient's estradiol level reached 300 IU/mL, a GnRH antagonist (Cetrotide, EMD-Serono, Rockland, MA, USA or Ganirelix, EMD-Serono, Rockland, MA, USA) was administered. In both protocols, when 2-3 follicles reach >17 mm by ultrasound an ovulatory dose of hCG (Pregnyl, EMD-Serono, Rockland, MA, USA) or Lupron (Leuprolide Acetate, Sandoz, Princeton, NJ, USA) was delivered. Thirty-six hrs later, the patient's oocyte retrieval was performed by a physician. Each CC mass was mechanically separated from its oocyte and rinsed in sperm wash medium (FUJIFILM Irvine

Scientific, Santa Ana, CA, USA), a medium containing 21 mM N-2-Hydroxyethylpiperazine-N'-2- ethanesulfonic acid (HEPES) and 4 mM sodium bicarbonate buffered modified human tubal fluid (HTF) and 5 mg/ mL human serum albumin to remove debris. For the PGT-A related studies, each CC mass and its associated oocyte/embryo were kept separate throughout the entire process. Cumulus cell masses were snap-frozen and maintained in liquid nitrogen (LN_2) until they were transported from the clinics to the University of South Carolina School of Medicine where they were stored in a freezer at -70°C until use. For the mitochondrial function assay associated RT-PCR, the CCs and MGCs were pooled together, and an aliquot of GCs were placed in RNAlater solution, (Life Technologies, Carlsbad, CA, USA) cooled for 24 hrs at 4˚C, snap-frozen and handled as above.

2.3 Embryo culture and ploidy assessment

Mature oocytes were inseminated via ICSI. Fertilization was confirmed by the presence of two pronuclei and two polar bodies 16-18 hrs after insemination. Embryos for the PGT-A studies were individually cultured in 20 µL LifeGlobal® global total media drops (Cooper Surgical, Trumbull, CT, USA) under oil (Ovoil, Vitrolife, Englewood, CO, USA) at 37°C, 6% CO_2, 5% O_2, 89% N_2 in a humidified atmosphere until day 5 or day 6 post retrieval. For PGT-A related studies, embryo morphologies were assessed using Gardner's blastocyst grading (Gardner et al., 2000), and 3-7 trophectoderm cells were biopsied and sent to Igenomix (Miami, FL, USA) for genetic testing using NGS. Frozen embryo transfers were performed using the highest quality euploid embryos. Live birth outcomes were obtained from

the patient's obstetrician, including delivery dates, gender, and if there were any maternal or neonatal interventions or complications. For mitochondrial related studies, embryos were group cultured in 50 µL LifeGlobal® global total media drops (Cooper Surgical) under oil (Vitrolife) at 37°C, 6% CO_2, 5% O_2, 89% N_2 in a humidified atmosphere until day 5 or day 6 post retrieval. Embryo morphologies were assessed using the American Society for Reproductive Medicine (ASRM) (Racowsky et al., 2010) criteria for day 3 embryos and day 5/6 blastocysts.

2.4 RNA Isolation and cDNA synthesis

RNA was isolated from each CC sample or pooled CC/MGC samples using the Direct-zol MiniPrep Kit with DNase treatment (Zymo Research, Irvine, CA, USA) following the manufacturer's instructions. Samples were removed from storage at -70°C and Ribozol (600-1000 µL) was added to each sample and incubated 5 min at room temperature (RT) to lyse cells. Lysates were transferred to clean RNase/DNase free microcentrifuge tubes. A 1:1 volume of 95-100% ethanol was added to tubes containing the Ribozol lysates and vortexed. Samples were loaded into Directzol spin columns and centrifuged at 15,000xg for 1 min in a refrigerated microfuge (Eppendorf, Hauppauge, NY, USA). Each spin was performed at 15,000xg in the same microfuge throughout this protocol. The flow-through was discarded. Each spin column was placed into a clean RNase/DNase free tube and 400 µL of RNA wash buffer was added into each column and centrifuged for 1 min. The flow-through was discarded. An 80 µL DNase mixture containing DNase, 1X DNase reaction buffer, and kit water was added into each column and incubated 15 min at room temperature. The columns were centrifuged

for 30 seconds and 400 µL RNA pre-wash buffer was added to the columns and they were centrifuged for an additional 1 min. The flow-through was discarded. Another 400 µL RNA pre-wash buffer was added and then centrifuged again, and the flow-through was discarded. A total of 700 µL RNA wash buffer was added to each column, centrifuged for 1 min, and the flow-through was discarded. Columns were centrifuged for another 2 min in order to dry the columns. Each column was transferred to a new RNase/DNase-free tube. 50µL RNase/DNase-free kit water was added to the columns for the pooled samples and 30 µL were added for the individual samples, and incubated at RT for 5 min. The columns were centrifuged for 2 min to elute RNA, and then kept on ice for immediate use or stored at -70°C. The RNA concentration and purity of individual CC masses was assessed at the wavelengths of 260 and 280 nm using a spectrophotometer with a 2 mm lid (NanoDrop 2000C, Thermo Scientific, Waltham, MA, USA). RNA concentration and purity for pooled samples were assessed at the wavelengths of 260 and 280 nm using a Biophotometer 6131 spectrophotometer (Eppendorf).

2.5 DNA Isolation

DNA was isolated from pooled GCs using the Direct-zol MiniPrep Kit as described above but omitting the DNase treatment step (Zymo Research). DNA concentration and purity were assessed at the wavelengths of 260 and 280 nm using a Biophotometer 6131 (Eppendorf).

2.6 cDNA synthesis

Each sample was reverse transcribed into cDNA using the iScript kit (Bio-Rad Laboratories, Hercules, CA, USA). RNA (15 µL), 4 µL of 5X iScript reaction

mix, and 1 µL of iScript Reverse Transcriptase enzyme were combined on ice, vortexed and pulsed down. Samples were allowed to sit for 2 min at RT before starting the program. The reverse transcription reaction was carried out in a thermocycler (Eppendorf), for 5 min at 25°C, 30 min at 42°C, and 5 min at 85°C. After cDNA synthesis, each sample of the cDNA was diluted with DNase/RNase-free water and stored at -20°C for subsequent qRT-PCR.

2.7 Quantitative Real-Time PCR

Synthesized primers were cartridge purified (Life Technologies). Primers included: *AMH*, *AREG*, *CALM1*, *CYP11A1*, *CYP19A1*, *FSHR*, *GJA4*, *GREM1*, *HSD3B1*, insulin-like growth factor 2 (*IGF2*), *IGFBP5*, inhibitor of growth protein 1 (*ING1*), inhibin beta A subunit (*INHBA*), *LHCGR*, mitochondrially encoded ATP synthase 8 (*MT-ATP8*), pappalysin-1 (*PAPPA*), *PGR*, *PGRMC1*, *PTGS2*, steroidogenic acute regulatory protein (*STARD1*), and *VCAN*. Primer sets may be found in Tables 3.2 and 4.3. Real-time PCR reactions were run with 2 or more wells per sample for 40-45 cycles and threshold cycle (Ct) values were averaged. The reactions included between 5-27 ng starting cDNA, 300 nM of each upstream and downstream primer, and 10 µL 2X SsoAdvanced Universal SYBR Green Supermix (Bio-Rad Laboratories) and sterilized PCR-grade water to a final volume to 20 µL per well. PCR-grade water was substituted for the cDNA as a negative control. PCR amplification was performed using the iCycler iQ Real-Time PCR Detection System (Bio-Rad Laboratories). TATA-box binding protein (*TBP*) mRNA was used as an internal control for cDNA samples (Nelson-Degrave et al., 2005) and actin beta (*ACTB*) DNA was used as an internal control for nuclear DNA

(nDNA) samples (Diez-Juan et al., 2015). Primer efficiency curves were determined on all amplicons. Single amplicons of the correct size were verified using agarose gels and by the presence of single melt-curve peaks. All primers not previously reported in the literature had their amplicons sequenced. mRNA and nDNA quantities were derived from a standard curve for each transcript using serial dilutions of its purified amplicon. *TBP* has extensively been tested as a control gene in our laboratory with human GCs under multiple conditions and treatments and has not been found to be regulated under any circumstances. Target mRNA values were expressed relative to values of the *TBP* mRNA control.

2.8 Quantification of mtDNA

Relative amounts of mtDNA and nDNA and were determined by qRT-PCR. The nuclear gene *ACTB* was selected as a reference gene to calculate mDNA content and the mtDNA gene *MT-ATP-8* was used to quantify mitochondrial genome content. The ratio of mtDNA:(2x nDNA) was used to determine mtDNA content.

2.9 Analysis of Mitochondrial Metabolic Substrates

Cumulus cells from each patient were rinsed in sperm washing medium (FUJIFILM Irvine Scientific) following oocyte retrieval and placed in a 5 mL tube. Follicular fluid containing MGCs from each patient was split between 50 mL tubes and centrifuged for 15 min at 300xg. Each spin was performed at 300xg in the same centrifuge throughout this protocol. Follicular fluid was decanted from the tubes and a filtered solution of hyaluronidase (50 mg/mL) from bovine testes (Sigma, Raleigh, NC, USA) was added to each MGC pellet and the CC tube and

incubated at 37°C for 10 min to remove cell clumps. Calcium/magnesium-free phosphate-buffered saline (PBS) (Gibco, Gaithersburg, MD, USA) was added to bring the pellet to ≥4 mL. Mural granulosa cells were layered on top of 35% over 70% Percoll solutions in 15 mL tubes and centrifuged for 30 min. A 30 µL assay mix containing 2x Biolog Mitochondrial Assay Solution (MAS) (Biolog, Hayward, CA, USA), 6x Redox Dye (Biolog), 24x saponin (90 µg/mL) for permeabilization (Alfa Aesar, Ward Hill, MA, USA), and sterile water was added to each well of the 96-well MitoPlate S-1 plates (Biolog) to incubate for 1 hour. Mural granulosa cells were partitioned into 1 or 2 bands with the blood pelleting to the bottom of the tubes. The upper band containing purified MGCs was removed, 25 mL of calcium/magnesium-free PBS (Gibco) and the CCs were combined. The mixture was poured through a 70-micron strainer. Pooled GCs were centrifuged for 20 min. The supernatant was decanted, and the pellet was resuspended in 1x MAS buffer (Biolog) to 2 mL. The GC/MAS mixture (0.5 mL) was removed and a 10 µL sample was counted on a hemocytometer. The remaining aliquot was centrifuged for 5 min. The supernatant was decanted and the pellet was placed in 0.5 mL RNAlater solution (Life Technologies), stored at 4°C for 24 hrs, and snap-frozen in LN_2 until it was transported to the University of South Carolina School of Medicine for further processing. The remaining 1.5 mL GC/MAS mixture was diluted to 3.0 mL with 1x Biolog MAS and a 10 µL sample was counted with a hemocytometer and averaged with the first cell count to determine the total cells in each sample. After 1 hr incubation, 30 µL of the GC/MAS suspension was added to each well of the MitoPlate S-1 plate. Permeabilized cells were assayed in triplicate for

mitochondrial activity using MitoPlate S-1 plates. The plates contained 31 cytoplasmic and mitochondrial metabolic substrates. Metabolism of substrates was assessed by a colorimetric change of a terminal electron acceptor tetrazolium redox dye at a wavelength of 590 nm read every 2.5 min for 50 cycles on a kinetic plate reader. Results were normalized to mtDNA copy number per sample and the negative control wells containing GC/MAS and assay mix without any additional substrates and positive control wells containing GC/MAS and assay mix with succinic acid. Slope ratio = [Slope (sample) – Slope (negative control)] / [Slope (positive control) – Slope (negative control)].

2.9 Statistics

Real-time PCR reactions were run with 2 or more wells per sample for 40-45 cycles and threshold cycle (Ct) values were averaged. The mRNAs were normalized against internal controls as described above. Statistical analysis of the results was performed using generalized linear mixed models (GLMMs) fitted by maximum likelihood using the R package lme4 (Bates et al., 2015). Substrates on in the mitochondrial function assay were run in triplicate on the same plate along with a negative control and a positive control. The slopes of the kinetic curves were averaged. Multiple linear regression models were estimated to predict the normalized average rate of each substrate's metabolism and mitochondrial metabolic score using Box-Cox transformation for normality (Box and Cox, 1964). Statistical analysis was performed using the statistical analysis environment R 3.6.2 (R Core Team, 2019).

Chapter 3

Cumulus cell Pappalysin-1, Luteinizing Hormone/ Choriogonadotropin Receptor, Amphiregulin and Hydroxy-delta-5-steroid dehydrogenase, 3 beta- and steroid delta-isomerase 1 mRNA levels associate with oocyte developmental competence and embryo outcomes[3]

---

[3]R.J. Kordus, A. Hossain, M.C. Corso, H. Chakarborty, G.F. Whitman-Elia, and H.A Lavoie. Journal of Assisted Reproduction and Genetics (2019) 36:1457–1469 https://doi.org/10.1007/s10815-019-01489-8 Reprinted here with permission of publisher.

3.1 Abstract

3.1.1 Purpose: To determine whether a selected set of mRNA biomarkers expressed in individual cumulus granulosa cell (CC) masses show association with oocyte developmental competence, embryo ploidy status, and embryo outcomes.

3.1.2 Methods: This prospective observational cohort pilot study assessed levels of mRNA biomarkers in 163 individual CC samples from 15 women stimulated in antagonist cycles. Nineteen mRNA biomarker levels were measured by real-time PCR and related to the development of their corresponding individually cultured oocytes and subsequent embryos, embryo ploidy status, and live birth outcomes.

3.1.3 Results: *PAPPA* mRNA levels were significantly higher in CC from oocytes that led to euploid embryos resulting in live births and aneuploid embryos compared to immature oocytes by ANOVA. *LHCGR* mRNA levels were significantly higher in CC of oocytes resulting in embryos associated with live birth compared to immature oocytes and oocytes resulting in arrested embryos by ANOVA. Using a General Linearized Mixed Model to assess ploidy status, CC *HSD3B1* mRNA levels in oocytes producing euploid embryos were significantly lower than other oocyte outcomes, collectively. When transferred euploid embryos outcomes were analyzed by ANOVA, *AREG* mRNA levels were significantly lower and *PAPPA* mRNA levels significantly higher in CC from oocytes that produced live births compared to transferred embryos that did not form a pregnancy.

3.1.4 Conclusions: Collectively, *PAPPA*, *LHCGR*, and *AREG* mRNA levels in CC may be able to identify oocytes with the best odds of resulting in a live birth, and

HSD3B1 mRNA levels may be able to identify oocytes capable of producing euploid embryos.

3.1.5 Key Words: cumulus cells, real-time PCR, mRNA levels, oocyte developmental competence, euploid embryo

3.2 Introduction

Successful in vitro fertilization (IVF) is highly dependent upon the quality of the oocytes harvested and the subsequent quality of embryos used for uterine transfer (Uyar et al., 2013). Several studies have shown that use of preimplantation genetic testing for aneuploidy (PGT-A) to select euploid embryos for uterine transfer increases implantation, ongoing pregnancy, and delivery rates (Chen et al., 2015a, Yang et al., 2012, Scott et al., 2013), whereas other studies showed PGT-A decreased pregnancy rates (Kushnir et al., 2016, Chang et al., 2016). Conflicting PGT-A findings might indicate that other methods beyond genetic screening are needed to improve IVF pregnancy rates. The differing PGT-A study results may also reflect the invasive methodology of PGT-A, which requires the removal of 3-10 cells from the trophectoderm. Increased numbers of trophectoderm cells per biopsy have been correlated with decreased implantation rates (Zhang et al., 2016). Therefore, a method for identifying oocytes that will produce euploid embryos with the greatest chances of leading to a live birth that does not require embryo manipulation would be advantageous.

Some non-invasive methods for assessing oocyte and embryo live birth potential include preimplantation embryo metabolomics and proteomics of secreted products (Uyar and Seli, 2014, Nel-Themaat and Nagy, 2011) and granulosa cell (GC) mRNA biomarkers (Kordus and LaVoie, 2017). The use of

GC biomarkers is based on knowledge that cumulus granulosa cells (CCs) and mural granulosa cells (MGCs) interact with oocytes and can reflect the health and maturational status of the oocyte (Tanghe et al., 2002, Uyar et al., 2013). GCs are obtained as a by-product of oocyte retrieval and can be rapidly assessed for mRNA levels by reverse transcription and quantitative polymerase chain reaction (PCR). Several studies suggest that CC biomarker mRNA levels from individual oocytes can be used to generate models capable of predicting pregnancy and live birth (Ekart et al., 2013, Iager et al., 2013, Wathlet et al., 2011).

Approaches to evaluate differentially expressed genes in CCs have employed large-scale microarray, transcriptome deep sequencing, PCR arrays and quantitative PCR (Kordus and LaVoie, 2017). In most cases the ploidy status of the embryos was not known, which could have altered the study outcomes. Only a handful of studies have examined CC mRNA levels in conjunction with oocyte or embryo ploidy status (Fragouli et al., 2012, Parks et al., 2016, Green et al., 2018). Taken together, a focused quantitative PCR analysis of CC target genes selected from prior studies combined with the ploidy status of the embryos should yield valuable information regarding mRNA biomarker usefulness in predicting live birth.

Many oocytes fail to fertilize, or when fertilized, arrest before reaching the blastocyst stage, or fail to develop into euploid blastocysts. We hypothesize that while many mature oocytes appear morphologically normal, the actual developmental competence of those oocytes is variable, and will be reflected by varying mRNA levels of specific biomarkers in their associated CCs. Furthermore, we propose that a CC mRNA biomarker model could potentially indicate whether

a mature oocyte, when fertilized, will result in a euploid embryo. In addition, we hypothesize that certain CC mRNA biomarkers and their levels will associate with oocytes that are capable of producing viable embryos which result in live births.

A comprehensive review of the human literature for potential CC candidate mRNA biomarkers was performed (Kordus and LaVoie, 2017), and genes were selected based on their functions. In some cases, the genes selected were based on data in non-human animals (Christenson et al., 2013, Vigone et al., 2013, Assidi et al., 2008, Blaha et al., 2015, Nivet et al., 2013, Saini et al., 2015, Glister et al., 2010). Gene products associated with oocyte maturation included calmodulin 1 (*CALM1*), gap junction alpha-4 protein (*GJA4*), gremlin (*GREM1*), and inhibitor of growth protein 1 (*ING1*). Genes associated with cumulus mass expansion included amphiregulin (*AREG*), prostaglandin-endoperoxide synthase 2 (*PTGS2*), and versican (*VCAN*). Genes encoding proteins mediating de novo steroidogenesis, estrogen, and progesterone production included aromatase (*CYP19A1*), cholesterol side-chain cleavage enzyme (*CYP11A1*), hydroxy-delta-5-steroid dehydrogenase, 3 beta- and steroid delta-isomerase 1 (*HSD3B1*), and steroidogenic acute regulatory protein (*STARD1*). Genes related to hormone modulation included insulin-like growth factor 2 (*IGF2*), insulin-like growth factor-binding protein 5 (*IGFBP5*), and inhibin beta A subunit (*INHBA*), and pappalysin-1 (*PAPPA*). Gene encoding hormone receptors included follicle-stimulating hormone receptor (*FSHR*), luteinizing hormone/choriogonadotropin receptor (*LHCGR*), progesterone receptor (*PGR*), and progesterone receptor, membrane component 1 (*PGRMC1*). The primary goal of this study was to determine if a

model of specific CC mRNA biomarker levels could identify a mature oocyte's ability to produce euploid embryos. The secondary goal of this study was to determine if specific CC mRNA biomarker levels could indicate oocytes capable of leading to euploid embryos with live birth outcomes.

3.3 Materials and methods

3.3.1 Study population, participants, and CC isolation

This study is a prospective observational cohort pilot study. In total, 164 individual CC masses were harvested from their corresponding oocytes from 15 patients undergoing infertility treatment with PGT-A at Advanced Fertility and Reproductive Endocrinology Institute (Columbia, SC, USA) from February 2015 through June 2016. Patient's either electively desired PGT-A or it was recommended based on the patient's diagnosis (Table 3.1). Patients with endometriosis or diminished ovarian reserve (DOR) were not included as prior work indicates these conditions alter GC gene expression (Greenseid et al., 2011, May-Panloup et al., 2012, Allegra et al., 2014, Barcelos et al., 2015). Patient demographics and cycle information (Table 3.1), blastocyst development, PGT-A results, and live birth data (Supplemental Table 3.1), as well as CC mRNA levels were collected. Each patient's ovaries were stimulated using an antagonist protocol until at least one follicle at 15 mm was present when a GnRH antagonist (Cetrotide, EMD-Serono, USA or Ganirelix, EMD-Serono, USA) was administered. When two follicles reached 18 mm or 50% of the follicles were ≥ 15 mm by ultrasound, an ovulatory dose of human chorionic gonadotropin (hCG) (Pregnyl, EMD-Serono, USA) or Lupron (Leuprolide Acetate, Sandoz, USA) was delivered.

Thirty-six hrs later patients underwent oocyte retrieval. Each CC mass was mechanically separated from its oocyte and rinsed in HTF-HEPES, medium (Irvine, USA) to remove debris. Each CC mass and its associated oocyte/embryo were kept separate throughout the entire process. A summary flowchart of the fate of the collected oocytes is shown in Figure 3.1. CC masses were snap frozen and maintained in LN_2 until they were transported to the University of South Carolina School of Medicine for further processing.

3.3.2 Embryo culture and ploidy assessment

Mature oocytes were inseminated via intracytoplasmic sperm injection. Fertilization was confirmed by the presence of two pronuclei and two polar bodies 16-18 h after insemination. Oocytes and embryos were individually cultured in 20 µL media drops (Global total, Global, USA) under oil (Ovoil, Vitrolife, USA) at 37°C, 6% CO2, 5% O2, 89% N2 in a humidified atmosphere until day 5 or day 6 post retrieval. Blastocyst morphologies were assessed using Gardner's blastocyst grading scale (Gardner et al., 2000), and 3-7 trophectoderm cells were biopsied and sent to Igenomix (Miami, FL, USA) for PGT-A using NGS. Fifteen FETs were performed using the highest quality euploid embryos (19 embryos total) for each patient. Live birth outcomes were obtained from the patient's obstetrician including delivery dates and if there were any maternal or neonatal interventions or complications.

3.3.3 RNA Isolation and cDNA synthesis

RNA was isolated from each CC mass using the Direct-zol MiniPrep Kit with DNase treatment (Zymo Research, Irvine, CA, USA). RNA concentration and

purity were assessed at the wavelengths of 260 and 280 nm using a spectrophotometer with a 2 mm lid (NanoDrop 2000C, Thermo Scientific, USA). Sample amounts varied between 80 and 360 ng RNA per individual sample. Each sample was reverse transcribed into cDNA using the Bio-Rad iScript kit (Hercules, CA, USA). The reverse transcription reaction was carried out in an Eppendorf thermocycler, for 5 min at 25°C, 30 min at 42°C, and 5 min at 85°C.

3.3.4 Quantitative Real-Time PCR

Gene primer sequences, annealing temperatures, and amplicon sizes can be found in Table 3.2. Synthesized primers were cartridge purified (Life Technologies, Carlsbad, CA, USA). PCR reactions were run with two or more wells per sample for 45 cycles and threshold cycle (Ct) values were averaged. The reaction included 2 µL of cDNA (6-27 ng starting RNA), 300 nM of each upstream and downstream primer, and 10 µL 2X SsoAdvanced Universal SYBR Green Supermix (Bio-Rad Laboratories, Hercules, CA, USA) and sterilized PCR-grade water to a final volume to 20 µL per well. PCR-grade water was substituted for the cDNA as a negative control. PCR amplification was performed using the iCycler iQ Real-Time PCR Detection System (Bio-Rad, USA). TATA-box binding protein (*TBP*) mRNA was used as an internal control (Nelson-Degrave et al., 2005). Single amplicons of correct size were verified using agarose gels and by the presence of single melt-curve peaks. mRNA quantities were derived from a standard curve for each mRNA made using serial dilutions of its purified amplicon. *TBP* has extensively been tested as a control gene in our laboratory with human granulosa cells under multiple conditions or treatments and has been found not to

be regulated under any circumstances. Target mRNA values were expressed relative to values of the *TBP* mRNA control.

3.3.5 Statistical analysis

The mRNA levels were normalized using log2 transformation. Principal Component Analysis (PCA) was conducted to explore the mRNA level correlation patterns between the CC samples. CC mRNA levels were compared between different oocyte and subsequent embryo developmental outcomes using repeated measures analysis of variance (ANOVA) to accommodate for the variable number of oocytes per patient followed by Tukey's post hoc tests for pairwise comparisons. The CC samples used for these studies were divided into the following categories: Immature oocytes, mature oocytes that failed fertilization, oocytes that produced embryos that arrested and were not appropriate for biopsy, oocytes that produced biopsied blastocysts that were aneuploid, and oocytes that produced biopsied blastocysts that were euploid. Oocytes that produced euploid embryos were further subdivided into embryos that resulted in live birth, embryos that resulted in a negative pregnancy, and embryos that were vitrified and not transferred. Each figure states which categories were used for the specific statistical analysis.

3.3.6 Statistical models

Models were estimated to predict multiple dichotomous oocyte developmental outcomes using generalized linear mixed models (GLMMs) fitted by maximum likelihood using the R package lme4 (Bates et al., 2015). The GLMMs included the normalized gene expressions as variables and used patients' demographics (age and body mass index (BMI) as controlling factors and adjusted

for two ovulation induction or trigger medications). Unstructured correlation patterns were used in fitted GLMMs to capture the correlation among the repeated observations from same individual. The statistical models aimed to include as many patients as possible. However, some of the genes had high proportion of missing values for some patients because of limited RNA amounts that were obtained from CC masses. To ensure maximum utilization of the data we started the modeling by including all the genes and proceeded backward dropping the genes one-by-one with highest proportion of missing observations until the fitted mixed-effects model attained computational convergence successfully. Since different patients had missing observations on different genes, exclusion of the missing values eventually reduced the number of patients and number of observations in the sample used to fit the model. The analysis sample size differed from model-to-model (for different response variables) as the maximum possible data points were used for a model to converge. Statistical significance in all analyses was determined at a 0.05 significance level. All the inference *P*-values were reported after adjusting for multiple comparisons (Hothorn et al., 2008). The predictive performances of the fitted models were assessed using Receiver Operating Characteristics (ROC) curves and Area Under ROC Curves (AUC). The AUC values of the models used in this study ranged from 0.75 to 1.00 implying the models exhibited good/very good to excellent predictive accuracy. Statistical analysis was performed using the statistical software R 3.4.4 (http://www.r.project.org/).

3.4 Results

In total, 164 CCs were harvested from 15 patients undergoing infertility treatment with PGT-A. Fifteen FETs were performed after PGT-A results were obtained. Eleven patients had single embryo transfers and four had double embryo transfers. In the four cases where two embryos were selected, one embryo of each gender was transferred. Eight patients gave birth to nine healthy children with no complications. 163 of 164 CC samples (n=15 patients) analyzed contained a sufficient amount of RNA to detect the endogenous control house-keeping gene, *TBP*. Due to limited starting sample RNA amounts, not all samples were able to be tested for each biomarker and the variations in sample size are noted in figures.

PCA was utilized to test the hypothesis that several of the CC genes we examined would be correlated with one another. The correlations of the CC mRNA levels of 151 observations from 14 patients were examined by creating a biplot within the multivariable dataset that contained the most biomarkers and individual patient observations that fit the model (Figure 3.2). The biplot is based on the first and second principal components (PC1 and PC2) of the log2-transformed mRNA levels of each individual CC mass. PC1 and PC2 explain 35.7% and 22.9% of the variability of the model, respectively. All genes shown were positively correlated to PC1. *HSD3B1*, *IGFBP5*, *PAPPA*, and *PGR* were all positively correlated with PC2 while *CYP11A1*, *CYP19A1*, and *INHBA* are negatively correlated with PC2. In addition, a significant ($P < 0.001$) strong positive correlation was observed between *CYP19A1* and *CYP11A1* ($r = .68$), and significant ($P < 0.001$) moderate

positive correlations were observed for *PGR* and *HSD3B* (*r* = .59), *CYP11A1* and *INHBA* (*r* = .50), *PGR* and *IGFBP5* (*r* = .41), and *PAPPA* and *INHBA* (*r* = .41).

We next wanted to test the hypothesis that the CC mRNA levels of the selected genes would vary by oocyte developmental competence and resulting embryo endpoint. To test this hypothesis, we analyzed all the CC mRNA level data by the resulting developmental outcome for each group of oocytes by repeated measures ANOVA followed by Tukey's post hoc test (adjusted *P*-values). *PAPPA* mRNA levels in CCs were higher in oocytes that resulted in euploid embryos that led to a live birth compared to immature oocytes and in oocytes that resulted in aneuploid embryos compared to immature oocytes, when comparing all groups ($P < 0.05$) (Figure 3.3). *LHCGR* mRNA levels in CCs were higher for oocytes that resulted in embryos which led to a live birth compared to immature oocytes and oocytes that resulted in arrested embryos compared to immature oocytes, when comparing all groups ($P < 0.05$). Other CC biomarkers showed no statistical differences between groups and their expression profiles are shown in Supplemental figure 3.1.

We also wanted to test the hypothesis that certain CC biomarker mRNA levels associated with oocytes giving rise to euploid embryos would be distinct from those giving rise to aneuploid embryos and those oocytes that resulted in arrested embryos or those that failed fertilization. Using a GLMM, the best fitting model examining whether CC biomarker mRNA expression associated with oocytes that became euploid embryos included 11 patients (n=78 CC masses) and *CYP11A1*, *CYP19A1*, *HSD3B1*, *IGFBP5*, *PAPPA*, *PGR*, *PGRMC1*, *ING1*,

LHCGR, and *STARD1* (Figure 3.4). CCs associated with oocytes that produced euploid embryos exhibited significantly ($P < 0.05$) lower CC *HSD3B1* mRNA levels than those oocytes that led to mature oocytes resulting in aneuploid blastocysts, oocytes producing embryos that arrested and did not reach the blastocyst stage, and mature oocytes that failed to fertilize, collectively (abnormal group). CC *ING1* mRNA levels associated with oocytes that produced euploid embryos trended toward being lower than CCs from oocytes that gave rise to the abnormal outcomes, collectively ($P = 0.061$).

A critical hypothesis we tested was that certain CC mRNA biomarker levels of oocytes giving rise to euploid embryos would be associated with live birth outcomes. CC mRNA levels from all 15 patients (n = 19 CC masses) were assessed for differences between oocytes yielding transferred embryos that resulted in a live birth and those that did not form a pregnancy, using repeated measures ANOVA followed by Tukey's post hoc test (adjusted *P*-values). *AREG* mRNA levels were significantly lower in CCs from oocytes that resulted in live births (n = 8 from 8 patients) compared to the no pregnancy group (n = 7 from 5 patients) ($P < 0.05$) (Figure 3.5). *PAPPA* mRNA levels were higher in CCs from oocytes producing euploid embryos that resulted in live births (n = 9 from 8 patients) compared to those that produced no pregnancy (n = 10 from 7 patients) ($P < 0.05$). The other biomarkers showed no statistical differences between groups.

Using a GLMM, we also compared the CC mRNA biomarkers associated with oocytes that resulted in euploid embryos producing a live birth compared to

oocyte outcomes not producing a live birth (non-viable group), collectively. The non-viable group included immature oocytes, mature oocytes resulting in aneuploid blastocysts, oocytes producing embryos that did not reach the blastocyst stage, and mature oocytes that failed to fertilize. The best fitting model for this comparison included 110 CC samples from 14 patients and included mRNA levels for *CYP11A*, *CYP19A1*, *IGFBP5*, *PAPPA*, *PGRMC1*, and *STARD1* (Supplemental Figure 3.2). As revealed in the fitted model higher CC *PAPPA* mRNA levels ($P < 0.05$) significantly increased the odds of an oocyte producing an embryo that resulted in a live birth (OR = 4.591, 95% CI: 1.098 to 19.201). The other five CC mRNA biomarkers did not significantly associate with live births.

3.5 Discussion

The key findings of this research were that higher *PAPPA*, higher *LHCGR*, and lower *AREG* mRNA levels in CCs were associated with oocytes that produced embryos capable of yielding live birth outcomes. In addition, lower CC *HSD3B1* mRNA was associated with oocytes that resulted in euploid embryos compared to other outcomes. Our premise was that although many retrieved oocytes in our study appeared mature, several oocytes would have mRNA expression profiles that were similar to those of immature oocytes. Aberrant mRNA levels would cause them to be incapable of forming euploid embryos and leading to live births. Therefore, an individual oocyte's developmental competence would be reflected in specific mRNA levels of their CC masses. For example, we predicted that an immature oocyte CC profile would differ from that of a mature oocyte CC profile capable of giving rise to a euploid embryo resulting in a successful pregnancy.

This was partly the case for CC *PAPPA* and *LHCGR* mRNA levels which were higher in CCs surrounding mature oocytes that gave rise to embryos resulting in live birth than immature oocytes (by ANOVA). However, by ANOVA the levels of CC *PAPPA* and *LHCGR* could not distinguish between oocytes giving rise to morphologically normal embryos that were aneuploid and transferred euploid embryos that resulted in live birth or no pregnancy. When utilizing the best fit GLMM, higher CC *PAPPA* levels continued to associate with oocytes giving rise to embryos with live birth compared to transferred embryos that did not result in pregnancies as well as other oocyte outcomes, collectively. In transferred embryos, lower CC *AREG* associated with oocytes giving rise to embryos with live birth outcomes by ANOVA analysis. Combining these data with that for CC *HSD3B1*, where lower levels were associated with euploid embryos, one can envision using these findings to create a future practical model where the CC levels of all four mRNA biomarkers could be used to predict which of a patient's cohort of oocytes and embryos will most likely be euploid and give rise to a live birth outcome. Although four biomarkers of the selected group exhibited significant differences in statistical models, this was a small pilot study and the data is limited by the small sample numbers for FETs. However, these results provide a starting point for a larger prospective future study.

Several of our analyses indicated *PAPPA* may be a reliable novel biomarker in CCs for identifying oocytes capable of leading to a live birth. *PAPPA* encodes a metalloproteinase that cleaves insulin like growth factor binding protein 4 (IGFBP4) and IGFBP5 (Laursen et al., 2001). Increased levels of *PAPPA* mRNA

and protein in peri-ovulatory follicles may be necessary to increase intrafollicular free IGFs through enhanced cleavage of IGFBPs (Firth and Baxter, 2002). IGFs are known to enhance gonadotropin signaling and FSH-induced LHCGR abundance (Wang and Chard, 1999). We also found that immature oocytes possessed lower CC *LHCGR* mRNA levels compared to all the other groups except oocytes that resulted in arrested embryos. Similarly, others have shown that CC *LHCGR* mRNA levels were higher in mature compared to immature oocytes (Maman et al., 2012). In addition, the ratio of CC *LHCGR* mRNA splice variants was previously reported to be higher in pregnant compared to non-pregnant patients (Papamentzelopoulou et al., 2012b).

Differential mRNA levels of steroidogenic genes in CCs may impact the fate of their associated oocytes. A previous study utilizing GCs pooled from multiple patients and follicles showed increased *CYP19A1* and *HSD3B1* mRNA levels in GCs from oocytes producing embryos that resulted in pregnancies compared to oocytes resulting in embryos that failed to develop (Hamel et al., 2008). In our study, lower CC *HSD3B1* mRNA levels associated significantly with oocytes which yielded euploid embryos. Additionally, *HSD3B1* and *PAPPA* both positively correlated with principal component 1 and 2 in our biplot analysis. The difference may have become apparent as we evaluated individual CC masses rather than pooling. Before including the trigger in our best fitting model, lower CC *CYP19A1* mRNA level was associated with live birth (P = 0.048, not shown), but showed only a trend when trigger medication was added to the model (P = 0.052; Supplemental figure 3.2). Given that different trigger medications can alter steroidogenic gene

expression (Borgbo et al., 2013), caution must be used in interpreting *HSD3B1* and *CYP19A1* mRNA data. Like *LHCGR*, *CYP19A1* is induced through FSH signaling, and *CYP19A1* is higher in dominant follicles of monovulatory species (Hayashi et al., 2010, Sisco et al., 2003, Kristensen et al., 2017).

Huang and colleagues found that higher *AREG* levels in CCs and MGCs were more likely to be associated with pregnancy (Huang et al., 2015). This differs from our study as we saw lower *AREG* levels in CCs from oocytes associated with live birth. As above, this discordant finding may be the result of pooling CCs and MGCs and/or the use four stimulation protocols in the Huang study. Our results are consistent with Feuerstein and colleagues who showed reduced *AREG* mRNA levels for CCs of oocytes that resulted in high-quality blastocysts (Feuerstein et al., 2007).

Two strengths of our study were that all patients received the same stimulation regimen, albeit with two differing trigger medications, and we excluded patients with endometriosis or DOR. Differing stimulation protocols have been reported to alter mRNA expression and bias results (Adriaenssens et al., 2010a, Assou et al., 2013, Grondahl et al., 2009). In previous studies, CCs and MGCs of patients with DOR (Greenseid et al., 2011, May-Panloup et al., 2012) or endometriosis (Allegra et al., 2014, Barcelos et al., 2015) exhibited altered mRNA expression relative to their control groups. For these reasons we excluded patients with these conditions.

As with any patient-driven clinical study, our study had limitations. Patient heterogeneity (Adriaenssens et al., 2010a, Hurwitz et al., 2010), patient age

(Hurwitz et al., 2010, Al-Edani et al., 2014) and differing trigger medications have been previously demonstrated to alter gene expression (Borgbo et al., 2013). A study design including younger patients with only male factor infertility using the same trigger medication would be a more ideal group to examine. Additionally, sample size may have influenced the findings. While we were able to analyze 163 samples, the samples were collected from 15 patients. Additionally, we were not able to analyze all genes for each of the samples as RNA amounts were a limiting factor with individual cumulus masses. With more patients, other mRNA expression level differences may have been apparent, and a larger prospective study is necessary to confirm the results we found and determine the predictive value of the CC mRNA levels for oocyte endpoints such as euploidy and live birth outcomes. Moreover, an argument can be made that looking at oocyte CC biomarkers and comparing the ploidy status of embryos disregards the potential that aneuploidy may have resulted from the paternal contribution to the embryos. We feel our study is still a valid assessment as aneuploidy is predominantly due to maternal origins (Rabinowitz et al., 2012). Finally, we cannot overlook the impact of uterine receptivity. Although we have no evidence of patient uterine receptivity issues, it is possible some non-implanting embryos were capable of leading to a live birth but were not able to implant due to a suboptimal uterine environment. A way to account for this would be to perform double embryo transfers with euploid embryos and assess CC mRNA expression for those where one implants and one does not (Green et al., 2018).

In conclusion, taken together the ideal oocyte developmental competence needed to produce live birth may be reflected by the interplay between *AREG, HSD3B1, LHCGR,* and *PAPPA* mRNA levels and likely their resulting proteins. The current data support that CC mRNA levels of these four biomarkers may be useful in assisted reproduction. A larger prospective study will be needed in to order to corroborate the results and to determine numerical ranges for levels of these biomarkers that could potentially have clinical value in selecting oocytes to fertilize or embryos for uterine transfer that will have the highest odds of yielding live birth.

3.6 Supplementary data

Supplementary data are available at Journal of Assisted Reproduction and Genetics online.

3.7 Funding

Supported by an ASPIRE-I grant from the University of South Carolina. MCC was supported by the University of South Carolina School of Medicine Research Program for Medical Students.

3.8 Compliance with ethical standards

3.8.1 Ethical Approval

"All procedures performed in studies involving human participants were in accordance with the ethical standards of the institutional and/or national research committee and with the 1964 Helsinki declaration and in its later amendments or comparable ethical standards." This study was approved by the University of South Carolina Institution Review Board (IRB registration number: 00000240).

3.8.2 Informed consent: Informed consent was obtained from all individual participants included in the study.

3.9 Conflict of interest: The authors declare no conflict of interest related to this study.

Table 3.1 Patient demographics and cycle information

Pt#	Age	BMI	Diagnosis/ PGT-A Reason	Cycle #	Day 3 FSH level (IU/ml)	E2 per oocyte (pg/ml)	# Oocytes	# Mature	# Fertilized	# Embryos biopsied	Trigger
1	27.8	25.3	Sex selection	3	5.4	141.9	8	8	8	4	hCG
2	36.4	26.4	Male factor	1	7.2	86.6	8	7	6	4	hCG
3	39.7	25	AMA	1	12	100.4	7	4	3	3	hCG
4	30	25.6	Donor	1	6	147.4	10	9	7	6	hCG
5	32.6	26.4	Translocation w/PGT-A	2	9.2	131.0	5	5	5	5	Lupron
6	35.9	21	Idiopathic	1	8.3	163.3	4	4	4	2	Lupron
7	39.7	38.8	AMA	1	11	145.5	9	9	6	5	Lupron
8	40	32	AMA + male factor	1	12	31.4	7	5	5	4	Lupron
9	33	18.8	Male factor	1	10	194.7	11	10	10	4	Lupron
10	42	20.3	AMA	1	6.6	108.2	5	5	5	3	hCG
11	36.1	29.2	Tubal factor	1	5.2	179.5	23	23	18	12	Lupron
12	37	20.7	AMA	1	11	142.2	16	15	14	8	Lupron
13	33.9	35	Male factor	2	10	183.1	11	10	8	2	hCG
14	28	28.4	PCO	1	5.9	184.2	24	6	5	4	hCG
15	39.7	31	AMA	1	7.5	132.6	16	14	14	7	Lupron

AMA = advanced maternal age, hCG = human chorionic gonadotropin, PGT-A = Pre-genetic testing for aneuploidy, PCO = polycystic ovaries,

Table 3.2 Primer set information

Gene	Primer sequences 5'--3'	Annealing temperature (°C)	Amplicon size (base pairs)	Reference or NCBI no.
AREG	For TGGACCTCAATGACACCTACTCTG Rev GGGCTTAACTACCTGTTCAACTCTG	62°	251	(Feuerstein et al., 2007)
CALM1	For TACTTCGTGTGCTCCGACCCAT Rev AGTCCACAGCCACAGCCTACTC	62	231	(Assidi et al., 2011)
CYP11A1	For GCAACGTGGAGTCGGTTTATGTC Rev GTGCAGGACACTGACGAAGTC	60	269	(Tsutsumi et al., 2008)
CYP19A1	For GCACATCCTCAATACCAGGTC Rev TTTGAGGGATTCAGCACAGAC	60	380	(Hamel et al., 2008)
FSHR	For ACCAAGCTTCGAGTCATCC Rev CATCTGCCTCTATCACCTCC	58	103	(Gonzalez-Fernandez et al., 2011)
GJA4	For CATCTCCCACATCCGCTACT Rev GAAGCCTGCCTCTAGCACAC	58	295	(Wang et al., 2009)
GREM1	For CGCCGCACTGACAGTATGAG Rev ACCTTGGGACCCTTTCTTTTTC	62	108	NG_013372.7
HSD3B1	For TGTGCCAGTCTTCATCTACAC Rev TGTTTTCCAGAGGCTCTTCTTC	60	101	(Hamel et al., 2008)
IGF2	For TTCCGCAGCTGTGACCTGGC Rev CCTCGAGCTCCTTGGCGAGC	62	229	NG_008849.1
IGFBP5	For AAGAAGCTGACCCAGTCCAA Rev GAATCCTTTGCGGTCACAAT	60	201	(Walker et al., 2007)
ING1	For GCCTGGTGTGAGGAGGACAA Rev CCCTATGAAAGGAATGGTTCCTT	62	124	(He et al., 2004)

Table 3.2 Continued

Gene	Primer sequences 5'--3'	Annealing temperature (°C)	Amplicon size (base pairs)	Reference or NCBI no.
INHBA	For AAGTCGGGGAGAACGGGTATGTGG Rev TCTTCCTGGCTGTTCCTGACTCG	62	123	(Seder et al., 2009)
LHCGR	For TGGAGAAGATGCACAATGGA Rev GGCAATTAGCCTCTGAATGG	60	122	(Yung et al., 2014)
PAPPA	For GTCATCTTTGCCTGGAAGGGAGAA Rev AGGGCTGTTCAACATCAGGATGAC	62	129	(Wagner et al., 2011)
PGR	For GTCATAGACCCCCGTTGCTA Rev GCTAAGCCAGCAAGAAATGG	60	124	(Guzman et al., 2013)
PGRMC1	For TCTGGACTGCACTGTTGTCCTTG Rev GCAAACACCTGTTCCTATTCTG	60	290	(Zachariades et al., 2011)
PTGS2	For GCTTTATGCTGAAGCCCTATGA Rev TCCAACTCTGCAGACATTTCC	60	70	(Adriaenssens et al., 2010b)
STARD1	For TACGTGGCTACTCAGCATCG Rev ACAGCAGGCTGGTCTTCAAC	60	157	(Chen et al., 2009)
TBP	For CACGGCACTGATTTTCAGTTC Rev TCTTGCTGCCAGTCTGGACT	62	79	(Nelson-Degrave et al., 2004)
VCAN	For GCACCTGTGTGCCAGGATA Rev CAGGGATTAGAGTGACATTCATCA	60	70	(Adriaenssens et al., 2010b)

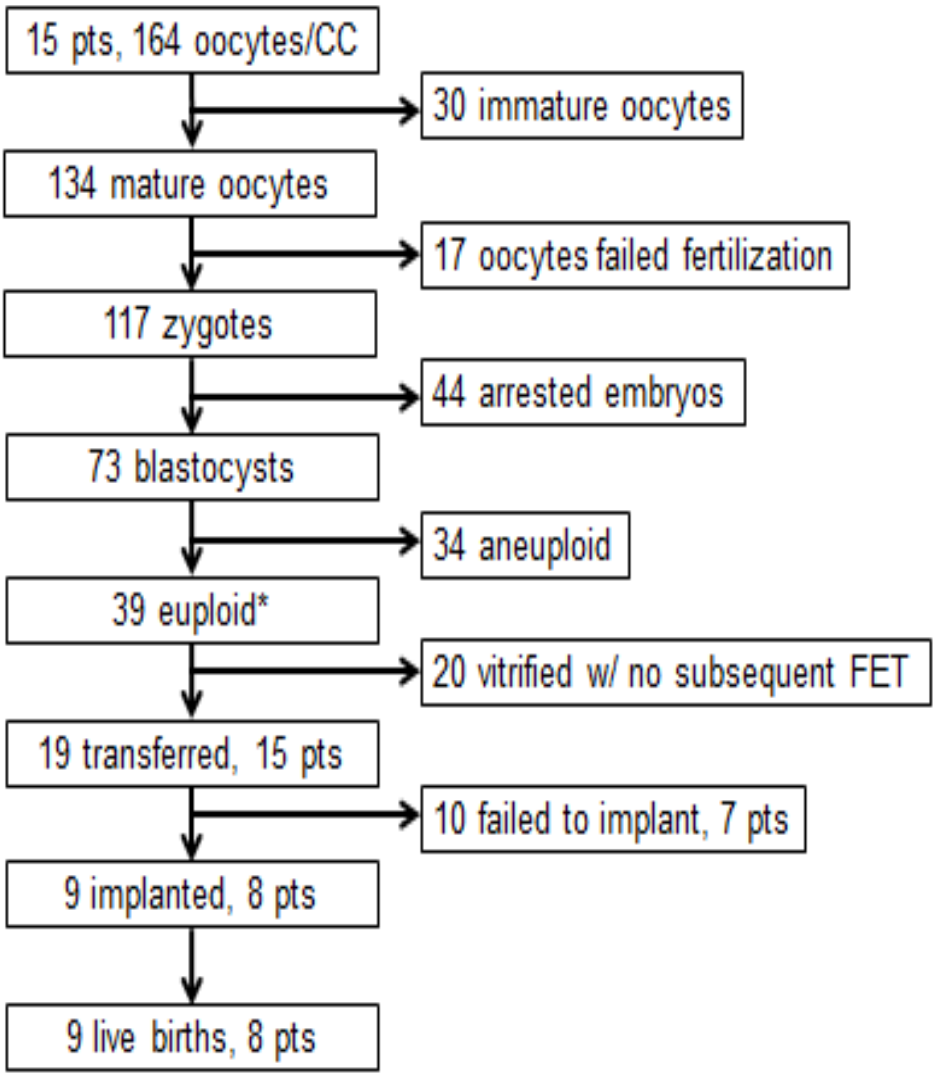

Figure 3.1 Flow diagram summarizing the study population from oocyte retrieval to final outcome. Oocytes (164) were retrieved from 15 patients and individually cultured. Individual CC masses from each oocyte were collected and mRNA was harvested from each mass. Of the 164 oocytes, 134 were mature and 30 were immature. All 134 were injected with sperm. Seventy-three of the fertilized oocytes became blastocysts and were biopsied for PGT-A testing and all were vitrified. PGT-A results indicated that 39 embryos were euploid and 34 were aneuploid. Nineteen of the euploid embryos were transferred and 20 remained in cryostorage. Ten embryos from 7 patients failed to implant while 9 embryos from 8 patients implanted and resulted in live births. *The control TBP mRNA did not amplify in one CC sample from an oocyte yielding a euploid embryo and was not included in the data analysis. RNA analyses were performed on n = 163 individual cumulus masses.

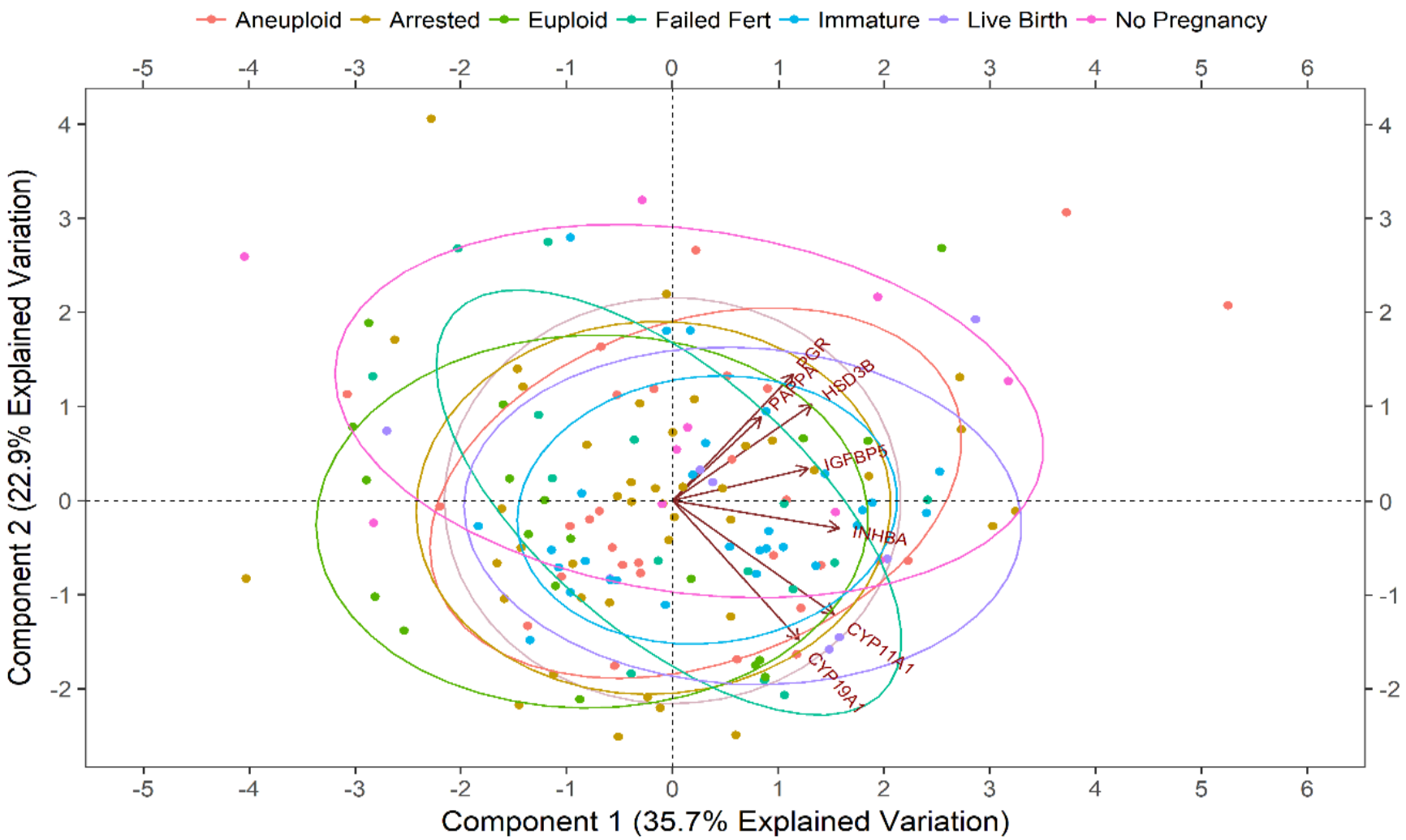
Aneuploid
Arrested
Euploid
Failed Fert
Immature
Live Birth
No Pregnancy
Component 2 (22.9% Explained Variation)
Component 1 (35.7% Explained Variation)
PGR
PAPPA
HSD3B
IGFBP5
INHBA
CYP11A1
CYP19A1

Figure 3.2 Principal Component Analysis Biplot for CC mRNA expression. Biplot of the log2-transformed mRNA levels for 7 genes from 14 patients along the first and second principal components (PC1 and PC2). PC1 accounted for 35.7% of the observed variance while PC2 accounted for 22.9% of the variance. Each data point represents an individual CC mass mRNA level associated with an individual oocyte (n=151 oocytes). The biplot demonstrates the relationship between individual CC mRNA level patterns and the correlation between the different genes. The closer the data points are to each other, the more similar the normalized CC gene expression patterns. The closer the arrows are to each other, the higher the correlation between the normalized CC gene expressions. Groups represent CC mRNA from oocytes with the following descriptions: Aneuploid = mature oocytes resulting in aneuploid embryos; Arrested = mature oocytes resulting in embryos that did not reach the blastocyst stage; Euploid = mature oocytes resulting in euploid blastocysts that were not transferred; Failed Fert = mature oocytes that did not fertilize; Immature = immature oocytes that were not fertilized; Live Birth = oocytes that resulted in euploid embryos that resulted in live births; No Pregnancy = oocytes that resulted in euploid embryos that did not result in a pregnancy

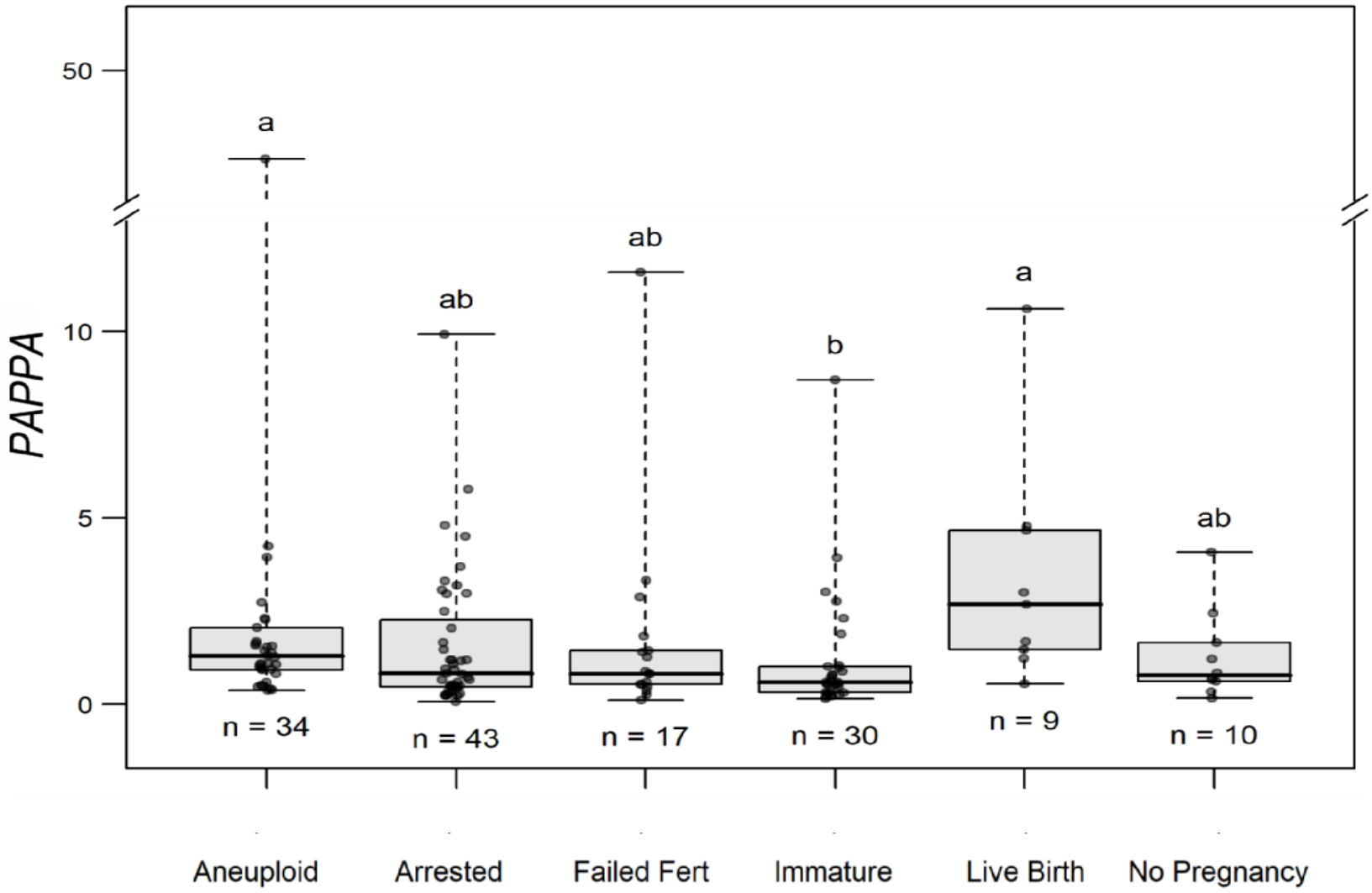
PAPPA
50
10
5
0
a
ab
ab
b
a
ab
n = 34
n = 43
n = 17
n = 30
n = 9
n = 10
Aneuploid
Arrested
Failed Fert
Immature
Live Birth
No Pregnancy

Figure 3.3 Biomarkers for CC mRNA expression associated with mature oocyte competence and embryo outcomes. To determine the differences in CC mRNA between groups where oocytes had different developmental and embryo outcomes, target mRNA levels were compared using repeated measures ANOVA followed by Tukey's post hoc test (adjusted *P*-values) for pairwise comparisons. Groups represent CC mRNA from oocytes with the following descriptions: Aneuploid = mature oocytes resulting in aneuploid embryos; Arrested = mature oocytes resulting in embryos that did not reach the blastocyst stage; Failed Fert = mature oocytes that did not fertilize; Immature = immature oocytes that were not fertilized; Live Birth = oocytes that resulted in transferred euploid embryos that resulted in live births; No Pregnancy = oocytes that resulted in transferred euploid embryos that did not result in a pregnancy. Data are presented as the median copy number (line inside box), first and third quartile (bottom and top of box), and highest and lowest data points (top and bottom of whiskers). Groups with different letters (a and b) exhibit significant differences ($P < 0.05$)

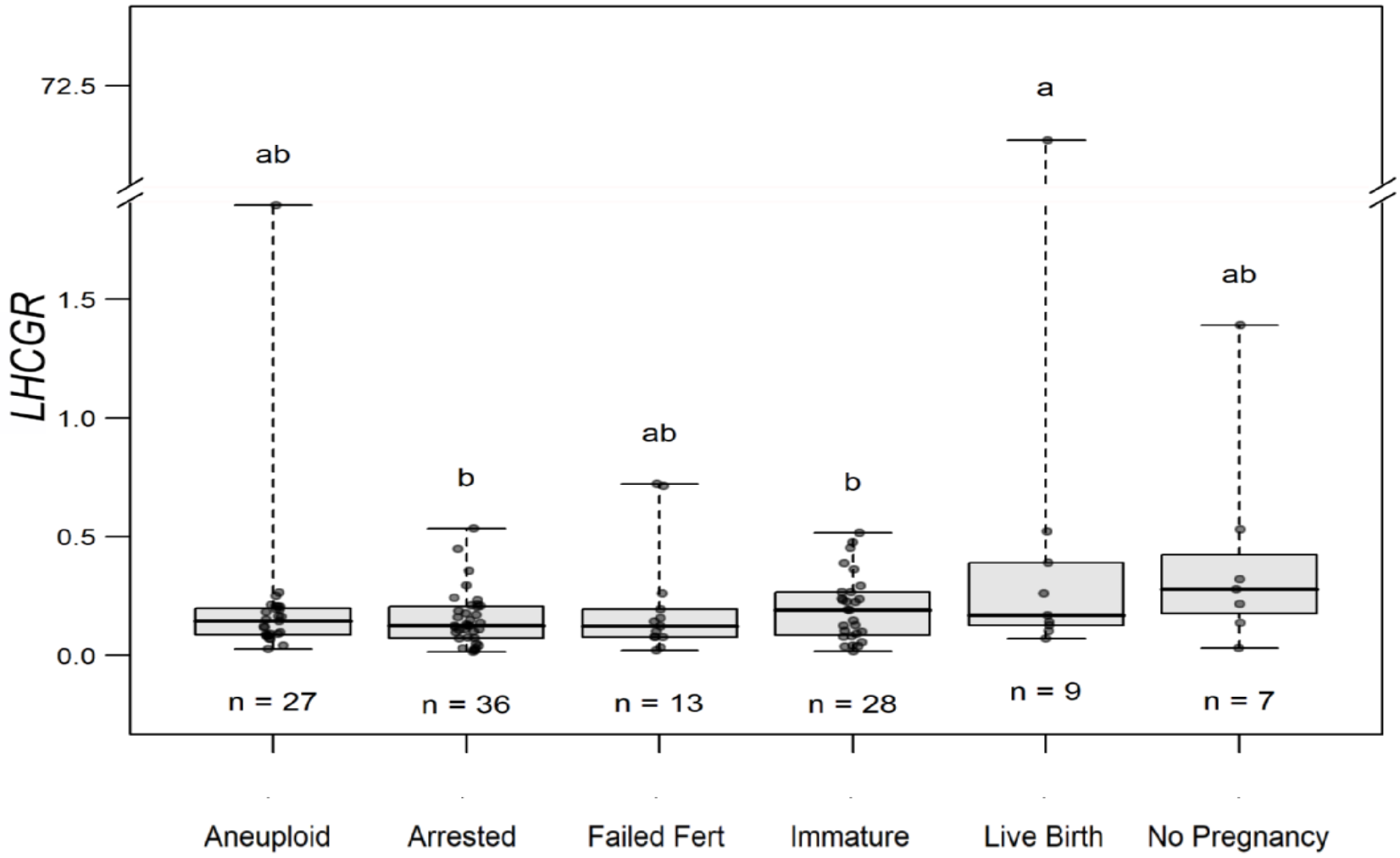

Figure 3.3 Continued

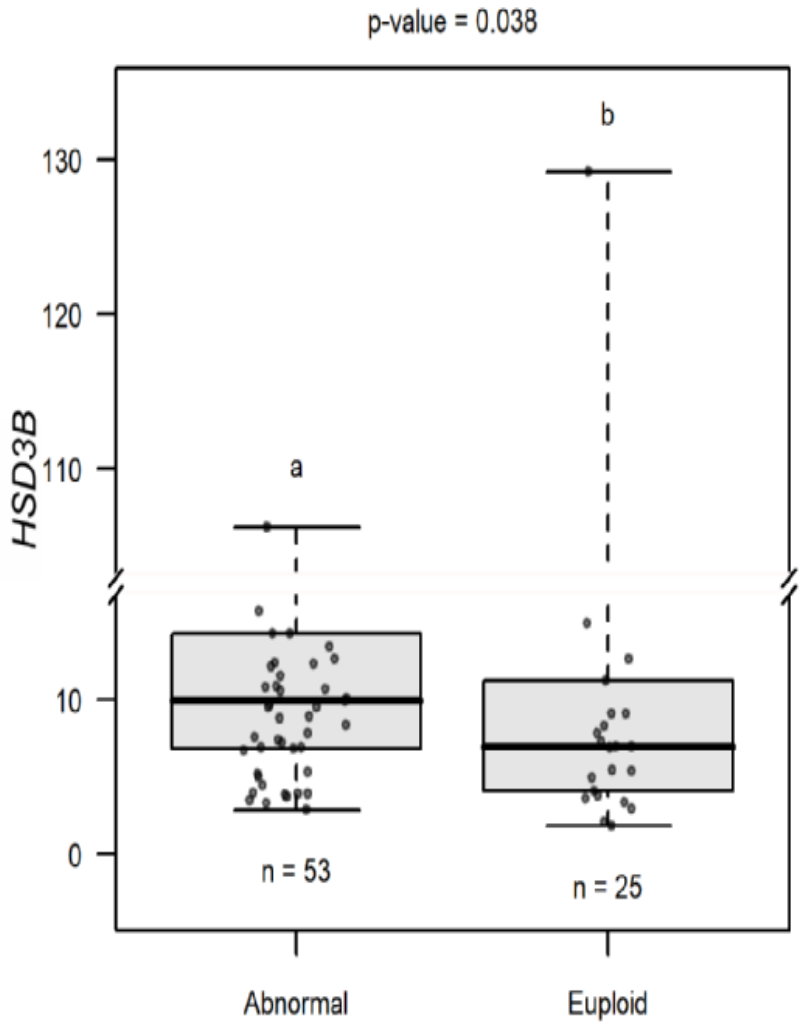
p-value = 0.038
HSD3B
130
120
110
10
0
a
b
n = 53
n = 25
Abnormal
Euploid

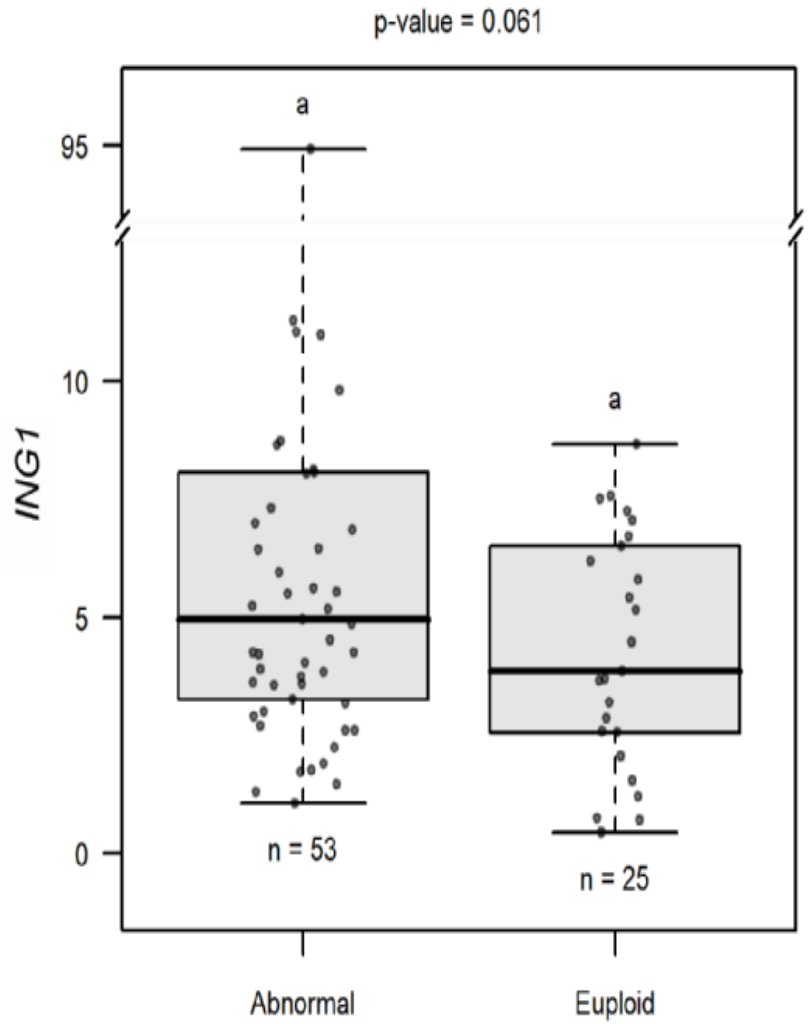
p-value = 0.061
ING1
95
10
5
0
a
a
n = 53
n = 25
Abnormal
Euploid

Figure 3.4 Biomarkers from the generalized linear mixed model associated with oocytes producing euploid embryos versus mature oocytes with other outcomes. To evaluate CC biomarker mRNA level association with oocytes capable of producing euploid embryos a model was fit with 78 CC samples from 11 patients and included the biomarkers: *CYP11A1, CYP19A1*, *HSD3B*, *IGFBP5*, *PAPPA*, *PGR*, *PGRMC1*, *ING1*, *LHCGR,* and *STARD1*. Higher *HSD3B* mRNA level significantly decreased the odds of an oocyte resulting in a euploid embryo (OR = 0.408, 95% CI: 0.175 to 0.953). Higher *ING1* mRNA levels marginally decreased the odds of an oocyte resulting in a euploid embryo (OR = 0.552, 95% CI: 0.297 to 1.027). Groups represent CC mRNA from oocytes with the following descriptions: Abnormal = mature oocytes resulting in aneuploid blastocysts, oocytes producing embryos that did not reach the blastocyst stage, and mature oocytes that failed to fertilize; Euploid = mature oocytes that resulted in euploid embryos regardless of whether they were transferred or remained vitrified. Data are presented as stated in figure 3.3 legend

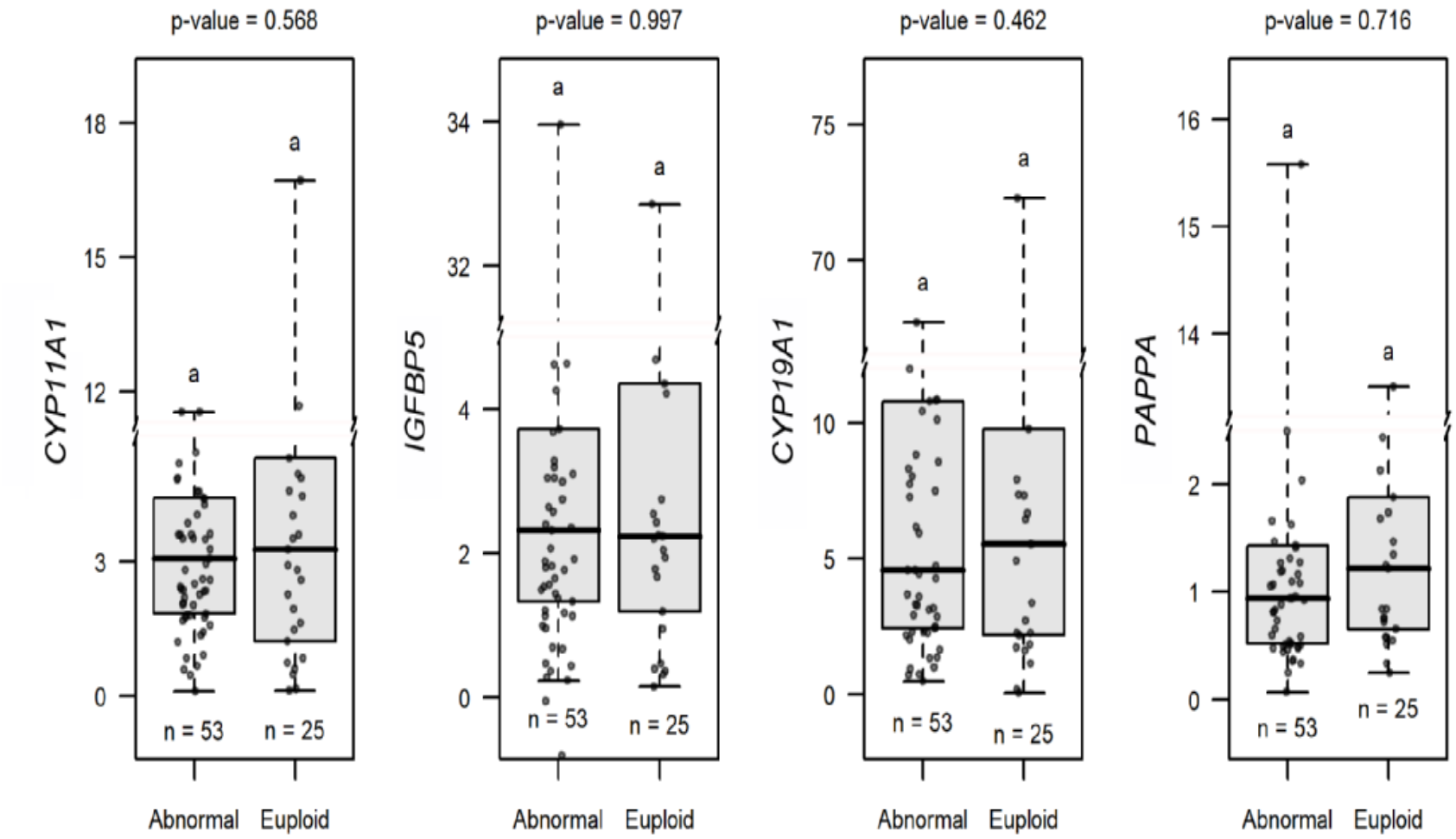

Figure 3.4 Continued

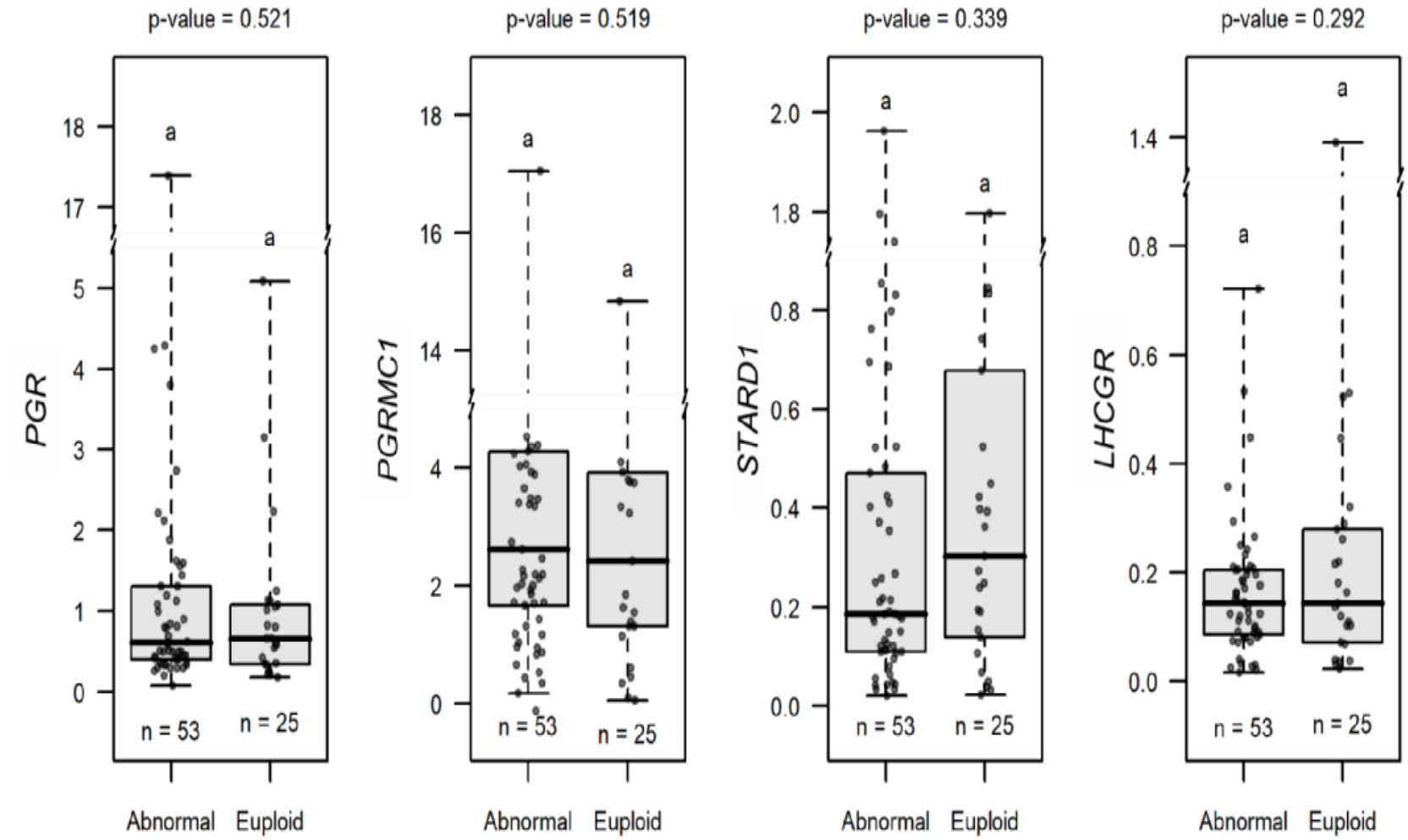

Figure 3.4 Continued

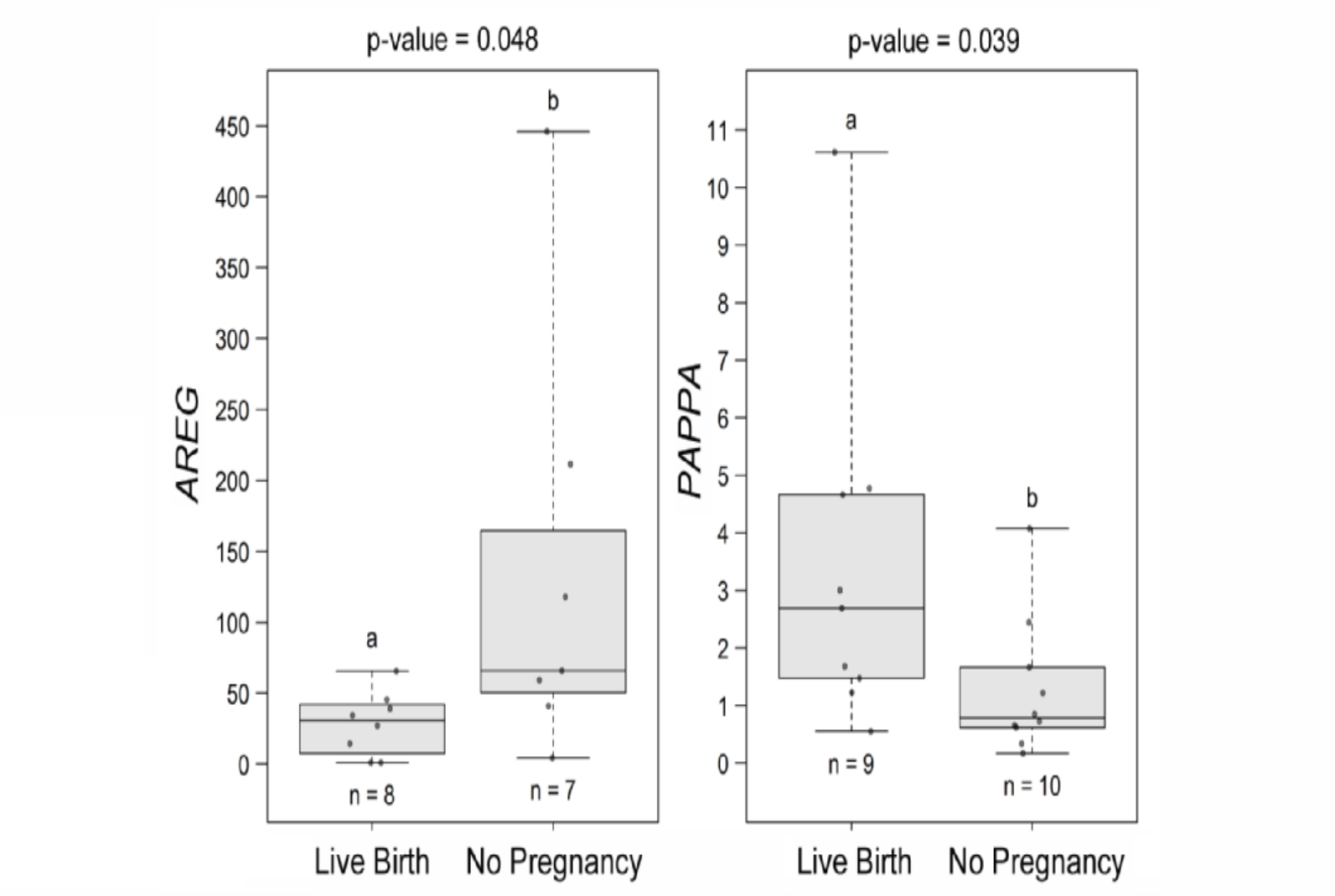
p-value = 0.048
AREG
450
400
350
300
250
200
150
100
50
0
a
b
n = 8
n = 7
Live Birth
No Pregnancy
p-value = 0.039
PAPPA
11
10
9
8
7
6
5
4
3
2
1
0
a
b
n = 9
n = 10
Live Birth
No Pregnancy

Figure 3.5 CC biomarkers associated with oocytes giving rise to euploid embryos with live birth or no pregnancy. Transferred embryos (n=19) from all 15 patients were assessed for mRNA level differences between those oocytes yielding embryos that resulted in a live birth and those that did not form a pregnancy using repeated measures ANOVA followed by Tukey's post hoc test (adjusted *P*-values) for pairwise comparisons. Of the transferred embryos, 9 resulted in live births. *AREG* mRNA levels were significantly lower in CCs from oocytes that resulted in live births (n = 8 from 8 patients) compared to the no pregnancy group (n = 7 from 5 patients) ($P < 0.05$). *PAPPA* mRNA expression was significantly increased in CCs from oocytes producing embryos that resulted in live births (n = 9 from 8 patients) compared to no pregnancy (n = 10 from 7 patients) ($P < 0.05$). *GREM1* mRNA levels (n = 3/group) were not significantly different and not shown. Data are presented as in figure 3.3 legend

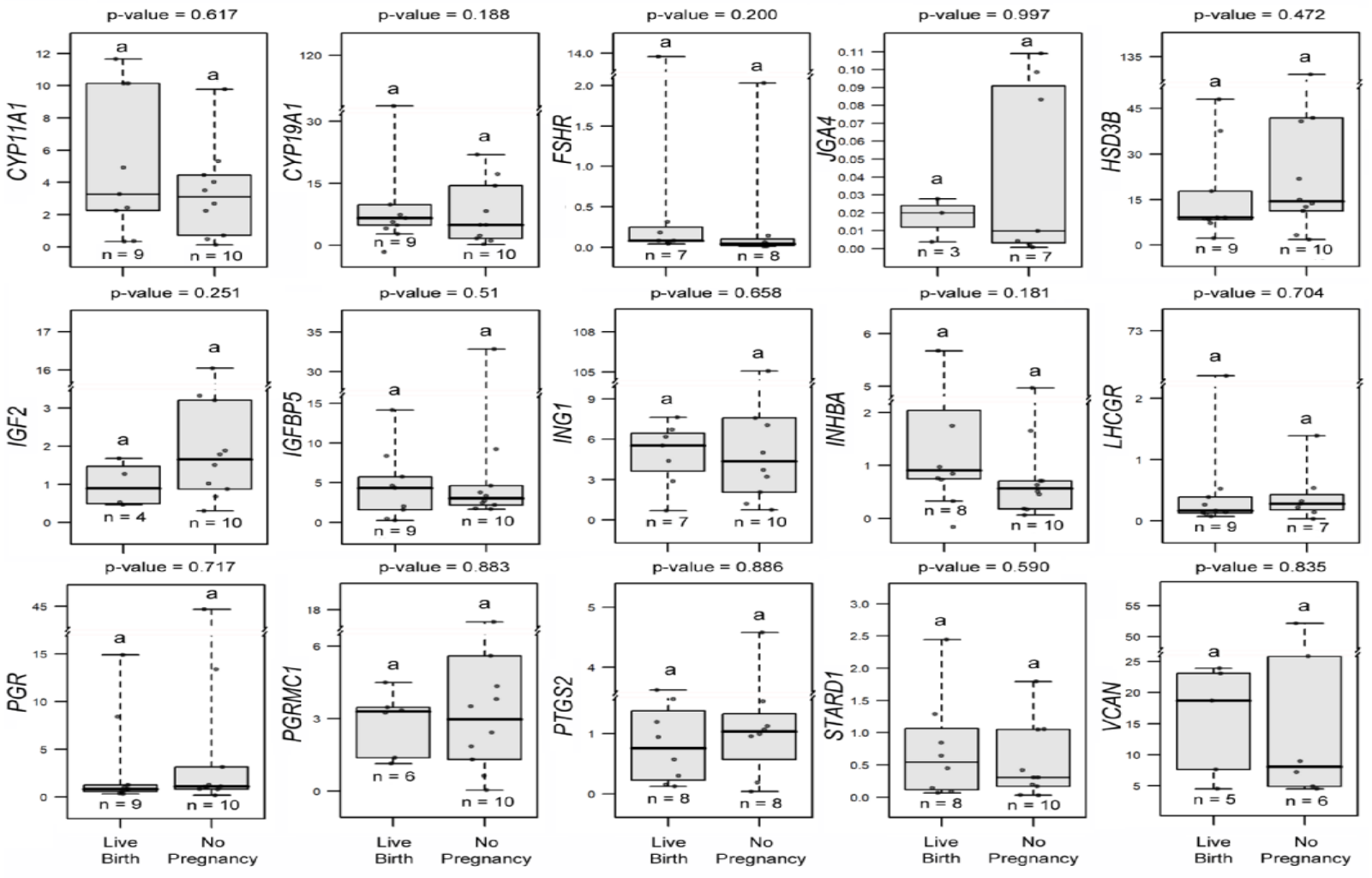

Figure 3.5 Continued

Table 3.3 Ploidy status and outcomes of biopsied embryos

Pt #	Embryo #	Ploidy Status	EXP	ICM	TROPH	ET	LB	NI	NT	NU
1	8	Euploid	5	A	B	X	X			
1	10	Euploid	2	B	B				X	
1	13	Euploid	5	B	B				X	
1	14	Euploid	3	B	B				X	
2	4	Euploid	6	A	B	X		X		
2	6	Monosomy	5	B	B					X
2	7	Monosomy	6	A	B					X
2	8	Monosomy	6	A	B					X
3	1	Euploid	5	A	B				X	
3	3	Monosomy	2	B	B					X
3	5	Triple Trisomy	5	A	B					X
3	7	Euploid	5	A	B	X	X			
4	2	Euploid	2	B	B	X	X			
4	4	Euploid	2	B	B				X	
4	7	Monosomy	2	B	B					X
4	8	Trisomy	2	B	B					X
4	11	Complex Aneuploid	2	B	B					X
4	12	Euploid	2	B	B				X	
5	3	Euploid	5	A	B	X	X			
5	4	Complex Aneuploid	5	C	C					X

Table 3.3 Continued

Pt #	Embryo #	Ploidy Status	EXP	ICM	TROPH	ET	LB	NI	NT	NU
5	6	Monosomy	5	A	B					X
5	8	Complex Aneuploid	3	B	B					X
5	9	XXX Super Female	5	A	A					X
6	2	Trisomy	5	A	B					X
6	6	Euploid	6	A	B	X		X		
7	3	Euploid	3	B	C	X		X		
7	6	Euploid	5	B	B				X	
7	7	Trisomy	5	B	B					X
7	8	Euploid	5	B	C	X		X		
7	11	Monosomy	2	B	B					X
8	2	Monosomy	5	A	B					X
8	3	Double Monosomy	3	C	C					X
8	6	Monosomy	5	A	A					X
8	7	Euploid	5	A	B	X	X			
9	1	Euploid	4	B	A	X		X		
9	2	Euploid	3	A	A				X	
9	10	Complex Aneuploid	2	B	B					X
9	15	Complex Aneuploid	2	B	B					X

Table 3.3 Continued

Pt #	Embryo #	Ploidy Status	EXP	ICM	TROPH	ET	LB	NI	NT	NU
10	1	Complex Aneuploid	4	B	C					X
10	4	Complex Aneuploid	4	B	C					X
10	5	Euploid	4	B	C	X	X			
11	3	Euploid	5	A	A	X	X			
11	6	Euploid	5	A	B				X	
11	7	Monosomy	5	B	B					X
11	8	Euploid	5	B	C				X	
11	13	Trisomy/Monosomy	5	B	A					X
11	14	Monosomy	5	A	B					X
11	15	Monosomy	5	A	A					X
11	17	Euploid	5	A	B				X	
11	18	Euploid	5	A	A				X	
11	19	Monosomy	3	A	B					X
11	20	Euploid	5	A	A	X	X			
11	22	Euploid	5	B	B				X	
12	5	Euploid	5	A	B	X	X			
12	6	Euploid	5	A	A				X	
12	7	Trisomy	5	A	A					X
12	8	Trisomy	5	B	B					X
12	12	Euploid	5	B	B				X	

Table 3.3 Continued

Pt #	Embryo #	Ploidy Status	EXP	ICM	TROPH	ET	LB	NI	NT	NU
12	14	Euploid	5	A	A				X	
12	16	Trisomy	5	A	A					X
12	17	Monosomy	5	A	B					X
13	3	Euploid	4	B	B				X	
13	7	Euploid	5	B	B	X		X		
14	2	Euploid	4	B	B	X		X		
14	4	Euploid	4	B	A	X		X		
14	5	Trisomy	4	A	B					X
14	14	Euploid	4	B	C				X	
15	3	Trisomy	4	A	A					X
15	4	Euploid	3	B	B	X		X		
15	6	Euploid	3	B	B				X	
15	8	Euploid	4	A	A				X	
15	10	Euploid	4	B	B				X	
15	11	Monosomy	4	A	B					X
15	17	Euploid	4	B	B	X		X		

EXP = blastocyst expansion grade; ICM = inner cell mass grade; Troph = trophectoderm grade; ET = transferred embryo; LB = live birth; NI = no implantation;
NT = not transferred (cryopreserved); NU = not used

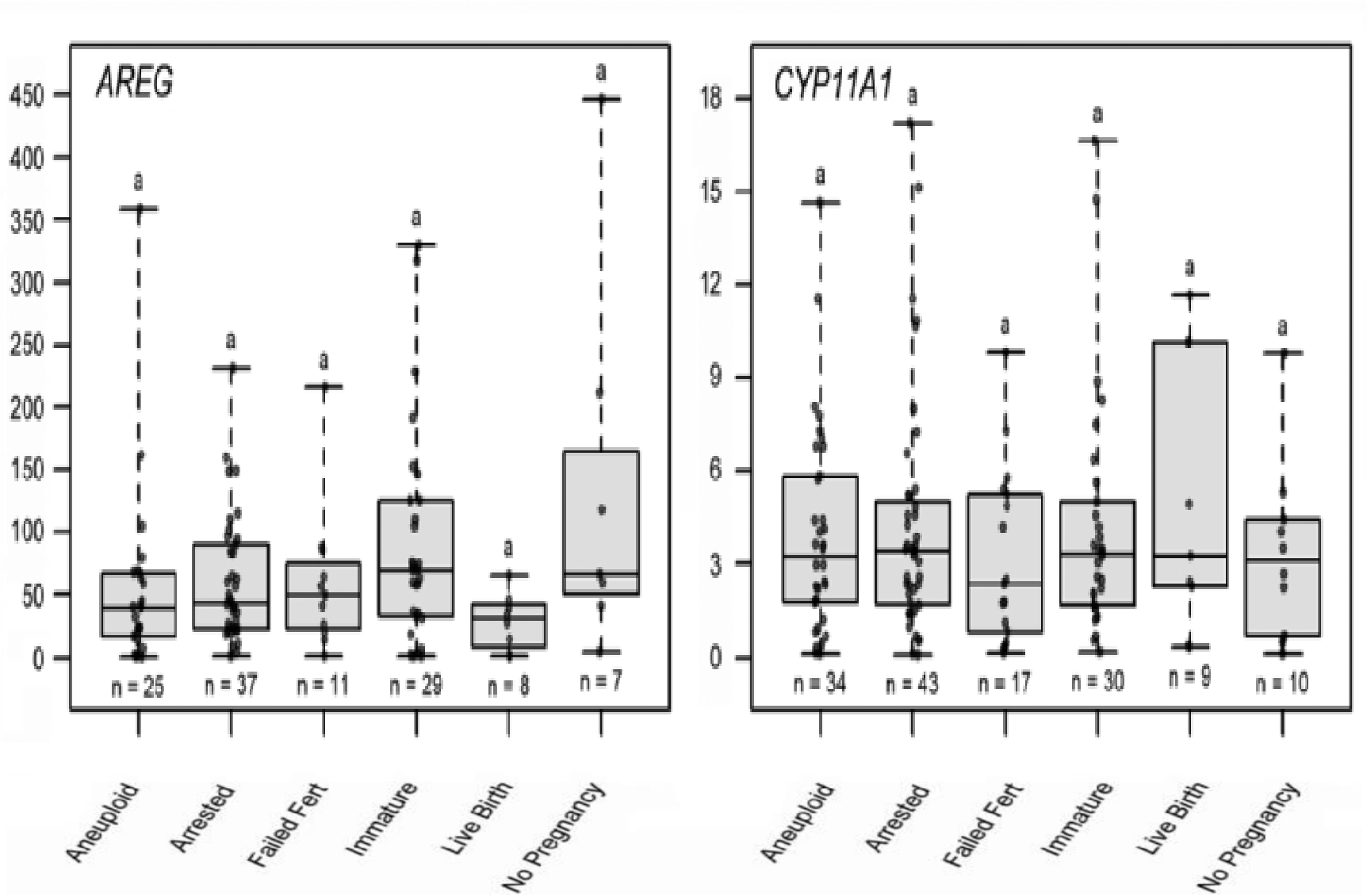
AREG
450
400
350
300
250
200
150
100
50
0
a
n = 25
n = 37
n = 11
n = 29
n = 8
n = 7
Aneuploid
Arrested
Failed Fert
Immature
Live Birth
No Pregnancy
CYP11A1
18
15
12
9
6
3
0
n = 34
n = 43
n = 17
n = 30
n = 9
n = 10
Aneuploid
Arrested
Failed Fert
Immature
Live Birth
No Pregnancy

Figure 3.6 Biomarkers for CC mRNA expression not associated with mature oocyte competence and embryo outcomes. To determine the differences in CC mRNA between groups where oocytes had different developmental and embryo outcomes target mRNA levels were compared using repeated measures ANOVA followed by Tukey's post hoc test (adjusted *P*-values) for pairwise comparisons. Groups represent CC mRNA from oocytes with the following descriptions: Aneuploid = mature oocytes resulting in aneuploid embryos; Arrested = mature oocytes resulting in embryos that did not reach the blastocyst stage; Failed Fert = mature oocytes that did not fertilize; Immature = immature oocytes that were not fertilized; Live Birth = oocytes that resulted in transferred euploid embryos that resulted in live births; No Pregnancy = oocytes that resulted in transferred euploid embryos that did not result in a pregnancy. No differences were seen in these biomarkers ($P > 0.05$). Data are presented as stated in figure 3 legend

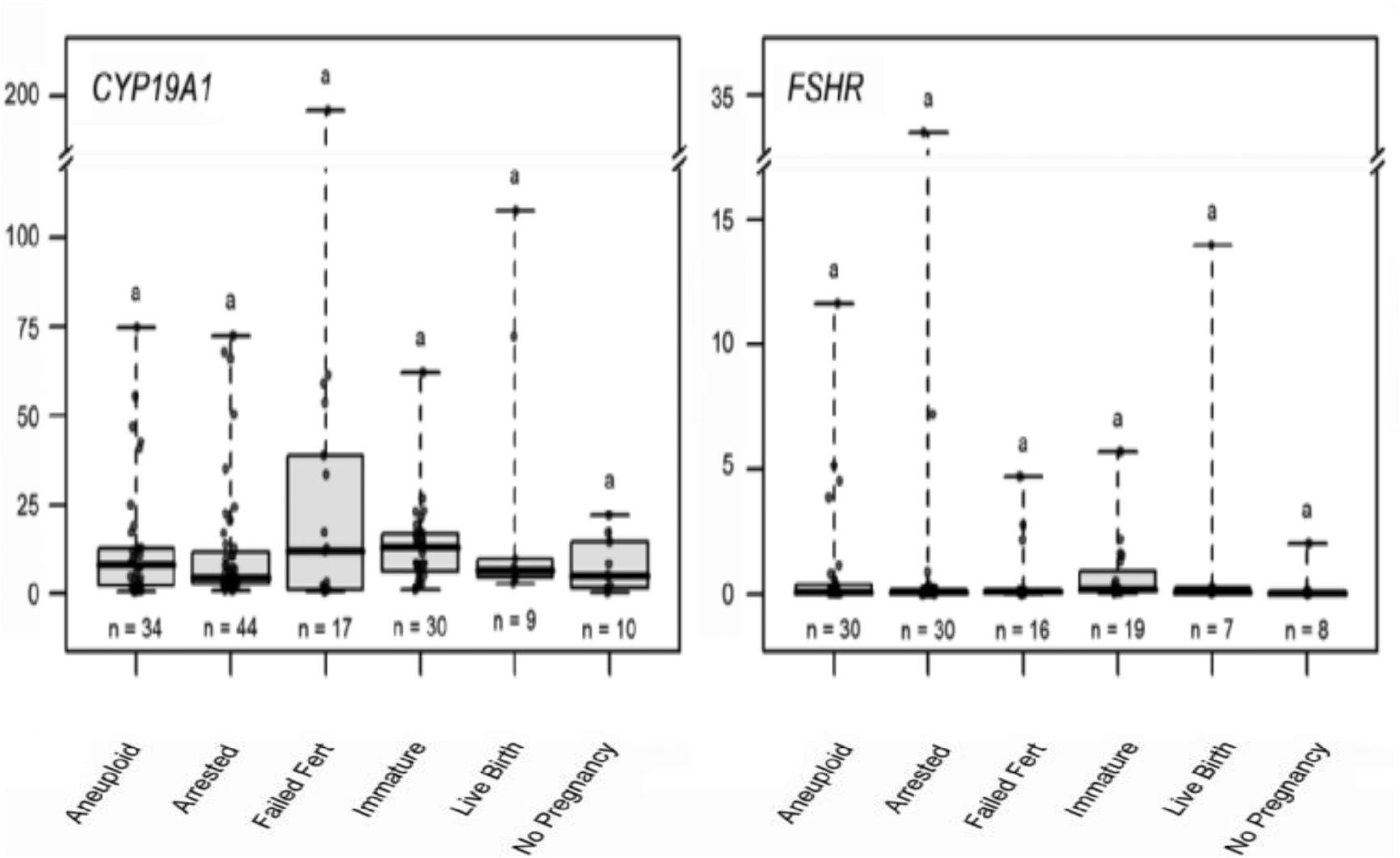

Figure 3.6 Continued

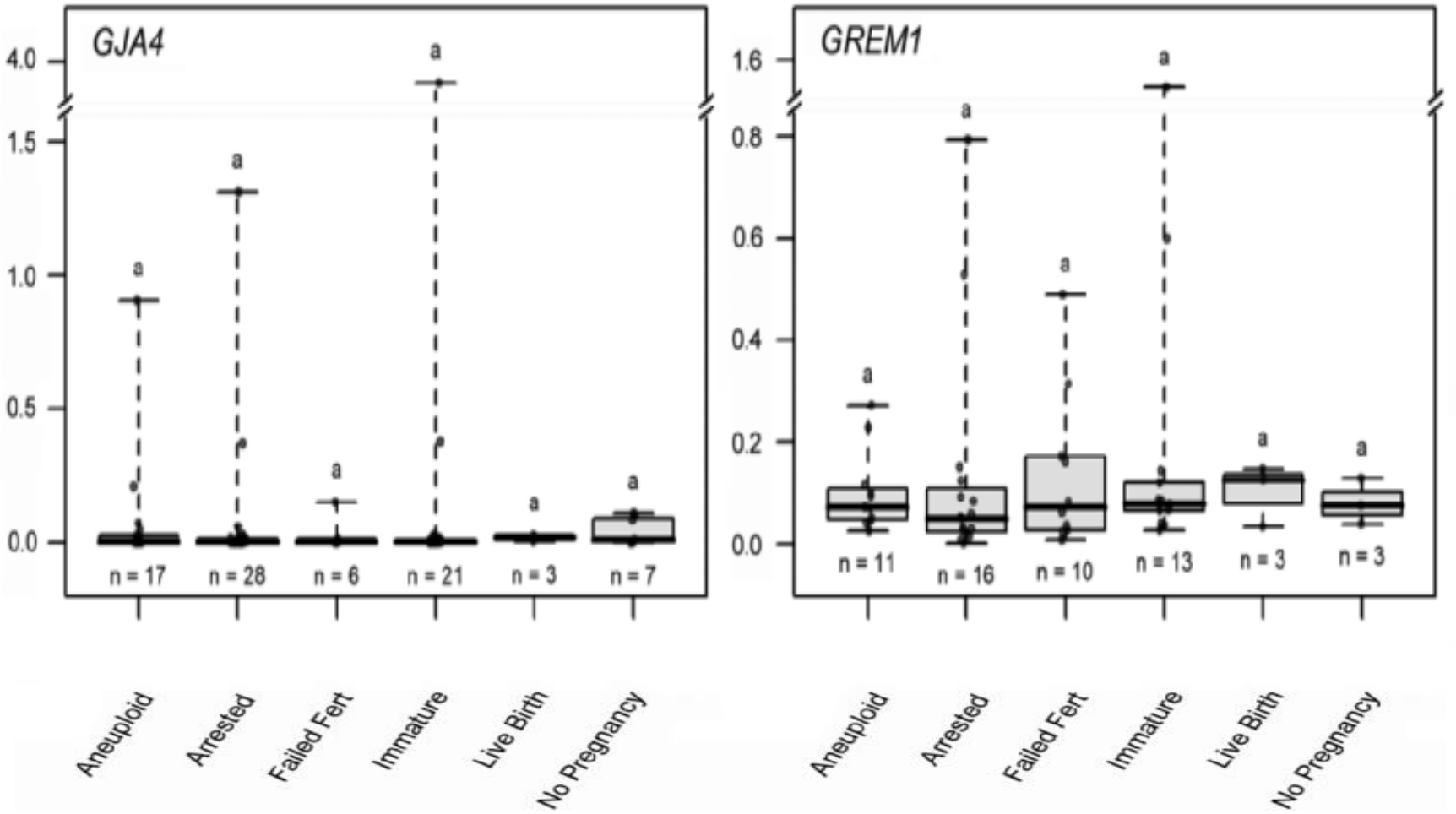

Figure 3.6 Continued

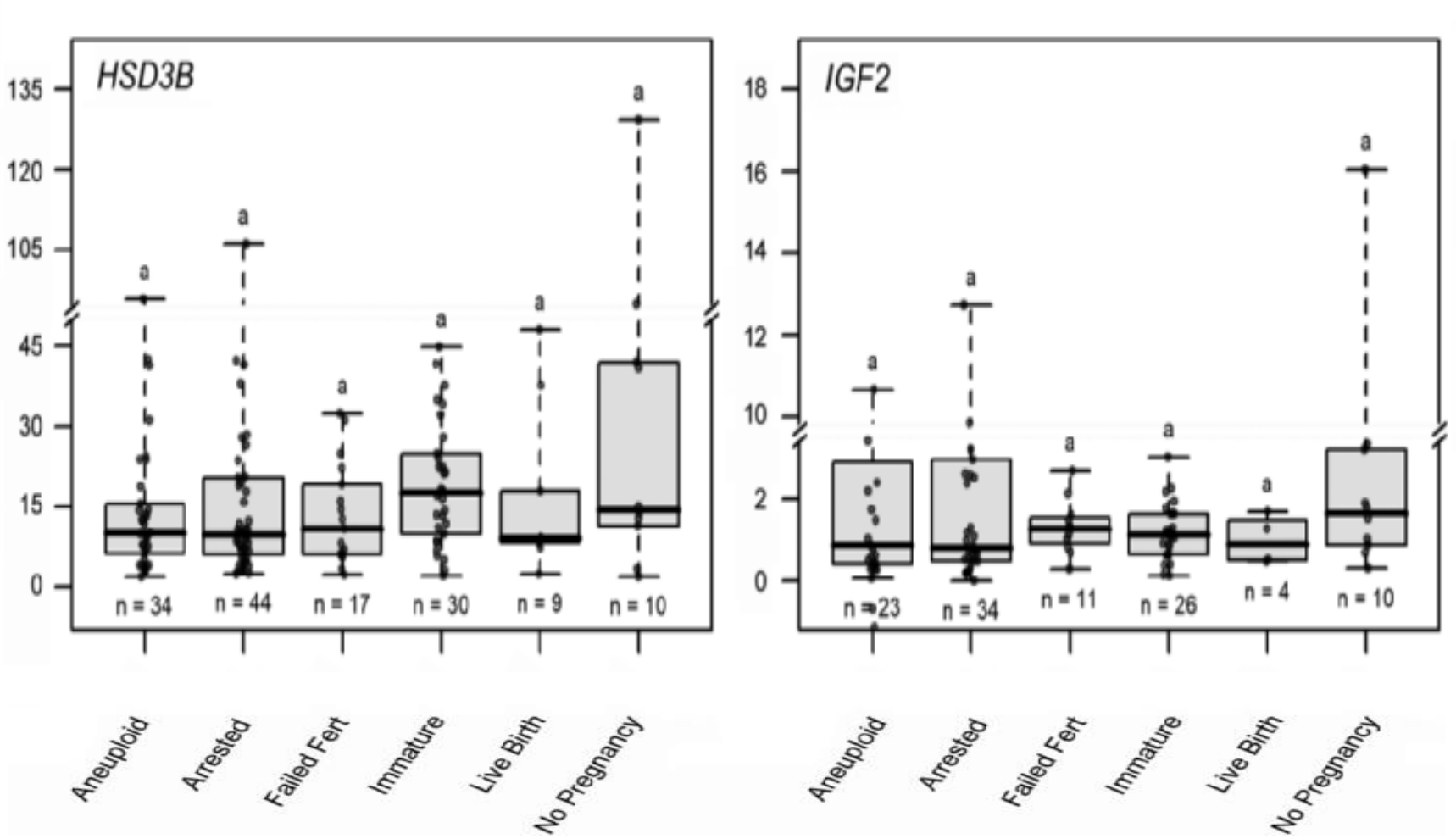

Figure 3.6 Continued

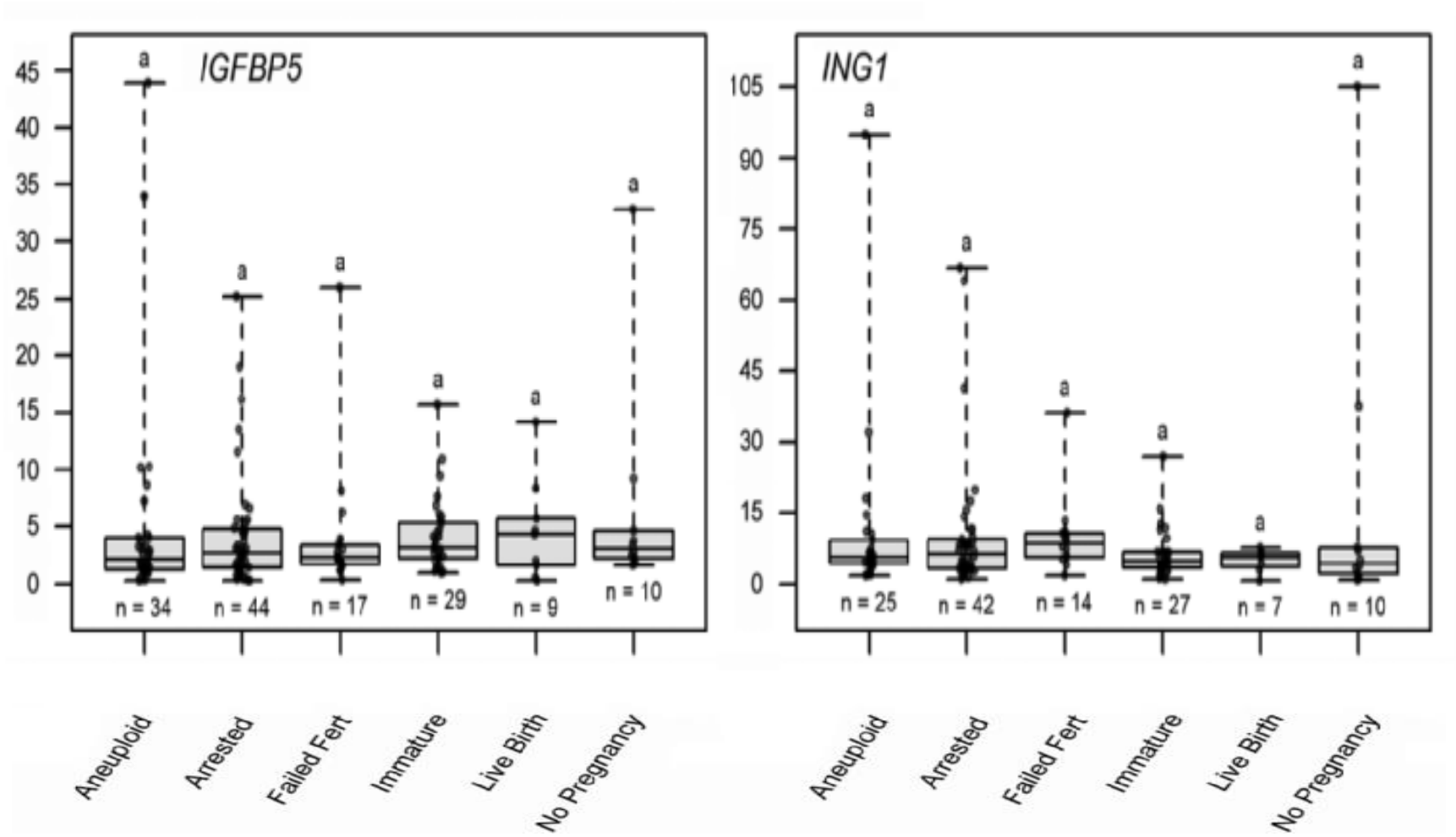

Figure 3.6 Continued

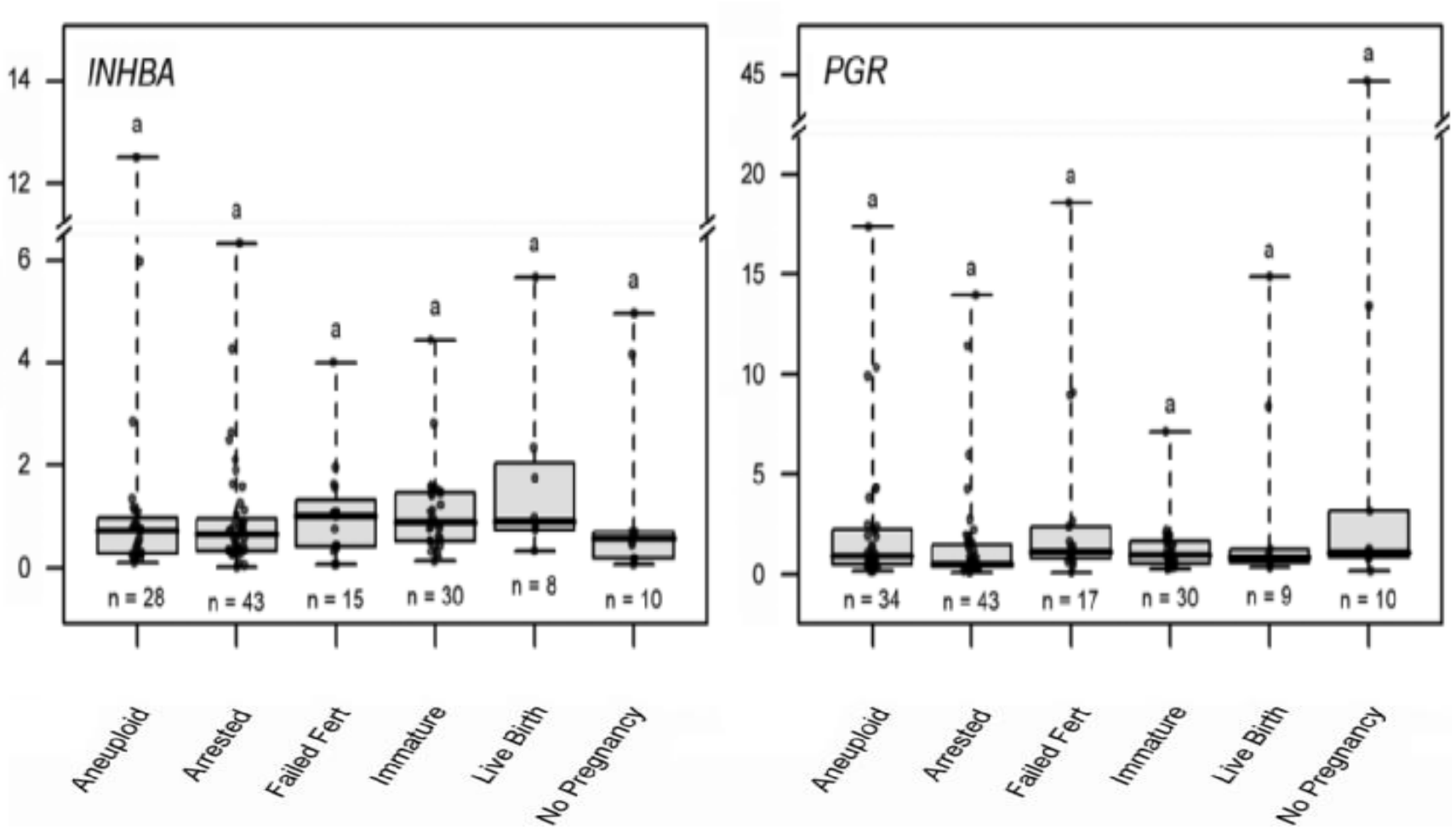

Figure 3.6 Continued

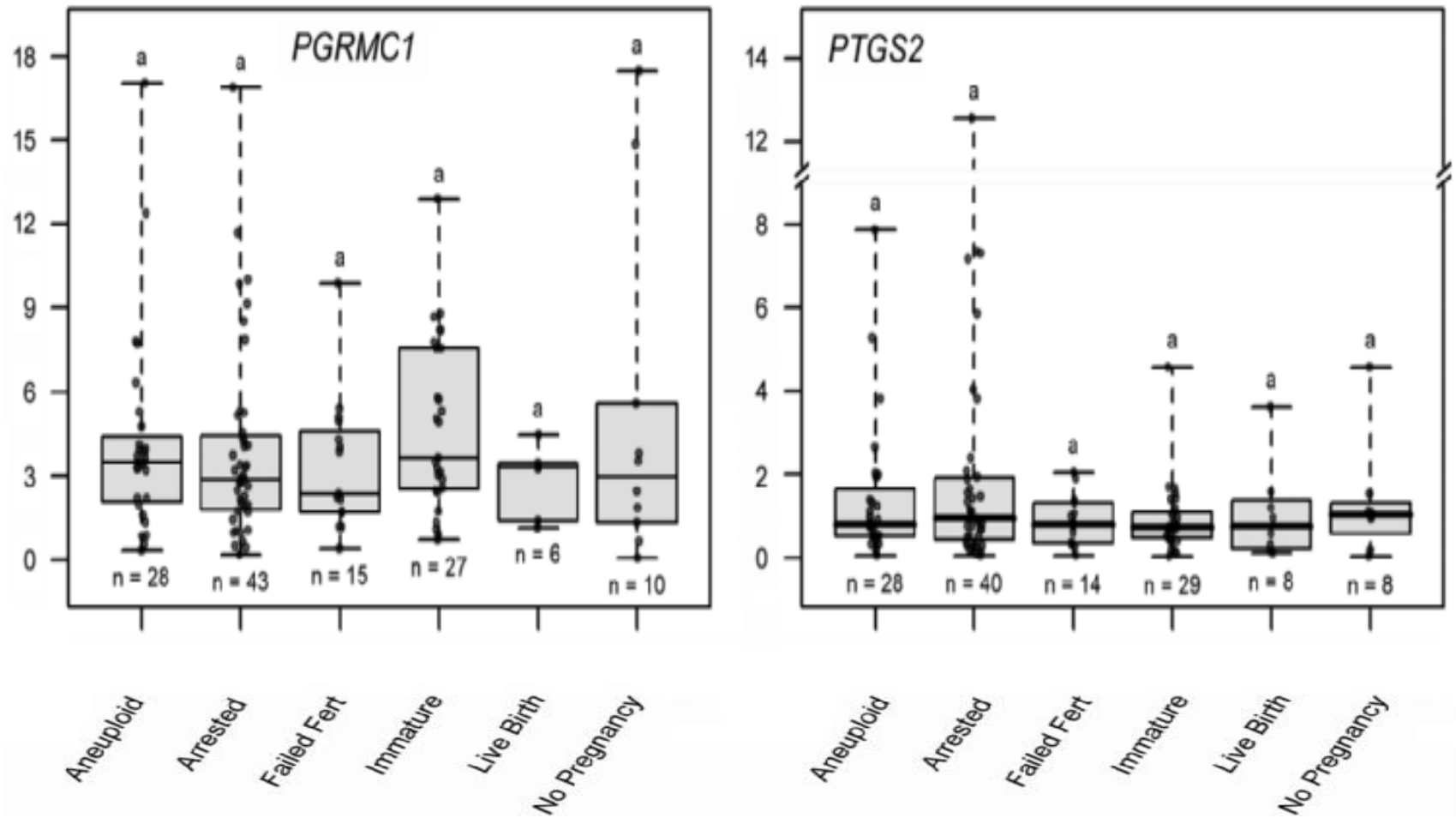

Figure 3.6 Continued

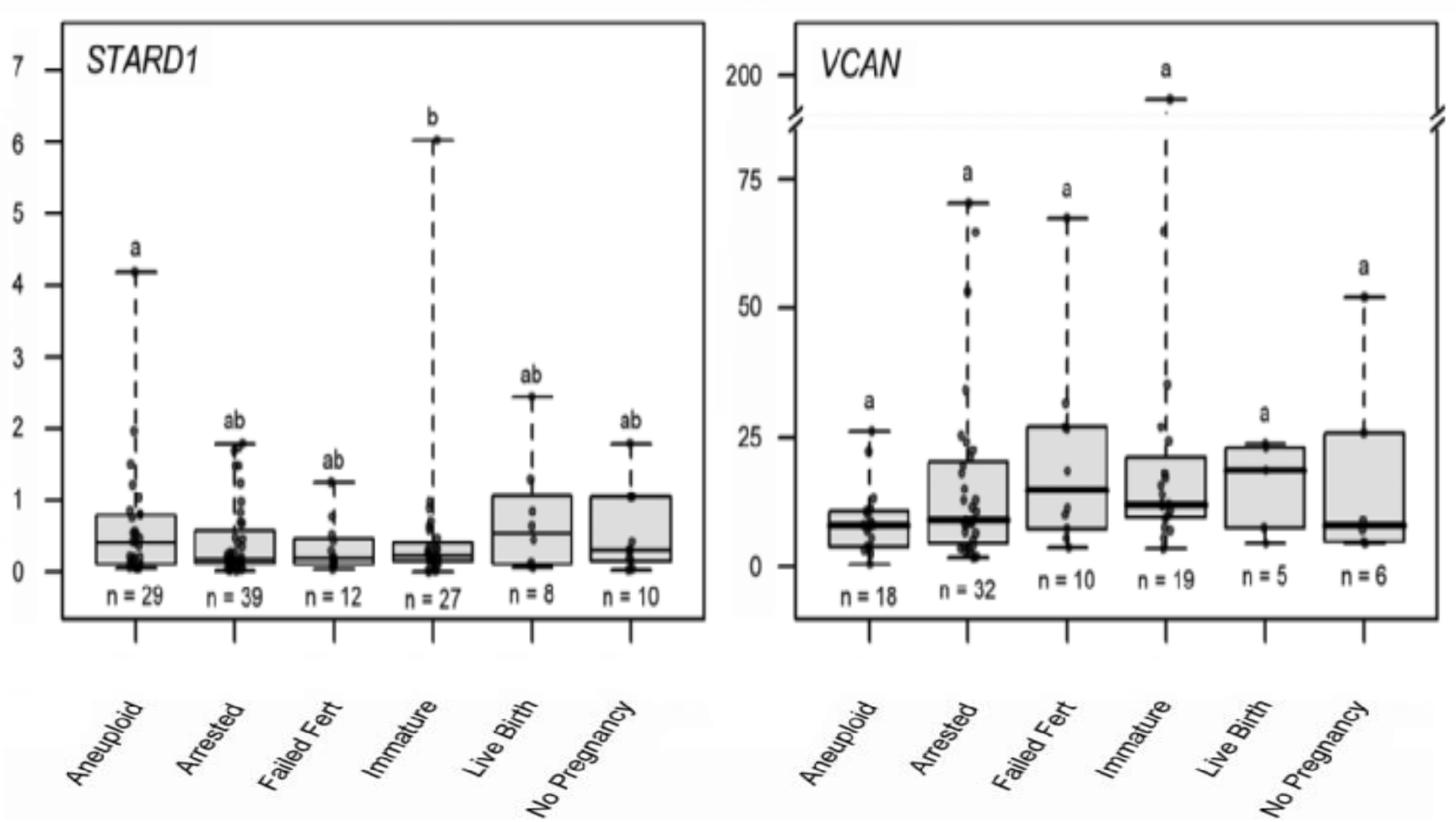

Figure 3.6 Continued

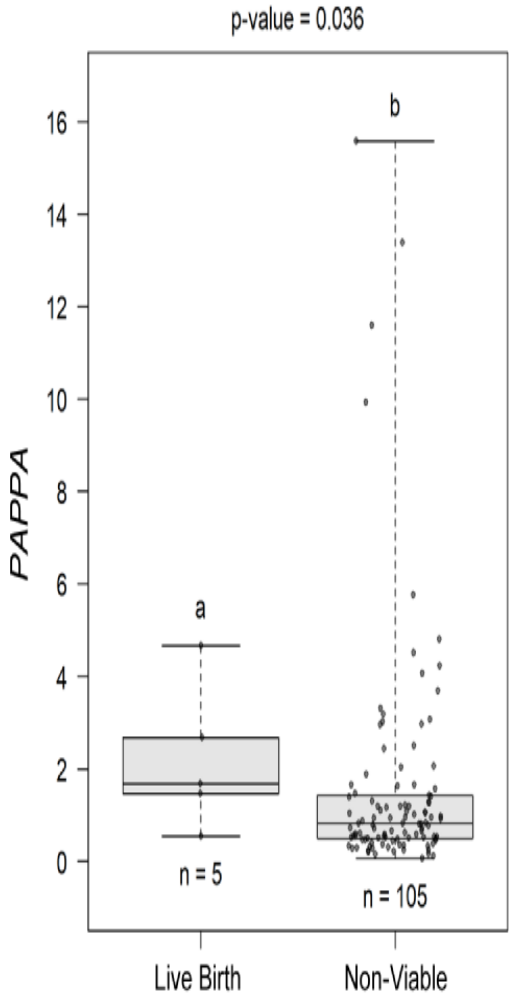

Figure 3.7 Generalized linear mixed model distinguishing CC from oocytes giving rise to live births and oocytes with outcomes not resulting in live birth, collectively. To evaluate the potential of CC biomarker mRNA levels to identify oocytes capable of producing euploid embryos resulting in a live birth versus groups not producing live births, the best fitting model included 110 CC samples from 14 patients and included biomarkers: *CYP11A1, CYP19A1*, *IGFBP5*, *PAPPA*, *PGRMC1,* and *STARD1*. Increased *PAPPA* mRNA expression ($P < 0.05$) significantly increased the odds of an oocytes producing an embryo resulting in a live birth (OR = 4.591, 95% CI: 1.098, to 19.201). All previously stated categories were included in this model except oocytes yielding euploid embryos that were not transferred. Groups represent CC mRNA from oocytes with the following descriptions: Live Birth = mature oocytes that resulted in euploid embryos that lead to live births; Non-Viable = immature oocytes, mature oocytes resulting in aneuploid blastocysts, oocytes producing embryos that did not reach the blastocyst stage, and mature oocytes that failed to fertilize, collectively. Data are presented as in figure 3 legend

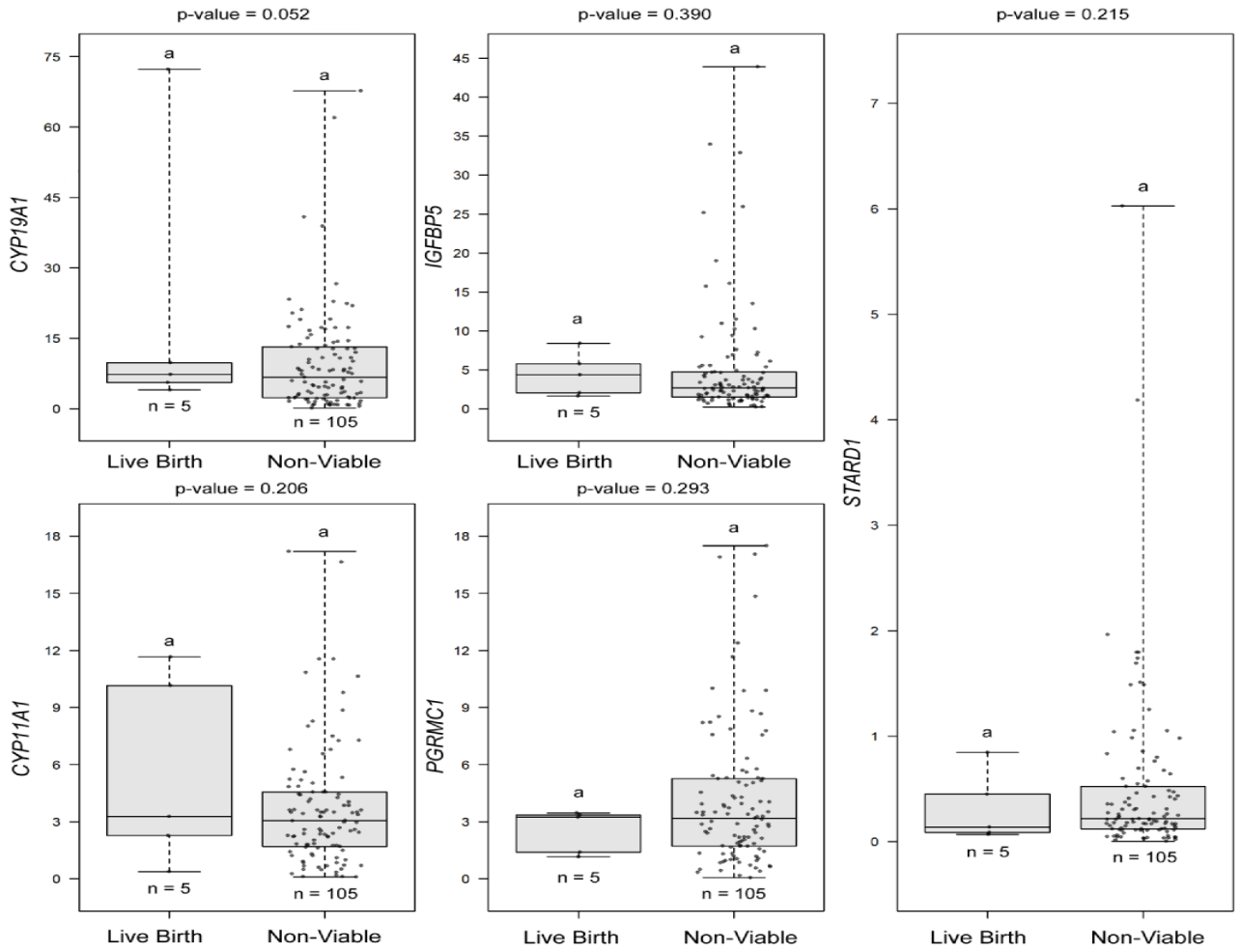

Figure 3.7 Continued

Chapter 4

Mitochondrial Metabolic Substrate Utilization in Granulosa Cells Reflects Body Mass Index and Total Follicle Stimulating Hormone Dosage in In Vitro Fertilization Patients[4]

---

[4]R.J. Kordus, A. Hossain, H.E. Malter, and H.A Lavoie. Submitted to Journal of Assisted Reproduction and Genetics

4.1 Abstract

4.1.1 Purpose: To utilize a novel mitochondrial function assay with pooled granulosa cells to determine whether mitochondrial function would differ by patient demographics and embryo development.

4.1.2 Methods: Prospective pilot study in a hospital based assisted reproductive program and public university. The study assessed mitochondrial metabolic substrate utilization and mRNA levels in pooled granulosa cells from 40 women undergoing in vitro fertilization during 2018 and 2019.

4.1.3 Results: In pooled granulosa cells, mitochondrial utilization of citric acid ($P < 0.01$), L-malic acid ($P < 0.05$), and octanoyl-L-carnitine ($P < 0.01$) were significantly lower with lower body mass index. Citric acid ($P < 0.05$), cis-acontic acid ($P < 0.01$), D-alpha-keto-glutaric acid ($P < 0.05$), L-glutamine ($P < 0.05$), and alanine-glycine ($P < 0.05$) were significantly lower with increasing FSH administered. Utilization of glycogen ($P < 0.05$) was significantly lower with lower fertilization rates and D-alpha-keto-glutaric acid ($P < 0.05$) was significantly lower in good 8-cell embryos. L-glutamine ($P < 0.05$) was significantly higher with lower blastocyst formation. Mitochondrial metabolic scores, which reflect overall mitochondrial activity of granulosa, were significantly higher with increased numbers of zygotes formed ($P < 0.05$), higher BMI ($P < 0.05$), less FSH administered ($P < 0.01$), and with greater numbers of mature oocytes ($P < 0.05$).

4.1.4 Conclusions: Body mass index and FSH dose administered were associated with mitochondrial utilization of citric acid, L-malic acid, octanoyl-L-carnitine, cis-acontic acid, D-alpha-keto-glutaric acid, L-glutamine, and alanine-

glycine. Glycogen, D-alpha-keto-glutaric acid, and L-glutamine may be possible biomarkers for embryo development.

4.1.5 Key Words: granulosa cells, in vitro fertilization, mitochondrial function assay, mitochondrial metabolic score, mitochondrial utilization

4.2 Introduction

Mitochondria are double-membrane organelles, which are believed to have originated from a symbiotic relationship between bacteria and host cells (Margulis, 1996). They are involved in apoptosis, calcium homeostasis, fatty acid oxidation, and metabolism. Mitochondria, the key source of power within eukaryotic cells, are responsible for generating 88% of a cell's total energy in the form of adenosine triphosphate (ATP) created during oxidative phosphorylation via mitochondrial membrane potential (Seyfried and Shelton, 2010). The remaining ATP required by the cell is produced from the processes of glycolysis and the tricarboxylic acid cycle through substrate-level phosphorylation. Oxidative phosphorylation is modulated by the cellular demand for ATP and the substrates available for processing within the cytoplasm. Glucose is the main substrate that will produce ATP via the intermediates of glycolysis. Pyruvate and other substrates of the glycolytic process will generate reducing equivalents, nicotinamide adenine dinucleotide hydride (NADH) and flavin adenine dinucleotide hydride ($FADH_2$), which will transfer electrons to the electron transport chain (ETC). The flow of electrons through the ETC will provide mitochondrial membrane potential ultimately producing ATP (Veatch et al., 2009).

Successful embryo development relies upon energy metabolism generated by ATP processed through the mitochondria to drive the cleavage of blastomeres and other cellular processes during early embryo development. While human oocytes contain the most mitochondrial of all cell types within the body, it is problematic to relate mitochondrial DNA (mtDNA) copy number and function to oocyte developmental competence; since the oocytes, and subsequent embryos, are required for clinical use. However, parallels between mtDNA content in human oocytes and granulosa cells (GCs), including both cumulus cells (CCs) and mural granulosa cells (MGCs), have been demonstrated (Boucret et al., 2015, Pawlak et al., 2016). Additionally, the metabolism of CCs directly affects their enclosed oocytes by providing the proper energy substrates required to complete meiosis and fertilization. Cumulus cells produce ATP and augment oocyte ATP supply during follicular growth. The CCs also provide pyruvate, generated from glycolysis, to their enclosed oocytes via gap junctions (Su et al., 2009, Sutton-McDowall et al., 2010). Further, mitochondrial function, measured by ATP production in CCs, has been shown to relate to proper human oocyte maturation and in vitro fertilization (IVF) outcomes (Dalton et al., 2014, Huang and Wells, 2010, Tsai et al., 2010).

Assessing mitochondrial substrate metabolism in GCs may allow for a non-invasive method for investigating oocyte competence and embryo development. Several studies have evaluated CCs, MGCs, and trophectoderm cells from blastocysts; and it appears there is a high correlation between the mtDNA content found in oocytes and CCs indicating that GC mtDNA might serve

as a biomarker for oocyte competence (Desquiret-Dumas et al., 2017, Diez-Juan et al., 2015, Fragouli and Wells, 2015, Ogino et al., 2016, Boucret et al., 2015). Furthermore, increased mtDNA GC copy numbers are associated with good quality embryos (Ogino et al., 2016, Desquiret-Dumas et al., 2017). Therefore, we hypothesized mitochondrial substrate utilization in pooled GCs, measured using a novel mitochondrial function assay, will also show correlations between various demographic and embryo endpoints.

The goal of this study was to see how individual substrates and total substrate utilization differed between patients based on age, serum anti-Mullerian hormone (AMH) level, body mass index (BMI), and number of mature oocytes retrieved per cohort. We also related individual and total substrate utilization to fertilization rates, day 3 embryo development, blastocyst development, and mRNA levels of selected genes to determine if one or more substrates can be used as a biomarker for IVF. In a recent investigation by our laboratory, several candidate mRNA transcripts in individual cumulus masses showed associations with viable embryos capable of leading to live births (Kordus et al., 2019), and these mRNAs were also investigated in this study. Genes of interest included, amphiregulin (*AREG*), which is associated with cumulus mass expansion; inhibitor of growth protein 1 (*ING1*), which is associated with oocyte maturation; aromatase (*CYP19A1*), cytochrome p450 family 11 subfamily A member 1 (*CYP11A1*), and hydroxy-delta-5-steroid dehydrogenase, 3 beta- and steroid delta-isomerase 1 (*HSD3B1*), which are associated with mediating de novo steroidogenesis, estrogen, and progesterone production; pappalysin-1 (*PAPPA*),

which is related to hormone modulation; and luteinizing hormone/choriogonadotropin receptor (*LHCGR*), which encodes for it's associated hormone receptor. We also examined *AMH* mRNA due to the relationship of serum AMH with ovarian reserve.

To our knowledge, this is the first study to examine a novel mitochondrial function assay to assess the metabolism of mitochondrial substrates in pooled GCs. The assay measures the rate of electron flow through the electron transport chain from 31 metabolic substrates that, when metabolized by cell preparations, produce NADH or $FADH_2$ using a tetrazolium dye (Bochner et al., 2001). The primary goal of this study was to determine if metabolic substrate utilization differed between patient groups and embryo cohorts. We also wanted to determine if a mitochondrial metabolic score could be generated from the overall metabolic rate of the substrates combined, that would be related to patient groups and primary embryo developmental endpoints.

4.3 Materials and methods

4.3.1 Study Population, Participants, and GC isolation

This study was a prospective cohort pilot study. In total, 817 pooled CCs and MGCs from 40 patients undergoing infertility treatment at Fertility Center of the Carolinas (Greenville, SC, USA) were analyzed (Figure 4.1). Of 58 starting patients, those with total GC numbers <650,000 per sample were excluded from the study (n=14), as well as patients with appropriate GC numbers where the positive assay control did not exhibit color change (n=4). Patient demographics and cycle information were collected for each cycle (Table 4.1). The patients'

assay data were compared based on age, serum AMH levels, BMI, and number of mature oocytes retrieved per cohort. Each patient's ovaries were stimulated using a long luteal protocol or an antagonist protocol. In the antagonist cycles, when one follicle reached 13 or 14 mm or the patient's estradiol level reached 300 IU/mL a GnRH antagonist (Cetrotide, EMD-Serono, USA or Ganirelix, EMD-Serono, USA) was administered. In both protocols, when 3 follicles reach >17 mm by ultrasound an ovulatory dose of human chorionic gonadotropin (hCG) (Pregnyl, EMD-Serono, USA) was delivered. Thirty-six hrs later patients underwent oocyte retrieval. Each CC mass was mechanically separated from it's oocyte and rinsed in medium (Sperm Wash Medium, Irvine, USA) to remove blood and debris and all CC masses per retrieval were combined in a single tube. The CCs and MGCs from each patient were taken to the research lab on ice for immediate processing.

4.3.2 Embryo culture and ploidy assessment

Mature oocytes were inseminated via intra-cytoplasmic sperm injection. Fertilization was confirmed by the presence of two pronuclei and two polar bodies 16-18 hrs after insemination. Embryos were group cultured in 50 µL LifeGlobal® global total media drops (Cooper Surgical, Trumbull, CT, USA) under oil (Ovoil, Vitrolife, Englewood, CO, USA) at 37°C, 6% CO_2, 5% O_2, 89% N_2 in a humidified atmosphere until day 5 or day 6 post retrieval. Embryo morphologies were assessed using the American Society for Reproductive Medicine (ASRM) (Racowsky et al., 2010) criteria for day 3 embryos and day 5/6 blastocysts.

4.3.3 Analysis of Mitochondrial Metabolic Substrates

Follicular fluid, containing MGCs from each patient, was split between 2 or more 50 mL tubes and centrifuged for 15 min at 300xg. A filtered solution of hyaluronidase (50 mg/mL) from bovine testes (Sigma, Raleigh, NC, USA) in media was added to each MGC pellet and the CC tube and incubated at 37°C for 10 min to dissociate cell clumps. Calcium/magnesium-free phosphate-buffered saline (PBS) (Gibco, Gaithersburg, MD, USA) was added to bring the pellet to approximately 4 mL. MGCs were purified by 35%-70% discontinuous Percoll gradient in 15 mL tubes and spun in a swinging bucket centrifuge for 30 min at 300xg. Assay mix (30 µL) containing 2x Biolog Mitochondrial Assay Solution (MAS) (Biolog, Hayward, CA, USA), 6x Redox Dye (Biolog), 24x saponin (90 µg/mL) for permeabilization (Alfa Aesar, Ward Hill, MA, USA), and sterile water were added to each well of the 96-well MitoPlate S-1 plates (Biolog) and incubated for 1 hr per manufacturer's instructions. Mural granulosa cells (the uppermost band in the gradient) were removed and combined with CCs in 25 mL of calcium/magnesium-free PBS (Gibco). The mixture was poured through a 70-micron strainer to remove any remaining cell clumps. Pooled GCs were centrifuged for 20 min, and the pellet was resuspended in 1x MAS (Biolog) to a volume of 2 mL. A 0.5 mL aliquot of the GC/MAS mixture was removed and a 10 µL sample was counted using a hemocytometer. This remainder of the aliquot was centrifuged for 5 min, and the pellet was placed in 0.5 mL RNAlater solution (Life Technologies), stored at 4°C for 24 hrs, and snap-frozen in LN_2 and stored until it was transported to the University of South Carolina School of Medicine and

stored at -70°C until processed. The remaining 1.5 mL GC/MAS mixture was diluted to 3.0 mL with 1x Biolog MAS and a 10 µL sample was counted with a hemocytometer. After 1 hr incubation at 37°C to allow all substrates to dissolve, 30 µL of the GC/MAS suspension was added to each well of the MitoPlate S-1 plate. Permeabilized cells were assayed in triplicate for metabolism of individual substrates (Table 4.2) using MitoPlate S-1 plates. Metabolism of substrates was assessed by a colorimetric change of a terminal electron acceptor tetrazolium redox dye at an optical density of 590 nm read every 2.5 min for 50 cycles on a kinetic plate reader (Figure 4.2). The slopes of the optical density absorbance readings were normalized to mtDNA copy number per sample (as described below) and the relative absorbance of the negative control wells containing GC/MAS without any additional substrates. To quantitatively compare the metabolism of each patient we developed a scoring system based on the aggregate slope ratios of all substrates normalized to the negative control and positive control wells. The mitochondrial metabolic score was the total of all the slope ratios of each substrate for each individual patient. Slope ratio = [Slope (sample) – Slope (negative control)] / [Slope (positive control) – Slope (negative control)] (Vanderstichel et al., 2015).

4.3.4 RNA Isolation and cDNA synthesis

RNA was isolated from each pooled CC/MCG sample per patient using the Direct-zol MiniPrep Kit with DNase treatment (Zymo Research, Irvine, CA, USA) following the manufacturer's instructions. RNA concentration and purity for pooled samples were assessed at the wavelengths of 260 and 280 nm using a

biophotometer 6131 spectrophotometer (Eppendorf). Each sample was reverse transcribed into cDNA using the iScript kit (Bio-Rad Laboratories, Hercules, CA, USA) following the manufacturer's instructions. The reverse transcription reaction was carried out in a thermocycler (Eppendorf), for 5 min at 25°C, 30 min at 42°C, and 5 min at 85°C.

4.3.5 DNA Isolation and Quantification

DNA was isolated from pooled GCs using the Direct-zol MiniPrep Kit (Zymo Research) as described above, omitting the DNase treatment step. DNA concentration and purity were assessed at the wavelengths of 260 and 280 nm using a biophotometer 6131 (Eppendorf). Relative amounts of mtDNA and nuclear DNA content (nDNA) and were determined by qRT-PCR (described below). The ratio of mtDNA:(2x nDNA) was used to determine mtDNA content.

4.3.6 Quantitative Real-Time PCR

Synthesized primers were cartridge purified (Life Technologies). Primers to amplify cDNA included: *AMH*, *AREG*, *CYP19A1*, *HSD3B1*, *ING1*, *LHCGR*, *PAPPA,* and TATA-box binding protein (*TBP*) (Table 4.3). The nuclear gene *ACTB* (beta-actin) was selected as a reference gene to calculate nDNA and the mtDNA gene mitochondrially encoded ATP synthase 8 (*MT-ATP-8*) was used to quantify mitochondrial genome content. Real-time PCR reactions were run with 2 or more wells per sample for 40-45 cycles and threshold cycle (Ct) values were averaged. The reactions included 5 ng starting cDNA, 300 nM of each upstream and downstream primer, and 10 µL 2X SsoAdvanced Universal SYBR Green Supermix (Bio-Rad Laboratories) and sterilized PCR-grade water to a final volume to 20 µL

per well. PCR-grade water was substituted for the cDNA as a negative control. PCR amplification was performed using the iCycler iQ Real-Time PCR Detection System (Bio-Rad Laboratories). *TBP* mRNA was used as an internal control for cDNA samples (Kordus et al., 2019) and actin beta (*ACTB*) DNA was used as an internal control for nuclear DNA (nDNA) samples (Diez-Juan et al., 2015). Target RNA and DNA quantities were derived from a standard curve made using serial dilutions of its purified amplicon. *TBP* has extensively been tested as a control gene in our laboratory with human GCs under multiple conditions and treatments and has not been found to be regulated under any circumstances. Target mRNA values were expressed relative to values of the *TBP* mRNA control.

4.3.7 Statistical analysis

Multiple linear regression models were estimated to predict the normalized average rate of each substrate's metabolism and mitochondrial metabolic score using Box-Cox transformation for normality (Box and Cox, 1964). Each substrate was assessed separately, and a mitochondrial metabolic score was created based on the slopes of the normalized absorbance readings of all substrates combined. The mitochondrial metabolic scores were normalized against the mtDNA content in each sample. The individual substrate rates and the mitochondrial metabolic scores were related to patient demographics. To determine the relationship between mitochondrial metabolic score and mRNA levels, Pearson's correlation analysis was used with both variables being Box-Cox transformed. We determined statistical significance of findings by $P < 0.05$ and considered the findings with 0.05

< P < 0.10 to be borderline significant. Statistical analysis was performed using the statistical analysis environment R 3.6.2 (R Core Team, 2019).

4.4 Results

In total, 817 oocytes and associated GCs were harvested from 40 patients undergoing fertility treatment. The CCs were combined with the MGCs from each patient. Thirty-seven out of 40 patients had at least one fresh or frozen embryo transfer (FET) and currently 49% of patients who did receive an ET either have ongoing pregnancies or have delivered a child.

We examined the mitochondrial metabolic profile of IVF patients using a novel mitochondrial function assay, Mitoplate S-1 which examined 31 different substrates. In hypothesis one, we tested whether individual substrate utilization by pooled granulosa mitochondria would differ according to age, serum AMH levels, BMI, and total number of mature oocytes retrieved per patient cohort. Absorbance readings in the assay reflected metabolism of utilization of substrates. To test this hypothesis, we analyzed the averaged normalized absorbance readings of each metabolic substrate within the comparison groups using a multiple linear regression model using Box-Cox transformation examining the independent variables of age, BMI, serum AMH, mature oocytes per cohort, antral follicle count, stimulation type, amount a HMG given, and amount of FSH administered. Age, BMI, serum AMH were divided into higher and lower groups as follows: Older age ≥ 34 years old and younger age < 34 years old; high BMI ≥ 26 kg/m^2 and low BMI < 26 kg/m^2; and higher serum AMH ≥ 3.5 ng/mL and lower serum AMH < 3.5 ng/ml. Based on the estimated multiple linear regression model

using observed data, patient mitochondrial utilization of citric acid ($P < 0.01$), L-malic acid ($P < 0.05$), and octanoyl-L-carnitine ($P < 0.01$) were found to be significantly lower (Figure 4.3), and mitochondrial utilization of cis-acontic acid ($P < 0.10$), D,L-beta-hydroxy-butyric acid ($P < 0.10$), and pyruvic acid/L-malic acid 100 µM ($P < 0.10$) were found to be borderline lower in patients with lower BMI in pooled GCs, while no other substrates demonstrated utilization differences by BMI in the model, after adjusting for the other factors in the model (Figure 4.4). Individuals with a greater number of mature oocytes were found to have a significant increase for alpha-keto-isocaproic acid mitochondrial utilization by pooled granulosa ($P < 0.01$) (Figure 4.5). No other substrates demonstrated utilization differences in the model (Figure 4.6). Additionally, patient mitochondrial utilization for citric acid ($P < 0.05$), cis-acontic acid ($P < 0.01$), D-alpha-keto-glutaric acid ($P < 0.05$), L-glutamine ($P < 0.05$), and alanine-glycine ($P < 0.05$) were found to be significantly lower (Figure 4.7), and mitochondrial utilization of D,L-isocitric acid ($P < 0.10$), D,L-beta-hydroxy-butyric acid ($P < 0.10$), L-glutamic acid ($P < 0.10$), acetyl-L-carnitine ($P < 0.10$), pyruvic acid/L-malic acid 100 µM ($P < 0.10$) were found to be borderline lower in pooled GCs of patients with higher administered FSH dosages, after adjusting for the other factors in the model while no other substrates demonstrated mitochondrial utilization differences for the number of mature oocytes in the model (Figure 4.8).

The second hypothesis tested was that a mitochondrial metabolic score generated from the aggregate metabolism of the pooled GCs would differ according to age, serum AMH levels, BMI, and total number of mature oocytes

retrieved per patient cohort. To test this, we analyzed the mitochondrial metabolic scores using a multiple linear regression model using Box-Cox transformation examining the independent variables of age, BMI, serum AMH level, number of mature oocytes, zygote fertilization, good 8-cell embryo development, and overall blastocyst formation per patient cohort. Based on the estimated multiple linear regression model using observed data, mitochondrial metabolic scores were found to be significantly higher in granulosa of patients with higher numbers of mature oocytes retrieved ($P < 0.05$), after adjusting for the other factors in the model (Figure 4.9). In a backward selected best fit model using only the BMI and total FSH dosage administered, mitochondrial metabolic scores were found to be significantly lower in pooled GCs of patients with a lower BMI ($P < 0.05$) (Figure 4.9), and significantly lower as the patient's FSH dose administered increased ($P < 0.01$) (Figure 4.9).

Our third hypothesis predicted that individual substrates metabolized by mitochondria in GCs of patients would differ by overall embryo cohort development. We created a multiple linear regression model using Box-Cox transformation looking at fertilization percentage, percentage good 8-cell embryo development on day 3, and percentage of blastocyst development by day 6. The 3 groups were divided into higher and lower groups as follows: higher fertilization percentage ≥ 80%, and lower fertilization percentage < 80%; higher good 8-cell development > 55% and lower good 8-cell development ≤ 55%; and higher percentage of blastocyst formation > 55% and lower percentage of blastocyst formation ≤ 55%. One patient was excluded from the blastocyst formation data as

she had an embryo transfer on day 3 with no additional embryos available for extended culture. Based on the estimated multiple linear regression model using observed data, mitochondrial utilization of glycogen ($P < 0.05$) was found to be significantly lower in pooled GCs of patients with lower fertilization percentage (Figure 4.10). No other substrates demonstrated utilization differences for fertilization in the model (Figure 4.11). In contrast, patient mitochondrial utilization of D-alpha-keto-glutaric acid ($P < 0.05$) was found to be significantly higher (Figure 4.10), and L-serine ($P < 0.10$) was found to be borderline higher in granulosa of patients with a lower percentage of good quality 8-cell embryos (Figure 4.12). In addition, patient mitochondrial utilization of D-gluconate-6-phosphate ($P < 0.10$), and D,L-isocitric acid ($P < 0.10$) was found to be borderline higher in patients with a lower percentage of blastocyst formation in pooled GCs, after adjusting for the other factors in the model (Figure 4.13). In a backward selected best fit model using only the percentage of good 8-cell embryos and percentage of blastocysts, GC mitochondrial utilization of L-glutamine ($P < 0.05$) was found to be significantly higher in patients with a lower percentage of blastocyst formation (Figure 4.10) and L-glutamine ($P < 0.10$) was found to be borderline higher in patients with a lower percentage of good quality 8-cell embryos in pooled GCs(Figure 4.12).

A fourth critical hypothesis we wanted to test was that a mitochondrial metabolic score generated from the aggregate metabolism of the pooled GCs would be associated with better overall embryo development. To test this hypothesis, we analyzed the patient mitochondrial metabolic score using a multiple linear regression model using Box-Cox transformation examining the independent

variables of age, BMI, AMH level, mature oocytes per cohort, zygote fertilization, good 8-cell embryo development, and overall blastocyst formation. Based on the estimated multiple linear regression model using observed data, mitochondrial metabolic scores were found to be significantly higher in granulosa cells of patients with higher overall number of fertilized zygotes ($P < 0.05$) in pooled GCs, after adjusting for the other factors in the model (Figure 4.14).

Finally, we wanted to test the hypothesis that the mitochondrial metabolic score would be differ with mRNA levels of the genes: *AMH, AREG*, *CYP19A1*, *CYP11A1*, *HSD3B1*, *ING1*, *LHCGR*, and *PAPPA*. In order to test this hypothesis, we used Pearson's correlation analysis with both variables being Box-Cox transformed, which demonstrated that *HSD3B* levels we borderline lower ($P < 0.10$) as the mitochondrial metabolic score decreased (Figure 4.13). No other mRNA levels varied.

4.5 Discussion

To our knowledge this is the first use of this mitochondrial function assay to investigate mitochondrial metabolic substrate utilization in the pooled GCs of IVF patients. The mitochondrial function assay plates utilized in our study contained 31 cytoplasmic and mitochondrial metabolic substrates to profile the metabolic capabilities of mitochondria in pooled GC from individual patients. Each well in the plate contained an individual chemical as the sole energy source. The substrates were metabolized through different biochemical pathways by entering the mitochondria through different transporters and they were then modified by various enzymes and dehydrogenases to produce NADH or $FADH_2$ (Figure 4.16).

Deviations in the mitochondrial metabolism of the substrates were detected by chemometric alterations in the energy-rich redox dye. As the cells metabolized the energy source, tetrazolium dye in the media was reduced, generating a purple color according to the amount of NADH or $FADH_2$ reducing equivalents generated and reflected the biochemical reactome of the substrates by the mitochondria (Bochner et al., 2001).

Our main goal was to determine if mitochondrial metabolic substrates in pooled GCs of IVF patients were significantly associated with patient age, serum AMH levels, BMI, or the number of mature oocytes retrieved per cohort. Secondly, we wanted to determine if mitochondrial substrate utilization was related to embryo cohort development. We hypothesized that mitochondria would metabolize the individual substrates at differing rates based on patient demographics and embryo cohort development. We also hypothesized that the overall mitochondrial metabolic utilization of all the substrates in the plate, combined, would allow us to score each patient's overall GC mitochondrial function and perhaps be used as a prediction tool for embryo development.

The key findings of our research were that GC mitochondrial utilization of the assay's metabolic substrates citric acid, L-malic acid, and octanoyl-L-carnitine were found to be significantly lower in patients with lower BMI indicating a potential increase in oxidative phosphorylation and perhaps reactive oxygen species production in overweight patients. Citric acid and L-malic acid are both components of the tricarboxylic acid cycle. The conversion of L-malic acid to oxaloacetate by malate dehydrogenase produces NADH which is processed

through the ETC. Octanoyl-L-carnitine is a medium chain fatty acid that catabolizes to several acetyl-CoA molecules and feeds into the tricarboxylic acid cycle. Granulosa cell utilization of citric acid, cis-acontic acid, D-alpha-keto-glutaric acid, L-glutamine, and alanine-glycine in the assay were found to be significantly lower in patients with higher administered FSH dosages using a multiple linear regression model. This indicates that the total FSH dose required to produce follicle maturation is associated with suppressed mitochondrial activity by the pool of granulosa. Cis-acontic acid and D-alpha-keto-glutaric acid are both components of the tricarboxylic acid cycle. The conversion of D-alpha-keto-glutaric acid by alpha-ketoglutarate dehydrogenase produces NADH which is processed through the ETC. L-glutamine, converted to alpha-ketoglutarate through glutamate dehydrogenase, enters the tricarboxylic acid cycle at that juncture. Alanine-gflycine will be converted into pyruvic acid and enters the tricarboxylic acid cycle after pyruvic acid is converted to acetyl-CoA. Four out the 7 substrates altered by either BMI and/or FSH were substrates directly involved in the citric acid cycle. Octanoyl-L-carnitine, modified by BMI, is involved in fatty acid metabolism. There is a commonality between the BMI and FSH dose-altered substrates. Both citric and cis-aconitic acid are modified by the enzyme aconitase in a reversible isomerization reaction. L-malic acid and alpha-keto-glutaric acid are both modified by dehydrogenases and undergo oxidation. The changes observed in the mitochondrial substrate utilization by GCs may indicate that dehydrogenase activity and oxidation reactions are altered by BMI and total FSH dosage administered.

Patients who fall within the obese range (>30 kg/m^2) of BMI have been shown to have almost 70% lower odds of becoming pregnant in their first IVF cycle compared to women who have lower BMI (Moragianni et al., 2012). Furthermore, high BMI and diabetes have both been shown to be related to alteration of mitochondrial function in mouse oocytes (Igosheva et al., 2010, Ou et al., 2012). In human GCs, mitochondrial membrane potential is decreased with higher BMI levels (Gorshinova et al., 2017), and gene expression has also been shown to be modified by BMI (Adriaenssens et al., 2010a, Kenigsberg et al., 2009, Robker et al., 2009). In our study BMI and FSH both altered the utilization of several mitochondrial metabolic substrates related to the tricarboxylic acid cycle. The findings that BMI and the total FSH dose administered alter mitochondrial metabolism in granulosa may be explained by the tendency of patients with higher BMI to receive higher doses of FSH during an IVF stimulation cycle (Fedorcsak et al., 2004). Interestingly, total FSH dosage was previously shown to have no impact on mitochondrial expression of a polycistronic RNA transcript in GCs of IVF patients (Saito et al., 2013), Citric acid and ATP levels have been shown to be reduced in diabetic mice suggesting reduced mitochondrial function due to increasing BMI (Wang et al., 2010). We found that the mitochondrial metabolic scores were significantly reduced when BMI was lower and total FSH dose administered was higher, when only BMI and FSH were in the backward selected models. Our results may indicate that increasing BMI causes an increase in oxidative phosphorylation and reactive oxygen species. This may or may not translate into an increase in ATP production. A recent study by Abraham and

colleagues demonstrated that fibroblasts from infants born to overweight mothers (compared to lean mothers) had significantly higher mitochondrial oxygen consumption rates and increased ATP production indicating mitochondrial inefficiency; cells also exhibited elevated ROS and oxidative stress (Abraham et al., 2018). One may expect that higher doses of FSH administered would show a similar increase in metabolic utilization since higher doses of FSH are associated with higher BMIs, however, we found the opposite effect in this study. This may indicate that GC from patients receiving higher FSH dose indeed suppress mitochondrial substrate utilization. Unfortunately, we did not assess ATP production in this study, but a future study may be able to assess the effect of BMI and FSH dose administered on substrate utilization and ATP production to see if BMI and FSH affect mitochondrial function independent of ATP production.

One of the key pathways for energy production is fatty acid oxidation. Lipotoxicity caused by excessive lipid accumulation and increased intracellular free fatty acid content leads to mitochondrial dysfunction which can compromise mitochondrial function through free fatty acid beta-oxidation and oxidative stress (Hauck and Bernlohr, 2016). Gorshinova and colleagues demonstrated reduced mitochondrial membrane potential in CCs with increasing BMI (Gorshinova et al., 2017). Surprisingly, octanoyl-L-carnitine is an interesting metabolite whose usage was altered in our experiments. Pyruvate, derived from the CCs surround the oocyte, and free fatty acid oxidization are the major sources of ATP production by oocyte mitochondria (Simerman et al., 2015). Octanoyl-L-carnitine has been shown to increase the respiration rate in saponin-treated heart muscles of rats

(Toleikis et al., 2001). The modulation of octanoyl-L-carnitine may indicate that patients with high BMI suffer from compromised mitochondrial function, due to lipotoxicity, causing the mitochondria to work harder in order to produce the same amount of ATP as a person with lower BMI.

We additionally hypothesized that oocyte maturity would be associated with altered mitochondrial metabolic function in granulosa cells as the amount of mtDNA in an oocyte has been previously shown to be important for oocyte maturity and fertilization (Reynier et al., 2001). Since mtDNA content in the oocytes has been shown to be associated with mtDNA content in the GCs (Boucret et al., 2015, Desquiret-Dumas et al., 2017, Ogino et al., 2016) we hypothesized that the mitochondrial metabolism of the GCs should reflect the mitochondrial metabolism of the oocyte and relate to an oocyte's overall developmental competence. The amount of mtDNA in oocytes has previously been demonstrated to be reduced in older patients and those with diminished ovarian reserve and mitochondrial membrane potential has been shown to decrease with advancing age (de Boer, 1999, Diez-Juan et al., 2015, May-Panloup et al., 2005b). However, mtDNA copy number alone does not account for how efficiently the mitochondria function. We observed a significant increase for alpha-keto-isocaproic acid metabolism by GCs in the assay as the number of mature oocytes increased. Alpha-keto-isocaproic acid is converted to leucine by way of a transamination reaction. Leucine then is converted to acetyl-CoA where it enters the tricarboxylic acid cycle. In our study, the calculated mitochondrial metabolic scores were significantly increased in a linear relationship with the total number of oocytes retrieved. Mitochondrial ATP

production and mitochondrial membrane potential in CCs have both been shown to correlate with the number of mature oocytes retrieved (Dumesic et al., 2016). Our observations may indicate there is a component of leucine metabolism that is related to final oocyte maturation.

We did not find any significant differences in mitochondrial metabolism related to age or serum AMH (Figure 4.17 and 4.18). AMH levels and advanced maternal age are closely related. Both AMH gene and protein expression are increased in GCs with advancing age (Kedem et al., 2014) while serum AMH levels in the blood decrease as the supply of oocytes dwindles with age (Knight and Glister, 2006). We performed correlation analysis between mtDNA copy number and patient age, BMI, serum AMH levels, and oocyte maturity and found no differences (Figure 4.19). The reason we may not have seen differences in these groups is because were we unable to look at patients with low oocyte yield, which normally fall in the low AMH and older patient groups. The minimum number of GCs needed to utilize the mitochondrial function assay required pooled CCs and MGCs from at least 10 oocytes. Therefore, older women and those with lower AMH levels in our study were still within a better prognostic group than patients with low oocyte yield due to age or diminished ovarian reserve. If we had been able to use fewer GCs for the assay and could have included patients with lower oocyte yield, we may have observed different results.

A secondary goal of this study was to determine if mitochondrial substrates in pooled GCs would relate to a patient's overall cohort development and yield potential substrate biomarkers to possibly predict embryo development or

pregnancy/live birth in future studies. The premise of this hypothesis was that one potential explanation for compromised oocyte, and subsequent embryo quality, has been postulated to be deficient mitochondrial function (Bentov et al., 2011). Embryo viability is related to the amount of energy produced by the mitochondria in the oocyte and surrounding GCs as early embryogenesis demands substantial amounts of energy produced by the mitochondria to drive the cleavage divisions (May-Panloup et al., 2005a, Reynier et al., 2001, Zhao et al., 2010). In fact, mitochondria with metabolic dysfunction may impair oocyte quality, overall embryo development, and live birth rates (Dumesic et al., 2016).

Glycogen is a cytoplasmic substrate which is converted through several steps to acetyl-CoA where it enters the tricarboxylic acid cycle. Mitochondrial utilization of glycogen was found to be significantly lower in patients with lower fertilization percentage. Mitochondrial metabolic scores significantly increased as the number of mature oocytes retrieved increased, while the scores decreased as the number of fertilized oocytes increased. This inverse relationship is likely due to the fact that GCs surrounding immature oocytes may exhibit increased mitochondrial activity which drops off as the oocyte matures and prepares for fertilization. Prior studies have demonstrated higher mean mtDNA levels in fertilized human oocytes compared to both unfertilized oocytes and degenerated oocytes (Reynier et al., 2001, Santos et al., 2006, Murakoshi et al., 2013). Our data appear to indicate that mitochondria in granulosa of oocytes that are better positioned to fertilize can utilize glycogen more efficiently to produce ATP than those granulosa of oocytes less likely to fertilize and perhaps the increase in ATP

is needed in order to complete fertilization. This data indicates that the mitochondrial metabolic score may be able to predict fertilization potential of a cohort of oocytes.

Mitochondrial utilization significantly increased for D-alpha-keto-glutaric acid in GCs from patients with lower good quality 8-cell embryos compared to those with high good quality 8-cell embryos. In addition, mitochondrial utilization of L-glutamine was found to be significantly higher in pooled GCs in patients with a lower percentage of blastocyst formation when using a backward selected model looking only at 8-cell embryos and blastocysts. L-glutamine was likely converted to alpha-keto-glutaric acid and used the same biochemical pathway in the assay. Increased mtDNA copy numbers in CCs have been shown to be associated with embryos that developed into high quality versus low-quality embryos and embryos more likely to implant than those that did not implant. It has been postulated that increased mitochondria within a blastocyst may serve to compensate for reduced mitochondrial energy production due to metabolic stress from reactive oxygen species and free radicals (Diez-Juan et al., 2015, Fragouli et al., 2015, Grindler and Moley, 2013, May-Panloup et al., 2016). In future studies use of a single substrate that showed significant differences based on embryo development could conceivably be optimized to test individual CC masses to examine the endpoints of individual embryo development, pregnancy, and live birth.

Finally, we wanted to test the hypothesis that the mitochondrial metabolic score, which reflects overall mitochondrial activity in the granulosa pool would be differ between mRNA levels of the selected genes. We selected *AMH* mRNA,

based on our original hypothesis that serum AMH levels would alter substrate utilization. We selected *AREG*, *CYP19A1*, *CYP11A1*, *HSD3B1*, *ING1*, *LHCGR*, and *PAPPA* as genes of interest based on a prior study our lab conducted with individual cumulus masses (Kordus et al., 2019). *HSD3B* levels were borderline lower ($P < 0.10$) as the mitochondrial metabolic score decreased, but none of these mRNAs showed significant regulation. In our prior study we examined individual CC masses from oocytes and their individual embryos. We believe we did not see any significant differences due to the use of pooled GCs in this study.

A strength of this study was that we were able to compare multiple substrates at once over a specified time course using the mitochondrial function assay. Another strength of this study was that we were able to assess mitochondrial function and not just mtDNA content. This study was limited by the number of GCs needed to analyze each substrate in triplicate in the mitochondrial function assay. We found that the threshold concentration of cells needed was approximately 7000 cells per well or just above 650,000 cells per plate in order to yield absorbance readings above the negative control values. Therefore, this necessitated pooling of the MGCs and the CCs to achieve the required number of cells per patient for the assay plate. Since we pooled the GCs, this caused us to have to examine at the embryo cohort as a whole, rather than individual embryos, which reduces the clinical utility of using this particular test to assess embryo development. Since this was a pilot study, our goal was to narrow the cohort of substrates down to a few which could be optimized in the future to analyze individual CC masses and then relate those results to individual oocytes and

resulting embryos in future studies. Specialized assay plates could be made with only the substrates of interest in the wells. Another limitation was the use of two stimulation protocols. A more ideal study would include patients undergoing a single stimulation protocol, either long luteal stimulation or antagonist stimulation.

Mitochondrial function and its relationship to human reproductive potential is poorly understood, and further research needs to be conducted regarding oocyte developmental competence and embryonic development. In this study we found mitochondrial metabolic function was altered with BMI and FSH dosage. We also found that there was a subset of mitochondrial metabolic substrates utilized by GCs that can potentially be used as novel biomarkers related to embryo development in future studies.

4.6 Supplementary data

Supplementary data are available at Journal of Assisted Reproduction and Genetics online.

4.7 Funding

Supported by an ASPIRE-I grant from the University of South Carolina.

4.8 Compliance with ethical standards

4.8.1 Ethical Approval

"All procedures performed in studies involving human participants were in accordance with the ethical standards of the institutional and/or national research committee and with the 1964 Helsinki declaration and in its later amendments or comparable ethical standards." This study was approved by Greenville Health

System (IRB number: Pro00072006) and the University of South Carolina Institution Review Board (IRB registration number: 00000240).

4.8.2 Informed consent: Informed consent was obtained from all individual participants included in the study.

4.9 Conflict of interest: The authors declare no conflict of interest related to this study.

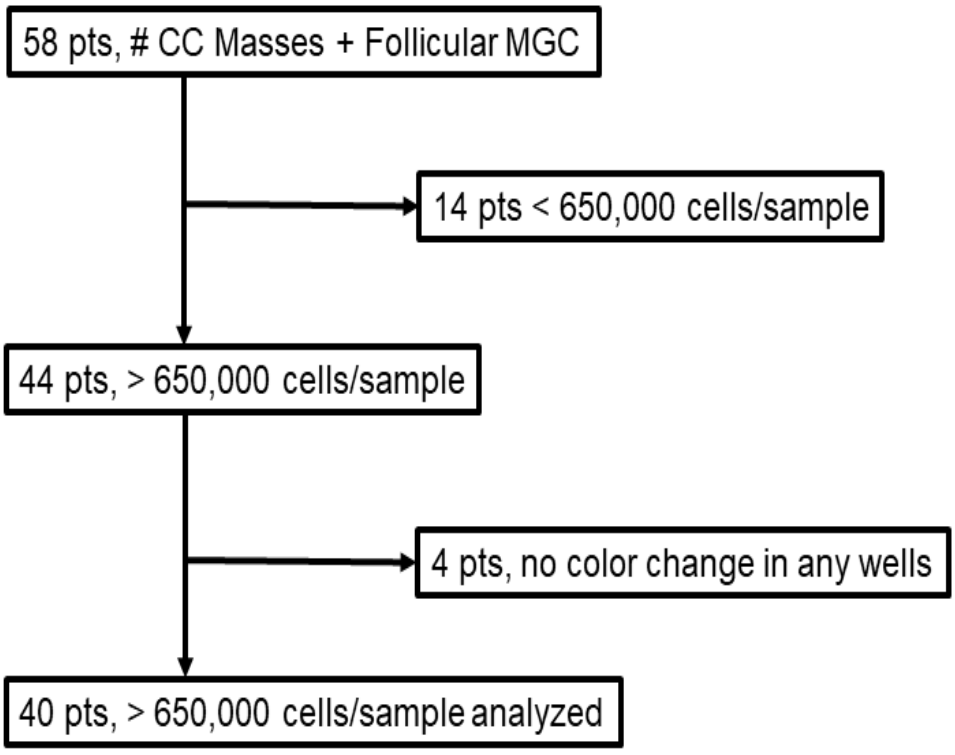

Figure 4.1 Flow diagram summarizing the study population from oocyte retrieval to final outcome. Oocytes, CC masses, and MGCs were collected from 58 patients (pts). Individual CC masses from each oocyte collected (n=817) were combined with the MGCs from each patient. Fourteen samples collected had an insufficient number of cells to visualize an appropriate color change in the wells of the assay plate and were excluded from the analysis. Four patients did exceed the minimum number of cells required to run the plate but no color changes were observed with the control wells and thus were excluded from the analysis, so the final number of patients analyzed was n = 40.

Table 4.1 Patient demographics and cycle information

Pt #	Age	BMI	Diag	AMH	AFC	STIM	HMG dose	FSH dose	# Mat oocyte	% Fert	% 8-C Good	% Blast	mtDNA content
1	34	23.1	MF	5.65	15	LL	300	825	22	77%	71%	47%	0.001184
2	24	19.4	MF	2.25	27	LL	600	1125	9	89%	25%	50%	0.001294
3	40	19.9	MF	3.86	20	LL	450	1488	20	90%	61%	61%	0.001562
4	26	21.6	PCO	4.34	30	LL	750	1425	9	67%	33%	33%	0.001663
5	32	19.1	RPL	1.98	11	AN	750	1700	14	86%	58%	50%	0.000311
6	38	21	AMA	1.52	11	AN	675	1575	11	82%	55%	66%	0.001355
7	36	29.7	RPL	2.48	26	AN	750	1800	25	92%	78%	73%	0.000824
8	36	27.9	DOR	0.55	7	AN	1200	3300	9	67%	83%	100%	0.000778
9	32	21.7	TUBAL	6.28	9	LL	525	1525	6	17%	0%	0%	0.000525
10	35	25.3	MF.OD. PCO	1.17	11	AN	675	2025	6	67%	0%	50%	0.000621
11	30	26.7	RPL	3.67	22	LL	825	2250	18	67%	50%	58%	0.000957
12	34	36.7	MF.OD. PCO	3.02	25	LL	525	1050	14	36%	0%	0%	0.000592
13	30	19	OD	2.5	22	LL	675	1425	13	85%	55%	54%	0.000927
14	29	26.2	MF	1.85	13	LL	750	1500	10	60%	67%	50%	0.001091
15	33	30.3	DOR	0.78	13	AN	600	1800	11	82%	67%	33%	0.001265
16	35	21.4	MF	5.48	22	LL	750	1875	15	73%	55%	64%	0.004323
17	37	29.4	OD. AMA	1.14	12	AN	675	2250	7	86%	50%	50%	0.006901
18	38	35.7	OD	2.63	12	AN	825	2475	16	94%	87%	47%	0.000297
19	33	28.3	DOR. OD	1.75	11	AN	825	3150	15	73%	55%	55%	0.001608
20	28	23	MF	6.8	18	LL	600	1050	11	46%	60%	20%	0.000809
21	22	19.3	IDIO	5.38	30	LL	225	787.5	25	80%	70%	80%	0.000432

Table 4.1 Patient demographics and cycle information continued

22	32	21.5	ENDO	4.73	20	LL	600	1275	24	58%	21%	57%	0.000362
23	31	29.7	OD	5.06	23	LL	750	1500	19	84%	38%	62%	0.001179
24	36	17.9	MF	1.26	23	LL	825	2475	12	58%	57%	43%	0.001328
25	31	29	PCO	11.5	27	LL	525	1050	10	90%	100%	78%	0.00098
26	35	31.3	OD	0.85	7	AN	750	2250	11	100%	55%	55%	0.000769
27	36	38.3	OD	1.92	9	LL	825	3000	12	92%	27%	9%	0.001229
28	37	33.1	OD	1.94	8	LL	825	3000	10	80%	62%	75%	0.000902
29	37	26.6	RPL BAL-TRAN	1.61	9	AN	1050	3000	6	100%	83%	67%	0.000570
30	34	25.8	MF	5.65	15	LL	300	775	25	84%	67%	52%	0.000354
31	27	25.8	AMEN	9.66	30	LL	600	938	16	88%	79%	57%	0.000201
32	33	23	RPL	5.13	30	LL	600	1050	22	68%	73%	73%	0.001147
33	34	29.3	UT	6.19	27	LL	675	1175	15	73%	64%	55%	0.00108
34	33	28.5	RPL	1.66	19	LL	675	1450	9	89%	50%	75%	0.000680
35	31	34.4	OD	4.68	27	LL	600	1100	26	42%	36%	55%	0.000739
36	28	29.8	OD	9.39	30	LL	750	1125	17	100%	88%	47%	0.000571
37	31	20.2	OD	5.47	19	LL	750	1950	10	70%	86%	71%	0.001878
38	38	33.1	AMA	3.15	30	AN	825	2625	22	82%	56%	72%	0.000675
39	31	18.9	OD	6.55	30	LL	675	1525	26	100%	62%	81%	0.000837
40	38	23.1	OD	9.97	30	LL	675	1350	11	73%	25%	0%	0.000944
median	**33**	**26**		**3.41**	**20**		**675**	**1512**	**19**	**81%**	**58%**	**55%**	**0.009145**
range	**22 - 40**	**17.9 - 38.3**		**0.55 - 11.5**	**7 - 30**		**225 - 1200**	**775 - 3300**	**10 - 41**	**17 - 100**	**0 - 100**	**0 - 100**	**0.000200 - 0.006901**

Table 4.1 Patient demographics and cycle information continued

8-C = 8-cell embryo, AFC = antral follicle count, AMEN = amenorrhea, AMA = advance maternal age, AMH = anti-Mullerian hormone, AN = antagonist stimulation, BAL-TRAN = balanced translocation, Blast = blastocyst, BMI = body mass index, Diag = diagnosis, DOR = diminished ovarian reserve, ENDO = endometriosis, FERT = fertilization, FSH = follicle stimulating hormone, HMG = human menopausal gonadotropin, IDIO = idiopathic, IUs = international units, LL = long luteal stimulation, MAT = mature, MF = male factor, mtDNA = mitochondrial DNA, PCO = polycystic ovaries, Pt = patient, OD = ovulatory dysfunction, RPL = recurrent pregnancy loss, STIM = stimulation type, TUBAL = tubal factor, UT = uterine anomaly

Table 4.2 List of Substrates on the Mitoplate-S-1 Mitochondrial Function Assay

Cytoplasmic substrates			
No substrate control	alpha-D-glucose	glycogen	D-glucose-1-phosphate
D-glucose-6-phosphate	D-gluconate-6-phosphate	L-lactic acid	D,L-alpha-glycerol-phosphate
Tricarboxylic acid cycle substrates			
pyruvic acid	citric acid	D,L-isocitric acid	cis-aconitic acid
D-alpha-keto-glutaric acid	succinic acid	fumaric acid	L-malic acid
Other mitochondrial substrates			
alpha-keto-butyric acid	D,L-beta-hydroxy-butyric acid	L-glutamic acid	L-glutamine
alanine-glycine	L-serine	L-ornithine	tryptamine
Other mitochondrial substrates with malic acid 100uM			
malic acid 100uM	octanoyl-L-carnitine	acetyl-l-carnitine	palmitoyl-D,L-carnitine
gamma-amino-butyric acid	alpha-keto-isocaproic acid	pyruvic acid	L-leucine

Table 4.3 Primer set information

Gene	Primer sequences 5'--3'	Annealing temperature (°C)	Amplicon size (base pairs)	Reference or NCBI no.
AMH	For GTGCTGCTGCTGAAGATG Rev CTCCGACAGGCTGATGAG	60	102	(Detti et al., 2018)
AREG	For TGGACCTCAATGACACCTACTCTG Rev GGGCTTAACTACCTGTTCAACTCTG	62	251	(Feuerstein et al., 2007)
ACTB	For AGCGGGAAATCGTGCGTGAC Rev AGGCAGCTCGTAGCTCTTCTC	60	116	(Diez-Juan et al., 2015)
CYP19A1	For GCACATCCTCAATACCAGGTC Rev TTTGAGGGATTCAGCACAGAC	60	380	(Hamel et al., 2008)
HSD3B1	For TGTGCCAGTCTTCATCTACAC Rev TGTTTTCCAGAGGCTCTTCTTC	60	101	(Hamel et al., 2008)
ING1	For GCCTGGTGTGAGGAGGACAA Rev CCCTATGAAAGGAATGGTTCCTT	62	124	(He et al., 2004)
LHCGR	For TGGAGAAGATGCACAATGGA Rev GGCAATTAGCCTCTGAATGG	60	122	(Yung et al., 2014)
MT-ATP8	For CTAAAATATTAAACACAAACTACCACCTACCTC Rev GTTCATTTTGGTTCTCAGGGTTTGTT TAA	60	92	(Diez-Juan et al., 2015)
PAPPA	For GTCATCTTTGCCTGGAAGGGAGAA Rev AGGGCTGTTCAACATCAGGATGAC	62	129	(Wagner et al., 2011)
TBP	For CACGGCACTGATTTTCAGTTC Rev TCTTGCTGCCAGTCTGGACT	62	79	(Nelson-Degrave et al., 2004)

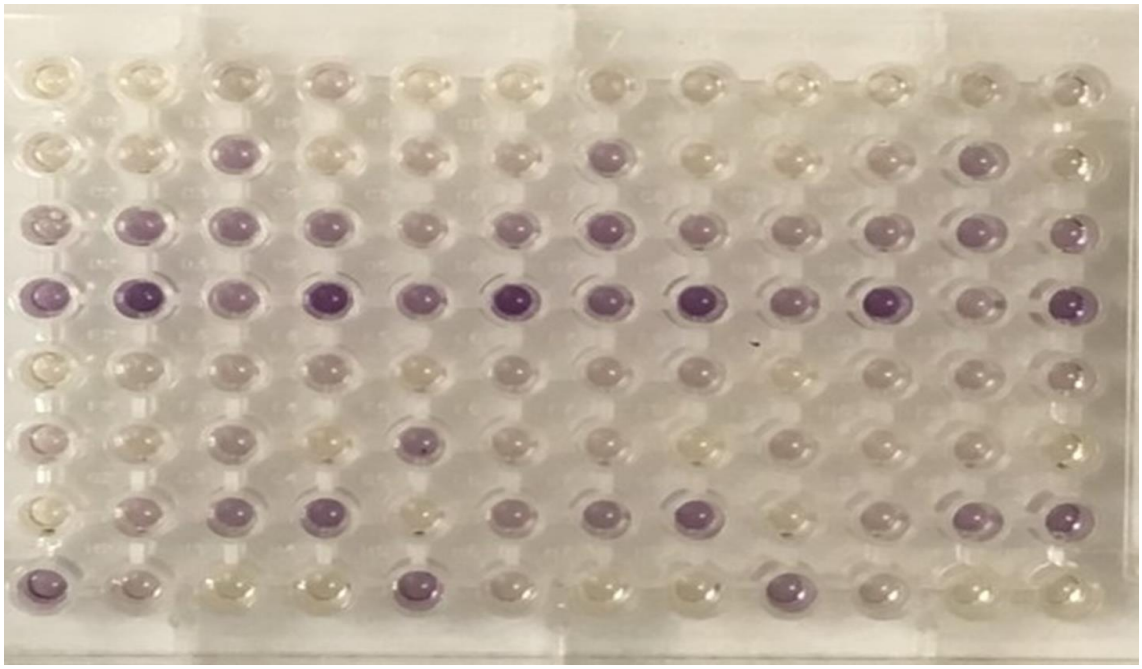

Figure 4.2 Sample mitochondrial functional assay Mitoplate-S-1. The mitochondrial function assay plates contained 31 cytoplasmic and mitochondrial metabolic substrates repeated in triplicate. Each well in the plate contained an individual chemical as the sole energy source. As the cells metabolized the energy source, tetrazolium dye in the media was reduced, generating a purple color according to the amount of NADH or $FADH_2$ reducing equivalents generated over 2.0 hrs. Absorbance readings in the assay reflected metabolism or utilization of substrates

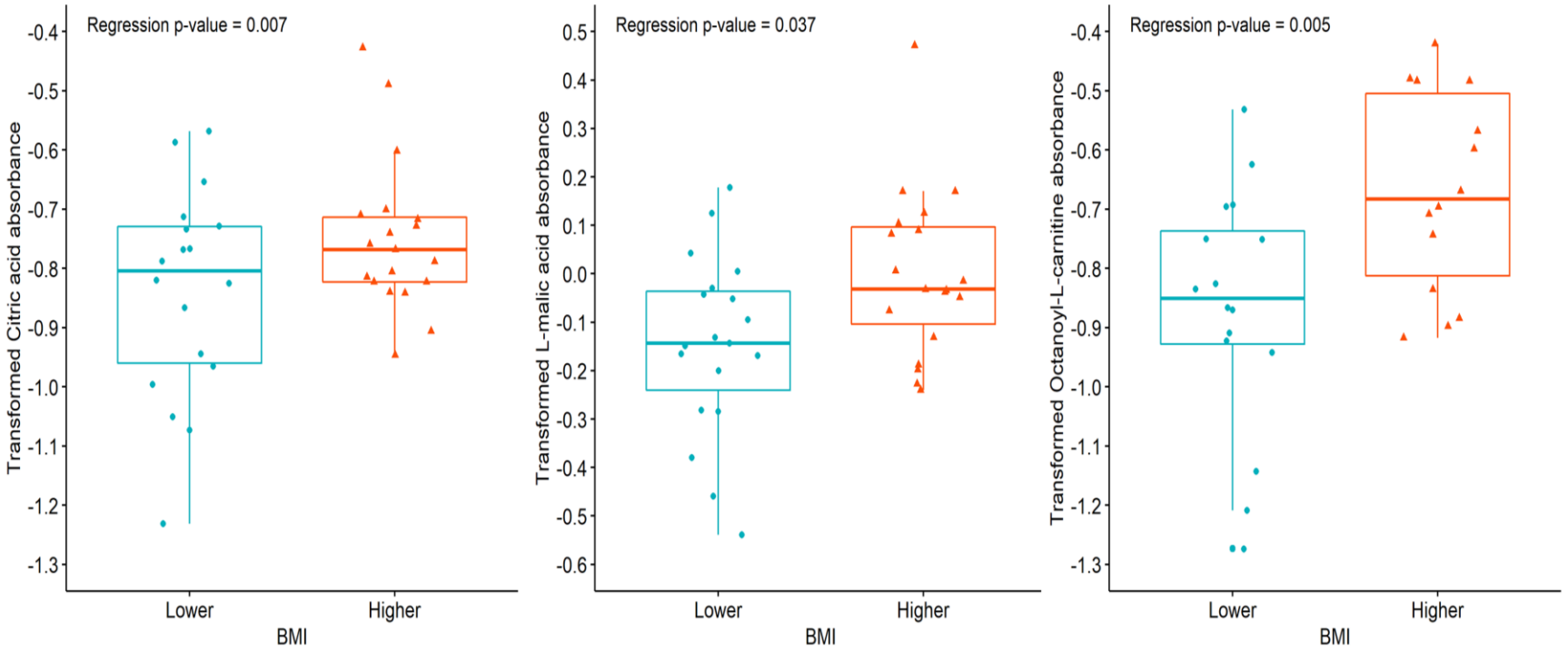

Figure 4.3 Substrates demonstrating significant mitochondrial utilization differences based on body mass index. To determine the differences in mitochondrial utilization, substrates were compared using a multiple linear regression model using Box-Cox transformation. BMI was divided into 2 groups with the higher group being patients with a BMI of ≥ to 26 kg/m^2 (n = 20) and the lower group being patients with a BMI of < 26 kg/m^2 (n = 20). Mitochondrial utilization of citric acid (P < 0.01), L-malic acid (P < 0.05), and octanoyl-L-carnitine (P < 0.01) were found to be significantly lower in pooled GCs of patients with lower BMI, after adjusting for the other factors in the model. Data are presented as the median (line inside box), first and third quartile (bottom and top of box), and the whiskers extend to 1.5 times the interquartile range beyond the first and third quartile.

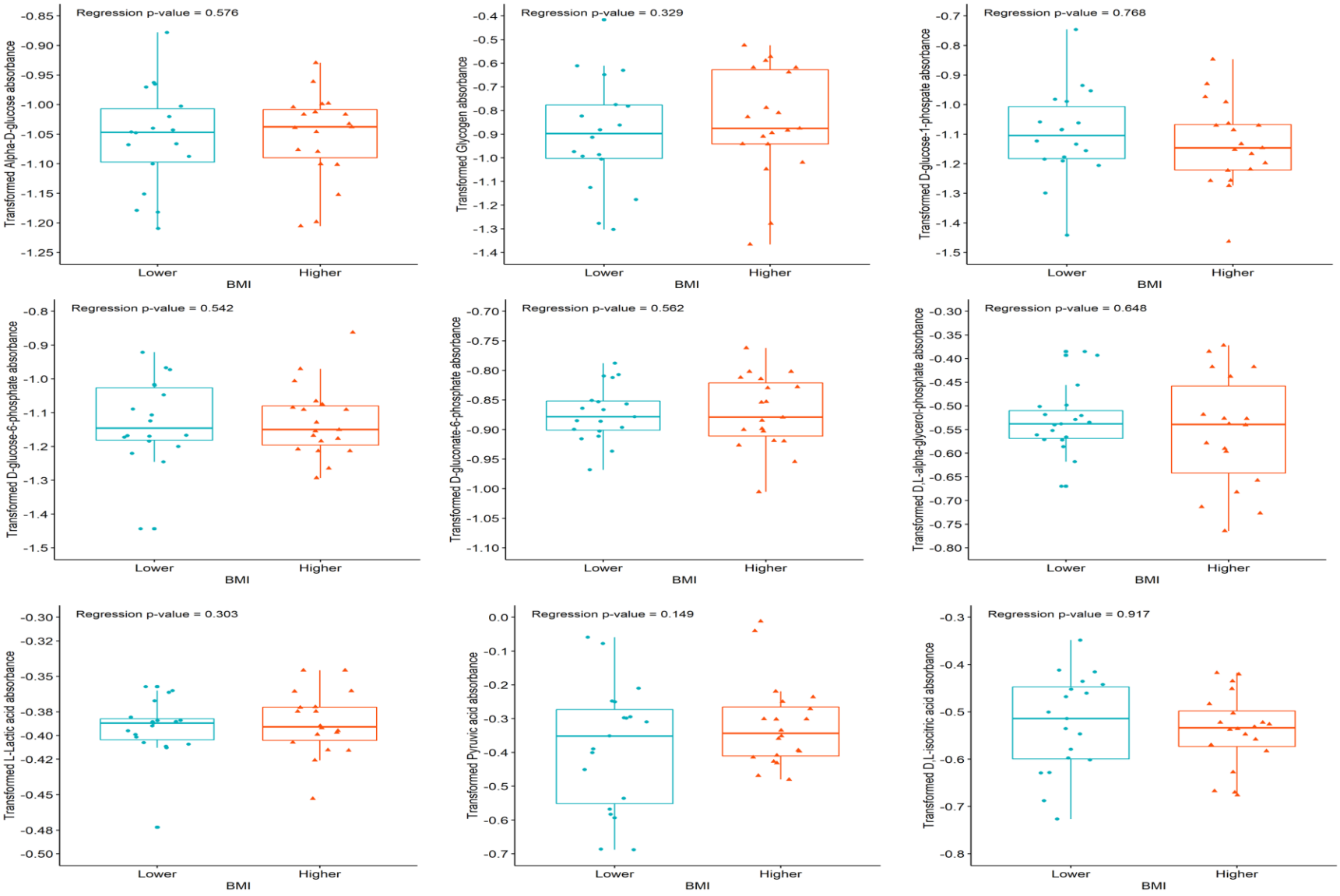
Regression p-value = 0.576
Transformed Alpha-D-glucose absorbance
Regression p-value = 0.329
Transformed Glycogen absorbance
Regression p-value = 0.768
Transformed D-glucose-1-phospate absorbance
Regression p-value = 0.542
Transformed D-glucose-6-phosphate absorbance
Regression p-value = 0.562
Transformed D-gluconate-6-phosphate absorbance
Regression p-value = 0.648
Transformed D,L-alpha-glycerol-phosphate absorbance
Regression p-value = 0.303
Transformed L-Lactic acid absorbance
Regression p-value = 0.149
Transformed Pyruvic acid absorbance
Regression p-value = 0.917
Transformed D,L-isocitric acid absorbance
Lower
Higher
BMI

Figure 4.4 Substrates demonstrating no significant mitochondrial utilization differences based on body mass index. To determine the differences in mitochondrial utilization, substrates were compared using a multiple linear regression model using Box-Cox transformation between BMI groups. BMI was divided into 2 groups with the higher group being patients with a BMI of ≥ to 26 kg/m^2 (n = 20) and the lower group being patients with a BMI of < 26 kg/m^2 (n = 20). Mitochondrial utilization of cis-acontic acid ($P < 0.10$), D,L-beta-hydroxy-butyric acid ($P < 0.10$), and pyruvic acid/L-malic acid 100 µM ($P < 0.10$) were found to be borderline lower in pooled GCs of patients with lower BMI, after adjusting for the other factors in the model. No other substrates showed any mitochondrial utilization differences. Data are presented as the median (line inside box), first and third quartile (bottom and top of box), and the whiskers extend to 1.5 times the interquartile range beyond the first and third quartle.

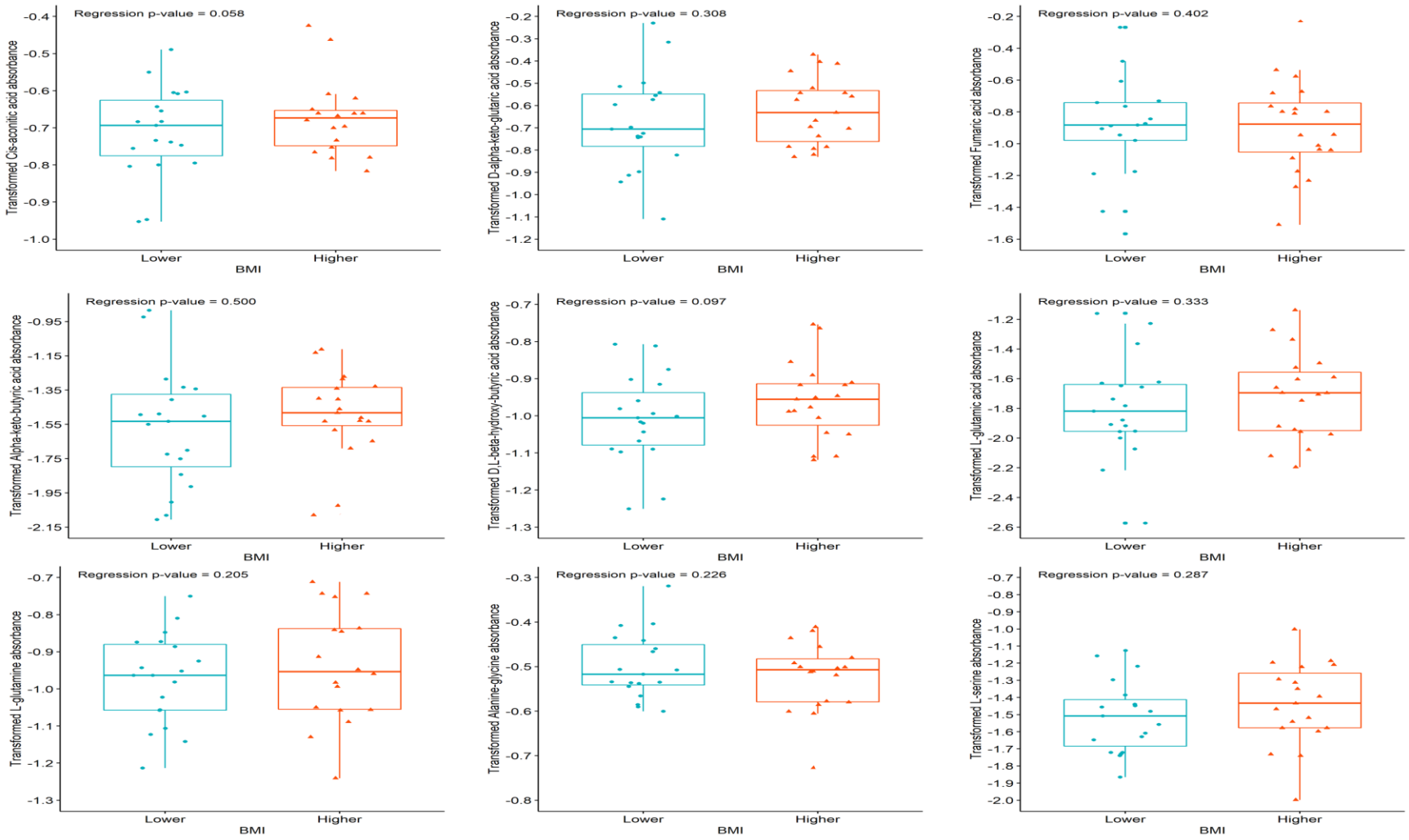

Figure 4.4 Continued

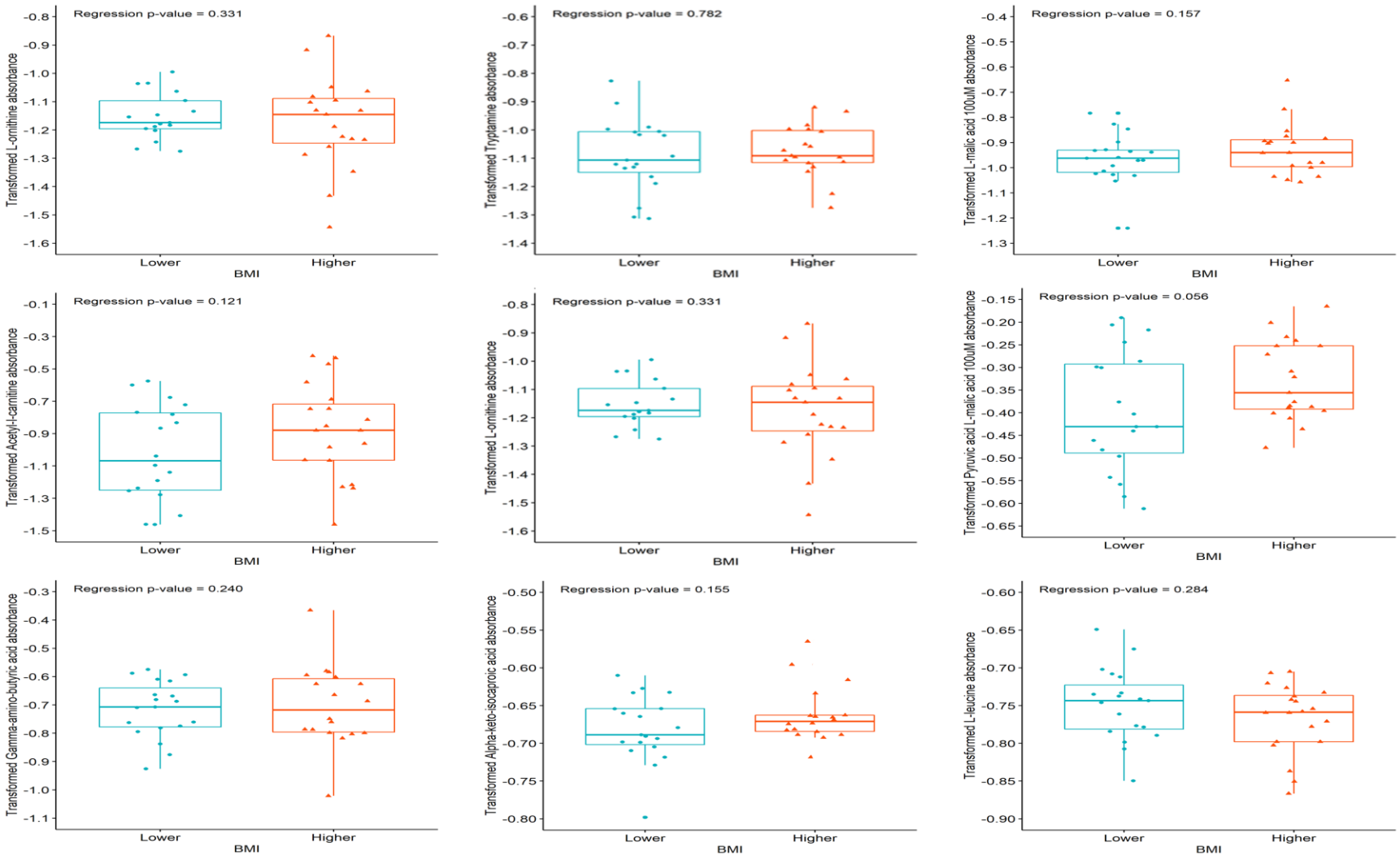

Figure 4.4 Continued

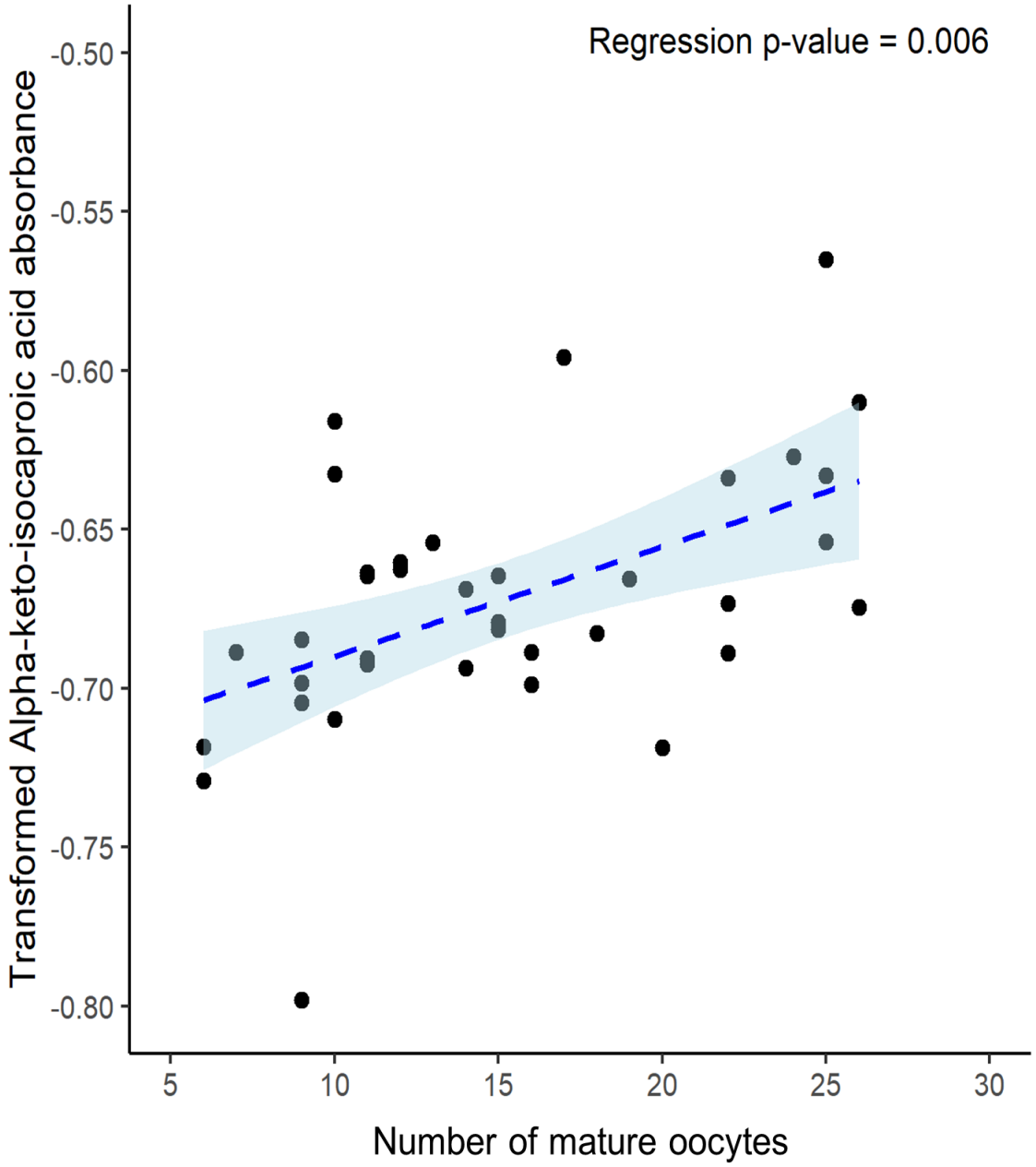

Figure 4.5 Substrates demonstrating significant mitochondrial utilization differences based on number of mature oocytes retrieved. To determine the differences in mitochondrial utilization, substrates were modeled using multiple linear regression after Box-Cox transformation for normality. Individuals with greater numbers of mature oocytes retrieved were found to have a significant increase in alpha-keto-isocaproic acid mitochondrial utilization ($P < 0.01$) in pooled GCs of patients, after adjusting for the other factors in the model. Data are presented as a scatter plot of the individual patient Box-Cox transformed values showing the trend line and the 95% confidence region.

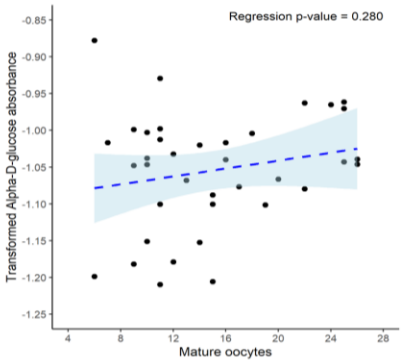
Regression p-value = 0.280
Transformed Alpha-D-glucose absorbance
Mature oocytes

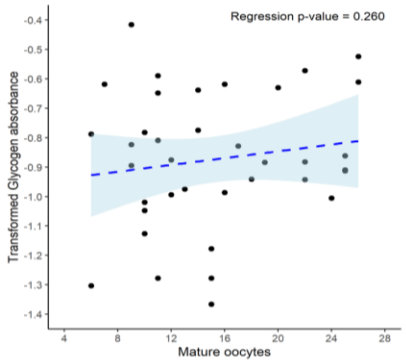
Regression p-value = 0.260
Transformed Glycogen absorbance
Mature oocytes

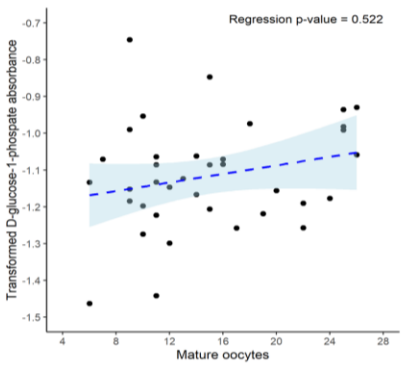
Regression p-value = 0.522
Transformed D-glucose-1-phospate absorbance
Mature oocytes

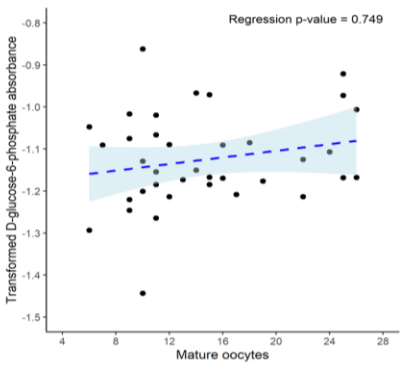
Regression p-value = 0.749
Transformed D-glucose-6-phosphate absorbance
Mature oocytes

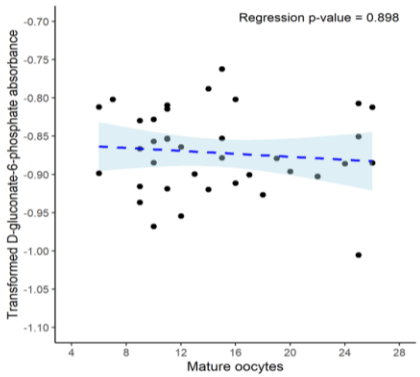
Regression p-value = 0.898
Transformed D-gluconate-6-phosphate absorbance
Mature oocytes

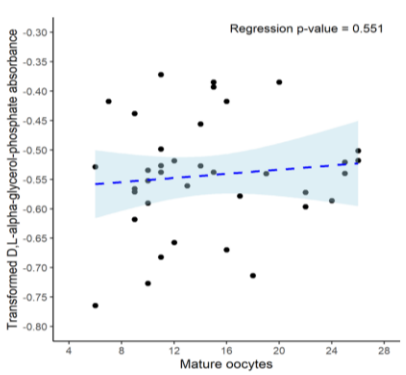
Regression p-value = 0.551
Transformed D,L-alpha-glycerol-phosphate absorbance
Mature oocytes

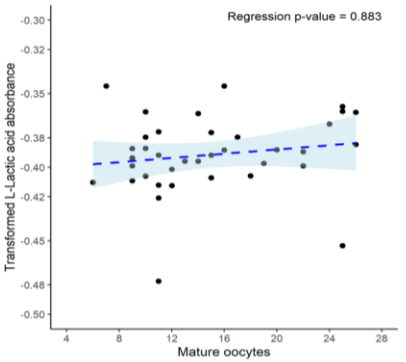
Regression p-value = 0.883
Transformed L-Lactic acid absorbance
Mature oocytes

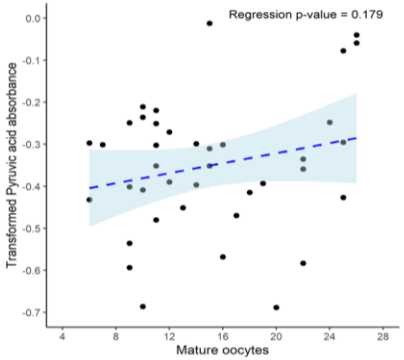
Regression p-value = 0.179
Transformed Pyruvic acid absorbance
Mature oocytes

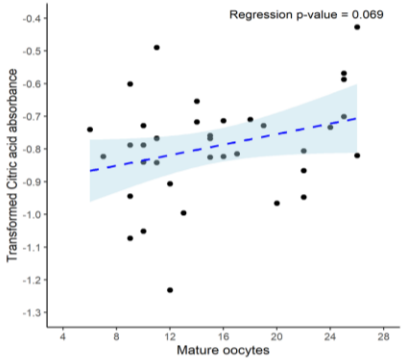
Regression p-value = 0.069
Transformed Citric acid absorbance
Mature oocytes

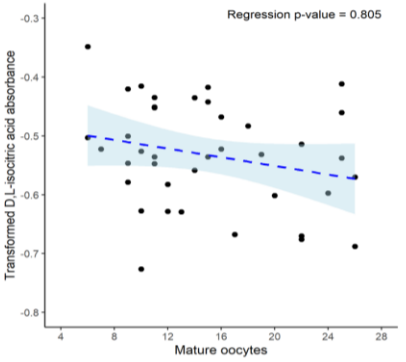
Regression p-value = 0.805
Transformed D,L-isocitric acid absorbance
Mature oocytes

Figure 4.6 Substrates demonstrating no significant mitochondrial utilization differences based on number of mature oocytes retrieved. To determine the differences in mitochondrial utilization, substrates were modeled using multiple linear regression after Box-Cox transformation for normality. No substrates in pooled GCs of patients demonstrated any significant mitochondrial utilization differences, after adjusting for the other factors in the model. Data are presented as a scatter plot of the individual patient Box-Cox transformed values showing the trend line and the 95% confidence region.

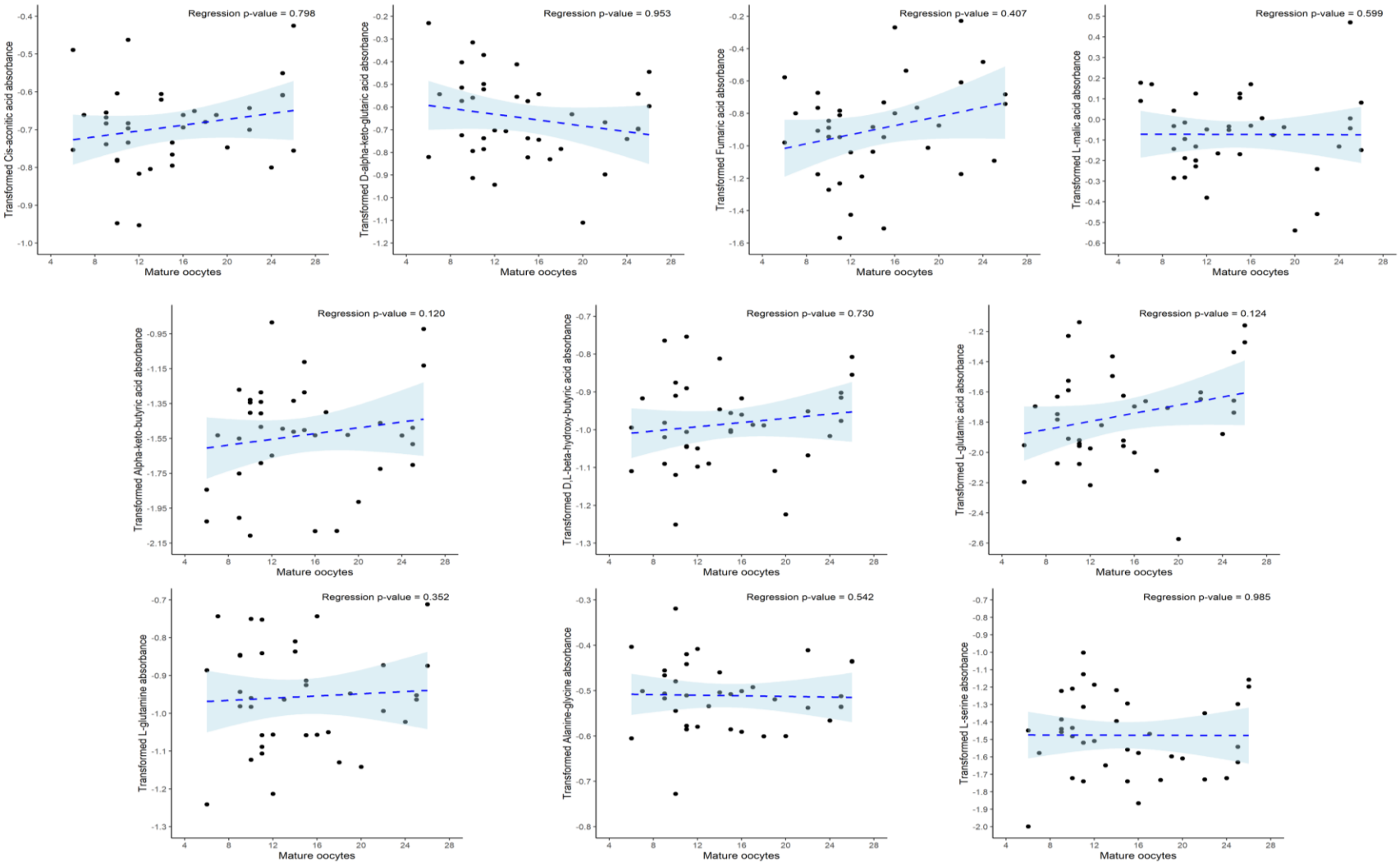

Figure 4.6 Continued

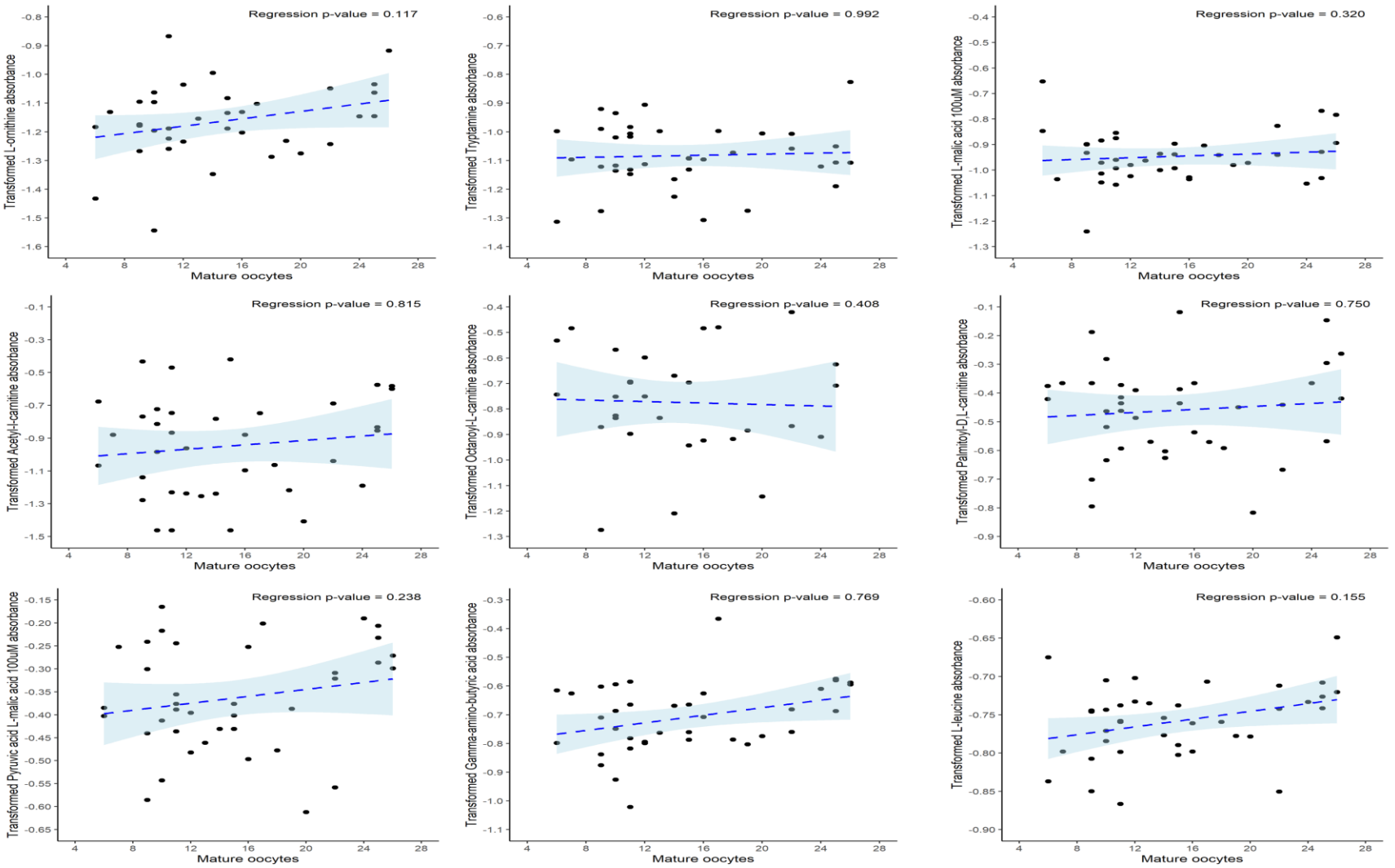

Figure 4.6 Continued

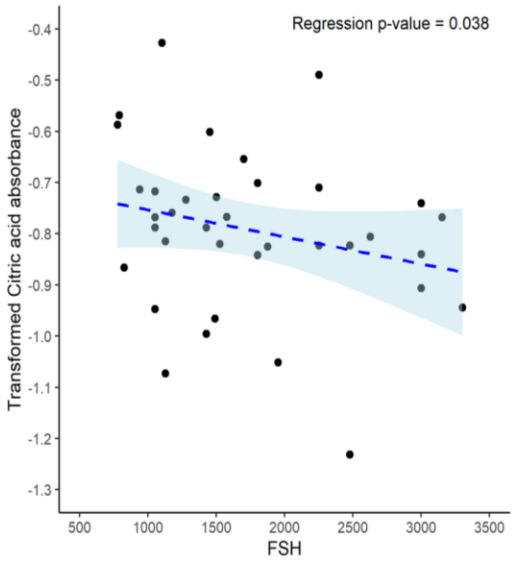
Regression p-value = 0.038
Transformed Citric acid absorbance
FSH

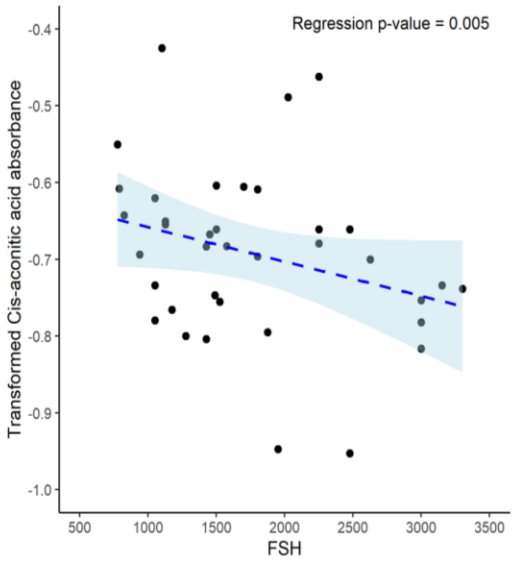
Regression p-value = 0.005
Transformed Cis-aconitic acid absorbance
FSH

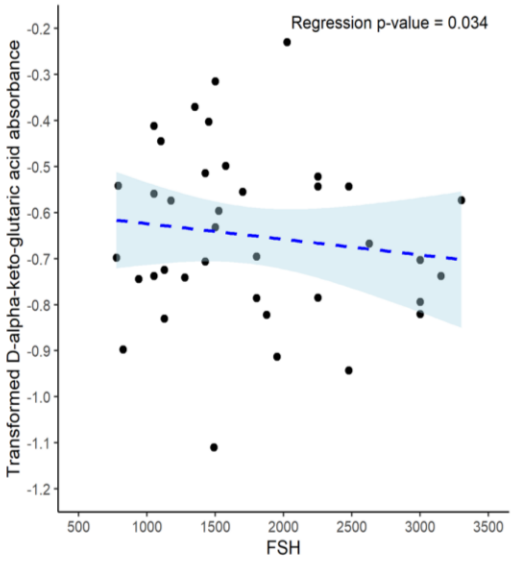
Regression p-value = 0.034
Transformed D-alpha-keto-glutaric acid absorbance
FSH

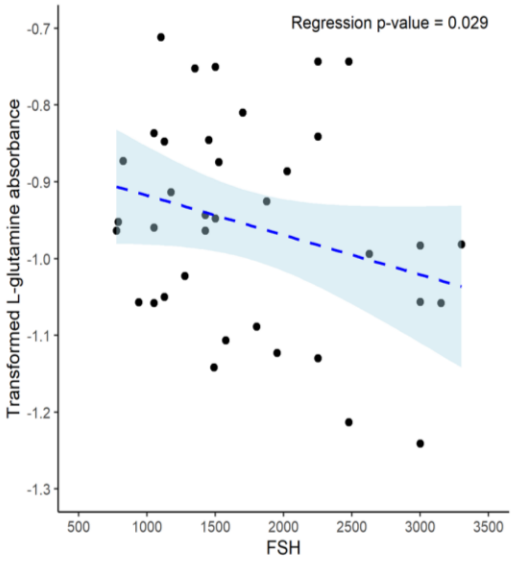
Regression p-value = 0.029
Transformed L-glutamine absorbance
FSH

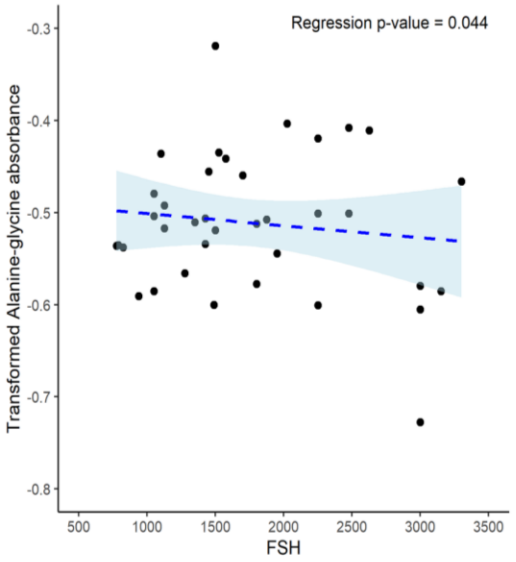
Regression p-value = 0.044
Transformed Alanine-glycine absorbance
FSH

Figure 4.7 Substrates demonstrating significant mitochondrial utilization differences based on total FSH dose administered. To determine the differences in mitochondrial utilization, substrates were modeled using multiple linear regression after Box Cox transformation for normality. Mitochondrial utilization for citric acid ($P < 0.05$), cis-acontic acid ($P < 0.01$), D-alpha-keto-glutaric acid ($P < 0.05$), L-glutamine ($P < 0.05$), and alanine-glycine ($P < 0.05$) in pooled GCs of patients were found to be significantly lower as total FSH dose administered increased, after adjusting for the other factors in the model. Data are presented as a scatter plot of the individual patient Box-Cox transformed values showing the trend line and the 95% confidence region.

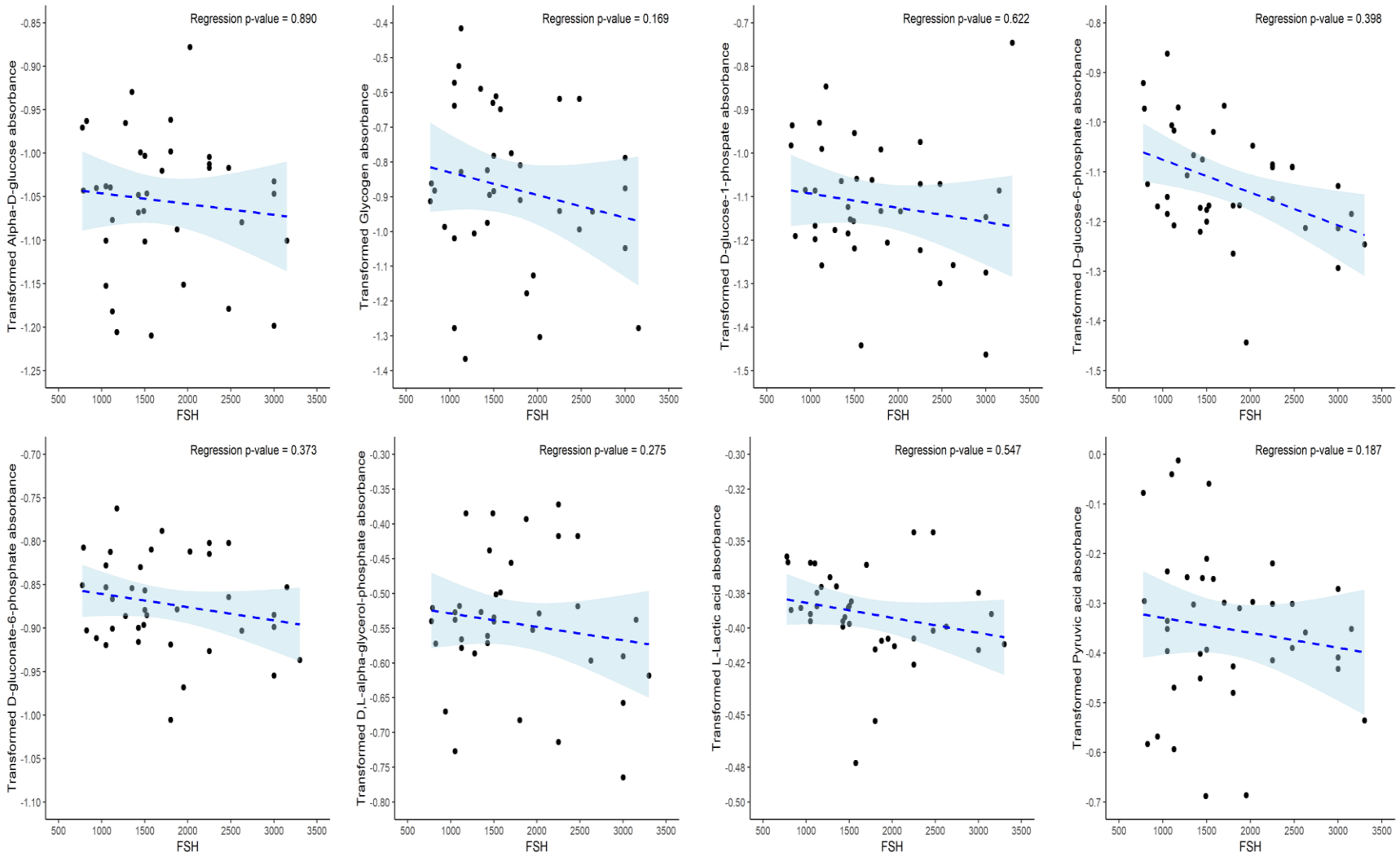
Regression p-value = 0.890
Transformed Alpha-D-glucose absorbance
FSH
Regression p-value = 0.169
Transformed Glycogen absorbance
FSH
Regression p-value = 0.622
Transformed D-glucose-1-phospate absorbance
FSH
Regression p-value = 0.398
Transformed D-glucose-6-phosphate absorbance
FSH
Regression p-value = 0.373
Transformed D-gluconate-6-phosphate absorbance
FSH
Regression p-value = 0.275
Transformed D,L-alpha-glycerol-phosphate absorbance
FSH
Regression p-value = 0.547
Transformed L-Lactic acid absorbance
FSH
Regression p-value = 0.187
Transformed Pyruvic acid absorbance
FSH

Figure 4.8 Substrates demonstrating no significant mitochondrial utilization differences based on total FSH dose administered. To determine the differences in mitochondrial utilization, substrates were modeled using multiple linear regression after Box-Cox transformation for normality. Mitochondrial utilization of D,L-isocitric acid ($P < 0.10$), D,L-beta-hydroxy-butyric acid ($P < 0.10$), L-glutamic acid ($P < 0.10$), acetyl-L-carnitine ($P < 0.10$), pyruvic acid/L-malic acid 100 µM ($P < 0.10$) were found to be borderline lower in pooled GCs of patients with higher administered FSH dosages, after adjusting for the other factors in the model. No other substrates showed any mitochondrial utilization differences. Data are presented as a scatter plot of the individual patient Box-Cox transformed values showing the trend line and the 95% confidence region.

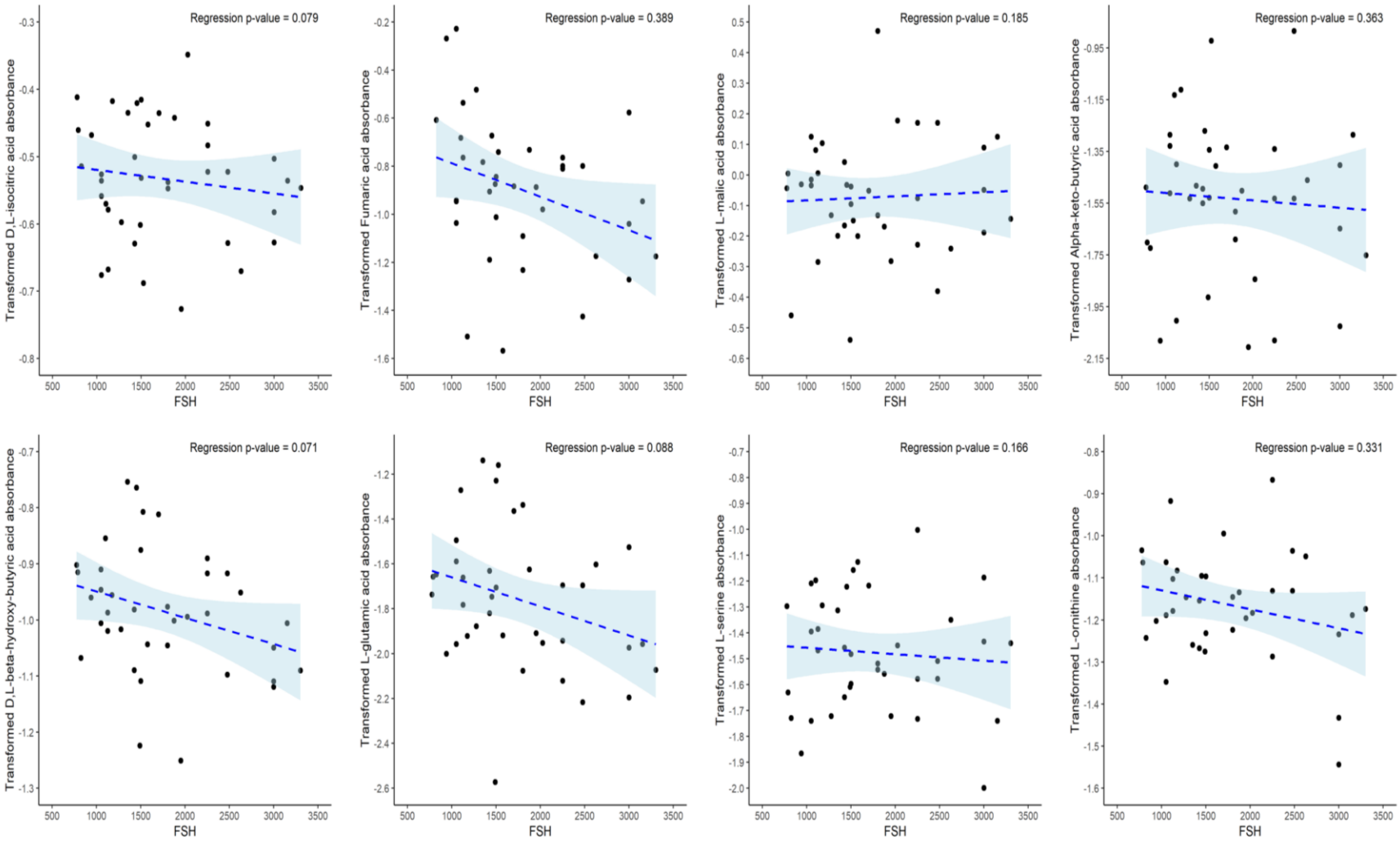

Figure 4.8 Continued

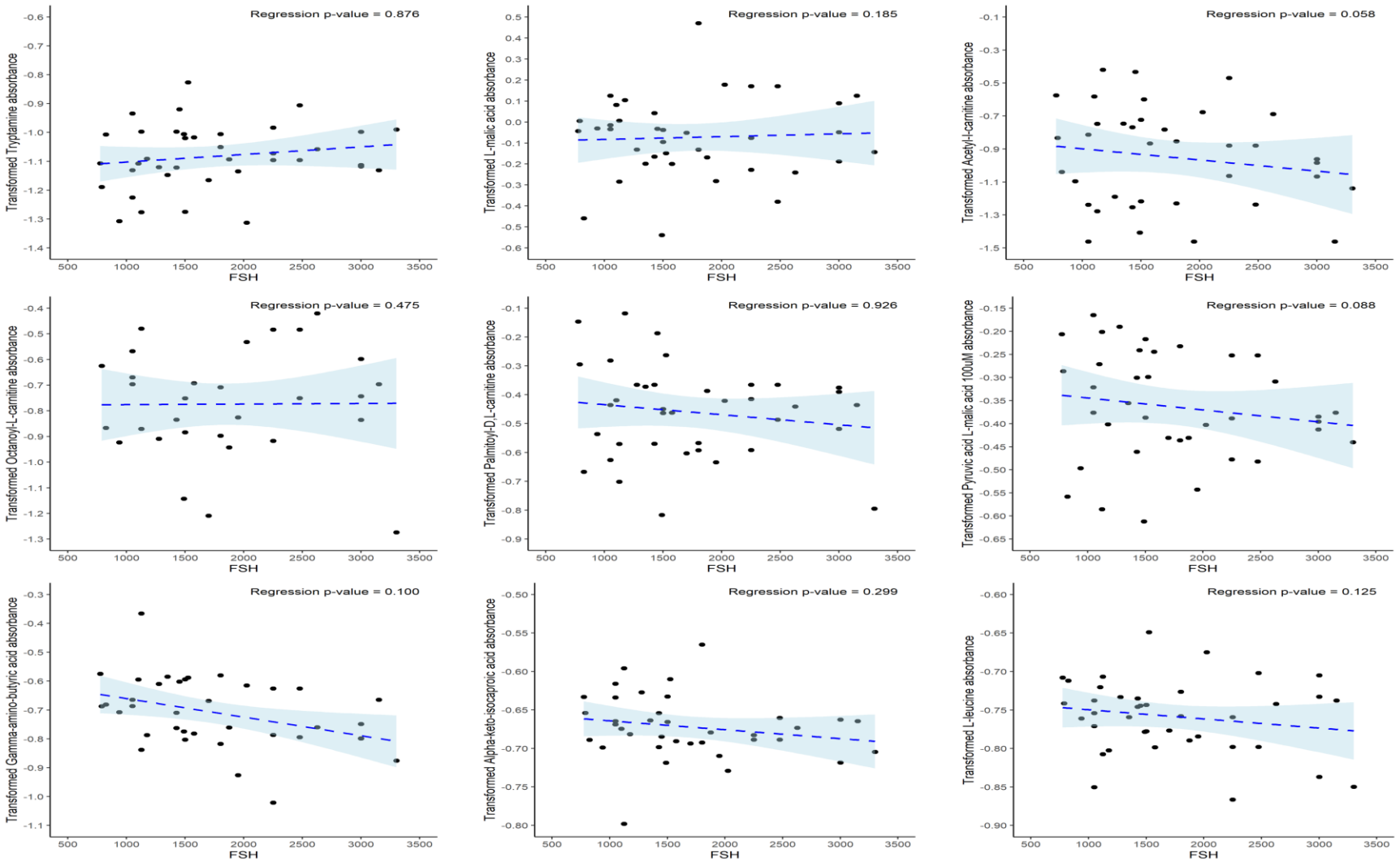

Figure 4.8 Continued

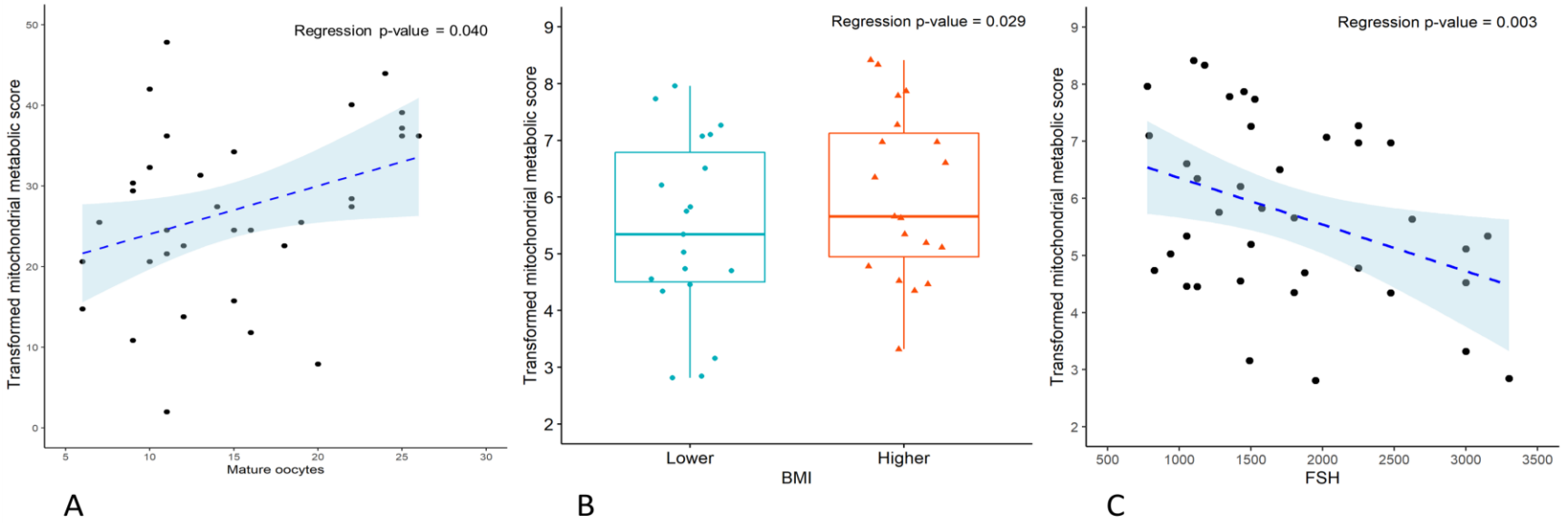

Figure 4.9 Mitochondrial metabolic scores demonstrating significant utilization differences based on BMI, total FSH dose, and number of mature oocytes retrieved. Mitochondrial metabolic scores were Box-Cox transformed for normality and modeled using multiple linear regression. **A)** Mitochondrial metabolic scores were found to be significantly higher in GCs of patients with higher numbers of mature oocytes retrieved ($P < 0.05$), after adjusting for the other factors in the model. In a backward selected best fit model using only the BMI and total FSH dosage administered, **B)** mitochondrial metabolic scores were found to be significantly lower in pooled GCs of patients with a lower BMI ($P < 0.05$). BMI was divided into 2 groups with the higher group being patients with a BMI of ≥ to 26 kg/m^2 (n = 20) and the lower group being patients with a BMI of < 26 kg/m^2 (n = 20). **C)** Mitochondrial metabolic scores were found to be significantly lower as the patient's FSH dose administered increased ($P < 0.01$). For BMI, transformed mitochondrial metabolic scores are presented as the median (line inside box), first and third quartile (bottom and top of box), and the whiskers extend to 1.5 times the interquartile range beyond the first and third quartile. For mature oocytes retrieved and FSH dose administered, the transformed scores are presented in a scatter plot of the individual patient values showing the trend line and the 95% confidence region.

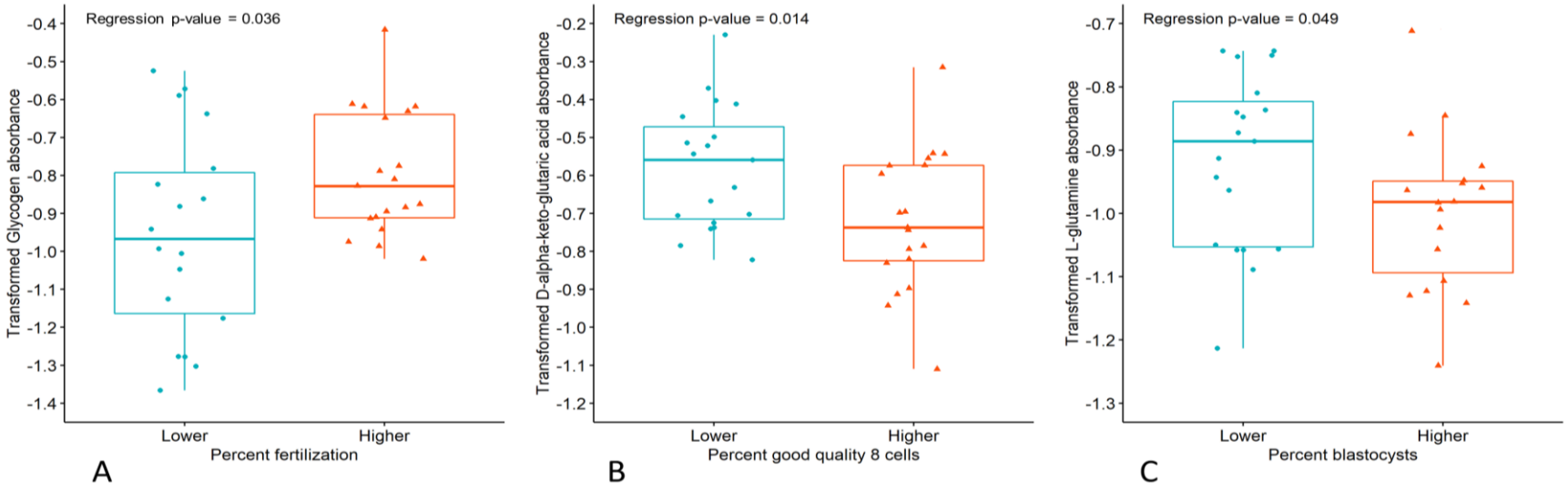

Figure 4.10 Substrates demonstrating significant mitochondrial utilization differences based on embryo cohort development. To determine the differences in mitochondrial utilization, substrates were modeled using multiple linear regression after Box-Cox transformation for normality. Cohorts were grouped as follows, higher fertilization percentage ≥ 80% (n = 22), and lower fertilization percentage < 80% (n = 18); Higher good 8-cell development > 55% (n = 22) and lower good 8-cell development ≤ 55% (n = 18); and higher percentage of blastocyst formation > 55% (n = 17) and lower percentage of blastocyst formation ≤ 55% (n = 22). One patient was excluded from the blastocyst formation data as she had an embryo transfer on day 3 with no additional embryos available for extended culture. **A)** Mitochondrial utilization of glycogen (P < 0.05) was found to be significantly lower in GCs of patients with lower fertilization percentage, **B)** mitochondrial utilization of D-alpha-keto-glutaric acid (P < 0.05) was found to be significantly higher in GCs from patients with a lower percentage of good quality 8-cell embryos, after adjusting for the other factors in the model. **C)** In a backward selected best fit model using only the percentage of good 8-cell embryos and percentage of blastocysts, mitochondrial utilization of L-glutamine (P < 0.05) was found to be significantly higher in GCs from patients with a lower percentage of blastocyst formation. Data are presented as the median (line inside box), first and third quartile (bottom and top of box), and the whiskers extend to 1.5 times the interquartile range beyond the first and third quartile.

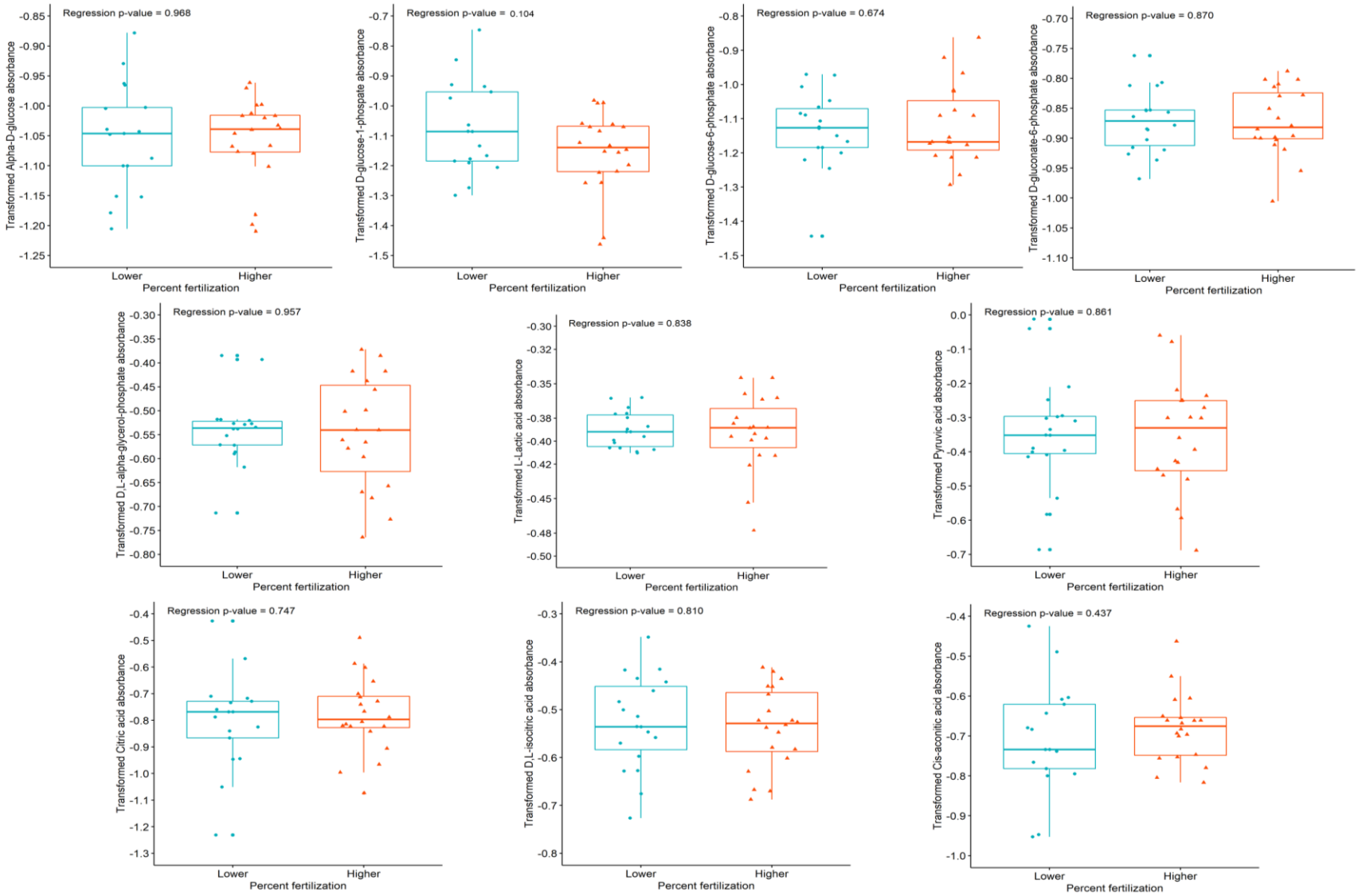
Regression p-value = 0.968
Transformed Alpha-D-glucose absorbance
Regression p-value = 0.104
Transformed D-glucose-1-phospate absorbance
Regression p-value = 0.674
Transformed D-glucose-6-phosphate absorbance
Regression p-value = 0.870
Transformed D-gluconate-6-phosphate absorbance
Regression p-value = 0.957
Transformed D,L-alpha-glycerol-phosphate absorbance
Regression p-value = 0.838
Transformed L-Lactic acid absorbance
Regression p-value = 0.861
Transformed Pyruvic acid absorbance
Regression p-value = 0.747
Transformed Citric acid absorbance
Regression p-value = 0.810
Transformed D,L-isocitric acid absorbance
Regression p-value = 0.437
Transformed Cis-aconitic acid absorbance
Lower
Higher
Percent fertilization

Figure 4.11 Substrates demonstrating no significant mitochondrial utilization differences based on fertilization percentage. To determine the differences in mitochondrial utilization, substrates were compared using a multiple linear regression model using Box-Cox transformation. The 2 groups were delineated by higher fertilization percentage ≥ 80% (n = 22), and lower fertilization percentage < 80% (n = 18). Data are presented as the median (line inside box), first and third quartile (bottom and top of box), and the whiskers extend to 1.5 times the interquartile range beyond the first and third quartile.

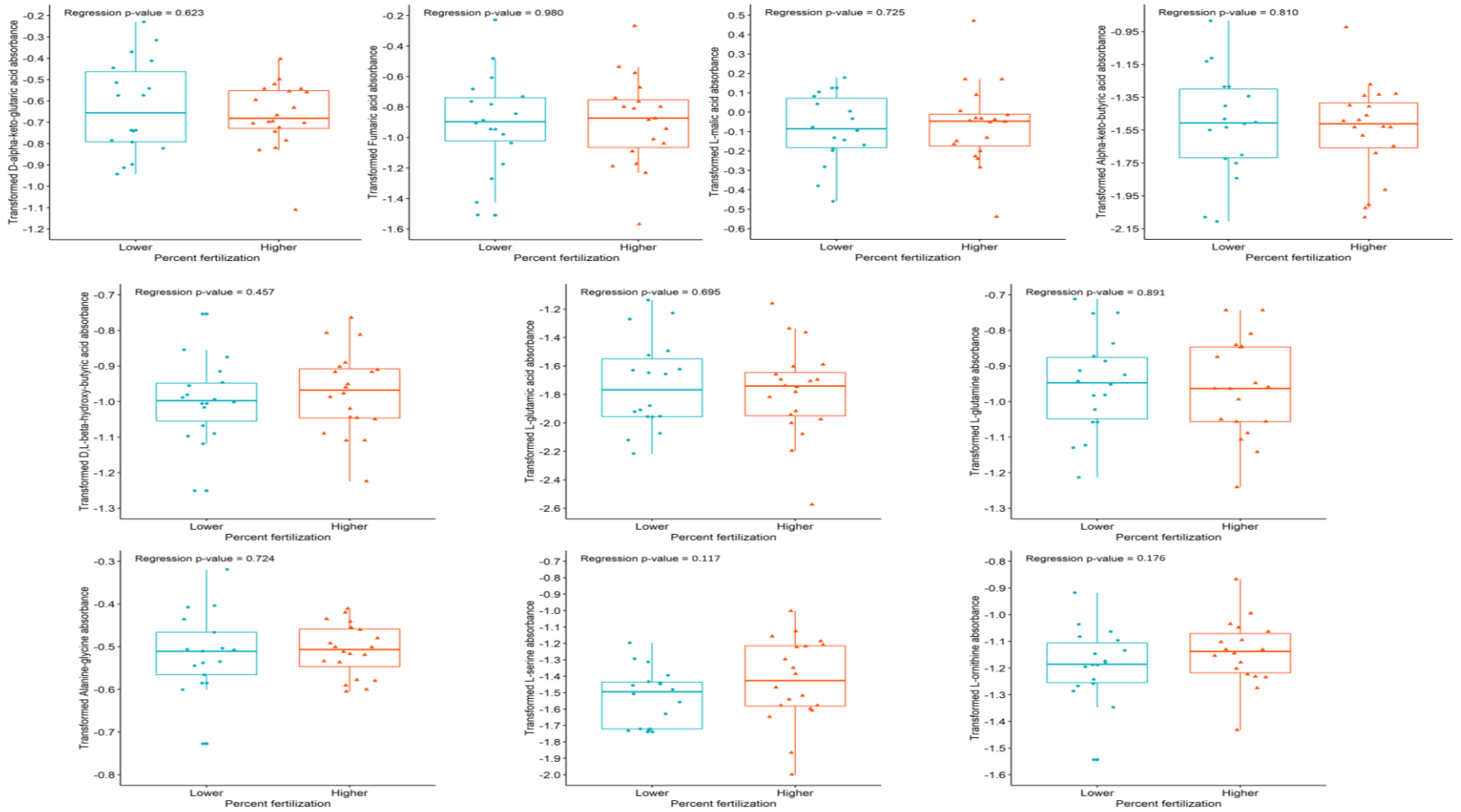

Figure 4.11 Continued

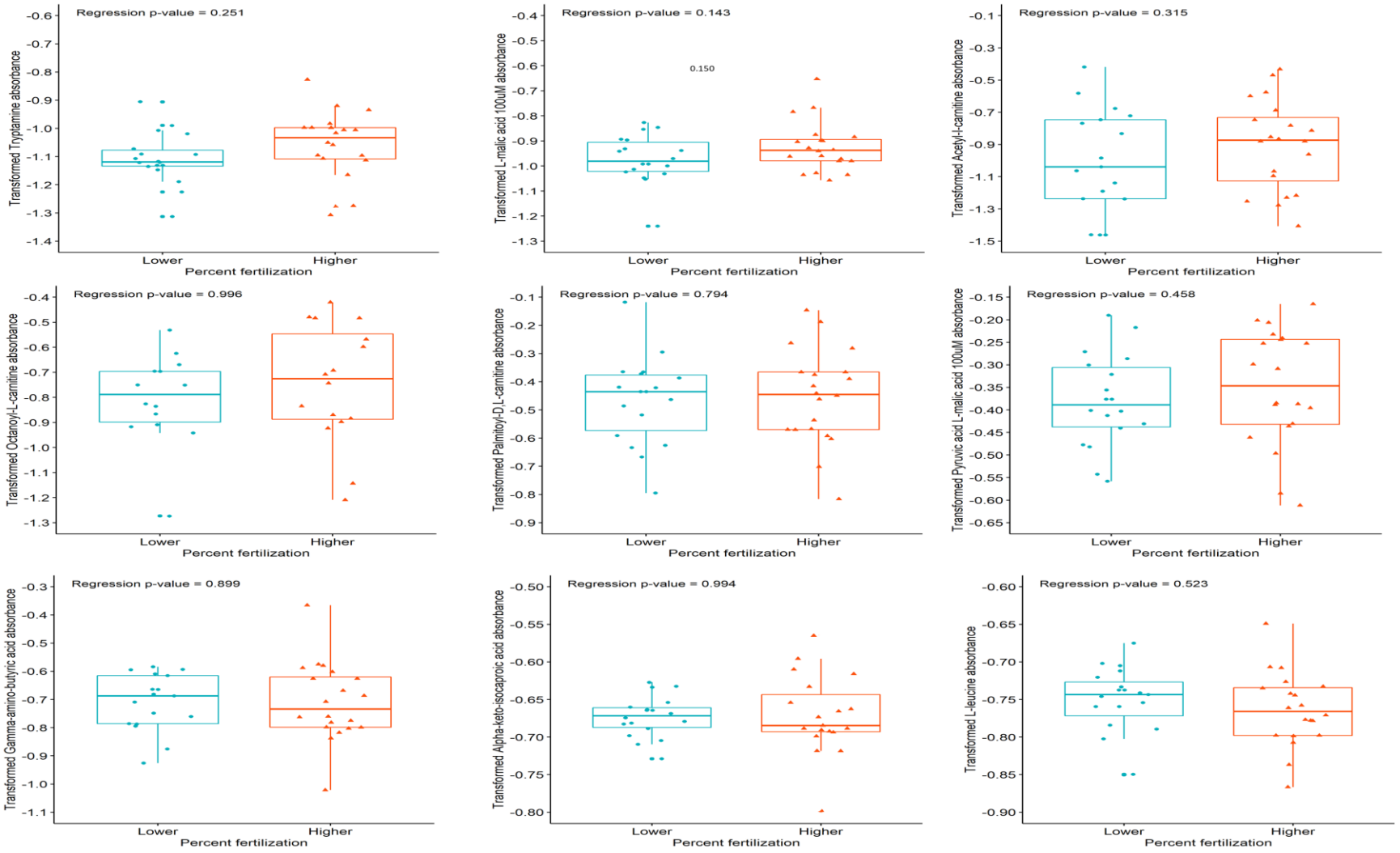

Figure 4.11 Continued

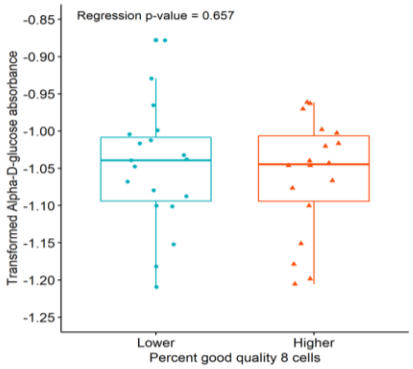
Regression p-value = 0.657
Transformed Alpha-D-glucose absorbance
-0.85
-0.90
-0.95
-1.00
-1.05
-1.10
-1.15
-1.20
-1.25
Lower
Higher
Percent good quality 8 cells

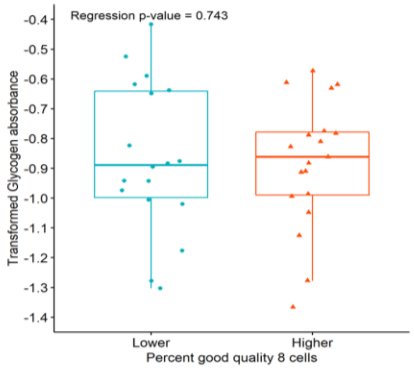
Regression p-value = 0.743
Transformed Glycogen absorbance
-0.4
-0.5
-0.6
-0.7
-0.8
-0.9
-1.0
-1.1
-1.2
-1.3
-1.4
Lower
Higher
Percent good quality 8 cells

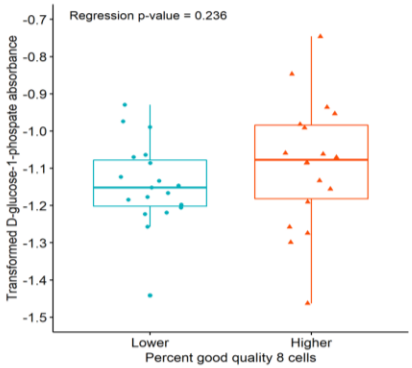
Regression p-value = 0.236
Transformed D-glucose-1-phospate absorbance
-0.7
-0.8
-0.9
-1.0
-1.1
-1.2
-1.3
-1.4
-1.5
Lower
Higher
Percent good quality 8 cells

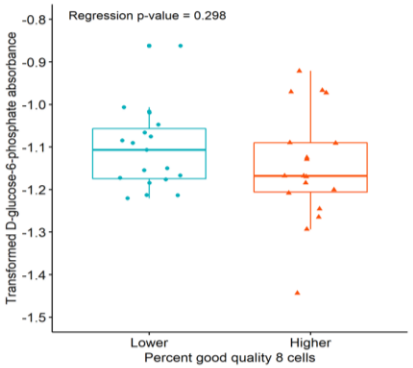
Regression p-value = 0.298
Transformed D-glucose-6-phosphate absorbance
-0.8
-0.9
-1.0
-1.1
-1.2
-1.3
-1.4
-1.5
Lower
Higher
Percent good quality 8 cells

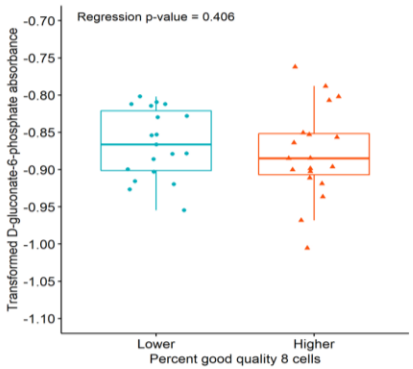
Regression p-value = 0.406
Transformed D-gluconate-6-phosphate absorbance
-0.70
-0.75
-0.80
-0.85
-0.90
-0.95
-1.00
-1.05
-1.10
Lower
Higher
Percent good quality 8 cells

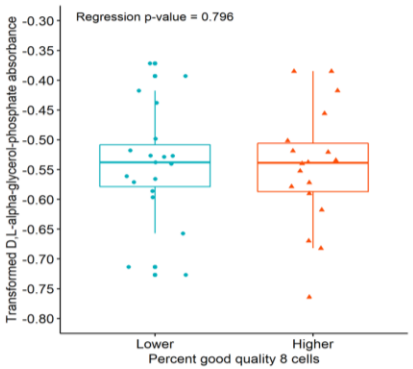
Regression p-value = 0.796
Transformed D,L-alpha-glycerol-phosphate absorbance
-0.30
-0.35
-0.40
-0.45
-0.50
-0.55
-0.60
-0.65
-0.70
-0.75
-0.80
Lower
Higher
Percent good quality 8 cells

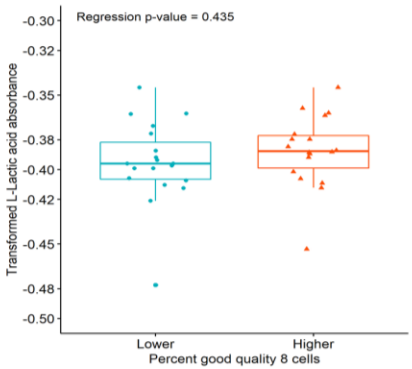
Regression p-value = 0.435
Transformed L-Lactic acid absorbance
-0.30
-0.32
-0.35
-0.38
-0.40
-0.42
-0.45
-0.48
-0.50
Lower
Higher
Percent good quality 8 cells

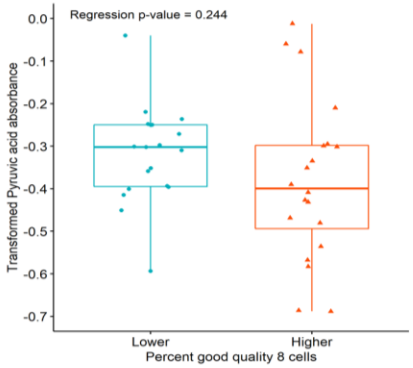
Regression p-value = 0.244
Transformed Pyruvic acid absorbance
0.0
-0.1
-0.2
-0.3
-0.4
-0.5
-0.6
-0.7
Lower
Higher
Percent good quality 8 cells

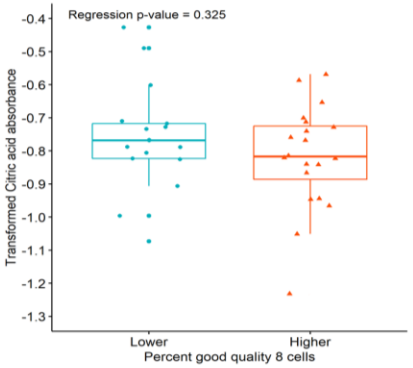
Regression p-value = 0.325
Transformed Citric acid absorbance
-0.4
-0.5
-0.6
-0.7
-0.8
-0.9
-1.0
-1.1
-1.2
-1.3
Lower
Higher
Percent good quality 8 cells

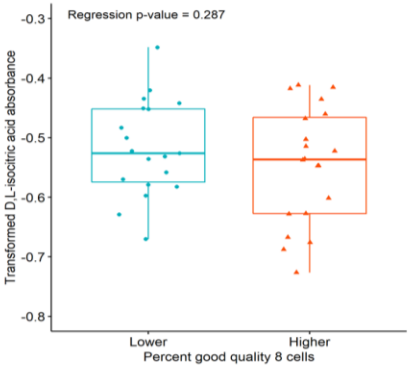
Regression p-value = 0.287
Transformed D,L-isocitric acid absorbance
-0.3
-0.4
-0.5
-0.6
-0.7
-0.8
Lower
Higher
Percent good quality 8 cells

Figure 4.12 Substrates demonstrating no significant mitochondrial utilization differences based on good 8-cell embryo development. To determine the differences in mitochondrial utilization, substrates were compared using a multiple linear regression model using Box-Cox transformation. The 2 groups were delineated by higher good 8-cell development > 55% (n = 22) and lower good 8-cell development ≤ 55% (n = 18). Mitochondrial utilization of L-serine ($P < 0.10$) was found to be borderline higher in GCs of patients with a lower percentage of good quality 8-cell embryos. In a backward selected best fit model using only the percentage of good 8-cell embryos and percentage of blastocysts, L-glutamine ($P < 0.10$) was found to be borderline higher in in pooled GCs from patients with a lower percentage of good quality 8-cell embryos. No other substrates showed significant differences. Data are presented as the median (line inside box), first and third quartile (bottom and top of box), and the whiskers extend to 1.5 times the interquartile range beyond the first and third quartile.

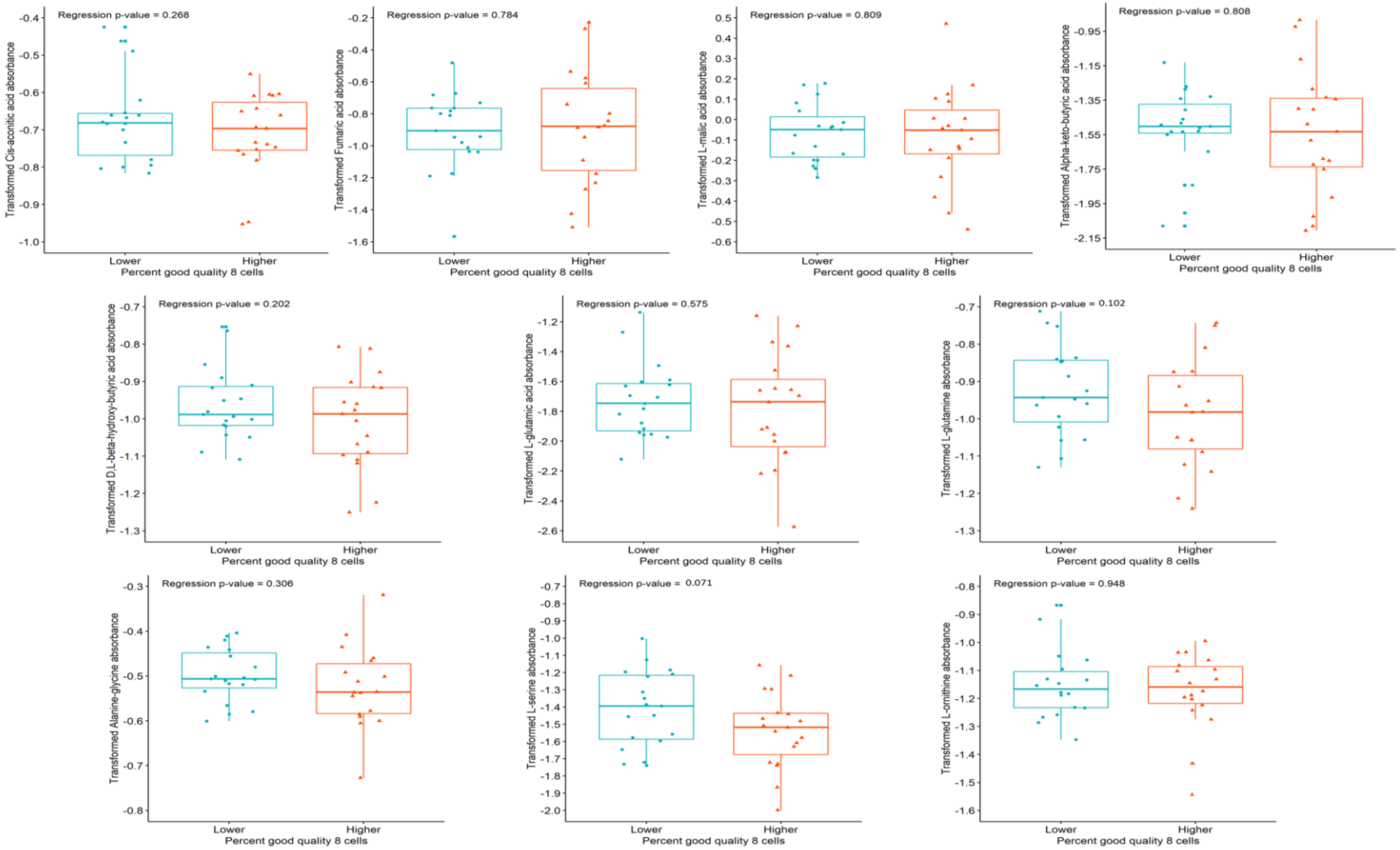

Figure 4.12 Continued

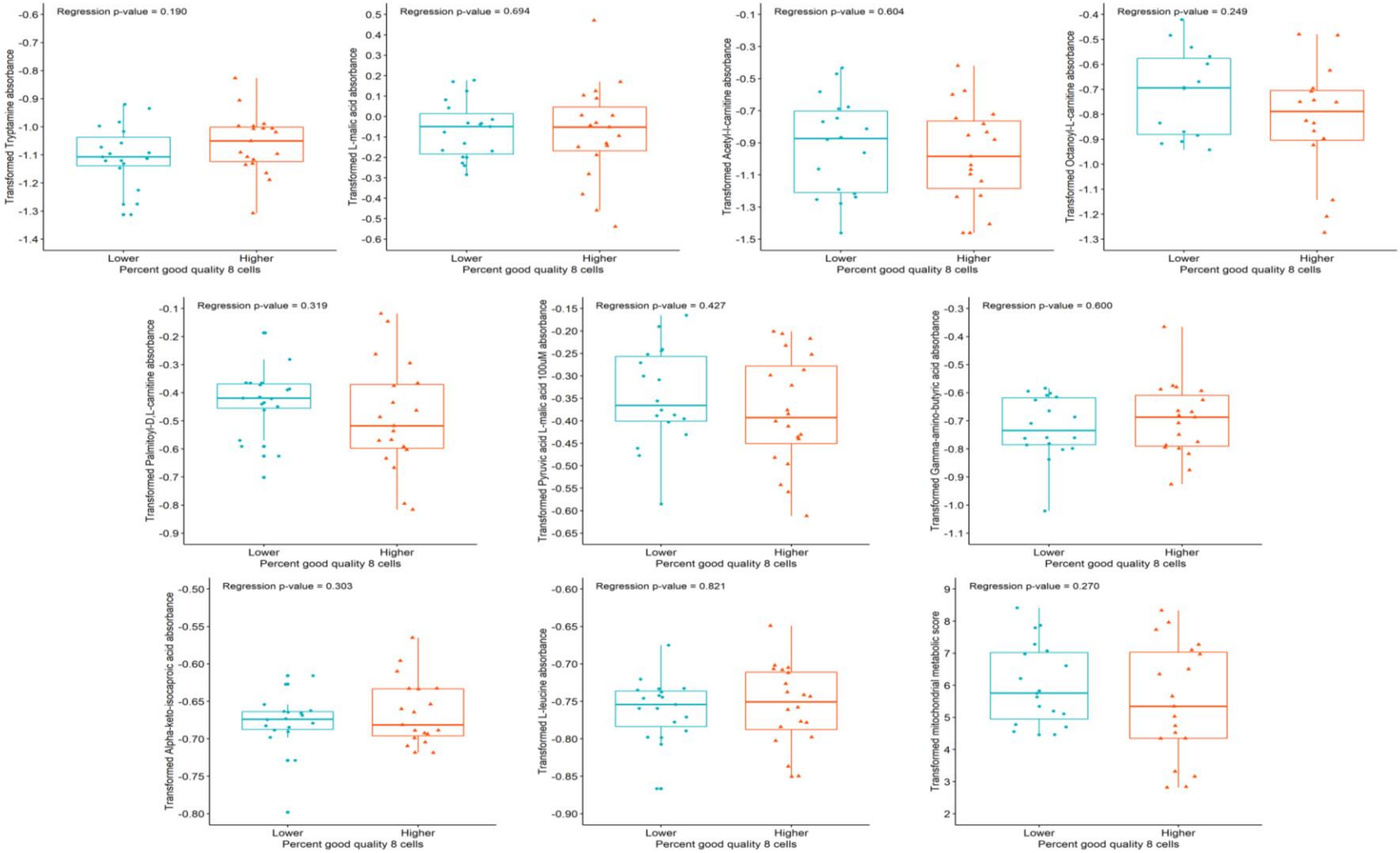

Figure 4.12 Continued

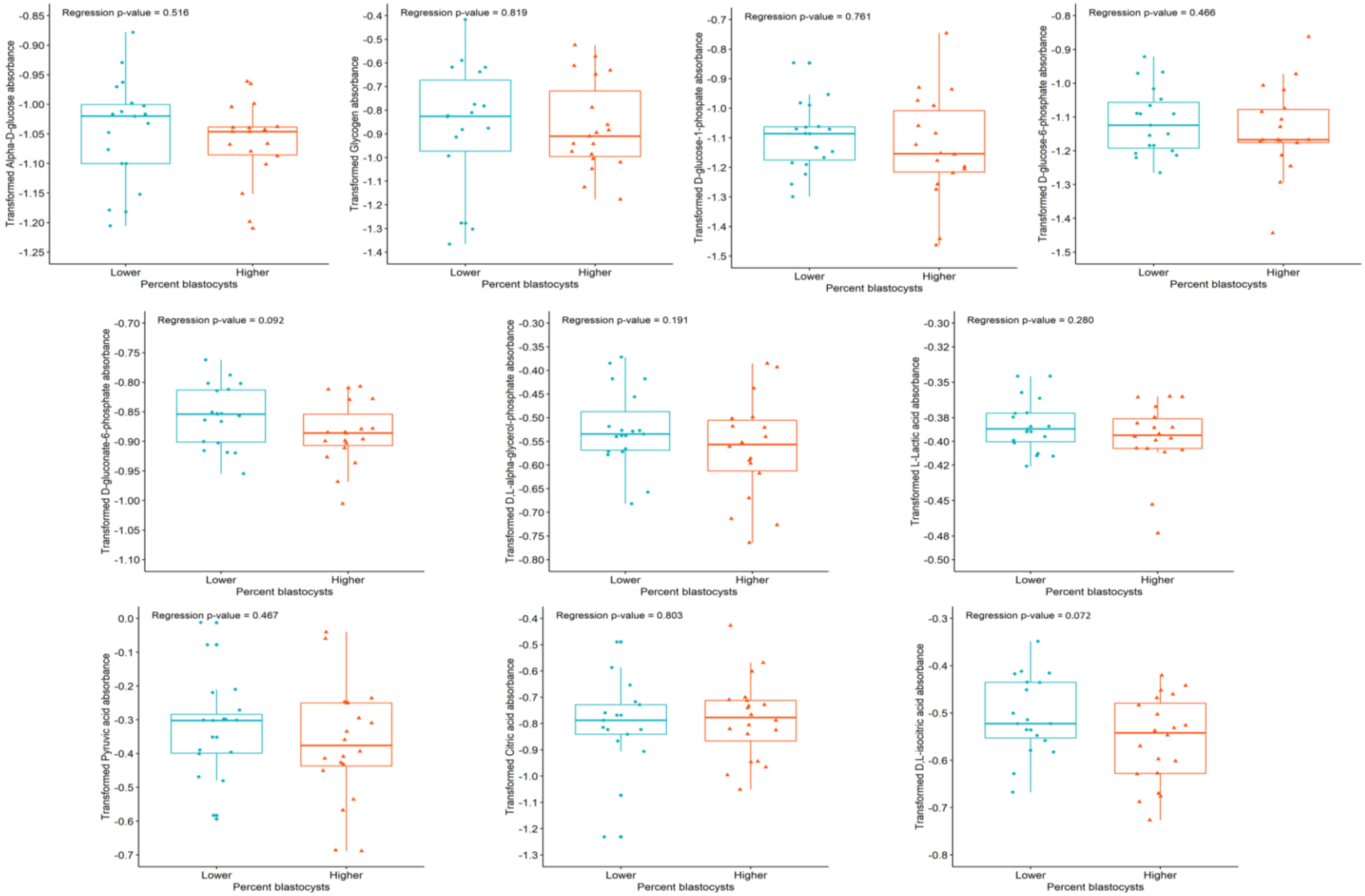
Regression p-value = 0.516
Transformed Alpha-D-glucose absorbance
Regression p-value = 0.819
Transformed Glycogen absorbance
Regression p-value = 0.761
Transformed D-glucose-1-phospate absorbance
Regression p-value = 0.466
Transformed D-glucose-6-phosphate absorbance
Regression p-value = 0.092
Transformed D-gluconate-6-phosphate absorbance
Regression p-value = 0.191
Transformed D,L-alpha-glycerol-phosphate absorbance
Regression p-value = 0.280
Transformed L-Lactic acid absorbance
Regression p-value = 0.467
Transformed Pyruvic acid absorbance
Regression p-value = 0.803
Transformed Citric acid absorbance
Regression p-value = 0.072
Transformed D,L-isocitric acid absorbance
Lower
Higher
Percent blastocysts

Figure 4.13 Substrates demonstrating no significant mitochondrial utilization differences based on blastocyst formation. To determine the differences in mitochondrial utilization, substrates were compared using a multiple linear regression model using Box-Cox transformation. The 2 groups were delineated by higher percentage of blastocyst formation > 55% (n = 17) and lower percentage of blastocyst formation ≤ 55% (n = 22). Mitochondrial utilization of D-Gluconate-6-phosphate ($P < 0.10$), and D,L-isocitric acid ($P < 0.10$) were found to be borderline higher in patients with a lower percentage of blastocyst formation in pooled GCs, after adjusting for the other factors in the model. No other substrates demonstrated significant differences. Data are presented as the median (line inside box), first and third quartile (bottom and top of box), and the whiskers extend to 1.5 times the interquartile range beyond the first and third quartile.

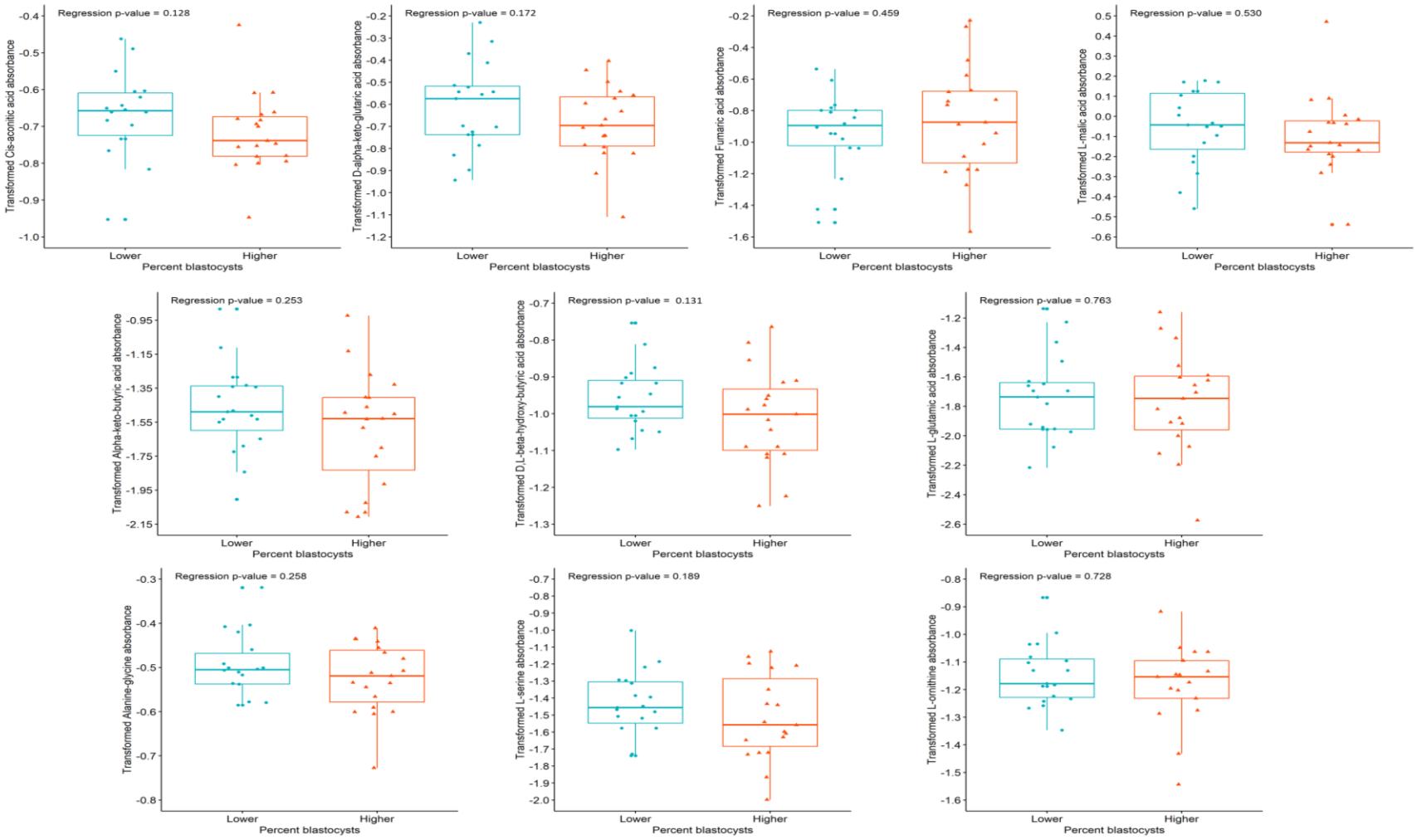

Figure 4.13 Continued

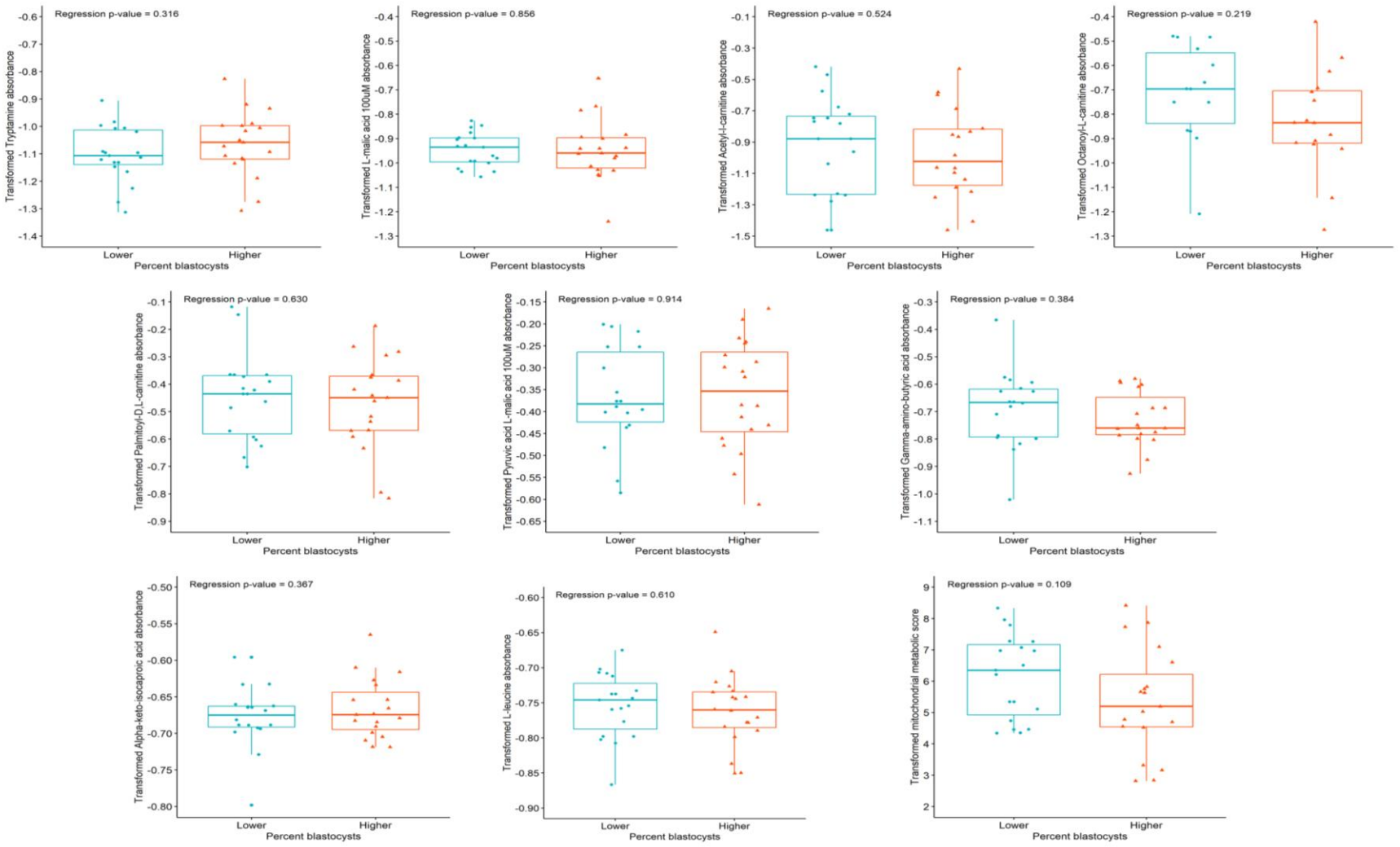

Figure 4.13 Continued

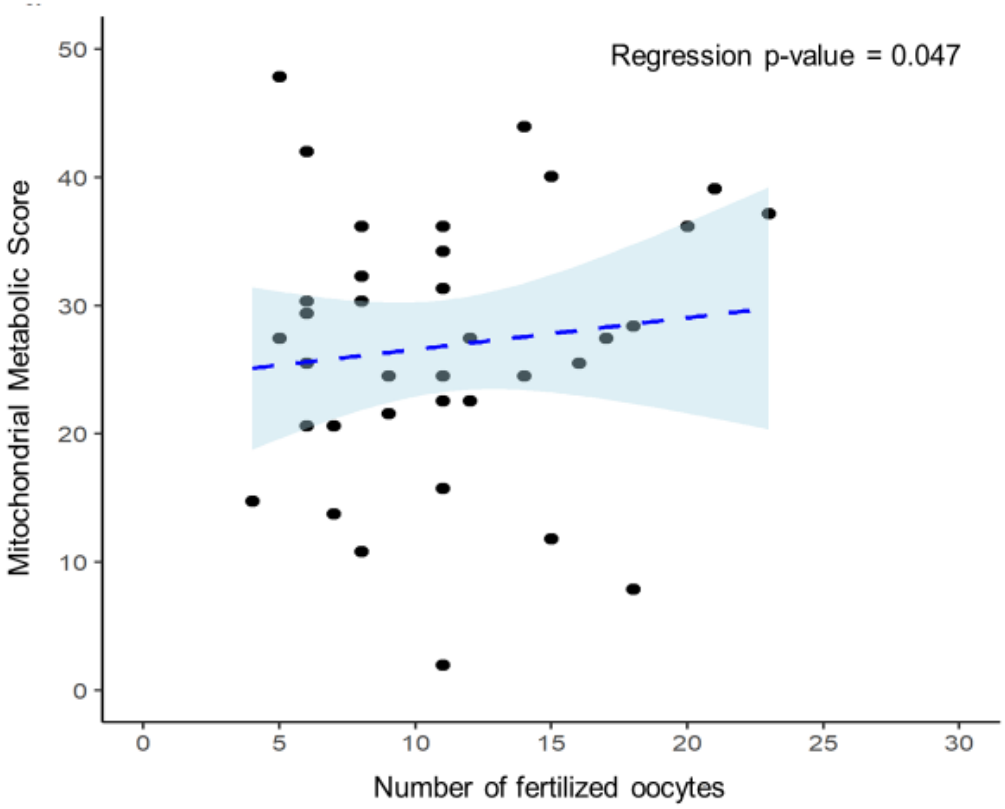

Figure 4.14 Mitochondrial metabolic scores demonstrating significant utilization differences based the total number of fertilized oocytes. Based on the estimated multiple linear regression model using observed data after Box-Cox transformation for normality, mitochondrial metabolic scores were found to be significantly higher in granulosa cells of patients with higher overall number of fertilized oocytes ($P < 0.05$) in pooled GCs, after adjusting for the other factors in the model, Data are presented as a scatter plot of the individual patient Box-Cox transformed values showing the trend line and the 95% confidence region.

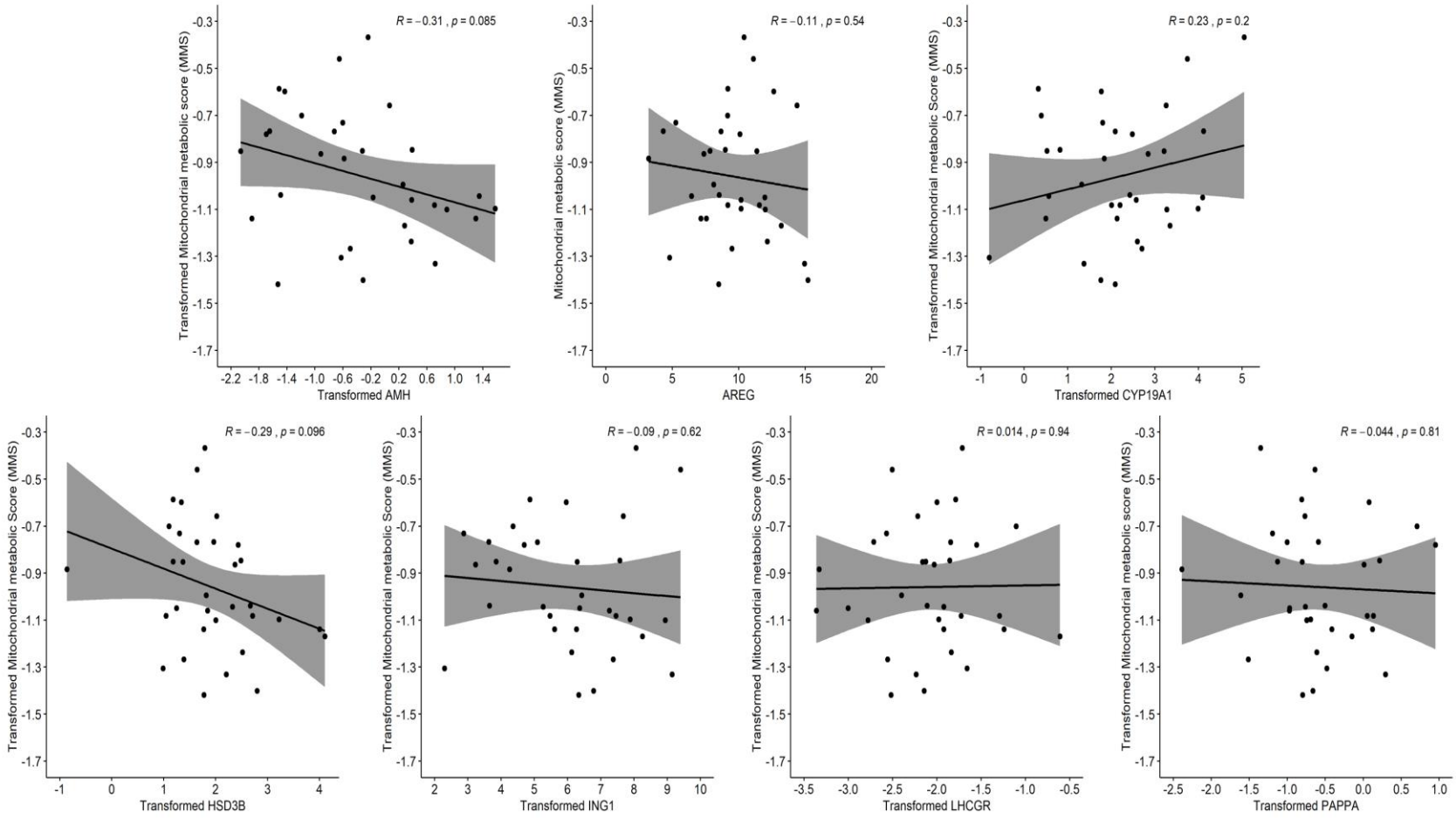

Figure 4.15 Mitochondrial metabolic scores based on mRNA levels. Based on Pearson's correlation analysis using data after Box-Cox transformation for normality, *HSD3B* mRNA levels were borderline significantly lower ($P < 0.10$) as the mitochondrial metabolic score decreased, Data are presented as a scatter plot of the individual patient Box-Cox transformed values showing the trend line and the 95% confidence region.

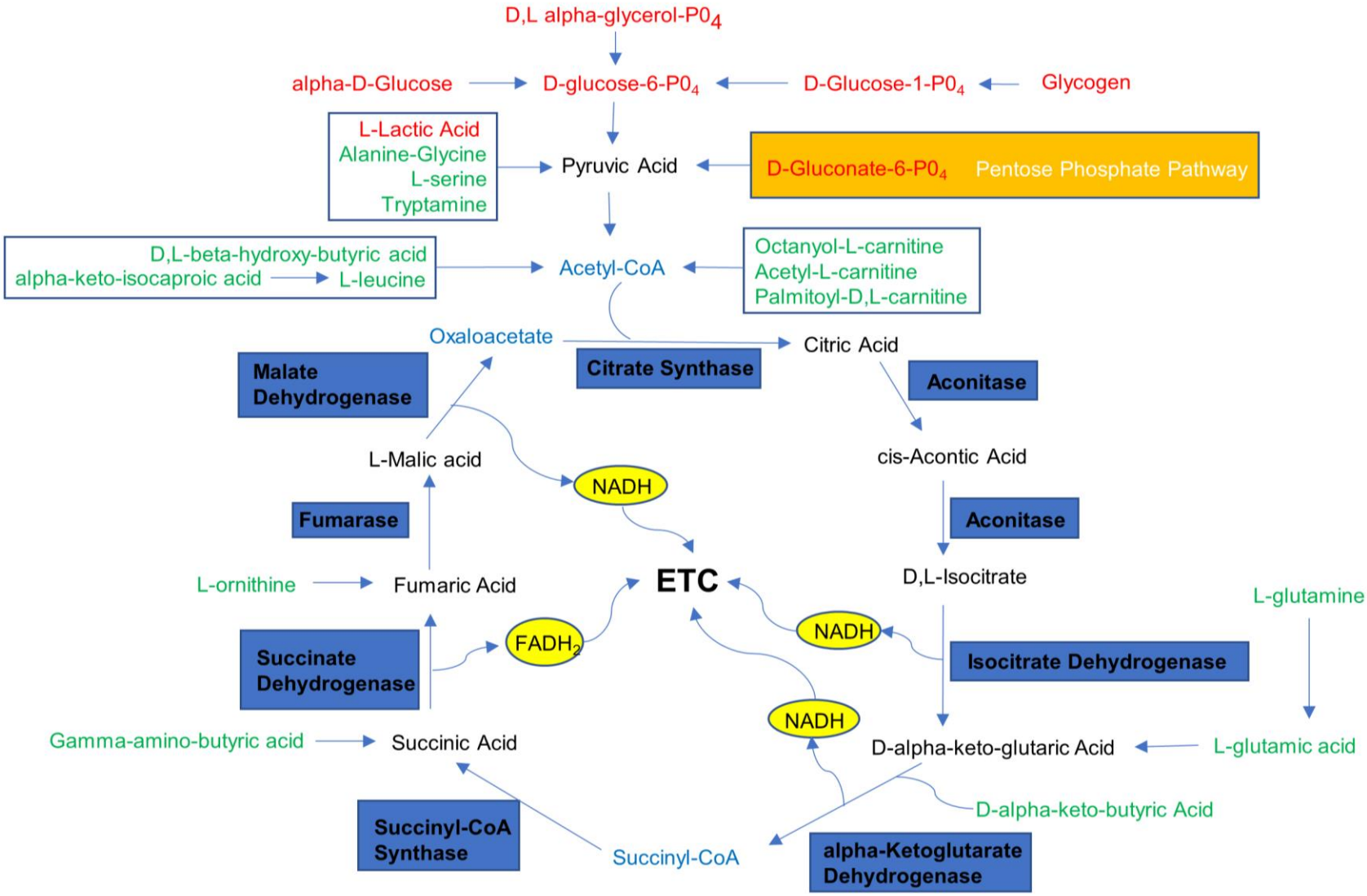
D,L alpha-glycerol-P0$_4$
alpha-D-Glucose
D-glucose-6-P0$_4$
D-Glucose-1-P0$_4$
Glycogen
L-Lactic Acid
Alanine-Glycine
L-serine
Tryptamine
Pyruvic Acid
D-Gluconate-6-P0$_4$
Pentose Phosphate Pathway
D,L-beta-hydroxy-butyric acid
alpha-keto-isocaproic acid
L-leucine
Acetyl-CoA
Octanyol-L-carnitine
Acetyl-L-carnitine
Palmitoyl-D,L-carnitine
Oxaloacetate
Citrate Synthase
Citric Acid
Malate Dehydrogenase
Aconitase
L-Malic acid
cis-Acontic Acid
NADH
Fumarase
Aconitase
L-ornithine
Fumaric Acid
ETC
D,L-Isocitrate
L-glutamine
NADH
FADH$_2$
Isocitrate Dehydrogenase
Succinate Dehydrogenase
NADH
Gamma-amino-butyric acid
Succinic Acid
D-alpha-keto-glutaric Acid
L-glutamic acid
D-alpha-keto-butyric Acid
Succinyl-CoA Synthase
Succinyl-CoA
alpha-Ketoglutarate Dehydrogenase

Figure 4.16 Tricarboxylic acid cycle diagram showing where the substrates of the mitochondrial function assay enter the cycle. This pathway diagram illustrates the various points where the substrates are converted and enter the tricarboxylic cycle. The substrates were metabolized through different biochemical pathways by entering the mitochondria through different transporters and they were then modified by various enzymes and dehydrogenases to produce NADH or $FADH_{2.}$ Blue = tricarboxylic acid constituents that are not substrates in the assay, Blue boxes = enzymes, Black = tricarboxylic acid cycle substrates, ETC = electron transport chain, $FADH_2$ = flavin adenine dinucleotide hydride, Green = other mitochondrial substrates, NADH = nicotinamide adenine dinucleotide hydride, Red = cystolic substrates.

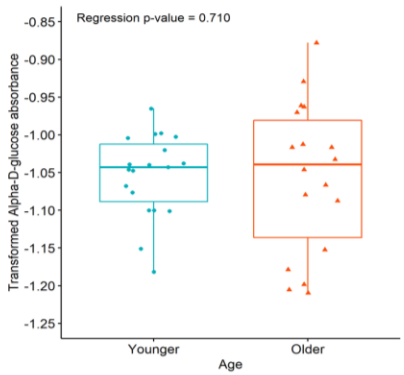
Regression p-value = 0.710
Transformed Alpha-D-glucose absorbance
Younger
Older
Age

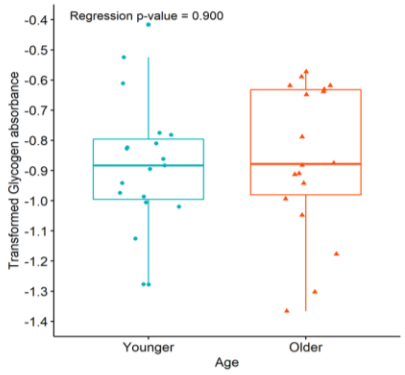
Regression p-value = 0.900
Transformed Glycogen absorbance
Younger
Older
Age

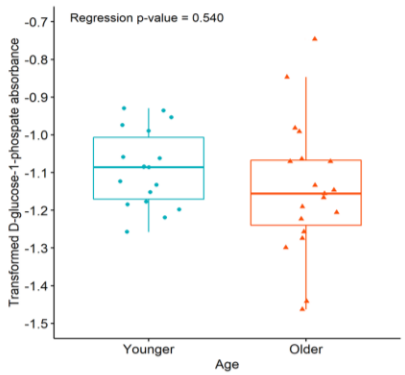
Regression p-value = 0.540
Transformed D-glucose-1-phospate absorbance
Younger
Older
Age

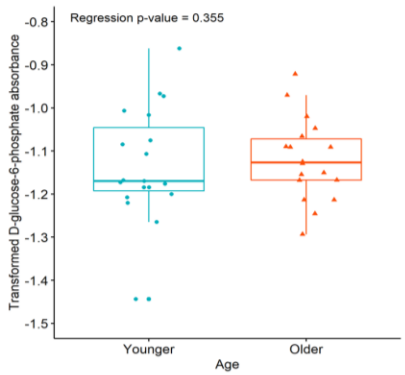
Regression p-value = 0.355
Transformed D-glucose-6-phosphate absorbance
Younger
Older
Age

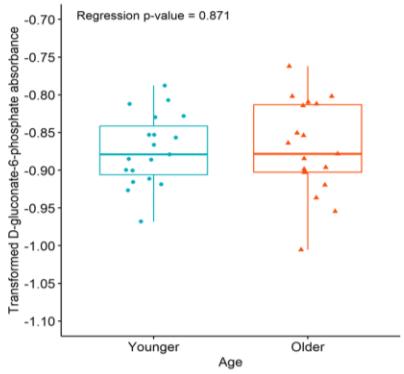
Regression p-value = 0.871
Transformed D-gluconate-6-phosphate absorbance
Younger
Older
Age

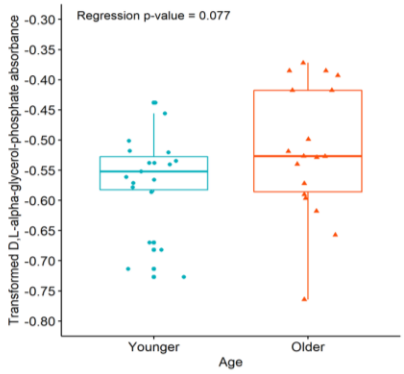
Regression p-value = 0.077
Transformed D,L-alpha-glycerol-phosphate absorbance
Younger
Older
Age

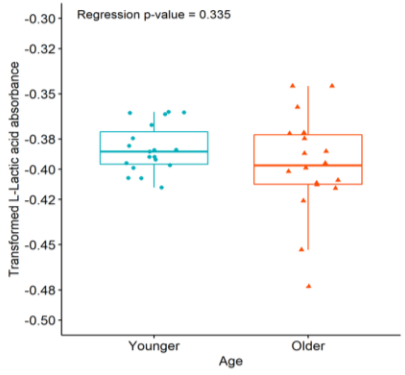
Regression p-value = 0.335
Transformed L-Lactic acid absorbance
Younger
Older
Age

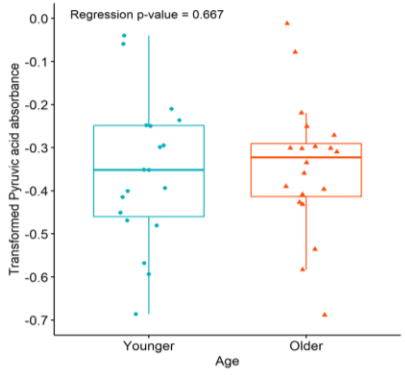
Regression p-value = 0.667
Transformed Pyruvic acid absorbance
Younger
Older
Age

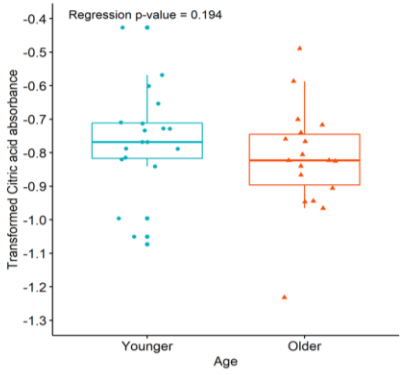
Regression p-value = 0.194
Transformed Citric acid absorbance
Younger
Older
Age

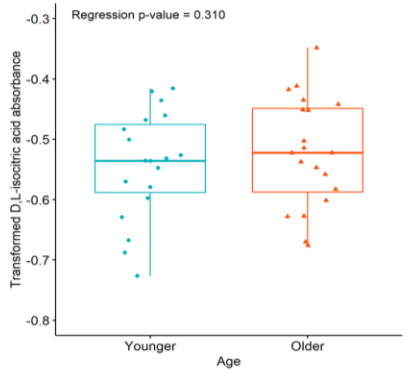
Regression p-value = 0.310
Transformed D,L-isocitric acid absorbance
Younger
Older
Age

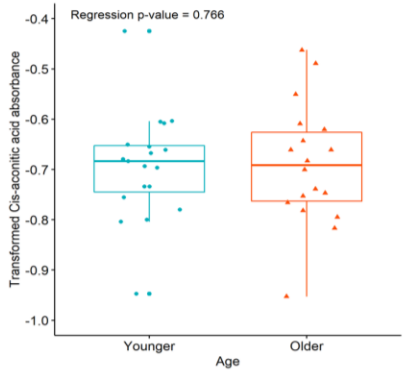
Regression p-value = 0.766
Transformed Cis-aconitic acid absorbance
Younger
Older
Age

Figure 4.17 Substrates demonstrating no significant mitochondrial utilization differences based on age. To determine the differences in mitochondrial utilization, substrates were modeled using multiple linear regression after Box-Cox transformation for normality. Age was divided into 2 groups with the older age being ≥ 34 years old (n = 19) and younger age being < 34 years old (n = 21). No substrates showed any statistically significant difference in mitochondrial utilization. Box-Cox transformed data are presented as the median (line inside box), first and third quartile (bottom and top of box), and the whiskers extend to 1.5 times the interquartile range beyond the first and third quartile.

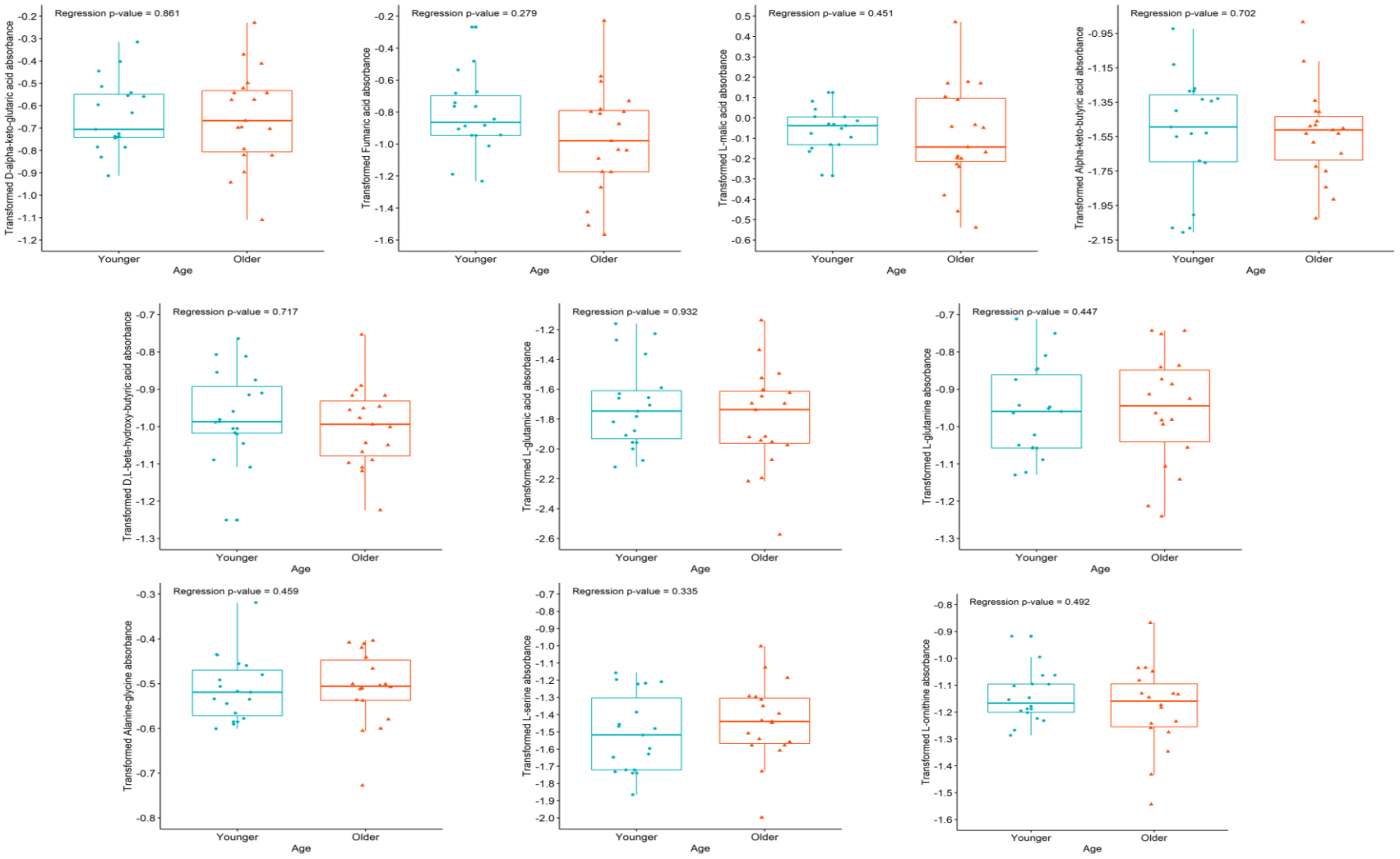

Figure 4.17 Continued

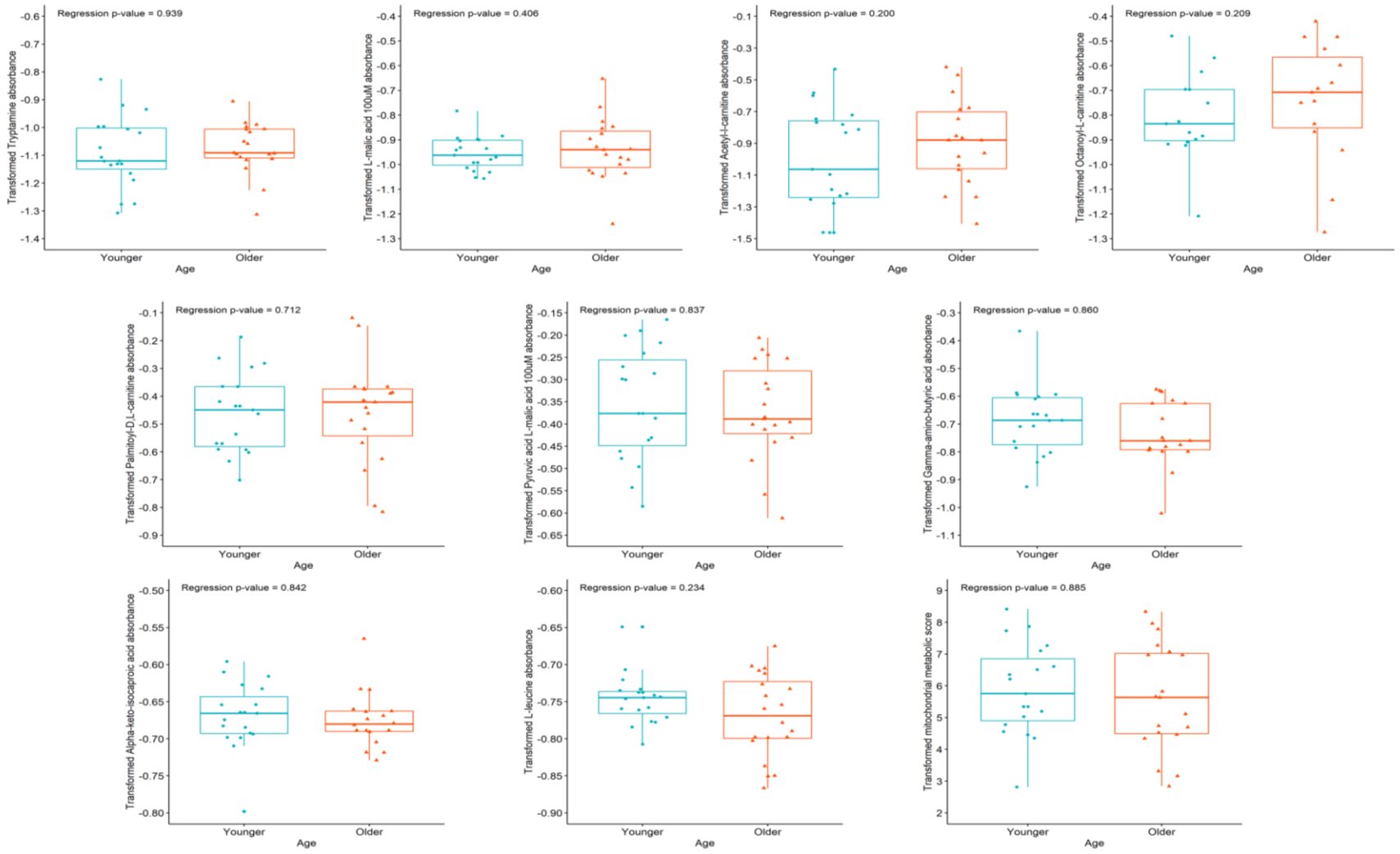

Figure 4.17 Continued

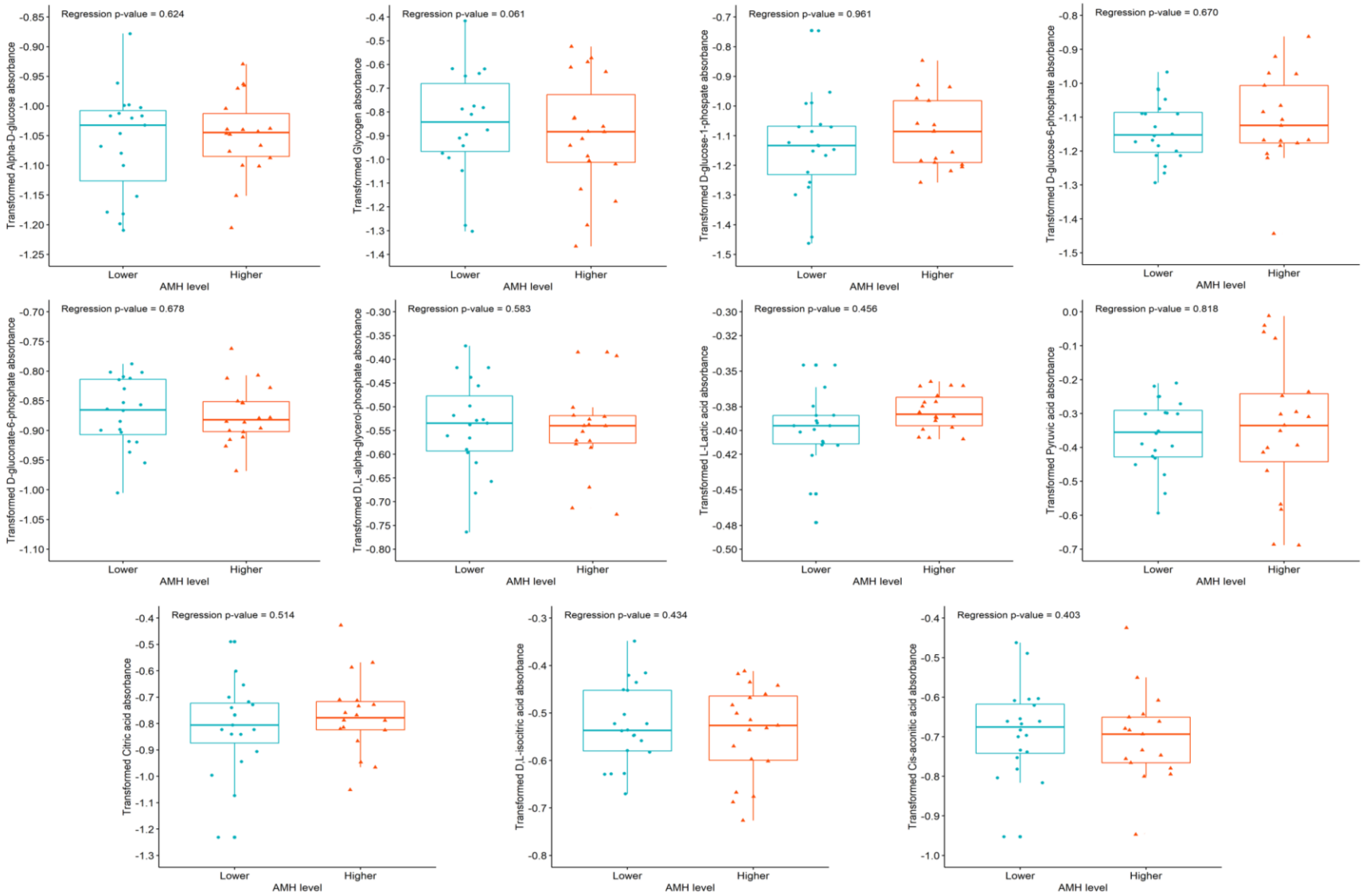
Regression p-value = 0.624
Transformed Alpha-D-glucose absorbance
Regression p-value = 0.061
Transformed Glycogen absorbance
Regression p-value = 0.961
Transformed D-glucose-1-phospate absorbance
Regression p-value = 0.670
Transformed D-glucose-6-phosphate absorbance
Regression p-value = 0.678
Transformed D-gluconate-6-phosphate absorbance
Regression p-value = 0.583
Transformed D,L-alpha-glycerol-phosphate absorbance
Regression p-value = 0.456
Transformed L-Lactic acid absorbance
Regression p-value = 0.818
Transformed Pyruvic acid absorbance
Regression p-value = 0.514
Transformed Citric acid absorbance
Regression p-value = 0.434
Transformed D,L-isocitric acid absorbance
Regression p-value = 0.403
Transformed Cis-aconitic acid absorbance
Lower
Higher
AMH level

Figure 4.18 Substrates demonstrating no significant mitochondrial utilization differences based on serum AMH levels. To determine the differences in mitochondrial utilization, substrates were modeled using multiple linear regression after Box-Cox transformation for normality. Serum AMH was divided into 2 groups with higher serum AMH being ≥ 3.5 ng/mL (n = 20) and lower serum AMH being < 3.5 ng/ml (n = 20). No substrates showed any statistically significant difference in mitochondrial utilization. Box-Cox transformed data are presented as the median (line inside box), first and third quartile (bottom and top of box), and the whiskers extend to 1.5 times the interquartile range beyond the first and third quartile.

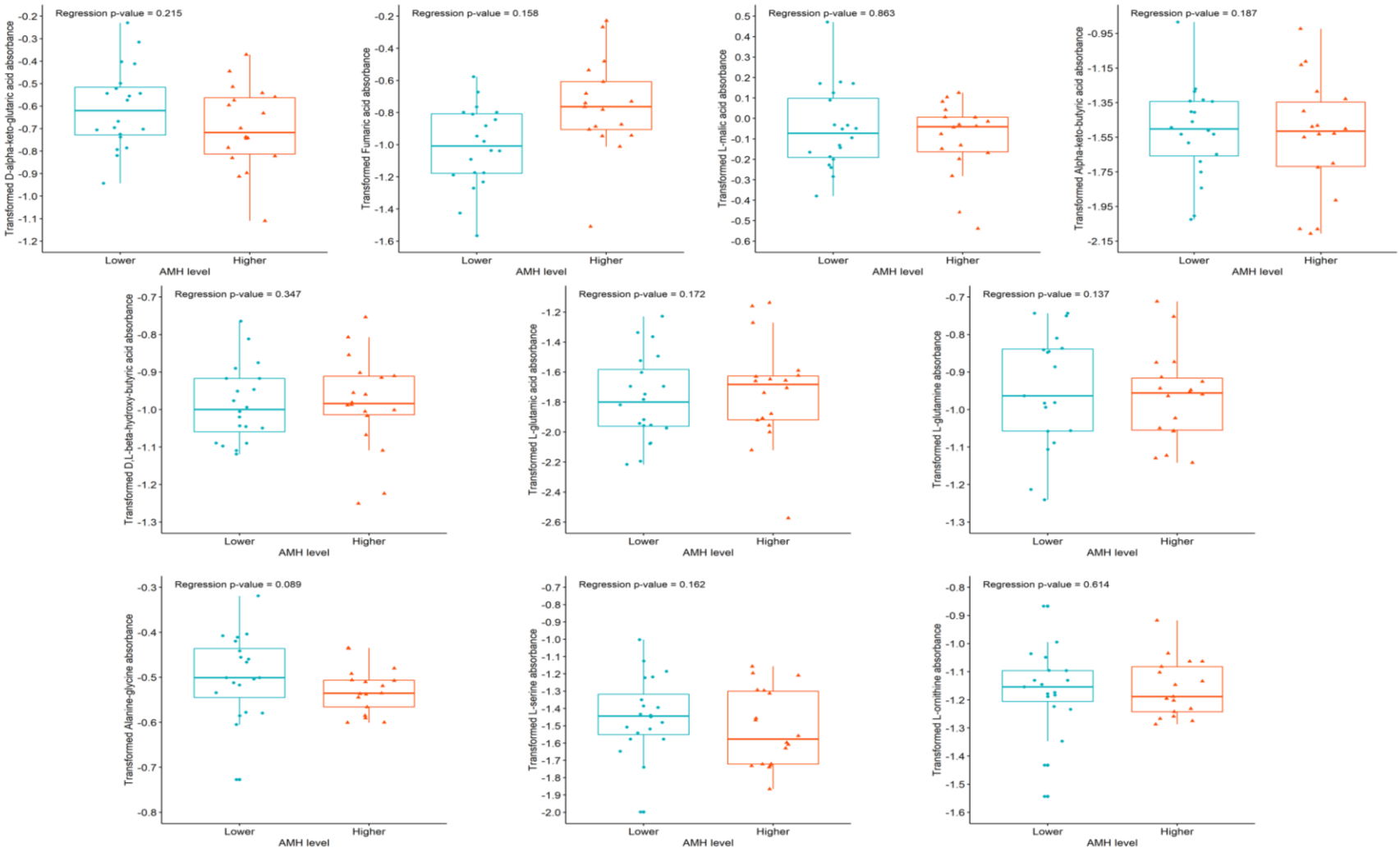

Figure 4.18 Continued

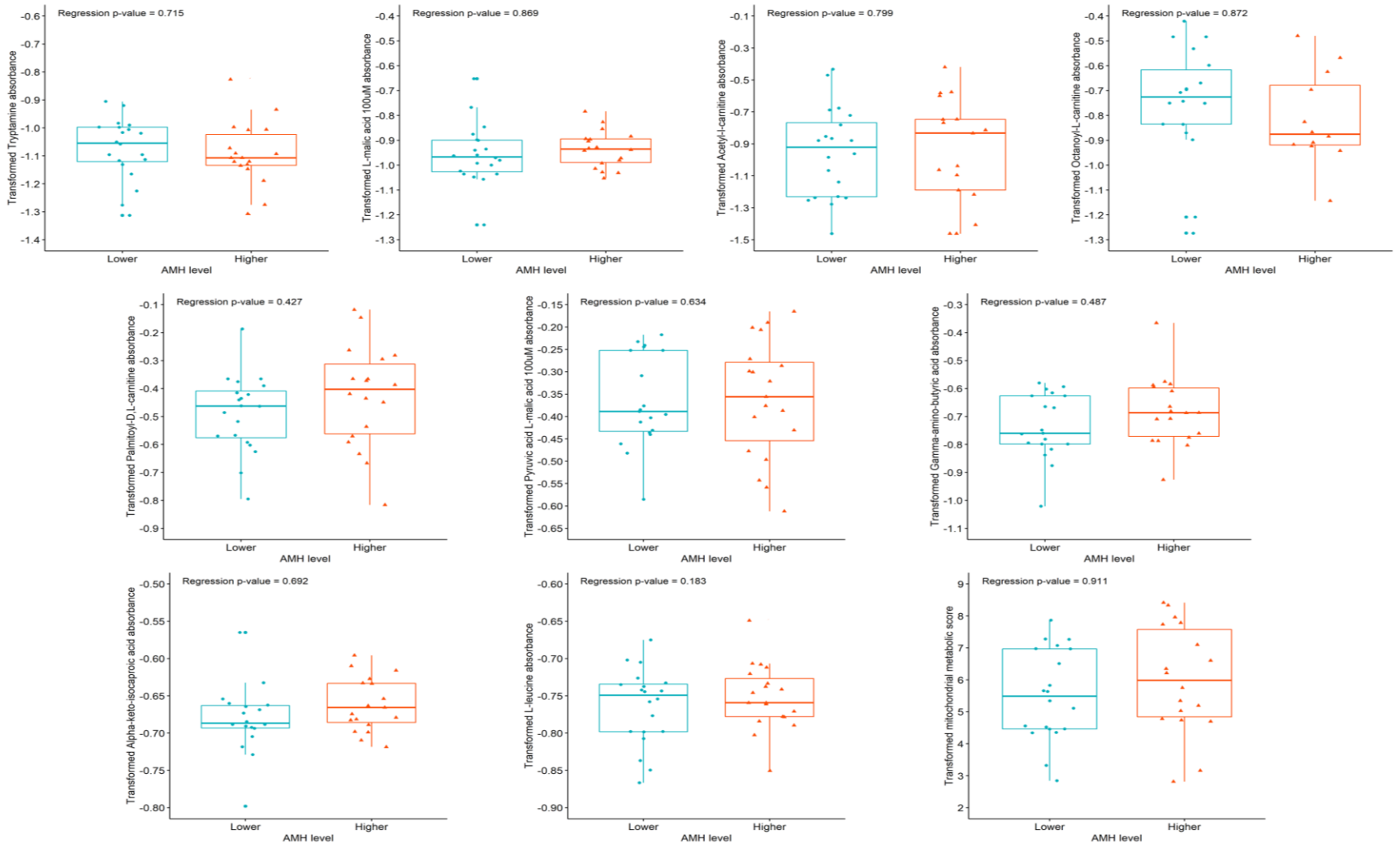

Figure 4.18 Continued

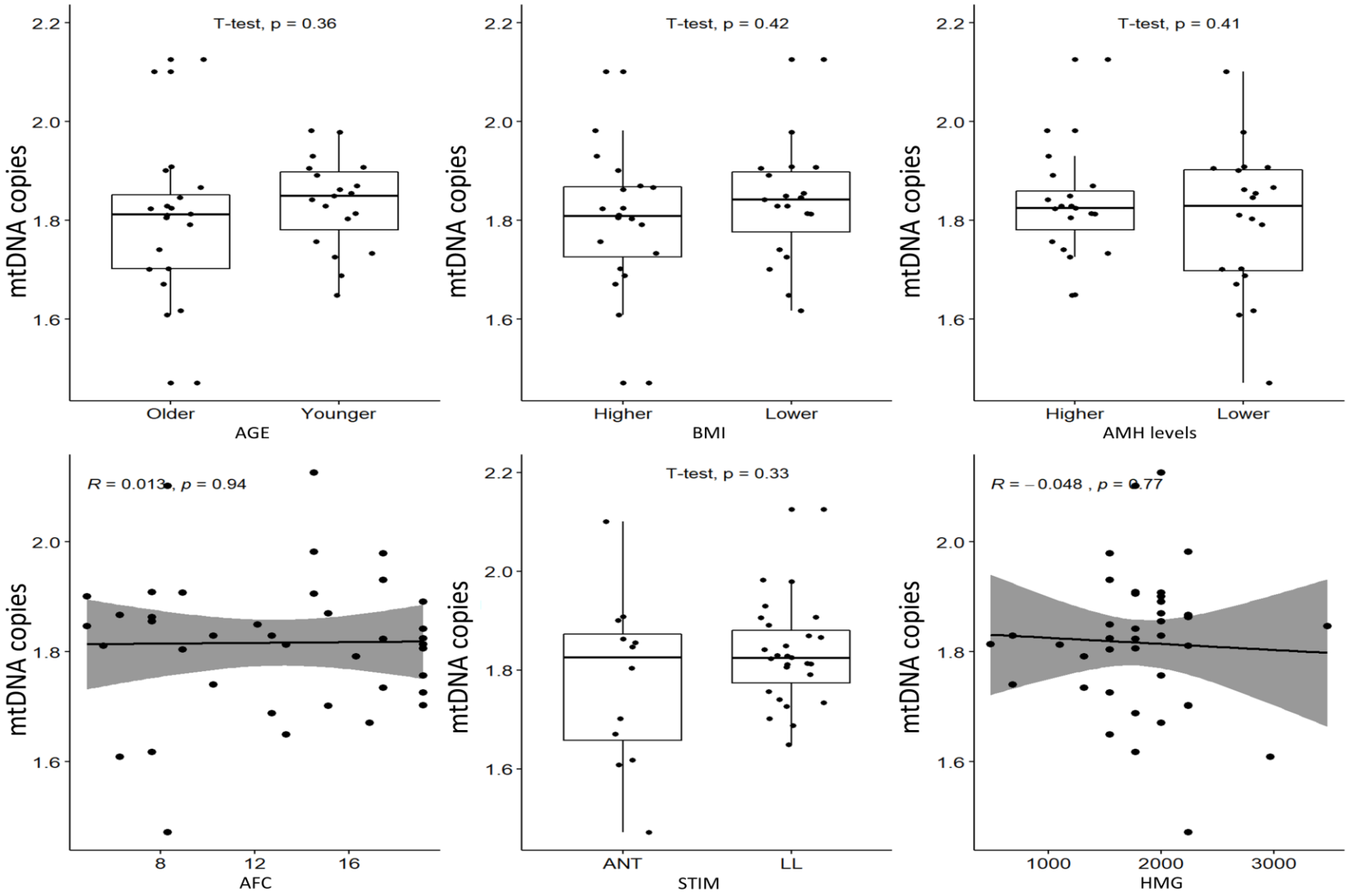
T-test, p = 0.36
mtDNA copies
2.2
2.0
1.8
1.6
Older
Younger
AGE
T-test, p = 0.42
Higher
Lower
BMI
T-test, p = 0.41
Higher
Lower
AMH levels
R = 0.013, p = 0.94
8
12
16
AFC
T-test, p = 0.33
ANT
LL
STIM
R = −0.048 , p = 0.77
1000
2000
3000
HMG

Figure 4.19 Pooled granulosa cell mtDNA content had no significant association with patient demographics nor oocyte outcomes. For categorical groups, Box-Cox transformed mtDNA values are presented as the median (line inside box), first and third quartile (bottom and top of box), and the whiskers extend to 1.5 times the interquartile range beyond the first and third quartile. Averages were compared using independent samples t-tests. For continuous variables, data are presented as a scatter plot of the individual patient Box-Cox transformed values showing the trend line and the 95% confidence region. Pearson's correlation coefficients were estimated and tested for statistical significance. 8-cells = 8-cell embryos, AFC = antral follicle count, AMH = anti-Mullerian hormone, ANT = antagonist stimulation, BMI = body mass index, FSH = follicle stimulating hormone, HMG = human menopausal gonadotropin, LL = long luteal stimulation, mtDNA = mitochondrial DNA, STIM = stimulation type

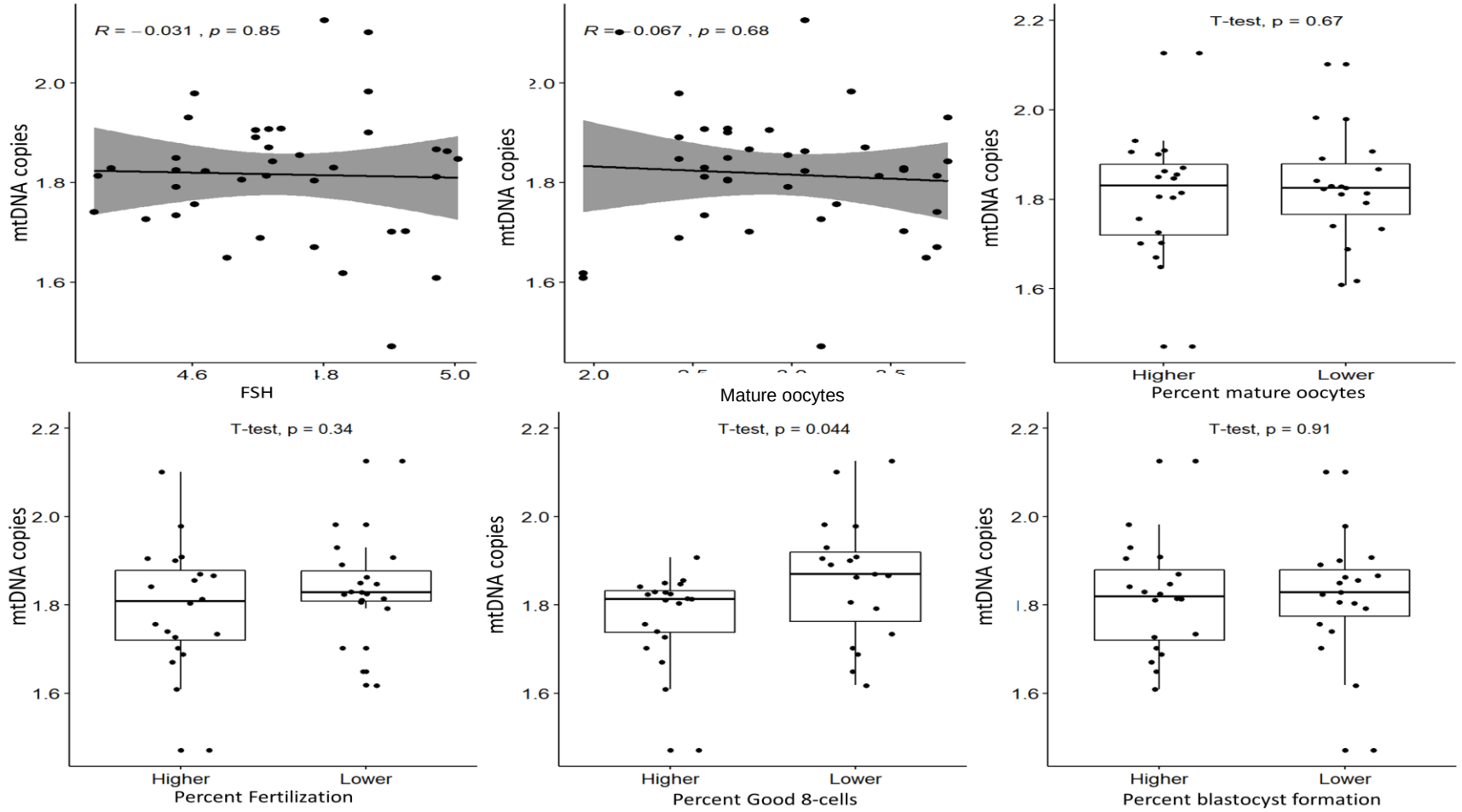

Figure 4.19 Continued

Chapter 5

General Discussion[5]

---

[5]R.J. Kordus and H.A. LaVoie. Granulosa cell biomarkers to predict pregnancy in ART: pieces to solve the puzzle. 2017. Reproduction. 153(2):R69-R83. Epub 2016 Nov 4. Review. Portions adapted from and reprinted here with permission of publisher

Granulosa cells within each follicle are composed of both the CCs and the MCGs that surround the individual oocytes. The fact that granulosa are easily collected as a by-product of the IVF process, and the fact that GCs are intimately related to oocyte maturation and developmental potential (Dumesic et al., 2015), make them ideal non-invasive materials to investigate various biomarkers to improve IVF outcomes. Multiple oocytes and their corresponding cumulus and mural granulosa cells are retrieved during assisted reproduction. As it is possible to isolate the CCs and MGCs associated with an individual oocyte from each retrieval, analyses of these cells may be valuable for screening biomarkers identifying embryos capable of producing a live birth. Appendices A-C summarize biomarker studies and indicate that CCs more often than MGCs exhibit biomarkers associated pregnancy and live birth outcomes (Kordus and LaVoie, 2017). Greater reliability of biomarkers being present in CCs seems logical as they are in direct contact with the oocyte at the time of retrieval from the ovary. Data from these studies suggest that the likelihood of a single expressed gene as a predictor of pregnancy is low, and that multiple genes and cycle characteristics are needed to create the best predictive models. Patient diagnoses, age, BMI, and IVF stimulation protocols; among other factors, can alter study outcomes. A homogeneous patient study population is critical in identifying GC biomarkers for predictive models. In addition, the paternal contributions to fertilization, embryo quality, and live birth outcomes is rarely addressed in studies, but should be considered. Stepwise multivariate analysis where multiple variables include levels of several of the most predictive mRNA biomarkers corrected for variations in

specific patient characteristics, may yield a reliable approach for selecting the best embryos with potential for live birth (Adriaenssens et al., 2010a). Predictive models that can be tested in multiple clinics will allow large scale validation of biomarkers and possibly transform procedures used for the selection of embryos for uterine transfer and improve assisted reproduction success rates.

Our long-term goal is to create a panel of granulosa biomarkers that can help improve a patient's odds of success using IVF on their first attempt. Ultimately, our objective is to obtain a biomarker panel that can help embryologists quickly and easily select an embryo, from a patient's cohort of embryos, which has the best chance of implanting in the uterus and leading to a heathy child. In our first set of aims, we prospectively examined mRNA transcripts in individual CC masses and related those biomarkers to individual oocyte, and subsequent embryo genetic status, oocyte developmental competence, and live birth outcomes. In this series of experiments, we contributed several important and original contributions to the field of IVF:

- We revealed for the first time that higher mRNA levels of a novel biomarker, *PAPPA*, may be a trustworthy biomarker in individual CCs associated with identifying oocytes capable of leading to a live birth.
- We confirmed that higher mRNA levels *LHCGR* and lower mRNA levels of *AREG* in CCs were associated with oocytes that formed embryos capable of leading to live birth.

- We concluded that collectively, CC *PAPPA*, *LHCGR*, and *AREG* mRNA may be able to be employed as a biomarker panel to identify oocytes with the best odds of resulting in a live birth.
- We indicated that lower CC mRNA levels of *HSD3B1* were associated with oocytes that developed into euploid embryos.

Since several studies previously investigated mRNA transcript biomarkers, we carefully selected transcripts that were potential biomarkers from several previous studies to validate and we also examined some novel transcripts. Our study was slightly different than other prior studies as we chose to examine mRNA transcripts levels in relation to oocyte maturity, abnormal embryo development, embryo ploidy status, and live birth outcomes. Relatively few studies have examined mRNA levels as related to ploidy status and IVF outcomes (Fragouli et al., 2010, Fragouli et al., 2012, Parks et al., 2016, Green et al., 2018).

We hypothesized that certain mRNA transcripts in individual CCs could be used to select individual oocytes, and their subsequent embryos, with the highest probability of leading to viable pregnancies and resulting in live births. We found that increased *PAPPA* and *LHCGR* mRNA levels were associated CCs surrounding mature oocytes that resulted in live births. Differences were also observed between immature oocytes compared to aneuploid embryos and immature oocytes compared to arrested embryos, respectively. This data indicates that embryos with increased CC mRNA levels of *PAPPA* and *LHCGR* should be preferentially selected first for uterine transfer, using these models, as they have been shown to be more likely to yield a live birth. This differential mRNA

expression between immature oocytes and mature oocytes leading live birth provides evidence for a potential optimal maturation window.

When comparing only transferred embryos within the entire biomarker panel, oocytes with decreased *AREG* and increased *PAPPA* mRNA levels in their CCs were more likely to produce a live birth. When applied to the best fitting live birth prediction model, which included a smaller subset of the biomarker panel, *PAPPA* and *CYP19A1* mRNA predicted live birth. This could indicate that *PAPPA* mRNA may be a reliable biomarker for identifying oocytes capable of leading to a live birth. *PAPPA* mRNA encodes a metalloproteinase that cleaves insulin-like growth factor binding protein 4 (IGFBP4) and IGFBP5 proteins and is found in follicular fluid (Conover et al., 1999, Laursen et al., 2001, Mazerbourg et al., 2001). It is a novel biomarker we chose to examine. *PAPPA* mRNA is present in antral follicles >5 mm through the pre-ovulatory stage and corpora lutea, but absent in pre-antral, small antral (1-2 mm), and atretic follicles (Hourvitz et al., 2000). Furthermore, *PAPPA* mRNA is present in cultured GCs from human follicles >8 mm (Conover et al., 2001) which coincides temporally with selection of the dominant follicle during the reproductive cycle (Baerwald et al., 2012). Increased levels of *PAPPA* mRNA and its resulting protein in GCs of peri-ovulatory follicles may be necessary to increase intrafollicular IGF availability. Cleavage of IGFBPs by PAPPA protein would release IGFs and result in an increase in free IGF available for signaling (Firth and Baxter, 2002). IGFs are known to enhance FSH and LH signaling and increase LHCGR abundance (Wang and Chard, 1999). Increased free IGF could potentially augment FSH and LH action on follicular cells

during oocyte maturation leading to an optimized follicular environment, and thus enhance the chances of falling within the optimal maturation window at the time of oocyte retrieval. Oocytes at optimal maturity would more likely yield euploid embryos and ultimately improve the chances of live birth.

FSHR and LHCGR are both G-coupled protein receptors. *FSHR* mRNA has previously been linked to good quality blastocyst development (Ekart et al., 2013). Papamentzelopoulou and colleagues demonstrated a relationship between *LHCGR* mRNA and pregnancy with the ratio of LH splice variants being higher in pregnant patients compared to non-pregnant patients (Papamentzelopoulou et al., 2012b). Webb and Campbell hypothesized that individual follicles have different sensitivities to FSH (Webb and Campbell, 2007); therefore, because FSH is known to induce the expression of LH receptors in GCs with follicular maturation, one might postulate that LHCGR expression is variable between individual follicles. Interestingly, others have shown that *LHCGR* mRNA expression in CCs was higher in mature, as opposed to immature oocytes, yet higher *LHCGR* mRNA expression resulted in lower fertilization rates (Maman et al., 2012). Consistent with these prior studies, we also found that immature oocytes had lower CC *LHCGR* mRNA levels compared to all the other groups, with the exception of arrested embryos. Haouzi and colleagues demonstrated that CC *LHCGR* mRNA expression varied between and within individual patient cohorts of mature oocytes (Haouzi et al., 2009). Measuring individual CCs *LHCGR* mRNA levels may also have allowed us to show a difference between oocytes that led to a live birth and those that did not.

Genes related to CC expansion and oocyte maturation may show altered mRNA levels when comparing mature and immature oocytes. AREG is an epidermal growth factor (EGF)-like family member previously shown to positively correlate with embryo quality as well as oocyte maturation and CC expansion in response to the LH surge (Freimann et al., 2004, Park et al., 2004, Zhang et al., 2005). AREG protein has shown correlations with good oocyte quality with in vitro matured porcine embryos (Sugimura et al., 2015) and human IVF derived good quality oocytes (Zamah et al., 2010). Huang and colleagues showed that increased *AREG* mRNA levels in CCs and MGCs were more likely to be associated with pregnancy (Huang et al., 2015). This differs from our study, as we saw decreased *AREG* mRNA levels in CCs from oocytes resulting in live birth. This discordant finding may be due to multiple reasons. In the Huang et al. study CCs and MGCs were pooled together. In addition, the participants were more diverse in terms of diagnoses than our study, and four different stimulation protocols were used. While the overall *AREG* mRNA levels per patient may have been increased, it is possible that the individual CC level for each oocyte leading to live birth was decreased. Our results are consistent with a study by Feuerstein and colleagues who showed reduced *AREG* mRNA levels for CCs of oocytes that resulted in high-quality blastocysts (Feuerstein et al., 2007).

Steroidogenesis is a major function of developing follicles. Granulosa cells and theca cells collectively produce androgens, estrogens, and progestins. Differential mRNA levels of steroidogenic genes in CCs may impact the fate of their associated oocytes. Previously both *CYP19A1* and *HSD3B1* showed

increased mRNA levels between pooled GCs from embryos that resulted in pregnancies compared to embryos that failed to develop (Hamel et al., 2008). In our study, decreased CC *HSD3B1* levels significantly increased the odds of an oocyte resulting in a euploid embryo. Additionally, *CYP19A1* mRNA was one of the biomarkers that borderline predicted live birth in our best fitting model. *CYP19A1* mRNA encodes aromatase, which converts androstenedione to estrone and testosterone to estradiol (Conley and Hinshelwood, 2001). HSD3B1 protein converts pregnenolone to progesterone (Simard et al., 2005). Like *LHCGR*, *CYP19A1* mRNA is induced through FSH signaling, and *CYP19A1* mRNA is more prevalent in dominant follicles of monovulatory species (Hayashi et al., 2010, Kristensen et al., 2017, Sisco et al., 2003). The optimal maturation window needed to produce live birth may be reflected by the interplay between these genes as seen in our study.

We also found decreased *ING1* levels showed a borderline increase in the odds of an oocyte resulting in a euploid embryo. *ING1* mRNA is a novel biomarker we examined. It encodes a tumor suppressor nuclear protein involved in both cell growth and apoptosis and is a member of the p53 signaling pathway (Garkavtsev et al., 1998). ING1 protein is known to modulate androgen receptor (AR) signaling (Esmaeili et al., 2016b, Esmaeili et al., 2016a, Tallen et al., 2009) and suppress angiogenesis (Tallen et al., 2009). We did not examine the mRNA expression of AR as Assidi and colleagues found no difference between AR mRNA expression of oocytes that formed a pregnancy and those that did not (Assidi et al., 2011).

There are multiple oocytes retrieved during an IVF cycle that would normally regress in a natural reproductive cycle and not ovulate. Although many of these supernumerary oocytes will reach the MII stage of development morphologically, the reason IVF cycles may yield lower percentages of oocytes leading to live birth is because they fall outside the optimal maturation window. We hypothesize that many mature appearing oocytes actually exhibit underlying pre- or post-mature biomarker expression patterns in their CCs and MGCs indicating those oocytes are incapable of producing high quality embryos that ultimately lead to live births.

Our study only evaluated what we believe to be immature versus mature oocyte mRNA expression. Evaluation of post-maturity may be more difficult in a clinical IVF setting. However, in vitro maturation studies in humans or in vivo studies in lower mammals may help examine the post-mature aspect of oocyte development. This concept has been recently demonstrated in CCs of CD-1 mice examined at various time points following hCG injection. Artini and colleagues demonstrated how the concept of the optimal maturation widow could be investigated (Artini et al., 2017). Oocytes that fell within the optimal maturation window exhibited lower levels of AKT serine/threonine kinase 1 (*Akt1*), BCL2-like 2 (*Bcl2l2*) and SHC adaptor protein 1 (*Shc1*) mRNAs (Figure 5.1).

Our second series of aims focused on identifying metabolic substrates utilized by mitochondria in pooled GCs to determine if any of the substrates were modulated in relation to patient age, serum AMH levels, BMI, percentage of mature oocytes within a patient cohort, and embryo developmental endpoints. Since the literature on mitochondria related to IVF outcomes is sparse and has focused

mainly on mtDNA content, we wanted to quantify mitochondrial activity and see if we could identify a group of metabolic substrates differentially utilized by mitochondria that could be used as biomarkers for IVF. In this series of experiments, we contributed several important and original contributions to the field of IVF:

- We were the first to demonstrate that a novel mitochondrial function assay using tetrazolium dye measuring NADH or $FADH_2$ reducing equivalents of individual substrates could be used to as a tool to investigate granulosa cell mitochondrial function.
- We showed that BMI, FSH dosage administered, and the number of mature oocytes retrieved per cohort associate with how mitochondria utilize certain substrates in pooled GCs including citric acid, L-malic acid, octanoyl-L-carnitine, cis-acontic acid, D-alpha-keto-glutaric acid, L-glutamine, and alanine-glycine.
- We established that there were individual mitochondrial substrates including, glycogen, D-alpha-keto-glutaric acid, and L-glutamine that were altered in relation to oocyte fertilization, embryo development on day 3, and embryo development to the blastocyst stage.
- We presented a mitochondrial metabolic scoring system, based on the mitochondrial function assay results, to interrogate different patient demographic groups and differences between embryo cohorts.

We discovered that citric acid, L-malic acid, and octanoyl-L-carnitine utillzation by mitochondria were significantly lower in patients with lower BMI. We expected to

find some differences in this patient demographic because impaired mitochondrial function including decreased mitochondrial membrane potential, lower ATP levels, and lower citric acid levels have been demonstrated to be associated with increasing BMI in mice (Wang et al., 2010, Igosheva et al., 2010, Ou et al., 2012). Further, obese patients have been shown to have reduced pregnancy and live birth rates (Koning et al., 2012, Petersen et al., 2013, Pinborg et al., 2013, Rittenberg et al., 2011). Additionally, we found increasing dosages of FSH lowered mitochondrial utilization of citric acid, cis-acontic acid, D-alpha-keto-glutaric acid, L-glutamine, and alanine-glycine. FSH dosage administered was previously shown to have no impact mitochondrial mRNA expression in GCs of IVF patients (Saito et al., 2013). However, our data may indicate there is a physiological metabolic effect in the mitochondria related to FSH dosage. We found that the mitochondrial metabolic scores were significantly reduced when BMI was lower and total FSH administered was higher. FSH and BMI are linked during IVF stimulation as patients with lower BMI tend to require lower doses of FSH than patients with higher BMI (Fedorcsak et al., 2004). These results seem to indicate that higher BMI increases, while increased dosages of FSH suppress, mitochondrial utilization of substrates related to dehydrogenase activity and oxidation reactions of the tricarboxylic acid cycle.

Alpha-keto-isocaproic acid mitochondrial utilization significantly increased as the number of mature oocytes increased. A prior study by Duran and colleagues demonstrated that ATP levels increase as oocytes mature from GVs to MII oocytes indicating an increase in mitochondrial metabolism as oocytes mature

(Duran et al., 2011). We calculated that the mitochondrial metabolic scores were significantly increased in a linear relationship with the total number of oocytes retrieved. Mitochondrial ATP production and mitochondrial membrane potential in CCs have both been shown to correlate with the number of mature oocytes retrieved (Dumesic et al., 2016). The data from all these studies seem to coincide as overall metabolism appears to increase with larger numbers of mature oocytes harvested, potentially indicating a need for higher ATP requirements as GCs help prepare the oocytes for fertilization.

The secondary goal of this study was more intimately related to our overall long-term goal. One hypothesis for poor oocyte quality and compromised embryo development is deficient mitochondrial function (Bentov et al., 2011). We wanted to determine if mitochondrial substrates in pooled GCs would relate to a patient's overall cohort development. Mitochondrial utilization of products of glycogen degradation were found to be significantly lower in patients with lower fertilization percentage. Mitochondrial metabolism significantly increased for D-alpha-keto-glutaric acid from patients with lower good quality 8-cell embryos and utilization of L-glutamine was found to be significantly higher in patients with a lower percentage of blastocyst formation, when using a backward selected model looking only at 8-cell embryos and blastocysts. Mitochondrial metabolic scores decreased as the number of fertilized zygotes increased. This data indicates that the mitochondrial metabolic score may be able to predict fertilization potential of a cohort of oocytes. Focusing on the substrates which yielded differential metabolic function, one could potentially analyze individual CC masses and then relate those results to individual

oocytes and resulting embryos in future studies. Specialized assay plates could be made with only the substrates of interest in the wells and optimized for fewer cells than the current commercial assay used.

Proper meiotic spindle formation and function are essential for proper oocyte fertilization and embryo development. Mitochondrial dysfunction has been associated with reduced ATP generation and meiotic spindle abnormalities (Sutton-McDowall et al., 2010) that may lead to compromised embryo development including fertilization failure (Reynier et al., 2001), aneuploidy (Schon et al., 2000), and abnormal cytokinesis and arrested development (Van Blerkom, 2004, Shoubridge and Wai, 2007, Ramalho-Santos et al., 2009). Reduction in ATP content generated by mitochondria may be a symptom of how substrate utilization is altered by the mitochondria, as seen in our research.

Finally, we wanted to investigate whether there was a relationship between the mRNA levels with individual CCs observed in our first aim and the mRNAs of the pooled GCs from the mitochondrial function assay experiments in our second aim. Examining the subset of genes from the first study which included *AREG*, *CYP19A1*, *CYP11A1*, *HSD3B1*, *ING1*, *LHCGR*, and *PAPPA,* lower *HSD3B* mRNA levels approached significance ($P < 0.10$) as the mitochondrial metabolic score decreased. A prior study demonstrated *HSD3B1* mRNA levels increased between pooled GCs from embryos that resulted in pregnancies compared to embryos that failed to develop (Hamel et al., 2008). In our first mRNA biomarker study lower CC *HSD3B1* mRNA levels significantly increased the odds of an oocyte resulting in a euploid embryo. Perhaps there is a link between *HSD3B* mRNA levels and

mitochondrial function relating to euploid embryo development that needs to be further evaluated.

We hypothesized mitochondrial substrate utilization may be altered based on studies that had previously shown mtDNA content differed in oocytes based on oocyte fertilization percentage (Santos et al., 2006, Reynier et al., 2001), mtDNA content in normal compared to diminished ovarian reserve in oocytes (May-Panloup et al., 2005b), and mtDNA content in trophectoderm biopsies of high quality embryos and embryos that formed pregnancies (Murakoshi et al., 2013, Diez-Juan et al., 2015, de Los Santos et al., 2018, Fragouli et al., 2017, Fragouli et al., 2015, Ravichandran et al., 2017). These prior studies did not look at CC mtDNA content, however, CC mtDNA content and oocyte mtDNA content have been shown to be positively correlated and increasing mtDNA content was demonstrated to be associated with better embryo development (Boucret et al., 2015, Ogino et al., 2016, Desquiret-Dumas et al., 2017). Specific mitochondrial substrate utilization may also indicate oocytes within the optimal maturation window. Oocytes with proper mitochondrial function capable of leading to pregnancy and live birth would be reflected in the metabolic utilization of the substrate biomarkers. In the same way we examined immature versus mature oocyte CC mRNA levels in study 1, one could examine mitochondrial function the same way. Cumulus cells from immature and mature oocytes could be collected and pooled by maturity. The assays could be performed when there are enough cells of each type to run a single replicate of the assay with a control in each assay

as a reference. The individual assays could then be combined and used to compare the mature and immature mitochondrial function.

Our studies have added valuable knowledge to the search for non-invasive biomarkers to help select the most viable embryos for uterine transfer. One could imagine combining embryo morphology, PGT-A testing, mRNA levels of select genes, and mitochondrial substrates to create a robust prediction model and ranking system to select the best embryos for transfer. Future studies will require prospective analysis of the models described above to determine the specificity and sensitivity of the biomarkers and the models and include larger samples sizes. Ideally, the models will be able to yield a method of ranking embryos from the most to least likely to lead to live birth. Examination of protein levels in CCs related to the biomarkers of interest by flow cytometry, enzyme-linked immunosorbent assay, or radioimmunoassay may be valuable to determine if protein content corroborates with mRNA levels. Biomarker studies for embryo selection are far from complete and further studies need to be conducted in order to reach the goal of being able to select the most viable embryos.

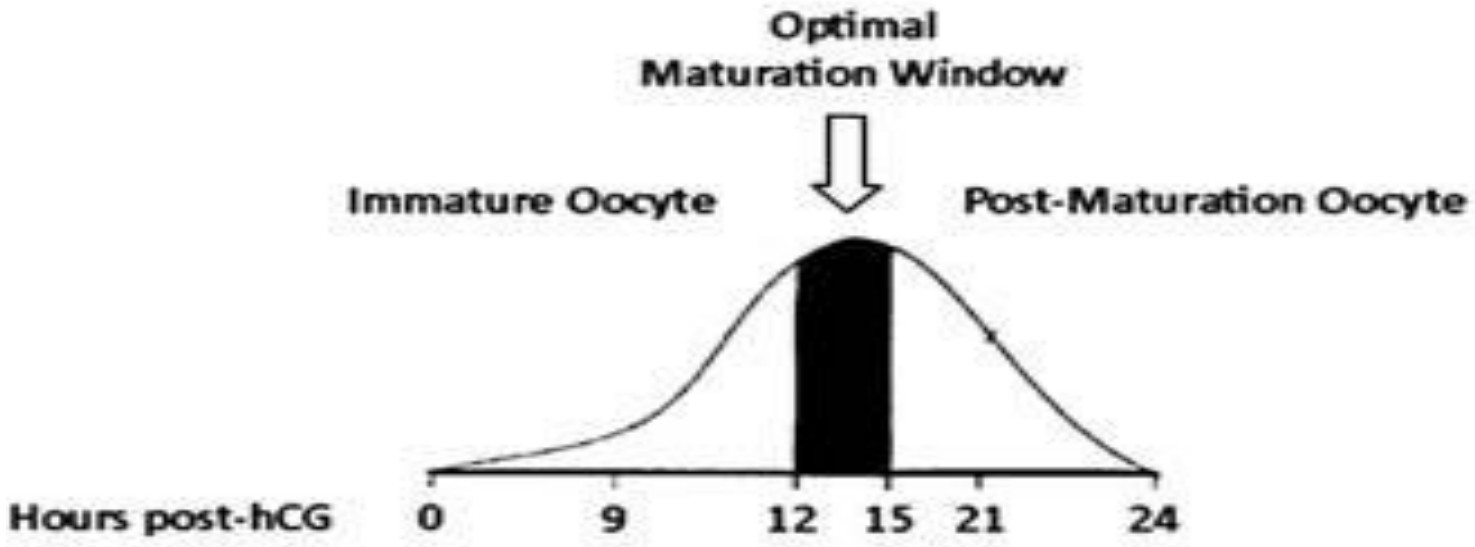

Figure 5.1. Example of an optimal maturation window in mice. The curve draws an oocyte maturation profile. Hours 0-9 represents immature oocytes, hrs 12-15 represent the optimal maturation window, and hrs 15-24 represent a post-mature maturation oocyte. Mouse oocytes that fell within the optimal maturation window exhibited lower levels of AKT serine/threonine kinase 1 (*Akt1*), BCL2-like 2 (*Bcl2l2*) and SHC adaptor protein 1 (*Shc1*) mRNAs (Artini et al., 2017). Reprinted with permission.

References

ABRAHAM, M., COLLINS, C. A., FLEWELLING, S., CAMAZINE, M., CAHILL, A., CADE, W. T. & DUNCAN, J. G. 2018. Mitochondrial inefficiency in infants born to overweight African-American mothers. *Int J Obes (Lond),* 42**,** 1306-1316.

ADRIAENSSENS, T., VAN VAERENBERGH, I., COUCKE, W., SEGERS, I., VERHEYEN, G., ANCKAERT, E., DE VOS, M. & SMITZ, J. 2019. Cumulus-corona gene expression analysis combined with morphological embryo scoring in single embryo transfer cycles increases live birth after fresh transfer and decreases time to pregnancy. *J Assist Reprod Genet,* 36**,** 433-443.

ADRIAENSSENS, T., WATHLET, S., SEGERS, I., VERHEYEN, G., DE, V. A., VAN DER ELST, J., COUCKE, W., DEVROEY, P. & SMITZ, J. 2010a. Cumulus cell gene expression is associated with oocyte developmental quality and influenced by patient and treatment characteristics. *Hum. Reprod,* 25**,** 1259-1270.

ADRIAENSSENS, T., WATHLET, S., SEGERS, I., VERHEYEN, G., DE VOS, A., VAN DER ELST, J., COUCKE, W., DEVROEY, P. & SMITZ, J. 2010b. Cumulus cell gene expression is associated with oocyte developmental quality and influenced by patient and treatment characteristics. *Hum Reprod,* 25**,** 1259-70.

AL-EDANI, T., ASSOU, S., FERRIERES, A., BRINGER, D. S., GALA, A., LECELLIER, C. H., AIT-AHMED, O. & HAMAMAH, S. 2014. Female aging alters expression of human cumulus cells genes that are essential for oocyte quality. *Biomed. Res. Int,* 2014**,** 964614.

ALLEGRA, A., RAIMONDO, S., VOLPES, A., FANALE, D., MARINO, A., CICERO, G., DE, L. G., SAMMARTANO, F., ALLEGRA, G. & ALESSANDRO, R. 2014. The gene expression profile of cumulus cells reveals altered pathways in patients with endometriosis. *J. Assist. Reprod. Genet,* 31**,** 1277-1285.

ANDERSON, E. & ALBERTINI, D. F. 1976. Gap junctions between the oocyte and companion follicle cells in the mammalian ovary. *J Cell Biol,* 71**,** 680-6.

ANDERSON, R. A., SCIORIO, R., KINNELL, H., BAYNE, R. A., THONG, K. J., DE SOUSA, P. A. & PICKERING, S. 2009. Cumulus gene expression as a predictor of human oocyte fertilisation, embryo development and competence to establish a pregnancy. *Reproduction,* 138**,** 629-637.

ARTINI, P. G., TATONE, C., SPERDUTI, S., D'AURORA, M., FRANCHI, S., DI EMIDIO, G., CIRIMINNA, R., VENTO, M., DI PIETRO, C., STUPPIA, L., GATTA, V., ITALIAN SOCIETY OF EMBRYOLOGY, R. & RESEARCH 2017. Cumulus cells surrounding oocytes with high developmental competence exhibit down-regulation of phosphoinositol 1,3 kinase/protein kinase B (PI3K/AKT) signalling genes involved in proliferation and survival. *Hum Reprod,* 32**,** 2474-2484.

ASSIDI, M., DUFORT, I., ALI, A., HAMEL, M., ALGRIANY, O., DIELEMANN, S. & SIRARD, M. A. 2008. Identification of potential markers of oocyte competence expressed in bovine cumulus cells matured with follicle-stimulating hormone and/or phorbol myristate acetate in vitro. *Biol Reprod,* 79**,** 209-22.

ASSIDI, M., MONTAG, M. & SIRARD, M. A. 2015. Use of both cumulus cells' transcriptomic markers and zona pellucida birefringence to select developmentally competent oocytes in human assisted reproductive technologies. *BMC. Genomics,* 16 Suppl 1**,** S9.

ASSIDI, M., MONTAG, M., VAN, D., V & SIRARD, M. A. 2011. Biomarkers of human oocyte developmental competence expressed in cumulus cells before ICSI: a preliminary study. *J. Assist. Reprod. Genet,* 28**,** 173-188.

ASSOU, S., ANAHORY, T., PANTESCO, V., LE, C. T., PELLESTOR, F., KLEIN, B., REYFTMANN, L., DECHAUD, H., DE, V. J. & HAMAMAH, S. 2006. The human cumulus--oocyte complex gene-expression profile. *Hum. Reprod,* 21**,** 1705-1719.

ASSOU, S., HAOUZI, D., DE, V. J. & HAMAMAH, S. 2010. Human cumulus cells as biomarkers for embryo and pregnancy outcomes. *Mol. Hum. Reprod,* 16**,** 531-538.

ASSOU, S., HAOUZI, D., DECHAUD, H., GALA, A., FERRIERES, A. & HAMAMAH, S. 2013. Comparative gene expression profiling in human cumulus cells according to ovarian gonadotropin treatments. *Biomed. Res. Int,* 2013**,** 354582.

ASSOU, S., HAOUZI, D., MAHMOUD, K., AOUACHERIA, A., GUILLEMIN, Y., PANTESCO, V., REME, T., DECHAUD, H., DE, V. J. & HAMAMAH, S. 2008. A non-invasive test for assessing embryo potential by gene expression profiles of human cumulus cells: a proof of concept study. *Mol. Hum. Reprod,* 14**,** 711-719.

BAERWALD, A., ANDERSON, P., YUZPE, A., CASE, A. & FLUKER, M. 2012. Synchronization of ovarian stimulation with follicle wave emergence in patients undergoing in vitro fertilization with a prior suboptimal response: a randomized, controlled trial. *Fertil. Steril,* 98**,** 881-887.

BARBEHENN, E. K., WALES, R. G. & LOWRY, O. H. 1974. The explanation for the blockade of glycolysis in early mouse embryos. *Proc Natl Acad Sci U S A,* 71**,** 1056-60.

BARCELOS, I. D., DONABELLA, F. C., RIBAS, C. P., MEOLA, J., FERRIANI, R. A., DE PAZ, C. C. & NAVARRO, P. A. 2015. Down-regulation of the CYP19A1 gene in cumulus cells of infertile women with endometriosis. *Reprod. Biomed. Online,* 30**,** 532-541.

BARRITT, J. A., COHEN, J. & BRENNER, C. A. 2000. Mitochondrial DNA point mutation in human oocytes is associated with maternal age. *Reprod Biomed Online,* 1**,** 96-100.

BARRITT, J. A., KOKOT, M., COHEN, J., STEUERWALD, N. & BRENNER, C. A. 2002. Quantification of human ooplasmic mitochondria. *Reprod Biomed Online,* 4**,** 243-7.

BATES, D., MACHLER, M., BOLKER, B. & WALKER, S. 2015. Fitting Linear Mixed-Effects Models Using lme4. *J. Stat. Softw.,* 67**,** 1-48.

BENKHALIFA, M., FERREIRA, Y. J., CHAHINE, H., LOUANJLI, N., MIRON, P., MERVIEL, P. & COPIN, H. 2014. Mitochondria: participation to infertility as source of energy and cause of senescence. *Int J Biochem Cell Biol,* 55**,** 60-4.

BENTOV, Y. & CASPER, R. F. 2013. The aging oocyte--can mitochondrial function be improved? *Fertil Steril,* 99**,** 18-22.

BENTOV, Y., YAVORSKA, T., ESFANDIARI, N., JURISICOVA, A. & CASPER, R. F. 2011. The contribution of mitochondrial function to reproductive aging. *J Assist Reprod Genet,* 28**,** 773-83.

BIGGERS, J. D., WHITTINGHAM, D. G. & DONAHUE, R. P. 1967. The pattern of energy metabolism in the mouse oocyte and zygote. *Proc Natl Acad Sci U S A,* 58**,** 560-7.

BLAHA, M., NEMCOVA, L., KEPKOVA, K. V., VODICKA, P. & PROCHAZKA, R. 2015. Gene expression analysis of pig cumulus-oocyte complexes stimulated in vitro with follicle stimulating hormone or epidermal growth factor-like peptides. *Reprod Biol Endocrinol,* 13**,** 113.

BOCHNER, B. R., GADZINSKI, P. & PANOMITROS, E. 2001. Phenotype microarrays for high-throughput phenotypic testing and assay of gene function. *Genome Res,* 11**,** 1246-55.

BORGBO, T., POVLSEN, B. B., ANDERSEN, C. Y., BORUP, R., HUMAIDAN, P. & GRONDAHL, M. L. 2013. Comparison of gene expression profiles in granulosa and cumulus cells after ovulation induction with either human chorionic gonadotropin or a gonadotropin-releasing hormone agonist trigger. *Fertil. Steril,* 100**,** 994-1001.

BORUP, R., THUESEN, L. L., ANDERSEN, C. Y., NYBOE-ANDERSEN, A., ZIEBE, S., WINTHER, O. & GRONDAHL, M. L. 2016. Competence Classification of Cumulus and Granulosa Cell Transcriptome in Embryos Matched by Morphology and Female Age. *PLoS. One,* 11**,** e0153562.

BOUCRET, L., JM, C. D. L. B., MORINIERE, C., DESQUIRET, V., FERRE-L'HOTELLIER, V., DESCAMPS, P., MARCAILLOU, C., REYNIER, P., PROCACCIO, V. & MAY-PANLOUP, P. 2015. Relationship between diminished ovarian reserve and mitochondrial biogenesis in cumulus cells. *Hum. Reprod,* 30**,** 1653-1664.

BOX, G. E. P. & COX, D. R. 1964. An Analysis of Transformations (with Discussion). *Journal of the Royal Statistical Society, Series B* 26(2)**,** 211-252.

BRANNIAN, J., EYSTER, K., MUELLER, B. A., BIETZ, M. G. & HANSEN, K. 2010. Differential gene expression in human granulosa cells from recombinant FSH versus human menopausal gonadotropin ovarian stimulation protocols. *Reprod. Biol. Endocrinol,* 8**,** 25.

BRAUDE, P. & ROWELL, P. 2003. Assisted conception. II--in vitro fertilisation and intracytoplasmic sperm injection. *BMJ,* 327**,** 852-5.

BUCCIONE, R., SCHROEDER, A. C. & EPPIG, J. J. 1990. Interactions between somatic cells and germ cells throughout mammalian oogenesis. *Biol Reprod,* 43**,** 543-7.

BUKOVSKY, A. 2005. Can ovarian infertility be treated with bone marrow- or ovary-derived germ cells? *Reprod Biol Endocrinol,* 3**,** 36.

BUKOVSKY, A., CAUDLE, M. R., SVETLIKOVA, M. & UPADHYAYA, N. B. 2004. Origin of germ cells and formation of new primary follicles in adult human ovaries. *Reprod Biol Endocrinol,* 2**,** 20.

BURGHARDT, R. C., BARHOUMI, R., SEWALL, T. C. & BOWEN, J. A. 1995. Cyclic AMP induces rapid increases in gap junction permeability and changes in the cellular distribution of connexin43. *J Membr Biol,* 148**,** 243-53.

BURNIK, P. T., VRTACNIK, B. E., LOVRECIC, L., KOPITAR, A. N. & MAVER, A. 2015a. No specific gene expression signature in human granulosa and cumulus cells for prediction of oocyte fertilisation and embryo implantation. *PLoS. One,* 10**,** e0115865.

BURNIK, P. T., VRTACNIK, B. E., MAVER, A., KOPITAR, A. N. & LOVRECIC, L. 2015b. Transcriptomic Analysis and Meta-Analysis of Human Granulosa and Cumulus Cells. *PLoS. One,* 10**,** e0136473.

BURNIK, P. T., VRTACNIK, B. E., MAVER, A. & LOVRECIC, L. 2015c. Specific gene expression differences in cumulus cells as potential biomarkers of pregnancy. *Reprod. Biomed. Online,* 30**,** 426-433.

CAPALBO, A., HOFFMANN, E. R., CIMADOMO, D., UBALDI, F. M. & RIENZI, L. 2017. Human female meiosis revised: new insights into the mechanisms of chromosome segregation and aneuploidies from advanced genomics and time-lapse imaging. *Hum Reprod Update,* 23**,** 706-722.

CATTEAU-JONARD, S., JAMIN, S. P., LECLERC, A., GONZALES, J., DEWAILLY, D. & DI, C. N. 2008. Anti-Mullerian hormone, its receptor, FSH receptor, and androgen receptor genes are overexpressed by granulosa cells from stimulated follicles in women with polycystic ovary syndrome. *J. Clin. Endocrinol. Metab,* 93**,** 4456-4461.

CDC 2019. Centers for Disease Control and Prevention/National Center for Health Statisitics. National Survey of Family Growth - I Listing. 2015-2017. URL http://www.cdc.gov/nchs/nsfg/key_statisticis/i_2015-2017.htm#infertility.

CECCHINO, G. N., SELI, E., ALVES DA MOTTA, E. L. & GARCIA-VELASCO, J. A. 2018. The role of mitochondrial activity in female fertility and assisted reproductive technologies: overview and current insights. *Reprod Biomed Online,* 36**,** 686-697.

CELIK, O., CELIK, N., GUNGOR, S., HABERAL, E. T. & AYDIN, S. 2015. Selective Regulation of Oocyte Meiotic Events Enhances Progress in Fertility Preservation Methods. *Biochem Insights,* 8**,** 11-21.
CHAN, C. C., LIU, V. W., LAU, E. Y., YEUNG, W. S., NG, E. H. & HO, P. C. 2005. Mitochondrial DNA content and 4977 bp deletion in unfertilized oocytes. *Mol Hum Reprod,* 11**,** 843-6.
CHANG, J., BOULET, S. L., JENG, G., FLOWERS, L. & KISSIN, D. M. 2016. Outcomes of in vitro fertilization with preimplantation genetic diagnosis: an analysis of the United States Assisted Reproductive Technology Surveillance Data, 2011-2012. *Fertil. Steril,* 105**,** 394-400.
CHAPPEL, S. 2013. The role of mitochondria from mature oocyte to viable blastocyst. *Obstet Gynecol Int,* 2013**,** 183024.
CHEN, M., WEI, S., HU, J. & QUAN, S. 2015a. Can Comprehensive Chromosome Screening Technology Improve IVF/ICSI Outcomes? A Meta-Analysis. *PLoS. One,* 10**,** e0140779.
CHEN, Q., SUN, X., CHEN, J., CHENG, L., WANG, J., WANG, Y. & SUN, Z. 2009. Direct rosiglitazone action on steroidogenesis and proinflammatory factor production in human granulosa-lutein cells. *Reprod Biol Endocrinol,* 7**,** 147.
CHEN, Y. C., CHANG, H. M., CHENG, J. C., TSAI, H. D., WU, C. H. & LEUNG, P. C. 2015b. Transforming growth factor-beta1 up-regulates connexin43 expression in human granulosa cells. *Hum. Reprod,* 30**,** 2190-2201.
CHIN, K. V., SEIFER, D. B., FENG, B., LIN, Y. & SHIH, W. C. 2002. DNA microarray analysis of the expression profiles of luteinized granulosa cells as a function of ovarian reserve. *Fertil. Steril,* 77**,** 1214-1218.
CHOI, J. & SMITZ, J. 2014. Luteinizing hormone and human chorionic gonadotropin: origins of difference. *Mol. Cell Endocrinol,* 383**,** 203-213.
CHRISTENSON, L. K., GUNEWARDENA, S., HONG, X., SPITSCHAK, M., BAUFELD, A. & VANSELOW, J. 2013. Research resource: preovulatory LH surge effects on follicular theca and granulosa transcriptomes. *Mol. Endocrinol,* 27**,** 1153-1171.
CILLO, F., BREVINI, T. A., ANTONINI, S., PAFFONI, A., RAGNI, G. & GANDOLFI, F. 2007. Association between human oocyte developmental competence and expression levels of some cumulus genes. *Reproduction,* 134**,** 645-650.
COLLADO-FERNANDEZ, E., PICTON, H. M. & DUMOLLARD, R. 2012. Metabolism throughout follicle and oocyte development in mammals. *Int J Dev Biol,* 56**,** 799-808.
CONLEY, A. & HINSHELWOOD, M. 2001. Mammalian aromatases. *Reproduction,* 121**,** 685-695.
CONOVER, C. A., FAESSEN, G. F., ILG, K. E., CHANDRASEKHER, Y. A., CHRISTIANSEN, M., OVERGAARD, M. T., OXVIG, C. & GIUDICE, L. C. 2001. Pregnancy-associated plasma protein-a is the insulin-like growth factor binding protein-4 protease secreted by human ovarian granulosa cells and is a marker of dominant follicle selection and the corpus luteum. *Endocrinology,* 142**,** 2155.

CONOVER, C. A., OXVIG, C., OVERGAARD, M. T., CHRISTIANSEN, M. & GIUDICE, L. C. 1999. Evidence that the insulin-like growth factor binding protein-4 protease in human ovarian follicular fluid is pregnancy associated plasma protein-A. *J. Clin. Endocrinol. Metab,* 84**,** 4742-4745.

CONTI, M., HSIEH, M., ZAMAH, A. M. & OH, J. S. 2012. Novel signaling mechanisms in the ovary during oocyte maturation and ovulation. *Mol Cell Endocrinol,* 356**,** 65-73.

COSKUN, S., OTU, H. H., AWARTANI, K. A., AL-ALWAN, L. A., AL-HASSAN, S., AL-MAYMAN, H., KAYA, N. & INAN, M. S. 2013. Gene expression profiling of granulosa cells from PCOS patients following varying doses of human chorionic gonadotropin. *J. Assist. Reprod. Genet,* 30**,** 341-352.

CUMMINS, J. M. 2000. Fertilization and elimination of the paternal mitochondrial genome. *Hum Reprod,* 15 Suppl 2**,** 92-101.

CUMMINS, J. M. 2001. Mitochondria: potential roles in embryogenesis and nucleocytoplasmic transfer. *Hum Reprod Update,* 7**,** 217-28.

DALTON, C. M., SZABADKAI, G. & CARROLL, J. 2014. Measurement of ATP in single oocytes: impact of maturation and cumulus cells on levels and consumption. *J Cell Physiol,* 229**,** 353-61.

DE BOER, K. A., JANSEN R.R.S., LEIGH D.A, MORTIMER D. 1999. Quantification of mtDNA copy number in the human secondary oocyte. . *Hum Reprod,* 14**,** 91-92.

DE LOS SANTOS, M. J., DIEZ JUAN, A., MIFSUD, A., MERCADER, A., MESEGUER, M., RUBIO, C. & PELLICER, A. 2018. Variables associated with mitochondrial copy number in human blastocysts: what can we learn from trophectoderm biopsies? *Fertil Steril,* 109**,** 110-117.

DEKEL, N., LAWRENCE, T. S., GILULA, N. B. & BEERS, W. H. 1981. Modulation of cell-to-cell communication in the cumulus-oocyte complex and the regulation of oocyte maturation by LH. *Dev Biol,* 86**,** 356-62.

DEMIRAY, S. B., GOKER, E. N. T., TAVMERGEN, E., YILMAZ, O., CALIMLIOGLU, N., SOYKAM, H. O., OKTEM, G. & SEZERMAN, U. 2019. Differential gene expression analysis of human cumulus cells. *Clin Exp Reprod Med,* 46**,** 76-86.

DESQUIRET-DUMAS, V., CLEMENT, A., SEEGERS, V., BOUCRET, L., FERRE-L'HOTELLIER, V., BOUET, P. E., DESCAMPS, P., PROCACCIO, V., REYNIER, P. & MAY-PANLOUP, P. 2017. The mitochondrial DNA content of cumulus granulosa cells is linked to embryo quality. *Hum Reprod,* 32**,** 607-614.

DETTI, L., FLETCHER, N. M., SAED, G. M., PEREGRIN-ALVAREZ, I. & UHLMANN, R. A. 2018. Anti-Mullerian Hormone (AMH) May Stall Ovarian Cortex Function Through Modulation of Hormone Receptors Other Than the AMH Receptor. *Reprod Sci,* 25**,** 1218-1223.

DEVJAK, R., FON, T. K., JUVAN, P., VIRANT, K., I, ROZMAN, D. & VRTACNIK, B. E. 2012. Cumulus cells gene expression profiling in terms of oocyte maturity in controlled ovarian hyperstimulation using GnRH agonist or GnRH antagonist. *PLoS. One,* 7**,** e47106.

DEVOTO, L., KOHEN, P., MUNOZ, A. & STRAUSS, J. F., 3RD 2009. Human corpus luteum physiology and the luteal-phase dysfunction associated with ovarian stimulation. *Reprod Biomed Online,* 18 Suppl 2**,** 19-24.
DHALI, A., JAVVAJI, P. K., KOLTE, A. P., FRANCIS, J. R., ROY, S. C. & SEJIAN, V. 2017. Temporal expression of cumulus cell marker genes during in vitro maturation and oocyte developmental competence. *J Assist Reprod Genet,* 34**,** 1493-1500.
DIEZ-JUAN, A., RUBIO, C., MARIN, C., MARTINEZ, S., AL-ASMAR, N., RIBOLDI, M., DIAZ-GIMENO, P., VALBUENA, D. & SIMON, C. 2015. Mitochondrial DNA content as a viability score in human euploid embryos: less is better. *Fertil Steril,* 104**,** 534-41 e1.
DOWNS, S. M. 1995. The influence of glucose, cumulus cells, and metabolic coupling on ATP levels and meiotic control in the isolated mouse oocyte. *Dev Biol,* 167**,** 502-12.
DOWNS, S. M. & UTECHT, A. M. 1999. Metabolism of radiolabeled glucose by mouse oocytes and oocyte-cumulus cell complexes. *Biol Reprod,* 60**,** 1446-52.
DUMESIC, D. A., GUEDIKIAN, A. A., MADRIGAL, V. K., PHAN, J. D., HILL, D. L., ALVAREZ, J. P. & CHAZENBALK, G. D. 2016. Cumulus Cell Mitochondrial Resistance to Stress In Vitro Predicts Oocyte Development During Assisted Reproduction. *J Clin Endocrinol Metab,* 101**,** 2235-45.
DUMESIC, D. A., MELDRUM, D. R., KATZ-JAFFE, M. G., KRISHER, R. L. & SCHOOLCRAFT, W. B. 2015. Oocyte environment: follicular fluid and cumulus cells are critical for oocyte health. *Fertil. Steril,* 103**,** 303-316.
DURAN, H. E., SIMSEK-DURAN, F., OEHNINGER, S. C., JONES, H. W., JR. & CASTORA, F. J. 2011. The association of reproductive senescence with mitochondrial quantity, function, and DNA integrity in human oocytes at different stages of maturation. *Fertil Steril,* 96**,** 384-8.
EDSON, M. A., NAGARAJA, A. K. & MATZUK, M. M. 2009. The mammalian ovary from genesis to revelation. *Endocr Rev,* 30**,** 624-712.
EGEA, R. R., PUCHALT, N. G., ESCRIVA, M. M. & VARGHESE, A. C. 2014. OMICS: Current and future perspectives in reproductive medicine and technology. *J. Hum. Reprod. Sci,* 7**,** 73-92.
EICHENLAUB-RITTER, U., VOGT, E., YIN, H. & GOSDEN, R. 2004. Spindles, mitochondria and redox potential in ageing oocytes. *Reprod Biomed Online,* 8**,** 45-58.
EICHENLAUB-RITTER, U., WIECZOREK, M., LUKE, S. & SEIDEL, T. 2011. Age related changes in mitochondrial function and new approaches to study redox regulation in mammalian oocytes in response to age or maturation conditions. *Mitochondrion,* 11**,** 783-96.
EKART, J., MCNATTY, K., HUTTON, J. & PITMAN, J. 2013. Ranking and selection of MII oocytes in human ICSI cycles using gene expression levels from associated cumulus cells. *Hum. Reprod,* 28**,** 2930-2942.
EMANUELE, M. A., WEZEMAN, F. & EMANUELE, N. V. 2002. Alcohol's effects on female reproductive function. *Alcohol Res Health,* 26**,** 274-81.

EPPIG, J. J. 2001. Oocyte control of ovarian follicular development and function in mammals. *Reproduction,* 122**,** 829-838.
EPPIG, J. J., FRETER, R. R., WARD-BAILEY, P. F. & SCHULTZ, R. M. 1983. Inhibition of oocyte maturation in the mouse: participation of cAMP, steroid hormones, and a putative maturation-inhibitory factor. *Dev Biol,* 100**,** 39-49.
EPPIG, J. J., O'BRIEN, M. & WIGGLESWORTH, K. 1996. Mammalian oocyte growth and development in vitro. *Mol. Reprod. Dev,* 44**,** 260-273.
ERNST, E. H., FRANKS, S., HARDY, K., VILLESEN, P. & LYKKE-HARTMANN, K. 2018. Granulosa cells from human primordial and primary follicles show differential global gene expression profiles. *Hum Reprod,* 33**,** 666-679.
ESMAEILI, M., JENNEK, S., LUDWIG, S., KLITZSCH, A., KRAFT, F., MELLE, C. & BANIAHMAD, A. 2016a. The tumor suppressor ING1b is a novel corepressor for the androgen receptor and induces cellular senescence in prostate cancer cells. *J. Mol. Cell Biol,* 8**,** 207-220.
ESMAEILI, M., PUNGSRINONT, T., SCHAEFER, A. & BANIAHMAD, A. 2016b. A novel crosstalk between the tumor suppressors ING1 and ING2 regulates androgen receptor signaling. *J. Mol. Med. (Berl),* 94**,** 1167-1179.
FAN, H. Y., LIU, Z., MULLANY, L. K. & RICHARDS, J. S. 2012. Consequences of RAS and MAPK activation in the ovary: the good, the bad and the ugly. *Mol. Cell Endocrinol,* 356**,** 74-79.
FEDORCSAK, P., DALE, P. O., STORENG, R., ERTZEID, G., BJERCKE, S., OLDEREID, N., OMLAND, A. K., ABYHOLM, T. & TANBO, T. 2004. Impact of overweight and underweight on assisted reproduction treatment. *Hum Reprod,* 19**,** 2523-8.
FEUERSTEIN, P., CADORET, V., DALBIES-TRAN, R., GUERIF, F., BIDAULT, R. & ROYERE, D. 2007. Gene expression in human cumulus cells: one approach to oocyte competence. *Hum. Reprod,* 22**,** 3069-3077.
FEUERSTEIN, P., PUARD, V., CHEVALIER, C., TEUSAN, R., CADORET, V., GUERIF, F., HOULGATTE, R. & ROYERE, D. 2012. Genomic assessment of human cumulus cell marker genes as predictors of oocyte developmental competence: impact of various experimental factors. *PLoS. One,* 7**,** e40449.
FIRTH, S. M. & BAXTER, R. C. 2002. Cellular actions of the insulin-like growth factor binding proteins. *Endocr. Rev,* 23**,** 824-854.
FORMAN, E. J., HONG, K. H., FERRY, K. M., TAO, X., TAYLOR, D., LEVY, B., TREFF, N. R. & SCOTT, R. T., JR. 2013. In vitro fertilization with single euploid blastocyst transfer: a randomized controlled trial. *Fertil. Steril,* 100**,** 100-107.
FORTIN, C. S., LEADER, A., MAHUTTE, N., HAMILTON, S., LEVEILLE, M. C., VILLENEUVE, M. & SIRARD, M. A. 2019. Gene expression analysis of follicular cells revealed inflammation as a potential IVF failure cause. *J Assist Reprod Genet,* 36**,** 1195-1210.
FORTUNE, J. E. 2003. The early stages of follicular development: activation of primordial follicles and growth of preantral follicles. *Anim Reprod Sci,* 78**,** 135-63.

FRAGOULI, E., BIANCHI, V., PATRIZIO, P., OBRADORS, A., HUANG, Z., BORINI, A., DELHANTY, J. D. & WELLS, D. 2010. Transcriptomic profiling of human oocytes: association of meiotic aneuploidy and altered oocyte gene expression. *Mol. Hum. Reprod,* 16**,** 570-582.

FRAGOULI, E., MCCAFFREY, C., RAVICHANDRAN, K., SPATH, K., GRIFO, J. A., MUNNE, S. & WELLS, D. 2017. Clinical implications of mitochondrial DNA quantification on pregnancy outcomes: a blinded prospective non-selection study. *Hum Reprod,* 32**,** 2340-2347.

FRAGOULI, E., SPATH, K., ALFARAWATI, S., KAPER, F., CRAIG, A., MICHEL, C. E., KOKOCINSKI, F., COHEN, J., MUNNE, S. & WELLS, D. 2015. Altered levels of mitochondrial DNA are associated with female age, aneuploidy, and provide an independent measure of embryonic implantation potential. *PLoS Genet,* 11**,** e1005241.

FRAGOULI, E. & WELLS, D. 2015. Mitochondrial DNA Assessment to Determine Oocyte and Embryo Viability. *Semin Reprod Med,* 33**,** 401-9.

FRAGOULI, E., WELLS, D., IAGER, A. E., KAYISLI, U. A. & PATRIZIO, P. 2012. Alteration of gene expression in human cumulus cells as a potential indicator of oocyte aneuploidy. *Hum. Reprod,* 27**,** 2559-2568.

FRANASIAK, J. M., FORMAN, E. J., HONG, K. H., WERNER, M. D., UPHAM, K. M., TREFF, N. R. & SCOTT, R. T., JR. 2014. The nature of aneuploidy with increasing age of the female partner: a review of 15,169 consecutive trophectoderm biopsies evaluated with comprehensive chromosomal screening. *Fertil Steril,* 101**,** 656-663 e1.

FREIMANN, S., BEN-AMI, I., DANTES, A., RON-EL, R. & AMSTERDAM, A. 2004. EGF-like factor epiregulin and amphiregulin expression is regulated by gonadotropins/cAMP in human ovarian follicular cells. *Biochem. Biophys. Res. Commun,* 324**,** 829-834.

FUCHS WEIZMAN, N., WYSE, B. A., GAT, I., BALAKIER, H., SANGARALINGAM, M., CABALLERO, J., KENIGSBERG, S. & LIBRACH, C. L. 2019. Triggering method in assisted reproduction alters the cumulus cell transcriptome. *Reprod Biomed Online,* 39**,** 211-224.

FUJINO, K., YAMASHITA, Y., HAYASHI, A., ASANO, M., MORISHIMA, S. & OHMICHI, M. 2008. Survivin gene expression in granulosa cells from infertile patients undergoing in vitro fertilization-embryo transfer. *Fertil. Steril,* 89**,** 60-65.

GARDNER, D. K., LANE, M., STEVENS, J., SCHLENKER, T. & SCHOOLCRAFT, W. B. 2000. Blastocyst score affects implantation and pregnancy outcome: towards a single blastocyst transfer. *Fertil. Steril,* 73**,** 1155-1158.

GARKAVTSEV, I., GRIGORIAN, I. A., OSSOVSKAYA, V. S., CHERNOV, M. V., CHUMAKOV, P. M. & GUDKOV, A. V. 1998. The candidate tumour suppressor p33ING1 cooperates with p53 in cell growth control. *Nature,* 391**,** 295-298.

GASCA, S., PELLESTOR, F., ASSOU, S., LOUP, V., ANAHORY, T., DECHAUD, H., DE, V. J. & HAMAMAH, S. 2007. Identifying new human oocyte marker genes: a microarray approach. *Reprod. Biomed. Online,* 14**,** 175-183.

GATTA, V., TATONE, C., CIRIMINNA, R., VENTO, M., FRANCHI, S., D'AURORA, M., SPERDUTI, S., CELA, V., BORZI, P., PALERMO, R., STUPPIA, L. & ARTINI, P. G. 2013. Gene expression profiles of cumulus cells obtained from women treated with recombinant human luteinizing hormone + recombinant human follicle-stimulating hormone or highly purified human menopausal gonadotropin versus recombinant human follicle-stimulating hormone alone. *Fertil. Steril,* 99**,** 2000-2008.

GEBHARDT, K. M., FEIL, D. K., DUNNING, K. R., LANE, M. & RUSSELL, D. L. 2011. Human cumulus cell gene expression as a biomarker of pregnancy outcome after single embryo transfer. *Fertil. Steril,* 96**,** 47-52.

GILCHRIST, R. B., LANE, M. & THOMPSON, J. G. 2008. Oocyte-secreted factors: regulators of cumulus cell function and oocyte quality. *Hum. Reprod. Update,* 14**,** 159-177.

GLEICHER, N., VIDALI, A., BRAVERMAN, J., KUSHNIR, V. A., BARAD, D. H., HUDSON, C., WU, Y. G., WANG, Q., ZHANG, L., ALBERTINI, D. F. & INTERNATIONAL, P. G. S. C. S. G. 2016. Accuracy of preimplantation genetic screening (PGS) is compromised by degree of mosaicism of human embryos. *Reprod Biol Endocrinol,* 14**,** 54.

GLISTER, C., SATCHELL, L. & KNIGHT, P. G. 2010. Changes in expression of bone morphogenetic proteins (BMPs), their receptors and inhibin co-receptor betaglycan during bovine antral follicle development: inhibin can antagonize the suppressive effect of BMPs on thecal androgen production. *Reproduction,* 140**,** 699-712.

GONZALEZ-FERNANDEZ, R., PENA, O., HERNANDEZ, J., MARTIN-VASALLO, P., PALUMBO, A. & AVILA, J. 2011. Patients with endometriosis and patients with poor ovarian reserve have abnormal follicle-stimulating hormone receptor signaling pathways. *Fertil. Steril,* 95**,** 2373-2378.

GORSHINOVA, V. K., TSVIRKUN, D. V., SUKHANOVA, I. A., TARASOVA, N. V., VOLODINA, M. A., MAREY, M. V., SMOLNIKOVA, V. U., VYSOKIKH, M. Y. & SUKHIKH, G. T. 2017. Cumulus cell mitochondrial activity in relation to body mass index in women undergoing assisted reproductive therapy. *BBA Clin,* 7**,** 141-146.

GOSDEN, R. G., LAING, S. C., FELICIO, L. S., NELSON, J. F. & FINCH, C. E. 1983. Imminent oocyte exhaustion and reduced follicular recruitment mark the transition to acyclicity in aging C57BL/6J mice. *Biol Reprod,* 28**,** 255-60.

GREEN, K. A., FRANASIAK, J. M., WERNER, M. D., TAO, X., LANDIS, J. N., SCOTT, R. T., JR. & TREFF, N. R. 2018. Cumulus cell transcriptome profiling is not predictive of live birth after in vitro fertilization: a paired analysis of euploid sibling blastocysts. *Fertil. Steril,* 109**,** 460-466.

GREENSEID, K., JINDAL, S., HURWITZ, J., SANTORO, N. & PAL, L. 2011. Differential granulosa cell gene expression in young women with diminished ovarian reserve. *Reprod. Sci,* 18**,** 892-899.
GRINDLER, N. M. & MOLEY, K. H. 2013. Maternal obesity, infertility and mitochondrial dysfunction: potential mechanisms emerging from mouse model systems. *Mol Hum Reprod,* 19**,** 486-94.
GRONDAHL, M. L., ANDERSEN, C. Y., BOGSTAD, J., BORGBO, T., BOUJIDA, V. H. & BORUP, R. 2012. Specific genes are selectively expressed between cumulus and granulosa cells from individual human pre-ovulatory follicles. *Mol. Hum. Reprod,* 18**,** 572-584.
GRONDAHL, M. L., BORUP, R., LEE, Y. B., MYRHOJ, V., MEINERTZ, H. & SORENSEN, S. 2009. Differences in gene expression of granulosa cells from women undergoing controlled ovarian hyperstimulation with either recombinant follicle-stimulating hormone or highly purified human menopausal gonadotropin. *Fertil. Steril,* 91**,** 1820-1830.
GRONDAHL, M. L., BORUP, R., VIKESA, J., ERNST, E., ANDERSEN, C. Y. & LYKKE-HARTMANN, K. 2013. The dormant and the fully competent oocyte: comparing the transcriptome of human oocytes from primordial follicles and in metaphase II. *Mol. Hum. Reprod,* 19**,** 600-617.
GRONDAHL, M. L., YDING, A. C., BOGSTAD, J., NIELSEN, F. C., MEINERTZ, H. & BORUP, R. 2010. Gene expression profiles of single human mature oocytes in relation to age. *Hum. Reprod,* 25**,** 957-968.
GUZMAN, L., ADRIAENSSENS, T., ORTEGA-HREPICH, C., ALBUZ, F. K., MATEIZEL, I., DEVROEY, P., DE, V. M. & SMITZ, J. 2013. Human antral follicles <6 mm: a comparison between in vivo maturation and in vitro maturation in non-hCG primed cycles using cumulus cell gene expression. *Mol. Hum. Reprod,* 19**,** 7-16.
HAAS, J., ZILBERBERG, E., NAHUM, R., MOR SASON, A., HOURVITZ, A., GAT, I. & ORVIETO, R. 2019. Does double trigger (GnRH-agonist + hCG) improve outcome in poor responders undergoing IVF-ET cycle? A pilot study. *Gynecol Endocrinol,* 35**,** 628-630.
HAMEL, M., DUFORT, I., ROBERT, C., GRAVEL, C., LEVEILLE, M. C., LEADER, A. & SIRARD, M. A. 2008. Identification of differentially expressed markers in human follicular cells associated with competent oocytes. *Hum. Reprod,* 23**,** 1118-1127.
HAMEL, M., DUFORT, I., ROBERT, C., LEVEILLE, M. C., LEADER, A. & SIRARD, M. A. 2010a. Genomic assessment of follicular marker genes as pregnancy predictors for human IVF. *Mol. Hum. Reprod,* 16**,** 87-96.
HAMEL, M., DUFORT, I., ROBERT, C., LEVEILLE, M. C., LEADER, A. & SIRARD, M. A. 2010b. Identification of follicular marker genes as pregnancy predictors for human IVF: new evidence for the involvement of luteinization process. *Mol. Hum. Reprod,* 16**,** 548-556.
HAMMOND, E. R., STEWART, B., PEEK, J. C., SHELLING, A. N. & CREE, L. M. 2015. Assessing embryo quality by combining non-invasive markers: early time-lapse parameters reflect gene expression in associated cumulus cells. *Hum Reprod,* 30**,** 1850-60.

HANUKOGLU, I. & JEFCOATE, C. R. 1980. Mitochondrial cytochrome P-450scc. Mechanism of electron transport by adrenodoxin. *J Biol Chem,* 255**,** 3057-61.
HANUKOGLU, I., SUH, B. S., HIMMELHOCH, S. & AMSTERDAM, A. 1990. Induction and mitochondrial localization of cytochrome P450scc system enzymes in normal and transformed ovarian granulosa cells. *J Cell Biol,* 111**,** 1373-81.
HAOUZI, D., ASSOU, S., MAHMOUD, K., HEDON, B., DE, V. J., DEWAILLY, D. & HAMAMAH, S. 2009. LH/hCGR gene expression in human cumulus cells is linked to the expression of the extracellular matrix modifying gene TNFAIP6 and to serum estradiol levels on day of hCG administration. *Hum. Reprod,* 24**,** 2868-2878.
HARRIS, S. E., LEESE, H. J., GOSDEN, R. G. & PICTON, H. M. 2009. Pyruvate and oxygen consumption throughout the growth and development of murine oocytes. *Mol Reprod Dev,* 76**,** 231-8.
HASEGAWA, J., YANAIHARA, A., IWASAKI, S., OTSUKA, Y., NEGISHI, M., AKAHANE, T. & OKAI, T. 2005. Reduction of progesterone receptor expression in human cumulus cells at the time of oocyte collection during IVF is associated with good embryo quality. *Hum. Reprod,* 20**,** 2194-2200.
HASSOLD, T., HALL, H. & HUNT, P. 2007. The origin of human aneuploidy: where we have been, where we are going. *Hum Mol Genet,* 16 Spec No. 2**,** R203-8.
HASSOLD, T. & HUNT, P. 2001. To err (meiotically) is human: the genesis of human aneuploidy. *Nat Rev Genet,* 2**,** 280-91.
HAUCK, A. K. & BERNLOHR, D. A. 2016. Oxidative stress and lipotoxicity. *J Lipid Res,* 57**,** 1976-1986.
HAYASHI, K. G., USHIZAWA, K., HOSOE, M. & TAKAHASHI, T. 2010. Differential genome-wide gene expression profiling of bovine largest and second-largest follicles: identification of genes associated with growth of dominant follicles. *Reprod. Biol. Endocrinol,* 8**,** 11.
HE, Y. Y., HUANG, J. L., SIK, R. H., LIU, J., WAALKES, M. P. & CHIGNELL, C. F. 2004. Expression profiling of human keratinocyte response to ultraviolet A: implications in apoptosis. *J. Invest Dermatol,* 122**,** 533-543.
HEBERT-SCHUSTER, M., ROTTA, B. E., KIRKPATRICK, B., GUIBOURDENCHE, J. & COHEN, M. 2018. The Interplay between Glucose-Regulated Protein 78 (GRP78) and Steroids in the Reproductive System. *Int J Mol Sci,* 19.
HEFFNER, L. J. 2004. Advanced maternal age--how old is too old? *N Engl J Med,* 351**,** 1927-9.
HERNANDEZ-OCHOA, I., KARMAN, B. N. & FLAWS, J. A. 2009. The role of the aryl hydrocarbon receptor in the female reproductive system. *Biochem Pharmacol,* 77**,** 547-59.
HILLIER, S. G. 2001. Gonadotropic control of ovarian follicular growth and development. *Mol Cell Endocrinol,* 179**,** 39-46.

HIRSHFIELD, A. N. 1989. Granulosa cell proliferation in very small follicles of cycling rats studied by long-term continuous tritiated-thymidine infusion. *Biol Reprod,* 41**,** 309-16.
HOTHORN, T., BRETZ, F. & WESTFALL, P. 2008. Simultaneous inference in general parametric models. *Biom. J,* 50**,** 346-363.
HOURVITZ, A., WIDGER, A. E., FILHO, F. L., CHANG, R. J., ADASHI, E. Y. & ERICKSON, G. F. 2000. Pregnancy-associated plasma protein-A gene expression in human ovaries is restricted to healthy follicles and corpora lutea. *J. Clin. Endocrinol. Metab,* 85**,** 4916-4920.
HSUEH, A. J., MCGEE, E. A., HAYASHI, M. & HSU, S. Y. 2000. Hormonal regulation of early follicle development in the rat ovary. *Mol Cell Endocrinol,* 163**,** 95-100.
HUANG, X., HAO, C., SHEN, X., LIU, X., SHAN, Y., ZHANG, Y. & CHEN, L. 2013. Differences in the transcriptional profiles of human cumulus cells isolated from MI and MII oocytes of patients with polycystic ovary syndrome. *Reproduction,* 145**,** 597-608.
HUANG, Y., ZHAO, Y., YU, Y., LI, R., LIN, S., ZHANG, C., LIU, P. & QIAO, J. 2015. Altered amphiregulin expression induced by diverse luteinizing hormone receptor reactivity in granulosa cells affects IVF outcomes. *Reprod. Biomed. Online,* 30**,** 593-601.
HUANG, Z. & WELLS, D. 2010. The human oocyte and cumulus cells relationship: new insights from the cumulus cell transcriptome. *Mol. Hum. Reprod,* 16**,** 715-725.
HUNTER, R. H., BOGH, I. B., EINER-JENSEN, N., MULLER, S. & GREVE, T. 2000. Pre-ovulatory graafian follicles are cooler than neighbouring stroma in pig ovaries. *Hum Reprod,* 15**,** 273-83.
HURWITZ, J. M., JINDAL, S., GREENSEID, K., BERGER, D., BROOKS, A., SANTORO, N. & PAL, L. 2010. Reproductive aging is associated with altered gene expression in human luteinized granulosa cells. *Reprod. Sci,* 17**,** 56-67.
IAGER, A. E., KOCABAS, A. M., OTU, H. H., RUPPEL, P., LANGERVELD, A., SCHNARR, P., SUAREZ, M., JARRETT, J. C., CONAGHAN, J., ROSA, G. J., FERNANDEZ, E., RAWLINS, R. G., CIBELLI, J. B. & CROSBY, J. A. 2013. Identification of a novel gene set in human cumulus cells predictive of an oocyte's pregnancy potential. *Fertil. Steril,* 99**,** 745-752.
IGOSHEVA, N., ABRAMOV, A. Y., POSTON, L., ECKERT, J. J., FLEMING, T. P., DUCHEN, M. R. & MCCONNELL, J. 2010. Maternal diet-induced obesity alters mitochondrial activity and redox status in mouse oocytes and zygotes. *PLoS One,* 5**,** e10074.
JAFFE, L. A. & EGBERT, J. R. 2017. Regulation of Mammalian Oocyte Meiosis by Intercellular Communication Within the Ovarian Follicle. *Annu Rev Physiol,* 79**,** 237-260.
JANSEN, R. P. & BURTON, G. J. 2004. Mitochondrial dysfunction in reproduction. *Mitochondrion,* 4**,** 577-600.
JANSEN, R. P. & DE BOER, K. 1998. The bottleneck: mitochondrial imperatives in oogenesis and ovarian follicular fate. *Mol Cell Endocrinol,* 145**,** 81-8.

JEPPESEN, J. V., KRISTENSEN, S. G., NIELSEN, M. E., HUMAIDAN, P., DAL, C. M., FADINI, R., SCHMIDT, K. T., ERNST, E. & YDING, A. C. 2012. LH-receptor gene expression in human granulosa and cumulus cells from antral and preovulatory follicles. *J. Clin. Endocrinol. Metab,* 97**,** E1524-E1531.

JINDAL, S., GREENSEID, K., BERGER, D., SANTORO, N. & PAL, L. 2012. Impaired gremlin 1 (GREM1) expression in cumulus cells in young women with diminished ovarian reserve (DOR). *J. Assist. Reprod. Genet,* 29**,** 159-162.

JOHNSON, M. T., FREEMAN, E. A., GARDNER, D. K. & HUNT, P. A. 2007. Oxidative metabolism of pyruvate is required for meiotic maturation of murine oocytes in vivo. *Biol Reprod,* 77**,** 2-8.

JONES, K. T. 2004. Turning it on and off: M-phase promoting factor during meiotic maturation and fertilization. *Mol Hum Reprod,* 10**,** 1-5.

KANG, H. J., MELNICK, A. P., STEWART, J. D., XU, K. & ROSENWAKS, Z. 2016. Preimplantation genetic screening: who benefits? *Fertil Steril,* 106**,** 597-602.

KAUR, S., ARCHER, K. J., DEVI, M. G., KRIPLANI, A., STRAUSS, J. F., III & SINGH, R. 2012. Differential gene expression in granulosa cells from polycystic ovary syndrome patients with and without insulin resistance: identification of susceptibility gene sets through network analysis. *J. Clin. Endocrinol. Metab,* 97**,** E2016-E2021.

KEDEM, A., YUNG, Y., YERUSHALMI, G. M., HAAS, J., MAMAN, E., HANOCHI, M., HEMI, R., ORVIETO, R., DOR, J. & HOURVITZ, A. 2014. Anti Mullerian Hormone (AMH) level and expression in mural and cumulus cells in relation to age. *J. Ovarian. Res,* 7**,** 113.

KENIGSBERG, S., BENTOV, Y., CHALIFA-CASPI, V., POTASHNIK, G., OFIR, R. & BIRK, O. S. 2009. Gene expression microarray profiles of cumulus cells in lean and overweight-obese polycystic ovary syndrome patients. *Mol. Hum. Reprod,* 15**,** 89-103.

KHAMSI, F. & ROBERGE, S. 2001. Differential effects of insulin-like growth factor-I and gonadotropins on the proliferative activity of two subgroups of granulosa cells: cumulus oophorus and mural granulosa cells. *Fertil. Steril,* 75**,** 997-1003.

KIRKEGAARD, K., AHLSTROM, A., INGERSLEV, H. J. & HARDARSON, T. 2015. Choosing the best embryo by time lapse versus standard morphology. *Fertil. Steril,* 103**,** 323-332.

KLIMCZAK, A. M., PACHECO, L. E., LEWIS, K. E., MASSAHI, N., RICHARDS, J. P., KEARNS, W. G., SAAD, A. F. & CROCHET, J. R. 2018. Embryonal mitochondrial DNA: relationship to embryo quality and transfer outcomes. *J Assist Reprod Genet,* 35**,** 871-877.

KNIGHT, P. G. & GLISTER, C. 2006. TGF-beta superfamily members and ovarian follicle development. *Reproduction,* 132**,** 191-206.

KOKS, S., VELTHUT, A., SARAPIK, A., ALTMAE, S., REINMAA, E., SCHALKWYK, L. C., FERNANDES, C., LAD, H. V., SOOMETS, U., JAAKMA, U. & SALUMETS, A. 2010. The differential transcriptome and ontology profiles of floating and cumulus granulosa cells in stimulated human antral follicles. *Mol. Hum. Reprod,* 16**,** 229-240.

KONING, A. M., MUTSAERTS, M. A., KUCHENBECKER, W. K., BROEKMANS, F. J., LAND, J. A., MOL, B. W. & HOEK, A. 2012. Complications and outcome of assisted reproduction technologies in overweight and obese women. *Hum Reprod,* 27**,** 457-67.

KORDUS, R. J., HOSSAIN, A., CORSO, M. C., CHAKRABORTY, H., WHITMAN-ELIA, G. F. & LAVOIE, H. A. 2019. Cumulus cell pappalysin-1, luteinizing hormone/choriogonadotropin receptor, amphiregulin and hydroxy-delta-5-steroid dehydrogenase, 3 beta- and steroid delta-isomerase 1 mRNA levels associate with oocyte developmental competence and embryo outcomes. *J Assist Reprod Genet,* 36**,** 1457-1469.

KORDUS, R. J. & LAVOIE, H. A. 2017. Granulosa cell biomarkers to predict pregnancy in ART: pieces to solve the puzzle. *Reproduction,* 153**,** R69-R83.

KRIEG, A. J., MULLINAX, S. R., GRIMSTAD, F., MARQUIS, K., CONSTANCE, E., HONG, Y., KRIEG, S. A. & ROBY, K. F. 2018. Histone demethylase KDM4A and KDM4B expression in granulosa cells from women undergoing in vitro fertilization. *J Assist Reprod Genet,* 35**,** 993-1003.

KRISTENSEN, S. G., MAMSEN, L. S., JEPPESEN, J. V., BOTKJAER, J. A., PORS, S. E., BORGBO, T., ERNST, E., MACKLON, K. T. & ANDERSEN, C. Y. 2017. Hallmarks of human small antral follicle development: implications for regulation of ovarian steroidogenesis and selection of the dominant follicle. *Front Endocrinol (Lausanne),* 8**,** 376.

KUPKA, M. S., D'HOOGHE, T., FERRARETTI, A. P., DE, M. J., ERB, K., CASTILLA, J. A., CALHAZ-JORGE, C., DE, G. C. & GOOSSENS, V. 2016. Assisted reproductive technology in Europe, 2011: results generated from European registers by ESHRE. *Hum. Reprod,* 31**,** 233-248.

KUSHNIR, V. A., DARMON, S. K., ALBERTINI, D. F., BARAD, D. H. & GLEICHER, N. 2016. Effectiveness of in vitro fertilization with preimplantation genetic screening: a reanalysis of United States assisted reproductive technology data 2011-2012. *Fertil. Steril*.

KUSHNIR, V. A., DARMON, S. K., BARAD, D. H. & GLEICHER, N. 2018. Degree of mosaicism in trophectoderm does not predict pregnancy potential: a corrected analysis of pregnancy outcomes following transfer of mosaic embryos. *Reprod Biol Endocrinol,* 16**,** 6.

KWON, H., CHOI, D. H., BAE, J. H., KIM, J. H. & KIM, Y. S. 2010. mRNA expression pattern of insulin-like growth factor components of granulosa cells and cumulus cells in women with and without polycystic ovary syndrome according to oocyte maturity. *Fertil. Steril,* 94**,** 2417-2420.

LARSEN, W. J. 2001. Human Embryology. Third edition. Churchill Livingstone.

LAURSEN, L. S., OVERGAARD, M. T., SOE, R., BOLDT, H. B., SOTTRUP-JENSEN, L., GIUDICE, L. C., CONOVER, C. A. & OXVIG, C. 2001. Pregnancy-associated plasma protein-A (PAPP-A) cleaves insulin-like growth factor binding protein (IGFBP)-5 independent of IGF: implications for the mechanism of IGFBP-4 proteolysis by PAPP-A. *FEBS Lett,* 504**,** 36-40.

LEE, H. J., JEE, B. C., KIM, S. K., KIM, H., LEE, J. R., SUH, C. S. & KIM, S. H. 2016. Expressions of aquaporin family in human luteinized granulosa cells and their correlations with IVF outcomes. *Hum Reprod,* 31**,** 822-31.

LEMMEN, J. G., RODRIGUEZ, N. M., ANDREASEN, L. D., LOFT, A. & ZIEBE, S. 2016. The total pregnancy potential per oocyte aspiration after assisted reproduction-in how many cycles are biologically competent oocytes available? *J. Assist. Reprod. Genet,* 33**,** 849-854.

LI, Y., LI, R. Q., OU, S. B., ZHANG, N. F., REN, L., WEI, L. N., ZHANG, Q. X. & YANG, D. Z. 2014. Increased GDF9 and BMP15 mRNA levels in cumulus granulosa cells correlate with oocyte maturation, fertilization, and embryo quality in humans. *Reprod. Biol. Endocrinol,* 12**,** 81.

LIANG, C. G., SU, Y. Q., FAN, H. Y., SCHATTEN, H. & SUN, Q. Y. 2007. Mechanisms regulating oocyte meiotic resumption: roles of mitogen-activated protein kinase. *Mol Endocrinol,* 21**,** 2037-55.

LINTERN-MOORE, S. & MOORE, G. P. 1979. The initiation of follicle and oocyte growth in the mouse ovary. *Biol Reprod,* 20**,** 773-8.

LIU, Q., ZHANG, J., WEN, H., FENG, Y., ZHANG, X., XIANG, H., CAO, Y., TONG, X., JI, Y. & XUE, Z. 2018. Analyzing the Transcriptome Profile of Human Cumulus Cells Related to Embryo Quality via RNA Sequencing. *Biomed Res Int,* 2018**,** 9846274.

LIU, Z., FAN, H. Y., WANG, Y. & RICHARDS, J. S. 2010. Targeted disruption of Mapk14 (p38MAPKalpha) in granulosa cells and cumulus cells causes cell-specific changes in gene expression profiles that rescue COC expansion and maintain fertility. *Mol. Endocrinol,* 24**,** 1794-1804.

LYNCH, M., KOSKELLA, B. & SCHAACK, S. 2006. Mutation pressure and the evolution of organelle genomic architecture. *Science,* 311**,** 1727-30.

MAGOFFIN, D. A. 2005. Ovarian theca cell. *Int J Biochem Cell Biol,* 37**,** 1344-9.

MAMAN, E., YUNG, Y., KEDEM, A., YERUSHALMI, G. M., KONOPNICKI, S., COHEN, B., DOR, J. & HOURVITZ, A. 2012. High expression of luteinizing hormone receptors messenger RNA by human cumulus granulosa cells is in correlation with decreased fertilization. *Fertil. Steril,* 97**,** 592-598.

MANNA, P. R., ROY, P., CLARK, B. J., STOCCO, D. M. & HUHTANIEMI, I. T. 2001. Interaction of thyroid hormone and steroidogenic acute regulatory (StAR) protein in the regulation of murine Leydig cell steroidogenesis. *J Steroid Biochem Mol Biol,* 76**,** 167-77.

MARGULIS, L. 1996. Archaeal-eubacterial mergers in the origin of Eukarya: phylogenetic classification of life. *Proc Natl Acad Sci U S A,* 93**,** 1071-6.

MARIEB, E. N. H., KATJA, 2016. Human Anatomy Physiology, 10th.

MARLOW, F. L. 2017. Mitochondrial matters: Mitochondrial bottlenecks, self-assembling structures, and entrapment in the female germline. *Stem Cell Res,* 21**,** 178-186.
MATZUK, M. M., BURNS, K. H., VIVEIROS, M. M. & EPPIG, J. J. 2002. Intercellular communication in the mammalian ovary: oocytes carry the conversation. *Science,* 296**,** 2178-2180.
MAY-PANLOUP, P., BOUCRET, L., CHAO DE LA BARCA, J. M., DESQUIRET-DUMAS, V., FERRE-L'HOTELLIER, V., MORINIERE, C., DESCAMPS, P., PROCACCIO, V. & REYNIER, P. 2016. Ovarian ageing: the role of mitochondria in oocytes and follicles. *Hum Reprod Update,* 22**,** 725-743.
MAY-PANLOUP, P., CHRETIEN, M. F., JACQUES, C., VASSEUR, C., MALTHIERY, Y. & REYNIER, P. 2005a. Low oocyte mitochondrial DNA content in ovarian insufficiency. *Hum Reprod,* 20**,** 593-7.
MAY-PANLOUP, P., FERRE-L'HOTELLIER, V., MORINIERE, C., MARCAILLOU, C., LEMERLE, S., MALINGE, M. C., COUTOLLEAU, A., LUCAS, N., REYNIER, P., DESCAMPS, P. & GUARDIOLA, P. 2012. Molecular characterization of corona radiata cells from patients with diminished ovarian reserve using microarray and microfluidic-based gene expression profiling. *Hum. Reprod,* 27**,** 829-843.
MAY-PANLOUP, P., VIGNON, X., CHRETIEN, M. F., HEYMAN, Y., TAMASSIA, M., MALTHIERY, Y. & REYNIER, P. 2005b. Increase of mitochondrial DNA content and transcripts in early bovine embryogenesis associated with upregulation of mtTFA and NRF1 transcription factors. *Reprod Biol Endocrinol,* 3**,** 65.
MAZERBOURG, S., OVERGAARD, M. T., OXVIG, C., CHRISTIANSEN, M., CONOVER, C. A., LAURENDEAU, I., VIDAUD, M., TOSSER-KLOPP, G., ZAPF, J. & MONGET, P. 2001. Pregnancy-associated plasma protein-A (PAPP-A) in ovine, bovine, porcine, and equine ovarian follicles: involvement in IGF binding protein-4 proteolytic degradation and mRNA expression during follicular development. *Endocrinology,* 142**,** 5243-5253.
MCGEE, E. A. & HSUEH, A. J. 2000. Initial and cyclic recruitment of ovarian follicles. *Endocr Rev,* 21**,** 200-14.
MCKENZIE, L. J., PANGAS, S. A., CARSON, S. A., KOVANCI, E., CISNEROS, P., BUSTER, J. E., AMATO, P. & MATZUK, M. M. 2004. Human cumulus granulosa cell gene expression: a predictor of fertilization and embryo selection in women undergoing IVF. *Hum. Reprod,* 19**,** 2869-2874.
MCREYNOLDS, S., DZIECIATKOWSKA, M., MCCALLIE, B. R., MITCHELL, S. D., STEVENS, J., HANSEN, K., SCHOOLCRAFT, W. B. & KATZ-JAFFE, M. G. 2012. Impact of maternal aging on the molecular signature of human cumulus cells. *Fertil. Steril,* 98**,** 1574-1580.
MEHLMANN, L. M. 2005. Stops and starts in mammalian oocytes: recent advances in understanding the regulation of meiotic arrest and oocyte maturation. *Reproduction,* 130**,** 791-9.
MENG, Y., QIAN, Y., GAO, L., CAI, L. B., CUI, Y. G. & LIU, J. Y. 2013. Downregulated expression of peroxiredoxin 4 in granulosa cells from polycystic ovary syndrome. *PLoS. One,* 8**,** e76460.

MILLER, W. L. 2005. Minireview: regulation of steroidogenesis by electron transfer. *Endocrinology,* 146**,** 2544-50.
MORAGIANNI, V. A., JONES, S. M. & RYLEY, D. A. 2012. The effect of body mass index on the outcomes of first assisted reproductive technology cycles. *Fertil Steril,* 98**,** 102-8.
MOTTA, P. M., NOTTOLA, S. A., MAKABE, S. & HEYN, R. 2000. Mitochondrial morphology in human fetal and adult female germ cells. *Hum Reprod,* 15 Suppl 2**,** 129-47.
MULLER-HOCKER, J., SCHAFER, S., WEIS, S., MUNSCHER, C. & STROWITZKI, T. 1996. Morphological-cytochemical and molecular genetic analyses of mitochondria in isolated human oocytes in the reproductive age. *Mol Hum Reprod,* 2**,** 951-8.
MUNNE, S., CHEN, S., COLLS, P., GARRISI, J., ZHENG, X., CEKLENIAK, N., LENZI, M., HUGHES, P., FISCHER, J., GARRISI, M., TOMKIN, G. & COHEN, J. 2007a. Maternal age, morphology, development and chromosome abnormalities in over 6000 cleavage-stage embryos. *Reprod. Biomed. Online,* 14**,** 628-634.
MUNNE, S., COHEN, J. & SIMPSON, J. L. 2007b. In vitro fertilization with preimplantation genetic screening. *N. Engl. J. Med,* 357**,** 1769-1770.
MUNNE, S., TOMKIN, G. & COHEN, J. 2009. Selection of embryos by morphology is less effective than by a combination of aneuploidy testing and morphology observations. *Fertil. Steril,* 91**,** 943-945.
MURAKOSHI, Y., SUEOKA, K., TAKAHASHI, K., SATO, S., SAKURAI, T., TAJIMA, H. & YOSHIMURA, Y. 2013. Embryo developmental capability and pregnancy outcome are related to the mitochondrial DNA copy number and ooplasmic volume. *J Assist Reprod Genet,* 30**,** 1367-75.
MURPHY, B. D. 2000. Models of luteinization. *Biol Reprod,* 63**,** 2-11.
NAGAOKA, S. I., HASSOLD, T. J. & HUNT, P. A. 2012. Human aneuploidy: mechanisms and new insights into an age-old problem. *Nat Rev Genet,* 13**,** 493-504.
NEL-THEMAAT, L. & NAGY, Z. P. 2011. A review of the promises and pitfalls of oocyte and embryo metabolomics. *Placenta,* 32 Suppl 3**,** S257-S263.
NELSON-DEGRAVE, V. L., WICKENHEISSER, J. K., COCKRELL, J. E., WOOD, J. R., LEGRO, R. S., STRAUSS, J. F., III & MCALLISTER, J. M. 2004. Valproate potentiates androgen biosynthesis in human ovarian theca cells. *Endocrinology,* 145**,** 799-808.
NELSON-DEGRAVE, V. L., WICKENHEISSER, J. K., HENDRICKS, K. L., ASANO, T., FUJISHIRO, M., LEGRO, R. S., KIMBALL, S. R., STRAUSS, J. F., III & MCALLISTER, J. M. 2005. Alterations in mitogen-activated protein kinase kinase and extracellular regulated kinase signaling in theca cells contribute to excessive androgen production in polycystic ovary syndrome. *Mol. Endocrinol,* 19**,** 379-390.
NISWENDER, G. D., JUENGEL, J. L., MCGUIRE, W. J., BELFIORE, C. J. & WILTBANK, M. C. 1994. Luteal function: the estrous cycle and early pregnancy. *Biol Reprod,* 50**,** 239-47.

NISWENDER, G. D., JUENGEL, J. L., SILVA, P. J., ROLLYSON, M. K. & MCINTUSH, E. W. 2000. Mechanisms controlling the function and life span of the corpus luteum. *Physiol Rev,* 80**,** 1-29.

NIVET, A. L., LEVEILLE, M. C., LEADER, A. & SIRARD, M. A. 2016. Transcriptional characteristics of different sized follicles in relation to embryo transferability: potential role of hepatocyte growth factor signalling. *Mol Hum Reprod,* 22**,** 475-84.

NIVET, A. L., VIGNEAULT, C., BLONDIN, P. & SIRARD, M. A. 2013. Changes in granulosa cells' gene expression associated with increased oocyte competence in bovine. *Reproduction,* 145**,** 555-65.

NSIAH-SEFAA, A. & MCKENZIE, M. 2016. Combined defects in oxidative phosphorylation and fatty acid beta-oxidation in mitochondrial disease. *Biosci Rep,* 36.

O'CONNOR, K. A., HOLMAN, D. J. & WOOD, J. W. 1998. Declining fecundity and ovarian ageing in natural fertility populations. *Maturitas,* 30**,** 127-36.

OGINO, M., TSUBAMOTO, H., SAKATA, K., OOHAMA, N., HAYAKAWA, H., KOJIMA, T., SHIGETA, M. & SHIBAHARA, H. 2016. Mitochondrial DNA copy number in cumulus cells is a strong predictor of obtaining good-quality embryos after IVF. *J Assist Reprod Genet,* 33**,** 367-371.

OU, X. H., LI, S., WANG, Z. B., LI, M., QUAN, S., XING, F., GUO, L., CHAO, S. B., CHEN, Z., LIANG, X. W., HOU, Y., SCHATTEN, H. & SUN, Q. Y. 2012. Maternal insulin resistance causes oxidative stress and mitochondrial dysfunction in mouse oocytes. *Hum Reprod,* 27**,** 2130-45.

OUANDAOGO, Z. G., FRYDMAN, N., HESTERS, L., ASSOU, S., HAOUZI, D., DECHAUD, H., FRYDMAN, R. & HAMAMAH, S. 2012. Differences in transcriptomic profiles of human cumulus cells isolated from oocytes at GV, MI and MII stages after in vivo and in vitro oocyte maturation. *Hum. Reprod,* 27**,** 2438-2447.

OUANDAOGO, Z. G., HAOUZI, D., ASSOU, S., DECHAUD, H., KADOCH, I. J., DE, V. J. & HAMAMAH, S. 2011. Human cumulus cells molecular signature in relation to oocyte nuclear maturity stage. *PLoS. One,* 6**,** e27179.

PAPAMENTZELOPOULOU, M., MAVROGIANNI, D., DINOPOULOU, V., THEOFANAKIS, H., MALAMAS, F., MARINOPOULOS, S., BLETSA, R., ANAGNOSTOU, E., KALLIANIDIS, K. & LOUTRADIS, D. 2012a. Detection of RUNX2 gene expression in cumulus cells in women undergoing controlled ovarian stimulation. *Reprod. Biol. Endocrinol,* 10**,** 99.

PAPAMENTZELOPOULOU, M., MAVROGIANNI, D., PARTSINEVELOS, G. A., MARINOPOULOS, S., DINOPOULOU, V., THEOFANAKIS, C., ANAGNOSTOU, E. & LOUTRADIS, D. 2012b. LH receptor gene expression in cumulus cells in women entering an ART program. *J. Assist. Reprod. Genet,* 29**,** 409-416.

PARK, J. Y., SU, Y. Q., ARIGA, M., LAW, E., JIN, S. L. & CONTI, M. 2004. EGF-like growth factors as mediators of LH action in the ovulatory follicle. *Science,* 303**,** 682-684.

PARKS, J. C., PATTON, A. L., MCCALLIE, B. R., GRIFFIN, D. K., SCHOOLCRAFT, W. B. & KATZ-JAFFE, M. G. 2016. Corona cell RNA sequencing from individual oocytes revealed transcripts and pathways linked to euploid oocyte competence and live birth. *Reprod. Biomed. Online,* 32**,** 518-526.

PAWLAK, P., CHABOWSKA, A., MALYSZKA, N. & LECHNIAK, D. 2016. Mitochondria and mitochondrial DNA in porcine oocytes and cumulus cells--A search for developmental competence marker. *Mitochondrion,* 27**,** 48-55.

PEPLING, M. E. & SPRADLING, A. C. 1998. Female mouse germ cells form synchronously dividing cysts. *Development,* 125**,** 3323-8.

PETERSEN, G. L., SCHMIDT, L., PINBORG, A. & KAMPER-JORGENSEN, M. 2013. The influence of female and male body mass index on live births after assisted reproductive technology treatment: a nationwide register-based cohort study. *Fertil Steril,* 99**,** 1654-62.

PINBORG, A., PETERSEN, G. L. & SCHMIDT, L. 2013. Recent insights into the influence of female bodyweight on assisted reproductive technology outcomes. *Womens Health (Lond),* 9**,** 1-4.

PRIBENSZKY, C., NILSELID, A. M. & MONTAG, M. 2017. Time-lapse culture with morphokinetic embryo selection improves pregnancy and live birth chances and reduces early pregnancy loss: a meta-analysis. *Reprod Biomed Online,* 35**,** 511-520.

PROVENZANO, M. & MOCELLIN, S. 2007. Complementary techniques: validation of gene expression data by quantitative real time PCR. *Adv. Exp. Med. Biol,* 593**,** 66-73.

RABINOWITZ, M., RYAN, A., GEMELOS, G., HILL, M., BANER, J., CINNIOGLU, C., BANJEVIC, M., POTTER, D., PETROV, D. A. & DEMKO, Z. 2012. Origins and rates of aneuploidy in human blastomeres. *Fertil. Steril,* 97**,** 395-401.

RACOWSKY, C., VERNON, M., MAYER, J., BALL, G. D., BEHR, B., POMEROY, K. O., WININGER, D., GIBBONS, W., CONAGHAN, J. & STERN, J. E. 2010. Standardization of grading embryo morphology. *J Assist Reprod Genet,* 27**,** 437-9.

RAMALHO-SANTOS, J., VARUM, S., AMARAL, S., MOTA, P. C., SOUSA, A. P. & AMARAL, A. 2009. Mitochondrial functionality in reproduction: from gonads and gametes to embryos and embryonic stem cells. *Hum Reprod Update,* 15**,** 553-72.

RAVICHANDRAN, K., MCCAFFREY, C., GRIFO, J., MORALES, A., PERLOE, M., MUNNE, S., WELLS, D. & FRAGOULI, E. 2017. Mitochondrial DNA quantification as a tool for embryo viability assessment: retrospective analysis of data from single euploid blastocyst transfers. *Hum Reprod,* 32**,** 1282-1292.

R CORE TEAM 2019. R: A language and environment for statistical computing. R. Foundation for Statisitcal Computing. Vienna, Austria. URL https://www.R-project.org/.

REYNIER, P., MAY-PANLOUP, P., CHRETIEN, M. F., MORGAN, C. J., JEAN, M., SAVAGNER, F., BARRIERE, P. & MALTHIERY, Y. 2001. Mitochondrial DNA content affects the fertilizability of human oocytes. *Mol Hum Reprod,* 7**,** 425-9.

RICHARDS, J. S. 1994. Hormonal control of gene expression in the ovary. *Endocr Rev,* 15**,** 725-51.

RICHARDS, J. S., RUSSELL, D. L., OCHSNER, S., HSIEH, M., DOYLE, K. H., FALENDER, A. E., LO, Y. K. & SHARMA, S. C. 2002. Novel signaling pathways that control ovarian follicular development, ovulation, and luteinization. *Recent Prog. Horm. Res,* 57**,** 195-220.

RICHARDSON, B. E. & LEHMANN, R. 2010. Mechanisms guiding primordial germ cell migration: strategies from different organisms. *Nat Rev Mol Cell Biol,* 11**,** 37-49.

RITTENBERG, V., SESHADRI, S., SUNKARA, S. K., SOBALEVA, S., OTENG-NTIM, E. & EL-TOUKHY, T. 2011. Effect of body mass index on IVF treatment outcome: an updated systematic review and meta-analysis. *Reprod Biomed Online,* 23**,** 421-39.

ROBKER, R. L., AKISON, L. K., BENNETT, B. D., THRUPP, P. N., CHURA, L. R., RUSSELL, D. L., LANE, M. & NORMAN, R. J. 2009. Obese women exhibit differences in ovarian metabolites, hormones, and gene expression compared with moderate-weight women. *J. Clin. Endocrinol. Metab,* 94**,** 1533-1540.

SAINI, N., SINGH, M. K., SHAH, S. M., SINGH, K. P., KAUSHIK, R., MANIK, R. S., SINGLA, S. K., PALTA, P. & CHAUHAN, M. S. 2015. Developmental competence of different quality bovine oocytes retrieved through ovum pick-up following in vitro maturation and fertilization. *Animal,* 9**,** 1979-85.

SAITO, N., YAMASHITA, Y., ONO, Y., HIGUCHI, Y., HAYASHI, A., YOSHIDA, Y., YAMAMOTO, H., KAWABE, S., KAMADA, M., TERAI, Y. & OHMICHI, M. 2013. Difference in mitochondrial gene expression in granulosa cells between recombinant FSH and hMG cycles under in vitro fertilization and transfer. *Reprod Med Biol,* 12**,** 99-104.

SANTOS, T. A., EL SHOURBAGY, S. & ST JOHN, J. C. 2006. Mitochondrial content reflects oocyte variability and fertilization outcome. *Fertil Steril,* 85**,** 584-91.

SART 2019. Society For Assisted Reproductive Technolgy. National Summary Report 2017. URL https://www.sartcorsonline.com/rptCSR_PublicMultYear.aspx?reportingYear=2017.

SCARICA, C., CIMADOMO, D., DOVERE, L., GIANCANI, A., STOPPA, M., CAPALBO, A., UBALDI, F. M., RIENZI, L. & CANIPARI, R. 2019. An integrated investigation of oocyte developmental competence: expression of key genes in human cumulus cells, morphokinetics of early divisions, blastulation, and euploidy. *J Assist Reprod Genet,* 36**,** 875-887.

SCHMIDT, J., WEIJDEGARD, B., MIKKELSEN, A. L., LINDENBERG, S., NILSSON, L. & BRANNSTROM, M. 2014. Differential expression of inflammation-related genes in the ovarian stroma and granulosa cells of PCOS women. *Mol. Hum. Reprod,* 20**,** 49-58.

SCHON, E. A., KIM, S. H., FERREIRA, J. C., MAGALHAES, P., GRACE, M., WARBURTON, D. & GROSS, S. J. 2000. Chromosomal non-disjunction in human oocytes: is there a mitochondrial connection? *Hum Reprod,* 15 Suppl 2**,** 160-72.

SCHOOLCRAFT, W. B., FRAGOULI, E., STEVENS, J., MUNNE, S., KATZ-JAFFE, M. G. & WELLS, D. 2010. Clinical application of comprehensive chromosomal screening at the blastocyst stage. *Fertil. Steril,* 94**,** 1700-1706.

SCOTT, R. T., JR., UPHAM, K. M., FORMAN, E. J., HONG, K. H., SCOTT, K. L., TAYLOR, D., TAO, X. & TREFF, N. R. 2013. Blastocyst biopsy with comprehensive chromosome screening and fresh embryo transfer significantly increases in vitro fertilization implantation and delivery rates: a randomized controlled trial. *Fertil. Steril,* 100**,** 697-703.

SEDER, C. W., HARTOJO, W., LIN, L., SILVERS, A. L., WANG, Z., THOMAS, D. G., GIORDANO, T. J., CHEN, G., CHANG, A. C., ORRINGER, M. B. & BEER, D. G. 2009. Upregulated INHBA expression may promote cell proliferation and is associated with poor survival in lung adenocarcinoma. *Neoplasia,* 11**,** 388-396.

SEIFER, D. B., DEJESUS, V. & HUBBARD, K. 2002. Mitochondrial deletions in luteinized granulosa cells as a function of age in women undergoing in vitro fertilization. *Fertil Steril,* 78**,** 1046-8.

SEYFRIED, T. N. & SHELTON, L. M. 2010. Cancer as a metabolic disease. *Nutr Metab (Lond),* 7**,** 7.

SHOUBRIDGE, E. A. & WAI, T. 2007. Mitochondrial DNA and the mammalian oocyte. *Curr Top Dev Biol,* 77**,** 87-111.

SIMARD, J., RICKETTS, M. L., GINGRAS, S., SOUCY, P., FELTUS, F. A. & MELNER, M. H. 2005. Molecular biology of the 3beta-hydroxysteroid dehydrogenase/delta5-delta4 isomerase gene family. *Endocr. Rev,* 26**,** 525-582.

SIMERMAN, A. A., HILL, D. L., GROGAN, T. R., ELASHOFF, D., CLARKE, N. J., GOLDSTEIN, E. H., MANRRIQUEZ, A. N., CHAZENBALK, G. D. & DUMESIC, D. A. 2015. Intrafollicular cortisol levels inversely correlate with cumulus cell lipid content as a possible energy source during oocyte meiotic resumption in women undergoing ovarian stimulation for in vitro fertilization. *Fertil Steril,* 103**,** 249-57.

SISCO, B., HAGEMANN, L. J., SHELLING, A. N. & PFEFFER, P. L. 2003. Isolation of genes differentially expressed in dominant and subordinate bovine follicles. *Endocrinology,* 144**,** 3904-3913.

SONG, W. H., BALLARD, J. W., YI, Y. J. & SUTOVSKY, P. 2014. Regulation of mitochondrial genome inheritance by autophagy and ubiquitin-proteasome system: implications for health, fitness, and fertility. *Biomed Res Int,* 2014**,** 981867.

STOCCO, C., TELLERIA, C. & GIBORI, G. 2007. The molecular control of corpus luteum formation, function, and regression. *Endocr Rev,* 28**,** 117-49.
STOUFFER, R. L., MARTINEZ-CHEQUER, J. C., MOLSKNESS, T. A., XU, F. & HAZZARD, T. M. 2001. Regulation and action of angiogenic factors in the primate ovary. *Arch Med Res,* 32**,** 567-75.
SU, Y. Q., SUGIURA, K. & EPPIG, J. J. 2009. Mouse oocyte control of granulosa cell development and function: paracrine regulation of cumulus cell metabolism. *Semin Reprod Med,* 27**,** 32-42.
SU, Y. Q., SUGIURA, K., WIGGLESWORTH, K., O'BRIEN, M. J., AFFOURTIT, J. P., PANGAS, S. A., MATZUK, M. M. & EPPIG, J. J. 2008. Oocyte regulation of metabolic cooperativity between mouse cumulus cells and oocytes: BMP15 and GDF9 control cholesterol biosynthesis in cumulus cells. *Development,* 135**,** 111-21.
SUGIMURA, S., RITTER, L. J., ROSE, R. D., THOMPSON, J. G., SMITZ, J., MOTTERSHEAD, D. G. & GILCHRIST, R. B. 2015. Promotion of EGF receptor signaling improves the quality of low developmental competence oocytes. *Dev. Biol,* 403**,** 139-149.
SUH, C. S., SONNTAG, B. & ERICKSON, G. F. 2002. The ovarian life cycle: a contemporary view. *Rev Endocr Metab Disord,* 3**,** 5-12.
SUTOVSKY, P., MORENO, R. D., RAMALHO-SANTOS, J., DOMINKO, T., SIMERLY, C. & SCHATTEN, G. 2000. Ubiquitinated sperm mitochondria, selective proteolysis, and the regulation of mitochondrial inheritance in mammalian embryos. *Biol Reprod,* 63**,** 582-90.
SUTTON-MCDOWALL, M. L., GILCHRIST, R. B. & THOMPSON, J. G. 2010. The pivotal role of glucose metabolism in determining oocyte developmental competence. *Reproduction,* 139**,** 685-95.
TALLEN, G., FARHANGI, S., TAMANNAI, M., HOLTKAMP, N., MANGOLDT, D., SHAH, S., SUZUKI, K., TRUSS, M., HENZE, G., RIABOWOL, K. & VON, D. A. 2009. The inhibitor of growth 1 (ING1) proteins suppress angiogenesis and differentially regulate angiopoietin expression in glioblastoma cells. *Oncol. Res,* 18**,** 95-105.
TANGHE, S., VAN, S. A., NAUWYNCK, H., CORYN, M. & DE, K. A. 2002. Minireview: Functions of the cumulus oophorus during oocyte maturation, ovulation, and fertilization. *Mol. Reprod. Dev,* 61**,** 414-424.
TATONE, C., AMICARELLI, F., CARBONE, M. C., MONTELEONE, P., CASERTA, D., MARCI, R., ARTINI, P. G., PIOMBONI, P. & FOCARELLI, R. 2008. Cellular and molecular aspects of ovarian follicle ageing. *Hum Reprod Update,* 14**,** 131-42.
TATONE, C., CARBONE, M. C., FALONE, S., AIMOLA, P., GIARDINELLI, A., CASERTA, D., MARCI, R., PANDOLFI, A., RAGNELLI, A. M. & AMICARELLI, F. 2006. Age-dependent changes in the expression of superoxide dismutases and catalase are associated with ultrastructural modifications in human granulosa cells. *Mol Hum Reprod,* 12**,** 655-60.

TAUGOURDEAU, A., DESQUIRET-DUMAS, V., HAMEL, J. F., CHUPIN, S., BOUCRET, L., FERRE-L'HOTELLIER, V., BOUET, P. E., DESCAMPS, P., PROCACCIO, V., REYNIER, P. & MAY-PANLOUP, P. 2019. The mitochondrial DNA content of cumulus cells may help predict embryo implantation. *J Assist Reprod Genet,* 36**,** 223-228.

TAYLOR, T. H., GITLIN, S. A., PATRICK, J. L., CRAIN, J. L., WILSON, J. M. & GRIFFIN, D. K. 2014. The origin, mechanisms, incidence and clinical consequences of chromosomal mosaicism in humans. *Hum Reprod Update,* 20**,** 571-81.

TE VELDE, E. R., SCHEFFER, G. J., DORLAND, M., BROEKMANS, F. J. & FAUSER, B. C. 1998. Developmental and endocrine aspects of normal ovarian aging. *Mol Cell Endocrinol,* 145**,** 67-73.

TOLEIKIS, A., LIOBIKAS, J., TRUMBECKAITE, S. & MAJIENE, D. 2001. Relevance of fatty acid oxidation in regulation of the outer mitochondrial membrane permeability for ADP. *FEBS Lett,* 509**,** 245-9.

TREFF, N. R., ZHAN, Y., TAO, X., OLCHA, M., HAN, M., RAJCHEL, J., MORRISON, L., MORIN, S. J. & SCOTT, R. T., JR. 2017. Levels of trophectoderm mitochondrial DNA do not predict the reproductive potential of sibling embryos. *Hum Reprod,* 32**,** 954-962.

TSAI, H. D., HSIEH, Y. Y., HSIEH, J. N., CHANG, C. C., YANG, C. Y., YANG, J. G., CHENG, W. L., TSAI, F. J. & LIU, C. S. 2010. Mitochondria DNA deletion and copy numbers of cumulus cells associated with in vitro fertilization outcomes. *J Reprod Med,* 55**,** 491-7.

TSUTSUMI, R., HIROI, H., MOMOEDA, M., HOSOKAWA, Y., NAKAZAWA, F., KOIZUMI, M., YANO, T., TSUTSUMI, O. & TAKETANI, Y. 2008. Inhibitory effects of cholesterol sulfate on progesterone production in human granulosa-like tumor cell line, KGN. *Endocr. J,* 55**,** 575-581.

UYAR, A. & SELI, E. 2014. Metabolomic assessment of embryo viability. *Semin. Reprod. Med,* 32**,** 141-152.

UYAR, A., TORREALDAY, S. & SELI, E. 2013. Cumulus and granulosa cell markers of oocyte and embryo quality. *Fertil. Steril,* 99**,** 979-997.

VAN BLERKOM, J. 2004. Mitochondria in human oogenesis and preimplantation embryogenesis: engines of metabolism, ionic regulation and developmental competence. *Reproduction,* 128**,** 269-80.

VAN BLERKOM, J. 2011. Mitochondrial function in the human oocyte and embryo and their role in developmental competence. *Mitochondrion,* 11**,** 797-813.

VAN BLERKOM, J., DAVIS, P. W. & LEE, J. 1995. ATP content of human oocytes and developmental potential and outcome after in-vitro fertilization and embryo transfer. *Hum Reprod,* 10**,** 415-24.

VAN LOENDERSLOOT, L. L., VAN, W. M., LIMPENS, J., BOSSUYT, P. M., REPPING, S. & VAN, D., V 2010. Predictive factors in in vitro fertilization (IVF): a systematic review and meta-analysis. *Hum. Reprod. Update,* 16**,** 577-589.

VANDERSTICHEL, R., DOHOO, I. & MARKHAM, F. 2015. Applying a kinetic method to an indirect ELISA measuring Ostertagia ostertagi antibodies in milk. *Can J Vet Res,* 79**,** 180-3.
VARRAS, M., POLONIFI, K., MANTZOURANI, M., STEFANIDIS, K., PAPADOPOULOS, Z., AKRIVIS, C. & ANTSAKLIS, A. 2012. Expression of antiapoptosis gene survivin in luteinized ovarian granulosa cells of women undergoing IVF or ICSI and embryo transfer: clinical correlations. *Reprod. Biol. Endocrinol,* 10**,** 74.
VEATCH, J. R., MCMURRAY, M. A., NELSON, Z. W. & GOTTSCHLING, D. E. 2009. Mitochondrial dysfunction leads to nuclear genome instability via an iron-sulfur cluster defect. *Cell,* 137**,** 1247-58.
VICTOR, A. R., BRAKE, A. J., TYNDALL, J. C., GRIFFIN, D. K., ZOUVES, C. G., BARNES, F. L. & VIOTTI, M. 2017. Accurate quantitation of mitochondrial DNA reveals uniform levels in human blastocysts irrespective of ploidy, age, or implantation potential. *Fertil Steril,* 107**,** 34-42 e3.
VIGONE, G., MERICO, V., PRIGIONE, A., MULAS, F., SACCHI, L., GABETTA, M., BELLAZZI, R., REDI, C. A., MAZZINI, G., ADJAYE, J., GARAGNA, S. & ZUCCOTTI, M. 2013. Transcriptome based identification of mouse cumulus cell markers that predict the developmental competence of their enclosed antral oocytes. *BMC Genomics,* 14**,** 380.
WAGNER, P. K., OTOMO, A. & CHRISTIANS, J. K. 2011. Regulation of pregnancy-associated plasma protein A2 (PAPPA2) in a human placental trophoblast cell line (BeWo). *Reprod. Biol. Endocrinol,* 9**,** 48.
WALKER, G., MACLEOD, K., WILLIAMS, A. R., CAMERON, D. A., SMYTH, J. F. & LANGDON, S. P. 2007. Insulin-like growth factor binding proteins IGFBP3, IGFBP4, and IGFBP5 predict endocrine responsiveness in patients with ovarian cancer. *Clin. Cancer Res,* 13**,** 1438-1444.
WANG, H. S. & CHARD, T. 1999. IGFs and IGF-binding proteins in the regulation of human ovarian and endometrial function. *J Endocrinol,* 161**,** 1-13.
WANG, H. X., TONG, D., EL-GEHANI, F., TEKPETEY, F. R. & KIDDER, G. M. 2009. Connexin expression and gap junctional coupling in human cumulus cells: contribution to embryo quality. *J. Cell Mol. Med,* 13**,** 972-984.
WANG, Q., FROLOVA, A. I., PURCELL, S., ADASTRA, K., SCHOELLER, E., CHI, M. M., SCHEDL, T. & MOLEY, K. H. 2010. Mitochondrial dysfunction and apoptosis in cumulus cells of type I diabetic mice. *PLoS One,* 5**,** e15901.
WATHLET, S., ADRIAENSSENS, T., SEGERS, I., VERHEYEN, G., JANSSENS, R., COUCKE, W., DEVROEY, P. & SMITZ, J. 2012. New candidate genes to predict pregnancy outcome in single embryo transfer cycles when using cumulus cell gene expression. *Fertil. Steril,* 98**,** 432-439.
WATHLET, S., ADRIAENSSENS, T., SEGERS, I., VERHEYEN, G., VAN, D., V, COUCKE, W., RON, E. R., DEVROEY, P. & SMITZ, J. 2011. Cumulus cell gene expression predicts better cleavage-stage embryo or blastocyst development and pregnancy for ICSI patients. *Hum. Reprod,* 26**,** 1035-1051.

WATHLET, S., ADRIAENSSENS, T., SEGERS, I., VERHEYEN, G., VAN, L. L., COUCKE, W., DEVROEY, P. & SMITZ, J. 2013. Pregnancy prediction in single embryo transfer cycles after ICSI using QPCR: validation in oocytes from the same cohort. *PLoS. One,* 8**,** e54226.

WEBB, R. & CAMPBELL, B. K. 2007. Development of the dominant follicle: mechanisms of selection and maintenance of oocyte quality. *Soc. Reprod. Fertil. Suppl,* 64**,** 141-163.

WEBB, R. J., MARSHALL, F., SWANN, K. & CARROLL, J. 2002. Follicle-stimulating hormone induces a gap junction-dependent dynamic change in [cAMP] and protein kinase a in mammalian oocytes. *Dev Biol,* 246**,** 441-54.

WEI, L. N., FANG, C., HUANG, R., LI, L. L., ZHANG, M. F. & LIANG, X. Y. 2012. [Change and significance of growth differentiation factor 9 and bone morphogenetic protein expression during oocyte maturation in polycystic ovary syndrome patients with ovarian stimulation]. *Zhonghua Fu Chan Ke. Za Zhi,* 47**,** 818-822.

WHITAKER, M. 1996. Control of meiotic arrest. *Rev Reprod,* 1**,** 127-35.

WILDING, M., DALE, B., MARINO, M., DI MATTEO, L., ALVIGGI, C., PISATURO, M. L., LOMBARDI, L. & DE PLACIDO, G. 2001. Mitochondrial aggregation patterns and activity in human oocytes and preimplantation embryos. *Hum Reprod,* 16**,** 909-17.

WYLIE, C. 1999. Germ cells. *Cell,* 96**,** 165-74.

YANAIHARA, A., OTSUKA, Y., IWASAKI, S., OKAI, T. & YANAIHARA, T. 2005. Strong expression of steroid sulfatase in human cumulus cells in patients with endometriosis. *Fertil. Steril,* 84**,** 464-467.

YANG, Z., LIU, J., COLLINS, G. S., SALEM, S. A., LIU, X., LYLE, S. S., PECK, A. C., SILLS, E. S. & SALEM, R. D. 2012. Selection of single blastocysts for fresh transfer via standard morphology assessment alone and with array CGH for good prognosis IVF patients: results from a randomized pilot study. *Mol. Cytogenet,* 5**,** 24.

YUNG, Y., MAMAN, E., OPHIR, L., RUBINSTEIN, N., BARZILAY, E., YERUSHALMI, G. M. & HOURVITZ, A. 2014. Progesterone antagonist, RU486, represses LHCGR expression and LH/hCG signaling in cultured luteinized human mural granulosa cells. *Gynecol. Endocrinol,* 30**,** 42-47.

ZACHARIADES, E., FOSTER, H., GOUMENOU, A., THOMAS, P., RAND-WEAVER, M. & KARTERIS, E. 2011. Expression of membrane and nuclear progesterone receptors in two human placental choriocarcinoma cell lines (JEG-3 and BeWo): Effects of syncytialization. *Int. J. Mol. Med,* 27**,** 767-774.

ZAMAH, A. M., HSIEH, M., CHEN, J., VIGNE, J. L., ROSEN, M. P., CEDARS, M. I. & CONTI, M. 2010. Human oocyte maturation is dependent on LH-stimulated accumulation of the epidermal growth factor-like growth factor, amphiregulin. *Hum Reprod,* 25**,** 2569-78.

ZHANG, M., SU, Y. Q., SUGIURA, K., XIA, G. & EPPIG, J. J. 2010. Granulosa cell ligand NPPC and its receptor NPR2 maintain meiotic arrest in mouse oocytes. *Science,* 330**,** 366-9.

ZHANG, S., LUO, K., CHENG, D., TAN, Y., LU, C., HE, H., GU, Y., LU, G., GONG, F. & LIN, G. 2016. Number of biopsied trophectoderm cells is likely to affect the implantation potential of blastocysts with poor trophectoderm quality. *Fertil. Steril,* 105**,** 1222-1227.

ZHANG, X., JAFARI, N., BARNES, R. B., CONFINO, E., MILAD, M. & KAZER, R. R. 2005. Studies of gene expression in human cumulus cells indicate pentraxin 3 as a possible marker for oocyte quality. *Fertil. Steril,* 83 Suppl 1**,** 1169-1179.

ZHAO, S. Y., QIAO, J., CHEN, Y. J., LIU, P., LI, J. & YAN, J. 2010. Expression of growth differentiation factor-9 and bone morphogenetic protein-15 in oocytes and cumulus granulosa cells of patients with polycystic ovary syndrome. *Fertil. Steril,* 94**,** 261-267.

APPENDIX A

Human pregnancy or live birth candidate biomarkers

shown to have differential mRNA expression

Gene name	Symbol	Function	Study Population	Samples	Reference
Down-regulated biomarkers					
Estrogen receptor 1	*ESR1*	Transcription factor	4 CC, 4 preg pts 4 CC, 4 not preg pts	Pooled	Artini *et al.* 2017
Nuclear factor I B	*NFIB*	Transcription factor	5 CC, preg pts 5 CC, not preg pts	Individual	Assou *et al.* 2008
Docking protein 5	*DOK5* *	Signal transduction	MGC, 16 & 28 preg pts MGC, 16 & 69 not preg	Pooled	Fortin *et al.* 2019
DnaJ heat shock protein family (Hsp40) member C15	*DNAJC15*	Heat shock protein	101 CC, 58 pts, multicenter	Individual	Iager *et al.* 2013
Microtubule associated tumor suppressor 1	*MTUS1*	Tumor suppressor			
Nucleoporin 133	*NUP133*	Nucleoporin			
Rhomboid like 2	*RHBDL2*	Serine protease			

APPENDIX A continued.

Gene name	Symbol	Function	Study Population	Samples	Reference
Zinc finger protein 93	*ZNF93*	Zinc finger protein			
Lysine demethylase 4A	*KDM4A*	Demethylase	31 CC, 31 MGC preg pts 53 CC, 51 MGC not preg	Pooled	Krieg *et al*. 2018
Lysine demethylase 4B	*KDM4B*	Demethylase			
Runt related transcription factor 2	*RUNX2*	Transcription factor	5 CC each, 41 pts	Pooled	Papamentzelopoulou *et al.* 2012a
Up-regulated biomarkers					
Forkhead box O4	*FOXO4*	Transcription factor	4 CC, 4 preg pts 4 CC, 4 not preg pts	Pooled	Artini *et al.* 2017
Chromodomain helicase DNA binding protein 9	*CHD9*	Chromatin remodeling	14 CC, 8 pts	Individual	Assidi *et al.*, 2011
Proteasome 26S subunit, non-ATPase 6	*PSMD6*	Proteasome subunit			
Ubiquilin 1	*UBQLN1*	Ubiquilin			
Dipeptidyl peptidase 8	*DPP8*	Peptidase	11 CC, 7 pts	Individual	Assidi *et al.*, 2015
Proteasome 26S subunit, non-ATPase 6	*PSMD6*	Proteasome subunit			
Ubiquilin 1	*UBQLN1*	Ubiquilin			
BCL2 like 11	*BCL2L11*	Apoptosis regulator	5 CC, preg 5 CC, not preg	Individual	Assou *et al.* 2008
Phosphoenolpyruvate carboxykinase 1	*PCK1*	Gluconeogenic enzyme			

APPENDIX A continued.

Gene name	Symbol	Function	Study Population	Samples	Reference
Pleckstrin homology like Domain family A member 1	*PHLDA1*	Apoptosis regulator	MGC, CC, 18 pts	Pooled	Hamel *et al.* 2010b
UDP-glucose pyrophosphorylase 2	*UGP2*	Glucogenic enzyme			
AT-rich interaction domain 1B	*ARID1B*	Chromatin remodeling	101 CC, 58 pts, multicenter	Individual	Iager *et al.* 2013
COX20, cytochrome c oxidase assembly factor	*COX20*	Electron transport chain			
Fibroblast growth factor 12	*FGF12*	Growth factor			
G protein-coupled receptor 137B	*GPR137B*	G protein-coupled receptor			
Nuclear receptor subfamily 2 group F member 6	*NR2F6*	Transcription factor	101 CC, 58 pts, multicenter	Individual	Iager *et al.* 2013
Solute carrier family 2 member 9	*SLC2A9*	Glucose transport			
Zinc finger protein 132	*ZNF132*	Zinc finger protein			
Bone morphogenetic protein 15	*BMP15*	Paracrine signaling	2426 CC, 196 pts	Pooled	Li Y *et al.*, 2014
Growth differentiation factor 9	*GDF9*	Paracrine signaling			

* Two separate analyses were performed in the same study
CC = cumulus cells; MGC = mural granulosa cells; pts = patients; preg = pregnant

APPENDIX B

Human pregnancy or live birth candidate biomarkers

with conflicting differential mRNA expression by qRT-PCR *

Gene	Symbol	Function	mRNA expression	Study Population	Samples	Reference
Activated leukocyte cell adhesion molecule	*ALCAM*	Cell adhesion	Live birth = not preg/loss Preg > not preg	270 CC, 25 pts 42 CC, 42 pts	Individual Individual	Ekart et al. 2013 Wathlet et al. 2011
Baculoviral IAP repeat containing 5	*BIRC5*	Apoptosis regulator	Preg = not preg Preg > not preg Preg = not preg	MGC, CC, 38 pts MGC, 28 pts CC, 29 pts	Pooled Pooled Pooled	Hamel et al. 2010a Fujino et al.2008 Varras et al. 2012
Calmodulin 1	*CALM1*	Calcium binding	Preg > not preg Preg > not preg Preg = not preg	14 CC, 8 pts 11 CC, 7 pts 39 CC, 39 pts	Individual Individual Individual	Assidi et al. 2011 Assidi et al. 2015 Burnik et al. 2015a
Calcium/calmodulin dependent protein kinase kinase ID	*CAMK1D*	Serine/threonine	Preg > not preg Preg > not preg ns trend	99 CC, 33 ICSI pts 47 CC, 47 ICSI pts	Individual Individual	Wathlet et al. 2012 Wathlet et al. 2013
Cell division cycle 42*DC42*		Cell cycle control	Preg > not preg Preg > not preg ns trend	30 MGC, CC, 18 pts ea MGC, CC, 38 pts	Pooled Pooled	Hamel et al. 2008 Hamel et al. 2010a
C-X-C motif ligand 2	*CXCL2*^	Inflammation	Preg < not preg Preg = not preg	16 MGC, 16 pts ea 28 MGC preg pts 69 MGC not preg pts	Pooled Pooled	Fortin *et al.* 2019 Fortin *et al.* 2019

APPENDIX B continued.

Gene	Symbol	Function	mRNA expression	Study Population	Samples	Reference
Cytochrome P450 family 19 subfamily A member 1	*CYP19A1*	Steroidogenic enzyme	Preg > not preg Preg = not preg	30 MGC, CC, 18 pts ea MGC, CC, 38 pts	Pooled Pooled	Hamel et al. 2008 Hamel et al. 2010a
Ephrin B2	*EFNB2*	Ephrin	Preg < not preg Preg > not Preg Preg > not preg	43 CC, 43 pts 99 CC, 33 ICSI pts 47 CC, 47 ICSI pts	Individual Individual Individual	Burnik et al. 2015c Wathlet et al. 2012 Wathlet et al. 2013
Ferredoxin 1	*FDX1*	Steroidogenic enzyme	Preg > not preg Preg = not preg	30 MGC, CC, 18 pts ea MGC, CC, 38 pts	Pooled Pooled	Hamel et al. 2008 Hamel et al. 2010a
Gremlin 1, DAN family BMP antagonist	*GREM1*	BMP antagonist	Live birth = not preg** Predicts pregnancy Preg > not preg	38 CC, 38 pts SET 108 CC, 8 ICSI pts 42 CC, 42 pts	Individual Pooled Individual	Gebhardt et al. 2011 Mckenzie et al. 2004 Wathlet et al. 201
Hyaluronan synthase 2	*HAS2*	Glycosyl-transferase	Live birth = not preg/loss Live birth = not preg Predicts pregnancy	270 CC, 25 pts 38 CC, 38 pts SET 108 CC, 8 ICSI pts	Individual Individual Pooled	Ekart et al. 2013 Gebhardt et al. 2011 Mckenzie et al. 2004
H4 clustered histone 3	*H4C3*	Histone	Preg > not preg Preg = not preg	14 CC, 8 pts 11 CC, 7 pts	Individual Individual	Assidi et al., 2011 Assidi et al., 2015
Hydroxy-delta-5-steroid dehydrogenase, 3 beta-and steroid delta-isomerase 1	*HSD3B1*	Steroidogenic enzyme	Preg > not preg Preg = not preg	30 MGC, CC, 18 pts ea MGC, CC, 38 pts	Pooled Pooled	Hamel et al. 2008 Hamel et al. 2010a
Inositol-trisphosphate 3-kinase A	*ITPKA*	Kinase	Preg = not preg Preg > not preg Preg > not Preg	39 CC, 41 pts 42 CC, 42 pts 99 CC, 33 ICSI pts	Individual Individual Individual	Burnik et al. 2015a Wathlet et al. 2011 Wathlet et al. 2012

APPENDIX B continued.

Gene	Symbol	Function	mRNA expression	Study Population	Samples	Reference
Luteinizing hormone/ choriogonadotropin receptor	*LHCGR*	G protein-coupled receptor	See note **	CC, 40 pts	Pooled	Papamentzelopoulou *et al.* 2012b
			Preg = not preg	MGC, CC, 111 pts	Pooled	Lee *et al.* 2016
			Preg = not preg	30 MGC, CC, 18 pts ea	Pooled	Hamel et al. 2008
Neuropilin 1 receptor	*NRP1*	Growth factor	Preg > not preg	14 CC, 8 pts	Individual	Assidi et al. 2011
			Preg > not preg	11 CC, 7 pts	Individual	Assidi et al., 2015
			Live birth = not preg/loss	270 CC, 25 pts	Individual	Ekart et al. 2013
			Preg = not preg	MGC, CC, 38 pts	Pooled	Hamel et al. 2010a
Neurotensin	*NTS^*	Neurotransmitter	Preg < not preg	28 MGC preg pts 69 MGC not preg pts	Pooled	Fortin *et al.* 2019
			Preg = not preg	16 MGC, 16 pts ea	Pooled	Fortin *et al.* 2019
Phosphoglycerate kinase 1	*PGK1*	Kinase	Preg = not preg	30 MGC, CC, 18 pts ea	Pooled	Hamel et al. 200
			Preg > not preg	MGC, CC, 38 pts	Pooled	Hamel et al. 2010a
Prostaglandin-endoperoxide synthase 2	*PTGS2*	Prostaglandin synthesis	Preg = not preg	39 CC, 41 pts	Individual	Burnik et al. 2015a
			Live birth > not preg	38 CC, 38 pts SET	Individual	Gebhardt et al. 2011
			Predicts pregnancy	108 CC, 8 ICSI pts	Pooled	Mckenzie et al. 2004
			Preg > not preg	42 CC, 42 pts	Individual	Wathlet et al. 2011
Pentraxin 3	*PTX3*	Immune response	Preg = not preg	90 CC, 45 pts	Individual	Cillo et al. 2007
			Preg > not preg	38 CC, 22 pts	Individual	Feuerstein et al. 2012
			Live birth > not preg ns trend	38 CC, 38 pts SET	Individual	Gebhardt et al. 2011
Regulator of G-protein signaling 2	*RGS2*	G protein signaling	Preg = not preg	43 CC, 43 pts	Individual	Burnik et al. 2015c
			Preg > not preg	38 CC, 22 pts	Individual	Feuerstein et al. 2012
			Preg = not preg	30 MGC, CC, 18 pts	Pooled	Hamel et al. 2008
			Preg > not preg	MGC, CC, 38 pts	Pooled	Hamel et al. 2010a
Syndecan 4	*SDC4*	Intracellular signaling	Preg > not preg	42 CC, 42 pts	Individual	Wathlet et al. 2011
			Preg = not preg	99 CC, 33 ICSI pts	Individual	Wathlet et al. 2012
Serpin family E member 2	*SERPINE2*	Peptidase inhibitor	Preg > not preg	30 MGC, CC, 18 pts	Pooled	Hamel et al. 2008
			Preg = not preg	MGC, CC 38 pts	Pooled	Hamel et al. 2010a

APPENDIX B continued.

Gene	Symbol	Function	mRNA expression	Study Population	Samples	Reference
Target of myb1 membrane trafficking protein	*TOM1*	Intracellular trafficking	Preg > not preg Preg = not preg	14 CC, 8 pts 11 CC, 7 pts	Individual Individual	Assidi et al. 2011 Assidi et al. 2015
Transient receptor potential cation channel subfamily M member 7	*TRPM7*	Ion channel	Preg > not preg Preg = not preg	42 CC, 42 pts 99 CC, 33 ICSI pts	Individual Individual	Wathlet et al. 2011 Wathlet et al. 2012
Taurine up-regulated 1 (non-protein coding)	*TUG1*	Long non-coding RNA	Preg = not preg Preg > not preg	14 CC, 8 pts 11 CC, 7 pts	Individual Individual	Assidi et al. 2011 Assidi et al. 2015
Versican	*VCAN*	Cell adhesion	Preg = not preg Live birth > not preg/loss Live birth > not preg^^ Preg > not preg Preg = not preg	43 CC, 43 pts 270 CC, 25 pts 38 CC, 38 pts SET 42 CC, 42 pts 99 CC, 33 ICSI pts	Individual Individual Individual Individual Individual	Burnik et al. 2015c Ekart et al. 2013 Gebhardt et al. 2011 Wathlet et al. 2011 Wathlet et al. 2012

* observed in two or more studies;

**Splice variants were present in greater quantities in pregnant vs not pregnant patients

^ Two separate analyses were performed in the same study

^^positive correlation with birth weight

CC = cumulus cells; MGC = mural granulosa cells; ICSI = intra-cytoplasmic sperm injection

SET = single embryo transfer; pts = patients; ea = each group; preg = pregnant, ns = not significant

Symbols: > greater than; = equivalent to, < less than

APPENDIX C

Human pregnancy or live birth candidate biomarkers

shown not to have differential mRNA expression by qRT-PCR

Genes	Symbol	Function	mRNA expression	Study Population	Samples	Reference
Aryl hydrocarbon	*AHR*	Transcription factor receptor	Live birth = not preg	38 CC, 38 pts SET	Individual	Gebhardt *et al.* 2011
Aldolase, fructose-bisphosphate A	*ALDOA*	Gluconeogenic enzyme	Live birth = not preg	38 CC, 38 pts SET	Individual	Gebhardt *et al.* 2011
Aquaporin 1 (Colton blood group)	AQP1	Passive H_2O transport	Preg = not preg	MCG, CC, 111 pts	Pooled	Lee *et al*. 2016
Aquaporin 2	AQP2	Passive H_2O transport	Preg = not preg	MCG, CC, 111 pts	Pooled	Lee *et al*. 2016
Aquaporin 3 (Gill blood group)	AQP3	Passive H_2O transport	Preg = not preg	MCG, CC, 111 pts	Pooled	Lee *et al*. 2016
Aquaporin 4	AQP4	Passive H_2O transport	Preg = not preg	MCG, CC, 111 pts	Pooled	Lee *et al*. 2016
Aquaporin 5	AQP5	Passive H_2O transport	Preg = not preg	MCG, CC, 111 pts	Pooled	Lee *et al*. 2016
Aquaporin 6	AQP6	Passive H_2O transport	Preg = not preg	MCG, CC, 111 pts	Pooled	Lee *et al*. 2016
Aquaporin 7	AQP7	Passive H_2O transport	Preg = not preg	MCG, CC, 111 pts	Pooled	Lee *et al*. 2016
Aquaporin 9	AQP9	Passive H_2O transport	Preg = not preg	MCG, CC, 111 pts	Pooled	Lee *et al*. 2016

APPENDIX C continued.

Genes	Symbol	Function	mRNA expression	Study Population	Samples	Reference
Aquaporin 11	AQP11	Passive H_2O transport	Preg = not preg	MCG, CC, 111 pts	Pooled	Lee *et al*. 2016
Aquaporin 12A	AQP12A	Passive H_2O transport	Preg = not preg	MCG, CC, 111 pts	Pooled	Lee *et al*. 2016
Androgen receptor	*AR*	Nuclear hormone receptor	Preg = not preg	14 CC, 8 pts	Individual	Assidi *et al.*, 2011
BTB domain and CNC homolog 2	*BACH2*	Transcription factor	Preg = not preg	30 MGC, CC, 18 pts ea	Pooled	Hamel *et al.* 2008
Calmodulin 2	*CALM2*	Calcium binding	Preg = not preg	42 CC, 42 pts	Individual	Wathlet *et al.* 2011
Calumenin	*CALU*	Calcium binding	Preg = not preg	14 CC, 8 pts	Individual	Assidi *et al.*, 2011
Chromogranin B	*CHGB*	Secretory protein	Preg = not preg	14 CC, 8 pts	Individual	Assidi *et al.*, 2011
C-X-C motif chemokine ligand 8	CXCL8^	Inflammation	Preg = not preg	MGC, 16 & 28 preg pts MGC, 16 & 69 not preg	Pooled	Fortin et al. 2019
Cytochrome P450 family 11 subfamily A member 1	*CYP11A1*	Steroidogenic enzyme	Preg = not preg	99 CC, 33 ICSI pts	Individual	Wathlet *et al.* 2012
Dihydro-pyrimidinase like 3	*DPYSL3*	Enzyme	Preg = not preg Preg = not preg	30 MGC, CC, 18 pts ea MGC, CC, 18 pts	Pooled Pooled	Hamel *et al.* 2008 Hamel *et al.* 2010b
Early growth response 1	*EGR1*	Transcription factor	Preg = not preg Preg = not preg	30 MGC, CC, 18 pts ea MGC, CC, 38 pts	Pooled Pooled	Hamel *et al.* 2008 Hamel *et al.* 2010a
Epiregulin	*EREG*	EGF ligand	Preg = not preg Preg = not preg	30 MGC, CC, 18 pts ea MGC, CC, 18 pts	Pooled Pooled	Hamel *et al.* 2008 Hamel *et al.* 2010b
Follicle stimulating hormone receptor	*FSHR*	G protein-coupled receptor	Live birth = not preg/loss	270 CC, 25 pts	Individual	Ekart *et al.* 2013

APPENDIX C continued.

Genes	Symbol	Function	mRNA expression	Study Population	Samples	Reference
Forkhead box O1	*FOXO1*	Transcription factor	Preg = not preg	8 CC, 8 pts	Pooled	Artini *et al.* 2017
Forkhead box O3	*FOXO3*	Transcription factor	Preg = not preg	8 CC, 8 pts	Pooled	Artini *et al.* 2017
GA binding protein transcription factor beta subunit 1	*GABPB1*	Transcription factor	Preg = not preg	MGC, CC, 18 pts	Pooled	Hamel *et al.* 2010b
Glutathione peroxidase 3	*GPX3*	Glutathione peroxidase	Preg = not preg	47 CC, 47 ICSI pts	Individual	Wathlet *et al.* 2013
Glutathione-disulfide reductase	*GSR*	Enzyme	Preg > not preg ns trend	47 CC, 47 ICSI pts	Individual	Wathlet *et al.* 2013
Glutathione S-transferase alpha 3	*GSTA3*	Glutathione peroxidase	Preg = not preg	47 CC, 47 ICSI pts	Individual	Wathlet *et al.* 2013
Glutathione S-transferase alpha 4	*GSTA4*	Glutathione peroxidase	Preg > not preg ns trend	47 CC, 47 ICSI pts	Individua l	Wathlet *et al.* 2013
Homeodomain interacting protein kinase 1	*HIPK1*	Serine/threonine kinase	Preg = not preg	39 CC, 41 pts	Individual	Burnik *et al.* 2015a
Homer scaffolding protein 1	*HOMER1*	Scaffold protein	Preg = not preg	MGC, CC, 18 pts	Pooled	Hamel *et al.* 2010b
Interleukin 1 beta	*IL1B*^	Cytokine	Preg = not preg	MGC, 16 & 28 preg pts MGC, 16 & 69 not preg	Pooled	Fortin et al. 2019
Interleukin 6 signal transducer	*IL6ST*	Signal transduction	Preg = not preg	30 MGC, CC, 18 pts ea	Pooled	Hamel *et al.* 2008

APPENDIX C continued.

Genes	Symbol	Function	mRNA expression	Study Population	Samples	Reference
Inhibin beta A subunit	*INHBA*	FSH secretion inhibitor	Preg = not preg	30 MGC, CC, 18 pts ea	Pooled	Hamel *et al.* 2008
Integral membrane protein 2A	*ITM2A*	Membrane protein	Preg = not preg	39 CC, 39 pts	Individual	Burnik *et al.* 2015a
Inositol 1,4,5-trisphosphate receptor type 1	*ITPR1*	IP3 receptor	Preg = not preg	47 CC, 47 ICSI pts	Individual	Wathlet *et al.* 2013
KH RNA binding domain containing, signal transduction associated 3	*KHDRBS3*	Signal transduction	Preg = not preg	39 CC, 39 pts	Individual	Burnik *et al.* 2015a
Keratin 6A	*KRT6A*	Filament protein	Preg = not preg	39 CC, 39 pts	Individua l	Burnik *et al.* 2015a
Lactate dehydrogenase A	*LDHA*	Lactate dehydrogenase	Live birth = not preg	38 CC, 38 pts SET	Individual	Gebhardt *et al.* 2011
LDL receptor related protein 8	*LRP8*	Apolipoprotein E and reelin receptor	Preg = not preg	MGC, CC, 18 pts	Pooled	Hamel *et al.* 2010b
Myristoylated alanine rich protein kinase C substrate	*MARCKS*	Actin binding	Preg = not preg	MGC, CC, 18 pts	Pooled	Hamel *et al.* 2010b
Nudix hydrolase 10	*NUDT10*	Hydrolase	Preg = not preg	39 CC, 39 pts	Individual	Burnik *et al.* 2015a
Parathyroid Hormone like hormone	*PTHLH*	Hormone	Preg = not preg	99 CC, 33 ICSI pts	Individual	Wathlet *et al.* 2012
Phospho-, fructokinase platelet	*PFKP**	Glycolytic enzyme	Live birth = not preg	38 CC, 38 pts SET	Individual	Gebhardt *et al.* 2011

APPENDIX C continued.

Genes	Symbol	Function	mRNA expression	Study Population	Samples	Reference
Progesterone receptor	*PGR*	Nuclear hormone receptor	Preg = not preg Preg = not preg Live birth = not preg/loss	MGC, CC, 18 pts 47 CC, 47 ICSI pts 270 CC, 25 pts	Pooled Individual Individual	Hamel *et al.* 2010b Wathlet *et al.* 2013 Ekart *et al.* 2013
Pirin	*PIR*	Iron-binding protein	Preg = not preg	MGC, CC, 18 pts	Pooled	Hamel *et al.* 2010b
Pyruvate kinase, muscle	*PKM*	Glycolytic enzyme	Live birth = not preg	38 CC, 38 pts SET	Individual	Gebhardt *et al.* 2011
Protein kinase N2	*PKN2*	Serine/Threonine kinase	Preg = not preg	14 CC, 8 pts	Individual	Assidi *et al.*, 2011
Prothymosin alpha	*PTMA^*	Immune response	Preg = not preg	MGC, 16 & 28 preg pts MGC, 16 & 69 not preg	Pooled	Fortin et al. 2019
Regulator of G-protein signaling 3	*RGS3*	G protein signaling	Preg > not preg ns trend	MGC, CC, 38 pts	Pooled	Hamel *et al.* 2010a
Ribosomal protein L9	*RPL9*	Ribosomal protein	Preg = not preg	14 CC, 8 pts	Individual	Assidi *et al.*, 2011
Scavenger receptor class B member 1	*SCARB1*	Lipoprotein receptor	Preg = not preg	30 MGC, CC, 18 pts ea	Pooled	Hamel *et al.* 2008
Semaphorin 3A membrane protein	*SEMA3A*	Secretion	Preg = not preg	MGC, CC, 18 pts	Pooled	Hamel *et al.* 2010b
Serpin family A member 3	*SERPINA3*	Peptidase inhibitor	Preg = not preg Preg = not preg	30 MGC, CC, 18 pts ea MGC and CC	Pooled Pooled	Hamel *et al.* 2008 Hamel *et al.* 2010a
Secreted frizzled related protein 1	*SFRP1*	Wnt signaling	Preg = not preg	MGC, CC, 18 pts	Pooled	Hamel *et al.* 2010b
Secreted frizzled related protein 2	*SFRP2*	Wnt signaling	Preg = not preg	270 CC from 25 pts	Individual	Ekart *et al.* 2013

APPENDIX C continued.

Genes	Symbol	Function	mRNA expression	Study Population	Samples	Reference
Solute carrier family 2 member 1	*SLC2A1*	Glucose transport	Preg = not preg	47 CC, 47 ICSI pts	Individual	Wathlet *et al.* 2013
Solute carrier family 2 member 4	*SLC2A4*	Glucose transport	Preg = not preg	270 CC, 25 pts	Individual	Ekart *et al.* 2013
SPHK1 interactor, AKAP domain containing	*SPHKAP*	PKA signaling	Preg = not preg	14 CC, 8 pts	Individual	Assidi *et al.*, 2011
Sprouty RTK Signaling antagonist 2	SPRY2	Kinase inhibitor	Preg = not preg	MGC, CC, 18 pts ea	Pooled	Hamel *et al.* 2008
SplA/ryanodine receptor domain and SOCS box containing 2	*SPSB2***	Signal transduction	Preg > not preg ns trend	38 CC, 22 pts	Individual	Fragouli *et al.*, 2012
Steroidogenic Acute Regulatory Protein	STARD1	Steroidogenesis	Preg = not preg	MCG, CC, 111 pts	Pooled	Lee *et al*. 2016
Stanniocalcin 1	*STC1*	Hormone	Preg = not preg	99 CC, 33 ICSI pts	Individual	Wathlet *et al.* 2012
			Preg = not preg	47 CC, 47 ICSI pts	Individual	Wathlet *et al.* 2013
Stanniocalcin 2	*STC2*	Hormone	Preg = not preg	99 CC, 33 ICSI pts	Individual	Wathlet *et al.* 2012
Steroid sulfatase (microsomal), isozyme S	*STS*	Sulfatase	Live birth = not preg	38 CC, 38 pts SET	Individual	Gebhardt *et al.* 2011
Synaptotagmin 11	*SYT11*	Protein trafficking	Preg = not preg	14 CC, 8 pts	Individual	Assidi *et al.*, 2011
T-box 6	*TBX6*	Transcription factor	Preg = not preg	39 CC, 41 pts	Individual	Burnik *et al.* 2015a

APPENDIX C continued.

Genes	Symbol	Function	mRNA expression	Study Population	Samples	Reference
Transforming growth factor beta 1	*TGFB1*	Growth factor	Preg = not preg	47 CC, 47 ICSI pts	Individual	Wathlet *et al.* 2013
Thrombospondin 1	*THBS1*	Adhesion protein	Preg = not preg	47CC, 47 ICSI pts	Individual	Wathlet *et al.* 2013
THO complex 2	*THOC2*	Transcription factor	Preg = not preg	14 CC, 8 pts	Individual	Assidi *et al.*, 2011
Transmembrane protein 64	*TMEM64*	Calcium signaling	Preg = not preg	39 CC, 41 pts	Individual	Burnik *et al.* 2015a
TNF alpha induced protein 6	*TNFAIP6*	Hyaluronin binding	Live birth = not preg Preg = not preg Preg = not preg	38 CC, 38 pts SET MGC, CC, 18 pts ea 108 CC, 8 ICSI pts	Individual Pooled Pooled	Gebhardt *et al.* 2011 Hamel *et al.* 2008 Mckenzie *et al.* 2004
Tumor protein p53 inducible protein 3	*TP53I3***	Dehydrogenase	Preg = not preg	38 CC, 22 pts	Individual	Fragouli *et al.*, 2012
UDP-glucose Pyrophos-phorylase 2	*UGP2*	Glycogenic enzyme	Preg > not preg	MGC, CC, 18 pts	Pooled	Hamel *et al.* 2010b
Tryptophan rich basic protein	*WRB*	Nuclear protein	Preg = not preg	39 CC, 39 pts	Individual	Burnik *et al.* 2015a
Tyrosine 3-monooxygenase/ tryptophan 5-monooxygenase activation protein zeta	*YWHAZ*	Signal transduction	Preg = not preg	MGC, CC, 18 pts	Pooled	Hamel *et al.* 010b

*positive correlation with birth weight; ** overexpressed in chromosomally normal oocytes

^ Two separate analyses were performed in the same study

CC = cumulus cells; MGC = mural granulosa cells; ICSI = intra-cytoplasmic sperm injection

SET = single embryo transfer; pts = patients; ea = each group; preg = pregnant, ns = not significant

Symbols: > greater than; = equivalent to, < less than

APPENDIX D

Permission to Reprint

Chapter 1

This is a License Agreement between Richard Kordus ("You") and Bioscientifica Limited ("Publisher") provided by Copyright Clearance Center ("CCC"). The license consists of your order details, the terms and conditions provided by Bioscientifica Limited, and the CCC terms and conditions.
All payments must be made in full to CCC.

Order Date	14-Apr-2020
Order license ID	1028524-2
ISSN	1741-7899
Type of Use	Republish in a thesis/dissertation
Publisher	SOCIETY FOR REPRODUCTION AND FERTILITY
Portion	Chapter/article

LICENSED CONTENT

Publication Title	Reproduction : the official journal of the Society for the Study of Fertility
Author/Editor	Society for the Study of Fertility, Society for Reproduction and Fertility, Society for Reproduction and Fertility., Society for the Study of Fertility.
Date	01/01/2001
Language	English
Country	United Kingdom of Great Britain and Northern Ireland
Rightsholder	Bioscientifica Limited
Publication Type	e-Journal
URL	http://www.jrf-journals.org.uk

REQUEST DETAILS

Portion Type	Chapter/article
Page range(s)	R69-R80
Total number of pages	12

Format (select all that apply)	Print, Electronic
Who will republish the content?	Academic institution
Duration of Use	Life of current edition
Lifetime Unit Quantity	Up to 499
Rights Requested	Main product
Distribution	Worldwide
Translation	Original language of publication
Copies for the disabled?	No
Minor editing privileges?	Yes
Incidental promotional use?	No
Currency	USD

NEW WORK DETAILS

Title	USING HUMAN GRANULOSA CELLS TO SELECT THE MOST COMPETENT EMBRYOS FOR UTERINE TRANSFER IN IN VITRO FERTILIZATION CYCLES
Instructor name	Holly A LaVoie
Institution name	University of South Carolina School of Medicine
Expected presentation date	2020-04-17

ADDITIONAL DETAILS

Order reference number	041320
The requesting person / organization to appear on the license	Richard Kordus

REUSE CONTENT DETAILS

Title, description or numeric reference of the portion(s)

Chapter 1 Introduction, Chapter 5 general discussion and and Appendices A-C

Editor of portion(s)	Richard Kordus
Volume of serial or monograph	N/A
Page or page range of portion	R69-R80
Title of the article/chapter the portion is from	

Introduction, General Discussion and Appendices A-C	
Author of portion(s)	Society for the Study of Fertility; Society for Reproduction and Fertility; Society for Reproduction and Fertility.; Society for the Study of Fertility.
Issue, if republishing an article from a serial	N/A
Publication date of portion	2016-11-04

Figure 1.1

https://www.freepik.com/free-vector/uterus-poster 3791876.htm

Freepik License

Free for personal and commercial purpose with attribution.

Insert the attribution line close to where you're using the resource. If it's not possible, place it in the credits section.

For example: "image: Freepik.com". This cover has been designed using resources from Freepik.com

Figure 1.2

Permissions
4th Floor, Auto Atlantic
Corner, Hertzog Boulevard & Heerengracht
Cape Town, 8001
South Africa
USGranting@pearson.com

Aug 6, 2019 PE Ref # 209708

Rich Kordus
890 West Faris Road, Suite 470
Greenville, SC 29605

Dear Rich,
You have our permission to include content from our text, HUMAN ANATOMY & PHYSIOLOGY, 10th Ed. by MARIEB, ELAINE N.; HOEHN, KATJA, in your dissertation or masters thesis at University of South Carolina School of Medicine.

Content to be included is:
Diagrammatic view of an ovary sectioned to reveal the follicles in its interior.

Please credit our material as follows:
MARIEB, ELAINE N.; HOEHN, KATJA, HUMAN ANATOMY & PHYSIOLOGY, 10th, ©2016. Reprinted by permission of Pearson Education, Inc., New York, New York.

Sincerely,
Michael Prince,
Permissions Granting Analyst

Figure 1.3

License Number	4635480776536
License date	Jul 24, 2019
Licensed Content Publisher	Oxford University Press
Licensed Content Publication	Human Reproduction Update
Licensed Content Title	Ovarian ageing: the role of mitochondria in oocytes and follicles
Licensed Content Author	May-Panloup, Pascale; Boucret, Lisa
Licensed Content Date	Oct 20, 2016
Licensed Content Volume	22
Licensed Content Issue	6
Type of Use	Thesis/Dissertation
Requestor type	Educational Institution/Non-commercial/ Not for-profit
Format	Print and electronic
Portion	Figure/table
Number of figures/tables	2

Will you be translating?	No
Title	USING HUMAN GRANULOSA CELLS TO SELECT THE MOST COMPETENT EMBRYOS FOR UTERINE TRANSFER IN IN VITRO FERTILIZATION CYCLES
Institution name	University of South Carolina School of Medicine
Expected presentation date	Aug 2019
Order reference number	072419A
Portions	Figures 1 and 2

Figure 1.4

License Number	4631931230675
License date	Jul 18, 2019
Licensed Content Publisher	Elsevier
Licensed Content Publication	Biochemical Pharmacology
Licensed Content Title	The role of the aryl hydrocarbon receptor in the female reproductive system
Licensed Content Author	Isabel Hernández-Ochoa,Bethany N. Karman,Jodi A. Flaws
Licensed Content Date	Feb 15, 2009
Licensed Content Volume	77
Licensed Content Issue	4
Licensed Content Pages	13
Type of Use	reuse in a thesis/dissertation
Portion	figures/tables/illustrations
Number of figures/tables/illustrations	1
Format	both print and electronic

Figure 1.5

EMANUELE, M. A., WEZEMAN, F. & EMANUELE, N. V. 2002. Alcohol's effects on female reproductive function. *Alcohol Res Health,* 26**,** 274-81.

Author information Copyright and License information Disclaimer
Copyright notice

Figure 1.6

EMANUELE, M. A., WEZEMAN, F. & EMANUELE, N. V. 2002. Alcohol's effects on female reproductive function. *Alcohol Res Health,* 26**,** 274-81.

Author information Copyright and License information Disclaimer
Copyright notice

Figure 1.7

HEBERT-SCHUSTER, M., ROTTA, B. E., KIRKPATRICK, B., GUIBOURDENCHE, J. & COHEN, M. 2018. The Interplay between Glucose-Regulated Protein 78 (GRP78) and Steroids in the Reproductive System. *Int J Mol Sci,* 19.

Figure 1.8

License Number	4631361052147
License date	Jul 17, 2019
Licensed Content Publisher	Georg Thieme Verlag KG
Licensed Content Publication	Seminars in Reproductive Medicine
Licensed Content Title	Mouse Oocyte Control of Granulosa Cell Development and Function: Paracrine Regulation of Cumulus Cell Metabolism

Licensed Content Author	You-Qiang Su, Koji Sugiura, John J. Eppig
Licensed Content Date	Jan 1, 2009
Licensed Content Volume	27
Licensed Content Issue	01
Type of Use	Dissertation/Thesis
Requestor type	non-commercial (non-profit)
Format	print and electronic
Portion	figures/tables/images
Number of figures/tables/images	1
Will you be translating?	no
Distribution quantity	50
Title	USING HUMAN GRANULOSA CELLS TO SELECT THE MOST COMPETENT EMBRYOS FOR UTERINE TRANSFER IN IN VITRO FERTILIZATION CYCLES
Institution name	University of South Carolina School of Medicine
Expected presentation date	Aug 2019
Order reference number	07172019A

Figure 1.9

NSIAH-SEFAA, A. & MCKENZIE, M. 2016. Combined defects in oxidative phosphorylation and fatty acid beta-oxidation in mitochondrial disease. *Biosci Rep,* 36.

Permission to reuse content from an article published by Portland Press:

- If the content that you are seeking to re-use is in a Portland Press article that is published open access under a CC BY licence NO permissions
- are required, although you must cite the published article and credit the authors when you re-use it (or part of it).

Figure 1.10

This Agreement between Richard J Kordus ("You") and Elsevier ("Elsevier") consists of your license details and the terms and conditions provided by Elsevier and Copyright Clearance Center.

License Number	4805541330368
License date	Apr 10, 2020

Licensed Content Publisher	Elsevier
Licensed Content Publication	Fertility and Sterility
Licensed Content Title	The nature of aneuploidy with increasing age of the female partner: a review of 15,169 consecutive trophectoderm biopsies evaluated with comprehensive chromosomal screening
Licensed Content Author	Jason M. Franasiak,Eric J. Forman,Kathleen H. Hong,Marie D. Werner,Kathleen M. Upham,Nathan R. Treff,Richard T. Scott
Licensed Content Date	Mar 1, 2014
Licensed Content Volume	101
Licensed Content Issue	3
Licensed Content Pages	9
Start Page	656
End Page	663.e1
Type of Use	reuse in a thesis/dissertation
Portion	figures/tables/illustrations
Number of figures/tables/illustrations	1
Format	both print and electronic
Are you the author of this Elsevier article?	No
Will you be translating?	No
Title	USING HUMAN GRANULOSA CELLS TO SELECT THE MOST COMPETENT EMBRYOS FOR UTERINE TRANSFER IN IN VITRO FERTILIZATION CYCLES
Institution name	U of SC, School of Medicine
Expected presentation date	Apr 2020
Order reference number	4102020
Portions	Figure 2A. Page 660

Chapter 3

This Agreement between Mr. Richard Kordus ("You") and Springer Nature ("Springer Nature") consists of your license details and the terms and conditions provided by Springer Nature and Copyright Clearance Center.

License Number	4613680844184
License date	Jun 21, 2019
Licensed Content Publisher	Springer Nature
Licensed Content Publication	Journal of Assisted Reproduction and Genetics
Licensed Content Title	Cumulus cell pappalysin-1, luteinizing hormone/choriogonadotropin receptor, amphiregulin and hydroxy-delta-5-steroid dehydrogenase, 3 beta- and steroid delta-isomerase 1 mRNA levels associate with oocyte developmental competence and embryo outcomes
Licensed Content Author	Richard J. Kordus, Akhtar Hossain, Michael C. Corso et al
Licensed Content Date	Jan 1, 2019
Type of Use	Thesis/Dissertation
Requestor type	academic/university or research institute
Format	print and electronic
Portion	full article/chapter
Will you be translating?	no
Circulation/distribution	<501
Author of this Springer Nature content	yes
Title	USING HUMAN GRANULOSA CELLS TO SELECT THE MOST COMPETENT EMBRYOS FOR UTERINE TRANSFER IN IN VITRO FERTILIZATION CYCLES
Institution name	University of South Carolina School of Medicine
Expected presentation date	Aug 2019
Order reference number	06212019

Chapter 5

This is a License Agreement between Richard Kordus ("You") and Bioscientifica Limited ("Publisher") provided by Copyright Clearance Center ("CCC"). The license consists of your order details, the terms and conditions provided by Bioscientifica Limited, and the CCC terms and conditions.
All payments must be made in full to CCC.

Order Date	14-Apr-2020
Order license ID	1028524-2

ISSN	1741-7899
Type of Use	Republish in a thesis/dissertation
Publisher	SOCIETY FOR REPRODUCTION AND FERTILITY
Portion	Chapter/article

LICENSED CONTENT

Publication Title	Reproduction : the official journal of the Society for the Study of Fertility
Author/Editor	Society for the Study of Fertility, Society for Reproduction and Fertility, Society for Reproduction and Fertility., Society for the Study of Fertility.
Date	01/01/2001
Language	English
Country	United Kingdom of Great Britain and Northern Ireland
Rightsholder	Bioscientifica Limited
Publication Type	e-Journal
URL	http://www.jrf-journals.org.uk

REQUEST DETAILS

Portion Type	Chapter/article
Page range(s)	R69-R80
Total number of pages	12
Format (select all that apply)	Print, Electronic
Who will republish the content?	Academic institution
Duration of Use	Life of current edition
Lifetime Unit Quantity	Up to 499
Rights Requested	Main product
Distribution	Worldwide
Translation	Original language of publication
Copies for the disabled?	No
Minor editing privileges?	Yes
Incidental promotional use?	No
Currency	USD

NEW WORK DETAILS

Title	USING HUMAN GRANULOSA CELLS TO SELECT THE MOST COMPETENT EMBRYOS FOR UTERINE TRANSFER IN IN VITRO FERTILIZATION CYCLES
Instructor name	Holly A LaVoie
Institution name	University of South Carolina School of Medicine

Expected presentation date	2020-04-17

ADDITIONAL DETAILS

Order reference number	041320
The requesting person / organization to appear on the license	Richard Kordus

REUSE CONTENT DETAILS

Title, description or numeric reference of the portion(s)

Chapter 1 Introduction, Chapter 5 general discussion and and Appendices A-C

Editor of portion(s)	Richard Kordus
Volume of serial or monograph	N/A
Page or page range of portion	R69-R80
Title of the article/chapter the portion is from	

Introduction, General Discussion and Appendices A-C

Author of portion(s)	Society for the Study of Fertility; Society for Reproduction and Fertility; Society for Reproduction and Fertility.; Society for the Study of Fertility.
Issue, if republishing an article from a serial	N/A
Publication date of portion	2016-11-04

Figure 5.1

This Agreement between Richard J Kordus ("You") and Oxford University Press ("Oxford University Press") consists of your license details and the terms and conditions provided by Oxford University Press and Copyright Clearance Center.

License Number	4805550398145
License date	Apr 10, 2020
Licensed content publisher	Oxford University Press
Licensed content publication	Human Reproduction

Licensed content title	Cumulus cells surrounding oocytes with high developmental competence exhibit down-regulation of phosphoinositol 1,3 kinase/protein kinase B (PI3K/AKT) signalling genes involved in proliferation and survival
Licensed content author	Artini, P G; Tatone, C
Licensed content date	Oct 26, 2017
Type of Use	Thesis/Dissertation
Institution name	
Title of your work	USING HUMAN GRANULOSA CELLS TO SELECT THE MOST COMPETENT EMBRYOS FOR UTERINE TRANSFER IN IN VITRO FERTILIZATION CYCLES
Publisher of your work	U of SC, School of Medicine
Expected publication date	Apr 2020
Permissions cost	0.00 USD
Value added tax	0.00 USD
Total	0.00 USD
Title	USING HUMAN GRANULOSA CELLS TO SELECT THE MOST COMPETENT EMBRYOS FOR UTERINE TRANSFER IN IN VITRO FERTILIZATION CYCLES
Institution name	U of SC, School of Medicine
Expected presentation date	Apr 2020
Order reference number	41020202
Portions	Figure 3A. Page 2479

Appendices

Order Date	14-Apr-2020
Order license ID	1028524-2
ISSN	1741-7899
Type of Use	Republish in a thesis/dissertation
Publisher	SOCIETY FOR REPRODUCTION AND FERTILITY
Portion	Chapter/article

LICENSED CONTENT

Publication Title	Reproduction : the official journal of the Society for the Study of Fertility
Author/Editor	Society for the Study of Fertility, Society for Reproduction and Fertility, Society for Reproduction and Fertility., Society for the Study of Fertility.
Date	01/01/2001
Language	English
Country	United Kingdom of Great Britain and Northern Ireland
Rightsholder	Bioscientifica Limited
Publication Type	e-Journal
URL	http://www.jrf-journals.org.uk

REQUEST DETAILS

Portion Type	Chapter/article
Page range(s)	R69-R80
Total number of pages	12
Format (select all that apply)	Print, Electronic
Who will republish the content?	Academic institution
Duration of Use	Life of current edition
Lifetime Unit Quantity	Up to 499
Rights Requested	Main product
Distribution	Worldwide
Translation	Original language of publication
Copies for the disabled?	No
Minor editing privileges?	Yes
Incidental promotional use?	No
Currency	USD

NEW WORK DETAILS

Title	USING HUMAN GRANULOSA CELLS TO SELECT THE MOST COMPETENT EMBRYOS FOR UTERINE TRANSFER IN IN VITRO FERTILIZATION CYCLES

Instructor name	Holly A LaVoie
Institution name	University of South Carolina School of Medicine
Expected presentation date	2020-04-17

ADDITIONAL DETAILS

Order reference number	041320
The requesting person / organization to appear on the license	Richard Kordus

REUSE CONTENT DETAILS

Title, description or numeric reference of the portion(s)

Chapter 1 Introduction, Chapter 5 general discussion and and Appendices A-C

Editor of portion(s)	Richard Kordus
Volume of serial or monograph	N/A
Page or page range of portion	R69-R80
Title of the article/chapter the portion is from	

Introduction, General Discussion and Appendices A-C

Author of portion(s)	Society for the Study of Fertility; Society for Reproduction and Fertility; Society for Reproduction and Fertility.; Society for the Study of Fertility.
Issue, if republishing an article from a serial	N/A
Publication date of portion	2016-11-04